ASSESSMENT OF ASPHALT MATERIALS TO RELIEVE REFLECTION CRACKING OF HIGHWAY SURFACINGS

by

MICHAEL DAVID FOULKES, B.Sc.

This thesis is submitted to the Council for National Academic Awards in partial fulfilment of the requirements for the Degree of Doctor of Philosophy.

This work was undertaken within the Department of Civil Engineering at Plymouth Polytechnic, Plymouth, in collaboration with the Transport and Road Research Laboratory (TRRL) U.K.

MARCH

1988

DECLARATION

While registered as a candidate for the degree for which this submission is made, the author has not been a registered candidate for any other award of the C.N.A.A. or of a University during the research programme.

All work described in this thesis is wholly original and was carried out by the author except where specifically noted by reference. Assistance received in the research work and preparation of this thesis is acknowledged.

Author: M.D. Foulkes

Supervisor: Prof.C.K. Kennedy

STATEMENT OF ADVANCED STUDIES

The author has undertaken the following advanced studies in connection with the programme of research.

DIRECTED READING

The published proceedings of the five conferences known as the "Ann Arbor" conferences held in 1962/7/72/7/82.

COURSES / SEMINARS / CONFERENCES

The author has attended the following meetings -

(i) Residential Course on 'Analytical Design of Bituminous Pavements' held at the University of Nottingham in 1984.

(ii) The 1985 'Deflectograph' Short Course held at Plymouth Polytechnic.

(iii) The 2nd International Conference on the Bearing Capacity of Road and Airfield Pavements, held at Plymouth Polytechnic in 1986.

(iv) Appropriate research seminars, lectures and other meetings of Professional Bodies throughout the period of the research.

ACKNOWLEDGEMENTS

The author is indebted to the many staff at Plymouth Polytechnic who gave freely of their time in support of this project.

The author wishes to express his gratitude in particular to Professor C.K. Kennedy, formerly Head of Department of Civil Engineering, Plymouth Polytechnic, and to Dr. D. Powell, Principal Scientific Officer of the Transport and Road Research Laboratory, who supervised this thesis and gave generously of their time for discussion and support.

Assistance was also afforded to the author by Mr. M. Nunn and Mr. H., Mayhew, Scientific Officers of the Transport and Road Research Laboratory whose enthusiasm contributed to the success of this project.

Thanks are also due to Mr. T.N. Brooker for his assistance and Mrs. S.K. Hicks for her patience.

Last but not least thanks to my wife, Moira for her support.

ASSESSMENT OF ASPHALT MATERIALS TO RELIEVE REFLECTION CRACKING OF HIGHWAY SURFACINGS

by M.D. Foulkes

ABSTRACT

The thesis investigates the mechanisms and restraints which influence transverse crack propagation through the bituminous surfacings of semi-flexible pavements. These pavements incorporate continuously laid cement bound roadbases which, during curing, crack into slabs of varying length, ranging from 4-25m.

Reciprocal crack growth can occur in the surfacing, known as 'reflection cracks', located through stresses concentrated at the discontinuities within the roadbase.

Three mechanisms have been identified and are described as contributing to reflection crack propagation. They have been analysed independently although the majority of conclusions drawn are applicable to their combined action. Their relative importance will vary with respect to pavement geometry, material properties, environmental conditions and traffic intensity.

The first mechanism, 'tensile fatigue', induces crack propagation vertically upward through the surfacing. Tensile strains are developed during daily and annual fluctuations of temperature, which cause expansion and contraction of the cement bound roadbase. This mechanism is most prominent on pavements with thin surfacings and long slab lengths. The rate of crack growth is dependent on the range of temperature within the roadbase, slab length, thermal characteristics of the roadbase material and resistance of the surfacing to this form of fatigue.

A model has been developed based on a combination of results from an extensive testing programme, the use of fracture mechanics theory and computer simulation of the condition. The results quantify the resistance shown by conventional bituminous mixes to reflection cracking in terms of their mix parameters. Also considered are the use of stress relieving membranes, reinforcement material and modified binders to inhibit crack growth.

The second mechanism,'tensile yield' is also thermally induced but associated with cold weather conditions. Temperature gradients through the pavement structure induce warping and contraction within the uppermost layers. Tensile strains developed at the surface can, under U.K. winter temperatures, exceed the ultimate yield strain of the wearing course material.

Preliminary investigations of four pavements constructed in the early 1970's to motorway specifications indicate that reflection cracking will initiate at the surface if the yield strain, as defined through tensile creep tests, is reduced through binder oxidization to a value of 0.5%. This mechanism will operate on pavements with greater structural layer thicknesses and is only partially dependent on slab length.

The influence of a further mechanism,'shear fatigue' induced through trafficking of the pavement, has been shown to be confined to the acceleration of crack growth in the final stages of propagation unless a breakdown of interlock occurs between adjoining roadbase slabs.

TABLE OF CONTENTS

		Page
1.0	Introduction	1
2.0	Composite Pavement Materials	5
2.1	Cement Stabilized Roadbases	5
2.2	Bituminous Surfacings	9
2.2.1	Material Specifications	9
2.2.1.1	Hot Rolled Asphalt	11
2.2.1.2	Dense Bitumen Macadam	11
2.2.1.3	Open Textured Macadam	11
2.2.2	Bituminous Material Properties	12
2.2.2.1	Stiffness Characteristics	12
2.2.2.2	Bitumen Stiffness	13
2.2.2.3	Mix Stiffness	15
2.2.3	The Effect of Service Conditions on the Susceptibility of Bituminous Mixes to Cracking	17
2.2.3.1	Bitumen Hardening	17
2.2.3.2	Void content	21
3.0	Pavement Design	23
3.1	Introduction	23
3.2	U.K. Empirical Design Guide	23
3.3	Analytical Design Guides	28
3.3.1	LR1132: General Design Considerations	28
3.3.2	LR1132: Lean Concrete Roadbase Design Considerations	39
4.0	Reflection Cracking	32
4.1	The Extent of the Reflection Cracking Problem	32
4.1.1	Crack Surveys	32
4.1.2	Overlaid Rigid Pavements	35
4.2	The effects of Pavement Deterioration Through Reflection Cracking	35
4.3	Causes of Reflection Cracking	36
4.3.1	Tensile Fatigue	37
4.3.2	Tensile Yield	39
4.3.2.1	Influence of Thermal Warping	39
4.3.2.2	Influence of Long Term Shrinkage	40
4.3.3	Shear Fatigue	40
4.3.4	Differential Settlement	41
4.4	A Review of Methods used to Inhibit Reflection Cracking	41
4.4.1	Aggregate Type and Mix Characteristics of Lean Concrete Roadbases	42
4.4.2	Depth of Bituminous Surfacings	42

page

4.4.3 Bituminous Mixes 43
4.4.4 Modified Binders 45
4.4.5 Bond Breaking Layers 46
4.4.6 Stress Absorbing Layers 47
4.4.7 Cushioning Layers 51
4.4.8 Cracking and Seating of Concrete Bases 51
4.4.9 Scarifying and Recycling or Overlaying 52
4.4.10 Overbanding 53
4.4.11 Surface Dressing 53
4.4.12 Overlays 53
4.4.13 Reconstruction 54
4.4.14 Conclusions 54

4.5 An Appraisal of Analytical Methods to Predict Crack Growth Through Bituminous Surfacings 56

4.5.1 Conclusions 66

5.0 Aims and Objectives of the Investigation 68

6.0 Mechanism of Tensile Fatigue 70

6.1 Introduction 70

6.1.1 The Mechanism 70
6.1.2 Development of a Predictive Model 71

6.2 Laboratory Simulation of The Tensile Fatigue Mechanism 72

6.2.1 Tensile Fatigue Test Rig 72
6.2.2 Control System 75
6.2.3 Test arrangement 76

6.3 Instrumentation and Data Logging 76

6.3.1 Introduction 76
6.3.2 Instrumentation of the Sample Beams For Crack Growth 78
6.3.3 Automatic Data Logging 81
6.3.4 The Derivation of Crack Length 82

6.4 Asphalt Test Mixes 86

6.4.1 Introduction 86
6.4.2 Mixes 86
6.4.2.1 Aggregates 87
6.4.2.2 Binder 87
6.4.2.3 Mix Preparation 87
6.4.3 Test Beams 88

6.5 The Concept of Accelerated Testing 88

6.5.1 Introduction 88
6.5.2 Experimental Verification 91
6.5.3 Results 91

6.6 Fracture Mechanics Approach 94

page

6.7 The Prediction Model 98

6.7.1 Introduction 98
6.7.2 Roadbase movements 98
6.7.3 Stress Intensity Factors 100
6.7.4 Material Fatigue Constants 100
6.7.5 Fatigue Life 100
6.7.6 Results 101

6.8 Stress Induced through Roadbase Movements 101

6.8.1 Crack opening widths 101
6.8.2 Temperature profiles within Composite Pavements under U.K. conditions 103
6.8.3 Coefficient of Thermal Expansion and and Contraction of Lean Concrete 107
6.8.4 Crack Spacings in Cement Bound Roadbases 109
6.8.4.1 Introduction 109
6.8.4.2 Theoretical Considerations 109
6.8.4.3 Crack Spacing Surveys 111
6.8.5 Sub-base Restraint 111

6.9 Mix stiffness of Bituminous Surfacings Relevant to Tensile Fatigue 114

6.9.1 Introduction 114
6.9.2 Calculations of Creep Stiffness 114
6.9.3 Tensile Yield Strain 116

6.10 Stress Intensity Factors 118

6.10.1 Introduction 118
6.10.2 Derivation of Stress Intensity factors using Finite Element Techniques 120
6.10.3 Description of Finite Element Model, F.E.1, used to Define Stress Intensity Factor 122
6.10.4 Modified Stress Intensity Factors in terms of Input Strain Parameters 124

6.11 Derivation of Fatigue Constants A and n 127

6.11.1 Introduction 127
6.11.2 Experimental Proceedure 128

6.12 Test Results 128

6.12.1 Introduction 128
6.12.2 Effect of Mix Parameters on Fatigue Constants 'A' and 'n' 130

6.13 Derivation of Annual Fatigue Life 130

6.13.1 Introduction 130
6.13.2 Program R.F.T. 100 138
6.13.3 Results 140

		page
7.0	Mechanism of Tensile Yield	157
7.1	Introduction	157
7.2	Study of M4 Reflection Cracking	158
7.3	Variations in the Material Properties of the M4	158
7.3.1	Contract 3	159
7.3.2	Contract 4	159
7.3.3	Contract 5	159
7.3.4	Contract 6	159
7.4	Discussion of Local Authority Report	160
7.5	Aims of the Investigation	162
7.6	Pavement Modelling	162
7.6.1	Introduction	162
7.6.2	Stiffness Data	162
7.6.3	Calculation of Coefficients of Thermal Contraction of Low Penetration Asphalts	164
7.6.3.1	Test procedure	165
7.6.3.2	The Thermal Coefficient of Contraction of Asphalts	165
7.7	Finite Element Model	167
7.7.1	Thermal Contraction and Warping	167
7.7.2	Description of the Model	169
7.8	Discussion of Model Results	171
7.9	Comparison of Field Observations with Model Results	178
7.10	Validation of Yield Strain Concept	180
7.10.1	Introduction	180
7.10.2	Further Investigations of Crack Development/ Yield Strain Relationships	180
7.10.2.1	M4 (Berkshire)	180
7.10.2.2	A38 (Litchfield By Pass)	185
7.10.2.3	M3 (Hampshire)	185
7.10.2.4	Redhouse Road (Northampton)	187
8.0	Mechanism of Shear Fatigue	189
8.1	Introduction	189
8.2	Field Test Data	189
8.3	Finite Element Model	192
8.3.1.	Model description	192
8.3.2	Stress Intensity Factor Curves	194

page

8.3.3 Deflected Shape 195

8.4 Laboratory Simulation of Traffic Loading Conditions 195

8.4.1 Rig Description 195
8.4.2 Instrumentation 195
8.4.3 Test Results 199

8.5 Analysis of Transverse Crack Frequency Data 200

8.5.1 Introduction 200
8.5.2 Crack Spacing 200

9.0 Geogrids as Crack Inhibitors 205

9.1 Introduction 205

9.2 Engineering Properties of Geogrids 207

9.3 Composite Sample Testing 210

9.4 Test results 213

9.4.1 Test Configuration (a) 213
9.4.2 Test Configuration (b) 213
9.4.3 Test Configuration (c) 213

10.0 Polymer Modified Binders as Crack Inhibitors 215

10.1 Introduction 215

10.2 Details of Modified Polymer Binder 216

10.3 Test Results 217

10.3.1. Tensile Fatigue Tests 217
10.3.2 Tensile Creep Tests 218

11.0 Engineering Significance of Results 219

11.1 General 219

11.1.1 Introduction 219
11.1.2 Crack Mechanisms 219
11.1.3 Dominant Crack Mechanisms 220

11.2 Factors Influencing Crack Growth 222

11.2.1 Slab Length 222
11.2.2 Thickness of Surfacing 223
11.2.3 Binder Grade 223
11.2.4 Binder Oxidation 223
11.2.5 Bitumen Content 224
11.2.6 Void Content 224
11.2.7 Aggregate Grading 225
11.2.8 Reinforcement 225
11.2.9 Stress Absorbing Layers 225

page

11.2.10 Mastic Debonded Zones 226
11.2.11 Modified Binders 226

11.3 Future Research 227

12.0 Conclusions 229

13.0 References 232

Appendix 1 Example Calculation of Stress Intensity Factor k_o

Appendix 2 Example Calculation of Fatigue Constants A and n

Appendix 3 Example on the Estimation of Reflection Cracking Fatigue life due to the Mechanism of Tensile Fatigue

Appendix 4 Modification of Predictive Method to Allow for Binder Hardening with Age

Appendix 5 Grading Envelopes for Test Mixes

Appendix 6 Basic Program Listings

Appendix 7 Input files to 'PAFEC' Finite Element package for the Investigation of the Crack Mechanisms.

LIST OF FIGURES

Fig.		Page
1.1	Flow chart depicting Structure of Thesis	4
2.1	Nomograph for determining the stiffness of Bitumens [13]	14
2.2	Ageing Data from Colnbrook By-Pass Experiment[18]	19
2.3	The Effect of Void Content on Bitumen Hardening - Results of the Zaca-Wigmore Asphalt Test Road [17]	19
3.1	Lean Concrete, Soil Cement and Cement bound Granular Roadbases - Minimum Thickness of Surfacing and Roadbase Specified by R.N.29. [7]	25
3.2	Design Curves for Roads with Lean Concrete Roadbase specified by LR1132 [1]	25
4.1	Dominant Reflection Cracking Mechanisms	38
4.2	Progression of Horizontal and Vertical Cracking[76]	62
4.3	Top Fibre Stress in Overlay due to J.R.C.P. Joint Movement[78]	65
4.4	Bottom Fibre Stress in Overlay due to J.R.C.P. Joint Movement [78]	65
4.5	Maximum Stress in Overlay due to 1 Deg.F. Temperature Differential in a rigid Pavement [78]	65
6.1	Elevation on Thermally Induced Reflection Cracking Simulation Rig	73
6.2	Input Data Simulating both Daily and Annual Expansion and Contraction of the Roadbase due to Thermal Variations	72
6.3	Portal Frame Mounted Strain Gauges	81
6.4	Plot of Pavement Surface Strain versus Crack Length from Linear Elastic Finite Element Model Output	83
6.5	The "Dugdale" model for Crack Tip Plasticity[106]	83
6.6	Strain ahead of given Increments of Crack on the Crack Path for Crack Opening Widths of 1.0mm and 1.4mm	84
6.7	Diagrammatic Presentation of the Plastic Zone ahead of the Crack Tip.	85
6.8	Correction to Crack Length given by Elastic Analysis related to Strain Yield of Bituminous Surfacing for u = 1.4mm	85
6.9	Verification of Concept of Accelerated Testing	92
6.10	Load versus Fatigue Cycles producing a Characteristic Gradient for Test Conditions and Sample Geometry	93

Fig.		Page
6.11	Verification of Relationship between Bitumen Stiffness and Fatigue Life for Crack Opening Fatigue Testing	93
6.12	Fundamental Modes of Fracture	97
6.13	Flow Chart depicting Method of Tensile Fatigue Model	99
6.14	Bi-Hourly Temperature/Depth Profiles for Bituminous, Concrete and Composite Pavements for January, April, July and October	105
6.15	Effect of Sub-Base Restraint on Roadbase Movement	113
6.16	Comparison of Stiffness Values between Tensile Creep Test and 3 point Bending	117
6.17	Definition of The Tensile Yield Point	117
6.18	Definition of the Principal Stresses for Derivation of the Stress Intensity Factor From Eq. 6.12	119
6.19	Derivation of Stress Intensity Factor k_o from Finite Element Model Output	121
6.20	Mesh Generation and Crack Opening Deflected Shape from Finite Element Model of Tensile Fatigue Mechanism	123
6.21	Stress Intensity Factor k_o versus Crack Length for given Ratio of Basecourse/Wearing Course Stiffness Values	125
6.22	Stress Intensity Factor (k_o) versus Crack Length for Bond Break between Surfacing and Roadbase	127
6.23	Expansion of Paris' Equation through Numerical Integration	129
6.24	Derivation of Fatigue Constants 'A' and 'n'.	129
6.25	Bitumen Stiffness versus Fatigue Constant 'A' for DBM Mixes (1)	136
6.26	Bitumen Stiffness versus Fatigue Constant 'A' for DBM Mixes (2)	137
6.27	Void Content versus Fatigue Constant 'A' for DBM mixes	137
6.28	Binder Grade versus Fatigue Constant 'n' for DBM mixes	137
6.29	Flow Chart of Program R.F.T. 100	141
6.30	Fatigue Life (Days) versus Aggregate Grading (mm) for 100mm Depth of DBM Material of Mid-Grading (BS4987)	142
6.31	Fatigue Life (Days) versus Binder Content (%) for 100mm Depth of 200pen. DBM Material of Mid-Grading (BS4987)	142

Fig.		Page
6.32	Fatigue Life (Days) versus Penetration Grade for 100mm Depth of DBM Material of Mid-Grading (BS4987)	143
6.33	Fatigue Life (Days) versus Void Content (%) for 100mm DEpth of DBM Material of Mid-Grading (BS4987)	143
6.34	Mix Stiffness and Fatigue Life Data for 20mm Nominal Size DBM with 50 pen binder, 4.2% Binder Content and 3% Voids	145
6.35	Mix Stiffness and Fatigue Life Data for 20mm Nominal Size DBM with 200 pen Binder, 4.2% Binder Content and 3% Voids	146
6.36	Mix Stiffness and Fatigue Life Data for 20mm Nominal Size DBM with 200 pen Binder, 4.7% Binder Content and 3% Voids	147
6.37	Mix Stiffness and Fatigue Life Data for 20mm Nominal Size DBM with 200 pen Binder, 5.2% Binder Content and 3% Voids	148
6.38	Mix Stiffness and Fatigue Life Data for 20mm Nominal Size DBM with 200 pen Binder, 6.2% Binder Content and 3% Voids	149
6.39	Mix Stiffness and Fatigue Life Data for 40mm Nominal Size DBM with 100 pen Binder, 4.2% Binder Content and 3% Voids	150
6.40	Mix Stiffness and Fatigue Life Data for 40mm Nominal Size DBM with 100 pen Binder, 4.2% Binder Content and 6% Voids.	150
6.41	Mix Stiffness and Fatigue Life Data for 40mm Nominal Size DBM with 100 pen Binder, 4.2% Binder Content and 8% Voids	152
6.42	Mix Stiffness and Fatigue Life Data for 40mm Nominal Size DBM with 100 pen Binder, 4.2% Binder Content and 11% Voids	153
6.43	Fatigue Lives for Oxidized H.R.A. and D.B.M. Wearing Course with 100 and 200 pen D.B.M. Basecourses and 20m Slab Length	155
6.44	Mix Stiffness and Fatigue Life of Debonded Surfacing Material Consisting of 40mm Nominal Size DBM with 100pen. Binder, 3% Void Content and 4.2% Binder Content	156
7.1	Void Content and Binder Pen. of Nearside Lane Contract 3 M4 Motorway([103])	161
7.2	Test Layout for the Derivation of Coefficient of Thermal Contraction of Asphalt Beams	166
7.3	Warping of Slab about its Mid Point	168
7.4	Finite Element Model, Mesh Orientation and Deformed Shape. Simulation of Thermal Contraction and Slab Warping of Pavement Structure	170
7.5	Thermal Gradients through Composite Pavements for Low Winter Temperatures	171

Fig.		Page
7.6	Stress Intensity Factor (k_o) versus Normalised Crack Length for Crack Initiation at the Surface and Crack Propagation downwards Due to Slab Warping and Thermal Contraction	172
7.7	Stress Intensity Factor (k_o) versus Crack Length for Crack Propagation Downwards	172
7.8	Comparison of Stress Intensity Factor Curves for Conditions of Crack Propagation from both the Base and the Surface	173
7.9	Horizontal Strain induced into the Wearing Course at an Initiated Crack for given Pavement Temperature Gradients	174
7.10	Tensile Creep Test Results from M4 Motorway (Berkshire) (Sheet 1)	176
7.11	Verification of Yield Strain Concept at Low Temperatures	177
7.12	Horizontal Crack Width for a Crack Fully Developed through the Surfacing and Vertical Warping Displacements at the Surface versus the Coefficient of Thermal Contraction of Asphalt	179
7.13	Tensile Creep Test Results from M4 Motorway (Berkshire) (Sheet 2)	181
7.14	Tensile Creep Test Results from A38 (Litchfield By-Pass)	182
7.15	Tensile Creep Test Results from Redhouse Road (Northampton)	183
7.16	Tensile Creep Test Results from M3 (Hampshire)	184
8.1	Modes of Crack Opening caused by Traffic	190
8.2	Trace of the Vertical Movement at a Joint caused by a Passing Vehicle	191
8.3	Dimensions and Loading on Finite Element Model F.E.3 Simulating Traffic Loading On Cracked Pavement Section	193
8.4	Example of Deflected Shape of Crack Pavement Section (Crack Length in Surfacing = 80mm)	193
8.5	Stress Intensity Factors for Thermal Tensile Fatigue and Traffic Loading versus Normalised Crack Length through Surfacing Layers	194
8.6	Deflection of Roadbase/Surfacing Interface at Crack Centre-line due to Load Case 1, from Finite Element Model F.E.3 Output	196
8.7	Differential Deflection of Roadbase/Surfacing Interface at Crack Centre-line due to Load Case 2 from Finite Element Model F.E.3 Output	196

Fig.		Page
8.8	Test Rig Configuration for Simulative Traffic Loading	198
8.9	Vertical Displacement Measurement Gauges	199
8.10	Lean Concrete Roadbase Compressive Strength versus Transverse Reflection Cracks per 200m Unit From Reflection Cracking Working Group (T.R.R.L)[2] Data for given Site Survey Conditions	202
8.11	Relative Crack Frequency versus the number of Cracks per 200m Unit for given Traffic Loadings. Data from Reflection Cracking Working Group (T.R.R.L)[2]	203
9.1	Dimensional Layout of Geogrids	206
9.2	Geogrid Strain at Failure versus Loading Rate in Direct Tension at 25°C for Materials (1) and (2)	208
9.3	Geogrid Maximum Stress versus Loading Rate in Direct Tension at 25°C for Materials (1) and (2)	208
9.4	Cyclic Tensile Testing of Geogrids at 25°C	211
9.5	Crack Length versus Fatigue Cycles for Reinforced and Unreinforced D.B.M. Samples	211
10.1	Results of Creep tests on a D.B.M. Mix incorporating both a Conventional Binder and a Polymer Modified Binder	216

LIST OF TABLES

Table		Page
2.1	Material and Grading Limits for Cement Stabilized Road Materials[4].	6
2.2	Strength Requirements for Cement Stabilized Roadbase Materials[4]	7
2.3	Recommended Bituminous Surfacings for Newly Constructed Flexible Pavements[7]	10
3.1	Construction Thickness for Flexible, Semi-Flexible and Rigid Pavements[7]	26
6.1	Test Mix Details	89
6.2	Daily Cyclic Crack Openings in the Roadbase, corrected for Sub-Base Friction Restraint Effects	102
6.3	Monthly Mean and Equivalent Values for the Daily Temperature Range in the Surfacing for the Determination of Bitumen Stiffness[80]	104
6.4	Monthly Mean and Equivalent Values for Daily Temperatures at the Top of the Roadbase for Calculation of Daily Crack Opening Movements[80]	104
6.5	The Influence of Aggregate Type on the Coefficient of Thermal Expansion of Concrete[91]	108
6.6	The Influence of Aggregate/Cement Content on the Coefficient of Thermal Expansion[92]	108
6.7	The Influence of Curing Condition of the Coefficient of Thermal Expansion[93]	109
6.8	Calculated Crack Spacings for Gravel Aggregate Lean Concrete Roadbase on Clinker Sub-base as a Function of Temperature Fall[94]	111
6.9	Results from Tests Investigating the Influence of Bitumen Content on the Cycles to Failure and Fatigue Constants.	131
6.10	Results from Tests Investigating the Influence of Void Content on the Cycles to Failure and Fatigue Constants	132
6.11	Results from Tests Investigating the Influence of Bitumen Grade on the Cycles to Failure and Fatigue Constants	133
6.12	Results from Tests Investigating the Influence of Aggregate Size on the Cycles to Failure and Fatigue Constants	134
6.13	Results from Tests Investigating the Influence of Material Type on the Cycles to Failure and Fatigue Constants	135

Table		Page
6.14	Limits to Mix Input Variables for Program R.F.T.100	139
7.1	Location, Pavement Construction Depths and Crack Spacings Details for Cores taken from the M4	163
7.2	Wearing Course - Mix Stiffness Data from Cores taken from Contracts 3 to 6	162
7.3	Analysis of Binder and Filler Contents and Recovered Binder Softening Points (SP_r)	164
7.4	Coefficients of Thermal Contraction for Various Grade Binders	167
7.5	Range of Stiffness and Thermal Coefficient Values defined for Individual Pavement Layers as Input Parameters for Finite Element Analysis of Crack Mechanism	169
7.6	Crack Spacing and Mix Details of the Three Locations Cored on the M4 Motorway, 88/8, 75/9 and 89/3	186
7.7	Yield Strain Values of Wearing Course Material from the Four Test Sites:- M4 (Berkshire), A38 (Litchfield By-Pass), M3 (Hampshire), Redhouse Road (Northampton)	186
8.1	Survey Sites and Traffic Data[2]	201

LIST OF PLATES

Plate		Page
1	Reflection Cracking on M4 Motorway and A30 Trunk Road	33
2	Tensile Fatigue Test Rig (1)	74
3	Tensile Fatigue Test Rig (2)	77
4	Crack Propagation Gauges	79
5	Portal Frame Gauges	80
6	Tensile Creep Test	115
7	Core on Cracked Section of the Redhouse Road (Northampton)	188
8	Traffic Loading Simulation Test	197
9	Tensile Testing of Geogrids	209
10	Geogrid as a Stress Reliever	212

1.0 INTRODUCTION

Design, specification and construction techniques have a direct influence on pavement performance. Deterioration of the pavement structure will inevitably occur. It may manifest itself as structural deformation or cracking, which would require major maintenance or as a surface condition such as loss of skid resistance. However, structural deterioration of the pavement can be minimised through adequate design. The current design guide for new road construction in the U.K.[1] permits the use of bituminous, wet mix granular and cement bound roadbase materials under the classification of 'flexible' pavements. Pavements incorporating the latter roadbase type and surfaced with a bituminous material are referred to as 'composite' pavements throughout this thesis.

The extent of road construction incorporating cement bound roadbases has fluctuated since its original introduction prior to the Second World War. During the 1960's and early 1970's, contractors elected, on initial cost grounds, to construct a large proportion of new trunk roads and motorway schemes in the U.K. using this type of roadbase rather than a permissible alternative. Since then its widespread use has declined due to a less favourable economic bias. There has also been concern that the incidence of reflection cracking may adversely affect performance. This form of cracking, which is the subject of the thesis, normally occurs as transverse cracks across the carriageway.

Field investigations[2] have shown that the cement bound roadbase cracks during the curing period forming transverse cracks usually at fairly regular spacing along the pavement. Reflection cracks are fractures in the bituminous surfacing above cracks in the roadbase, which are caused by movements within the road structure. The consequences of this effect therefore require consideration, prior to new pavement construction and overlay maintenance programmes.

The reaction of local authority engineers to the phenomenon of reflection cracking has been varied. It is described by some as a minor maintenance problem of little structural significance while regarded by others as a serious form of pavement deterioration. A working group established by the Transport and Road Research

Laboratory in 1984 [2] provided data on 1000km of roads constructed with cement bound roadbases completed between 1960 and 1975. It was concluded that less than half of the 200m long sub-units surveyed exhibited transverse cracking and the roadbases were generally performing well.

Nevertheless, reflection cracks can be the source of early deterioration[3], accelerating the need for maintenance and reducing the service life of the pavement. Deterioration in the form of ravelling and spalling of the surface occurs adjacent to these cracks which impairs the riding quality of the pavement. Furthermore, intrusion of water into the crack opening results in a loss of bond between the pavement layers and a decrease in subgrade support.

Many remedies have been proposed and tried but as yet no proven method to eliminate reflection cracking has been developed. Current methods of overlay design[3] are based on deflection measurements and concede the possibility of reflection cracking by specifying a minimum thickness of overlay with which to retard reflection cracks. Similarly, the latest review of the design guide for new construction[1] also specifies an increased thickness of bituminous surfacing to inhibit reflection cracking.

An extensive research effort, predominantly in the United States, has failed to formulate a model to predict the rate of crack propagation through the full depth of bituminous surfacing. The mechanisms causing reflection cracking and the factors involved have to be identified before effective measures to prevent reflection cracking can be devised. Three possible crack mechanisms have been studied. The first mechanism, 'Tensile Fatigue', assumes that cracks propagate vertically upwards through the surfacing as a result of strains developed from daily and annual thermal fluctuations within the roadbase. The second mechanism, 'Tensile Yield', is also thermally induced and is associated with cold weather conditions which cause warping and contraction within the surfacing layer. If the ultimate yield strain of the surfacing material is exceeded reflection cracks will initiate at the surface and propagate downwards. The third mechanism assumes that cracks are caused by shear stresses induced by wheel loads travelling over the cracked roadbase.

The thesis describes an investigation into these three mechanisms of reflection cracking. Analytical models have been studied and laboratory tests have been conducted to obtain the required input data for these models. The aim of the research has been to identify the important material and structural factors that influence reflection cracking with the view to designing roads or maintenance treatments that resist this form of cracking. The research approach adopted is shown as a flow diagram in fig. 1.1.

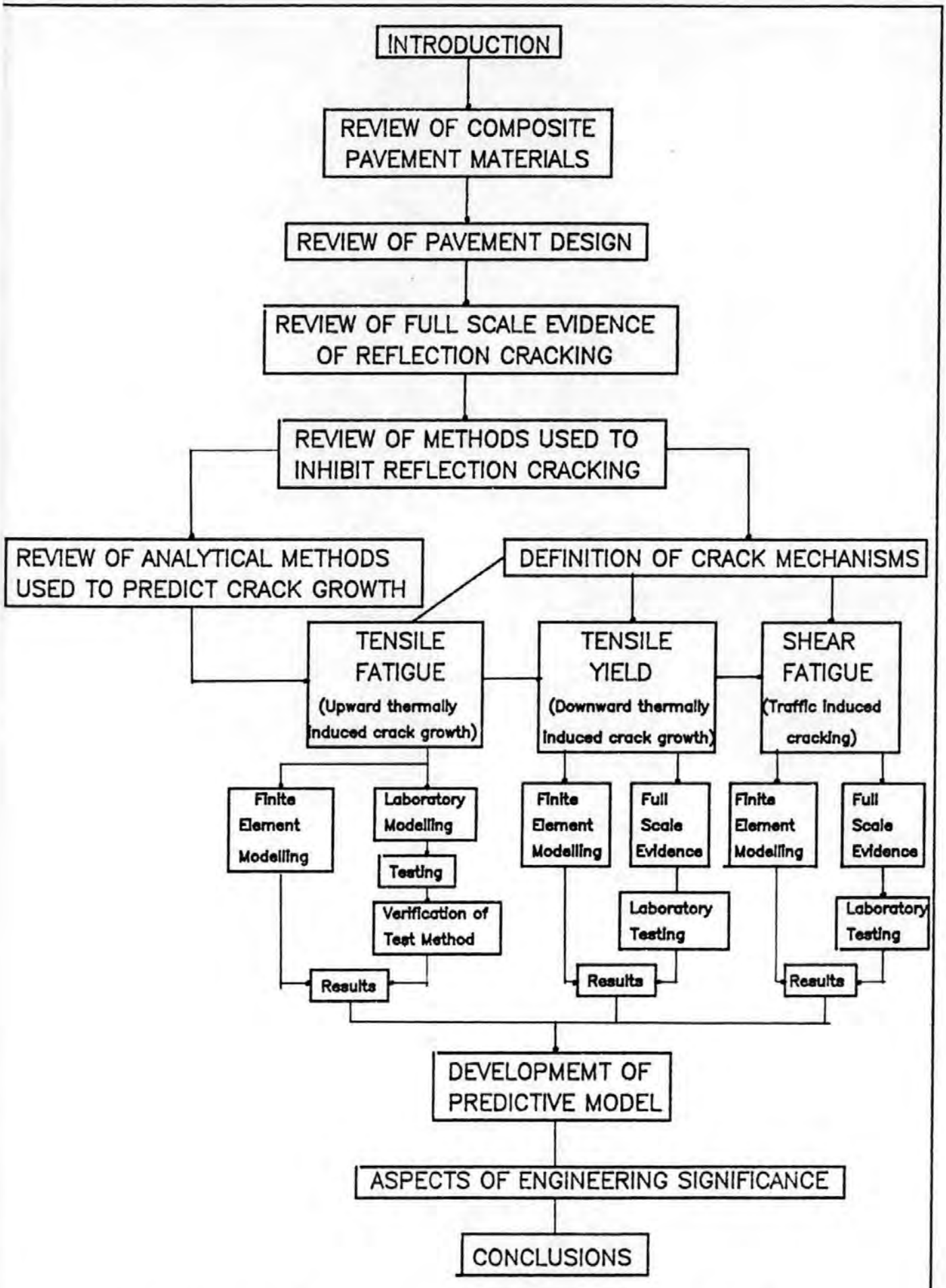

FIG.1.1 FLOW CHART DEPICTING STRUCTURE OF THESIS

2.0 COMPOSITE PAVEMENT MATERIALS

2.1 CEMENT STABILISED ROADBASES

In the United Kingdom, pavements are classified for design purpose as either rigid (concrete) or flexible. The categories of flexible roads reflect the type of roadbase used; bituminous, granular and cemented. The Specification for Highway Works, 1986[105] makes separate provision for four classes of cement stabilised material given as CBM1, CBM2, CBM3, and CBM4. This specification has been only recently implemented and discussion on the provisions contained within the 1976 version are more relevant to the prediction models described within this thesis which are based upon existing structures. CBM1, CBM2 and CBM3 are referred to in the Specification for Road and Bridge Works, 1976 [4], as soil - cement, cement bound granular material and lean concrete. The materials and corresponding grading limits are set out in tables 2.1 and 2.2.

The use of lean concrete was permitted for all pavement loading classifications[7] and therefore has been the most extensively used cement stabilised roadbase material. Since its introduction the specification for lean concrete has been periodically modified in an attempt to reduce crack susceptibility and to produce more economic mixes. An historical perspective in the use of cement stabilised materials in the U.K. is provided by Williams[5]. A short summary is presented here.

Initially, on trial schemes in the 1940's, an aggregate/cement ratio of 8:1 was adopted but this was subsequently modified, to conserve cement, to a ratio of 12:1. A bituminous surfacing thickness of 80mm was specified. As many of the roads with this construction developed cracking even leaner mixes were specified. The premise was that, under the action of restrained thermal contraction, lower strength material would crack more frequently and thus reduce the crack widths, making it less likely that cracks would propagate through the surfacing. In areas of the country which used gravel aggregates an aggregate/cement ratio of 15:1 to 20:1 was generally adopted. However, where crushed rock was available a ratio of 24:1 was favoured as it was considered that the angular shape and rough

TABLE 2.1 MATERIAL AND GRADING LIMITS FOR CEMENT STABILIZED ROAD MATERIAL
(After the Specifications for Road and Bridge Works 1976)

CEMENT STABILISED MATERIAL	MATERIAL FOR PROCESSING	LIMITS OTHER THAN GRADING
Soil-Cement	Soil, Chalk, Pulverised Fuel Ash, Burnt Shale, Washed or Processed Granular Material Crushed Rock or Slag	Sulphate content ⟩ 1% (⟩ 0.25% if cohesive) Liquid limit ⟩ 45% Plastic limit ⟩ 20%
Cement Bound Granular Material	Naturally occurring Gravel-Sand, Washed or Processed Granular Material, Crushed Rock or Slag	Sulphate content ⟩ 1%
Lean Concrete	Naturally occurring Material, to BS 882 Slag Coarse Aggregate, to BS 1047	Flakiness index ⟩ 35

GRADING REQUIREMENTS

B.S. Sieve Size	Soil Cement finer than:	Cement-Bound Granular Material	Lean Concrete (37.5mm) nominal	Lean Concrete (20mm) nominal
(75mm)	–	–	100	–
(50mm)	100	100	–	–
(37.5mm)	95	95 – 100	95 – 100	100
(20mm)	45	45 – 100	45 – 80	80 – 100
(10mm)	35	35 – 100	–	–
3/16in.(5mm)	25	25 – 100	30 – 40	35 – 45
No.25(600μ)	8	8 – 65	8 – 30	10 – 35
No.52(300μ)	5	5 – 40	–	–
No.100(150μ)	–	–	0 – 6	0 – 6
No.200(75μ)	0	0 – 10	–	–

TABLE 2.2 STRENGTH REQUIREMENTS FOR CEMENT STABILIZED ROADBASE MATERIAL
(After the Specification for Road and Bridge Works 1976)

	STRENGTH REQUIREMENTS	
Soil Cement (Clause 805)	1.7 day crushing strength, average of 5 specimens	$< 2.8 MN/m^2$ on cylinders $< 3.5 MN/m^2$ on cubes
	Specimens compacted to field density 2.5 successive batches of 5 specimens Root mean square value of coefficient of variation $\geq 40\%$	
Cement-Bound Granular	1. As for soil-cement, but only on cubes 2. As for soil-cement, but rms value $\geq 25\%$	
Lean Concrete	1. 28-day cube strength, average of 3 cubes ≥ 1 in any consecutive 5 averages to be $< 10 MN/m^2$ or $> 20 MN/m^2$ Cubes compacted to refusal: field density specified separately. 2. If(a) Overall average of 5 x 3 values $< 11 MN/m^2$ or $20.5 MN/m^2$ (b) Average range exceeds 50% of overall average strength then " ..... different materials or mix proportions ...." 3. 7-day cube strength, average of 3 cubes, $< 7 MN/m^2$ or $> 14 MN/m^2$ If > 1 in any consecutive 5 averages $< 7 MN/m^2$ or $> 14 MN/m^2$ "the cement content shall be increased ..."	

texture of the rock particles would ensure favourable load transfer across cracks.

The continued occurrence of reflection cracking prompted TRRL investigations into very lean mixes (35:1) in an experimental road in Whitchurch, Glamorgan in 1959. It was observed that the progressive reduction in cement content overcame to some extent the problem of cracking but only at the cost of all the potential benefits associated with the use of a cemented material.

With the advent of motorway construction during the early 1960's stronger mixes were specified on the grounds that roadbase failures would be difficult to rectify but in 1963, once again, the use of lower aggregate/cement ratios of 15:1 to 20:1 were specified for all types of aggregate, together with a proportionally greater thickness of bituminous surfacing material. This was expected to reduce thermal changes in the cement bound layer and inhibit crack development to beyond the design life.

Until 1963 the specification for lean concrete was solely in terms of its aggregate/cement ratio and aggregate grading but, on revision, a set of minimum strength criteria and field density requirements was introduced which jointly defined the end product. However, when used with naturally cementing aggregates such as limestone this specification produced high strength lean concrete mixes. Subsequent stipulation in the 1976 edition of the specification[4] limited the 28 day cube strength to between 10 and 20N/mm^2.

It is questionable[5] whether the reliance on an achievement of a selected cube strength will deal with the reflection cracking problem. Furthermore, the specification of higher strength mixes may induce roadbase failures.

The 1976 Specification for Road and Bridge Works[4] also modified the aggregate gradings from those given in previous codes. In the earlier major road schemes the practice varied regarding the quality of the aggregate, with widespread use of as-raised material. Under the revised gradings this material is restricted to the category of cement bound granular material.

To gain a uniformity in the measurement of site strength parameters the 1976 specification[4] also required that test cubes be compacted to refusal density. This involved using a vibrating hammer to compact the material in a mould to its maximum density in accordance with BS1881[6]. Previously, cube strength results were prone to considerable variation as the compaction differed according to the diligence of the individual involved in the production of the cubes.

As field density is a critical factor in determining the subsequent performance of cement stabilized materials an average density from three determinations is stipulated, which may not fall to below 95% of the theoretical density with zero air voids.

2.2 BITUMINOUS SURFACINGS

2.2.1 Material Specifications

In the design of new flexible roads in the U.K., the thickness and type of bituminous surfacing material are specified in terms of the cumulative number of standard axles the pavement is required to carry during its design life. Both thickness and type of surfacing are dependent on roadbase type (granular, bituminous or cement bound). The relevant extract from the 1970 design guide[7] is given in table 2.3.

Bituminous material is mineral aggregate mixed with either tar or bitumen, which may be low viscosity cutback bitumen, bitumen emulsion or tar/bitumen mixture.Traditionally in the U.K. bituminous road materials can be classified under three basic mix types which are

a) Hot Rolled Asphalt[8]
b) Dense Bitumen (or Tar) Macadam[9]
c) Open Textured Macadam[9]

However, the mix design of asphalt surfacings rarely recognises the different functions these layers perform when laid over cement stabilized, bituminous or unbound roadbases and the consequent need for different material properties.

TABLE 2.3

Recommended Bituminous Surfacings for Newly Constructed Flexible Pavements (After RN29)

Traffic (cumulative number of standard axles)			
Over 11 millions (1)	2.5-11 millions (2)	0.5-2.5 millions (3)	Less than 0.5 millions (4)
Wearing course (crushed rock or slag coarse aggregate only) Min.thickness 40mm Rolled asphalt to BS 594 (pitch-bitumen binder may be used) (Clause 907)		Wearing course Min.thickness 20mm Rolled asphalt to BS 594 (pitch-bitumen binder be used)(Clause 907) Dense tar surfacing to BTIA Specif.(Clause909) Cold asphalt to BS 1690 (Clause 913)(to be surface-dressed immediately or as soon as possible Dense bitumen macadam to BS 1621 (Clause 908) Open texture bitumen macadam to BS 1621 (Clause 912)	Two-course (a) Wearing course Min thickness 20mm Cold asphalt to BS 169)(Clause 910) Coated macadam to BS 802, BS 1621, BS 1241 or BS 2040 (Clause 913, 912 or 908) (b) Basecourse Coated macadam to BS 802, BS 1621, BS 1241 or BS 2040 (Clause 906 or 905) Single course Rolled asphalt to BS 594 (pitch-bitumen may be used) Dense tar surfacing to BTIA Specification (Clause 909) Medium-textured tarmacadam to BS 802 (Clause 913)(to be surface-dressed immediately or as soon as possible Dense bitumen macadam to BS 1621 (Clause 908) 60mm of single course tarmacadam to BS 802 (Clause 906) or BS 1241 (to be surface-dressed immediately or as soon as poss. 60mm of single course bitumen macadam to BS 1621 (Clause 905) BS 2040
Basecourse Min.thickness 60mm. Rolled asphalt to BS 594 (Clause 902) Dense bitumen macadam or dense tarmac (crushed rock or slag only (Clause 903 or 904)	Basecourse Rolled asphalt to BS 594 (Clause 902) Dense bitumen macadam or dense tarmac (Clause 903 or 904)	Basecourse Rolled asphalt to BS 594 (Clause 902) Dense bitumen macadam or dense tarmacadam (Clause 903 or 904)	

2.2.1.1. Hot Rolled Asphalt

Hot Rolled Asphalt is a hot mix, hot lay, bituminous material adopted for its properties of stability and durability. It is gap graded. The coarse aggregate bulks the mixture and contributes to its stability. The high bitumen and fine aggregate content form a sand/filler mortar which produces the primary influence on the mechanical properties of the mix. Its resistance to deformation is therefore dependent on the use of a bitumen of a suitable grade. The fine aggregates form the major proportion of the mortar while the filler stiffens and strengthens the binder. Its widest use is that of a wearing course material providing a dense impervious mix from the time of laying. The high stiffness associated with this type of mix reduces the stresses transmitted to the roadbase and formation due to traffic loading.

2.2.1.2. Dense Bitumen Macadam

Dense Bitumen Macadam is also a hot mix, hot lay, bituminous material but of continuous grading. The induced stresses exerted on Dense Bitumen Macadams are dissipated through its mechanism of stone contact which therefore requires aggregates of high crushing strength which combines with its continuous grading to produce an interlocking matrix. The binder acts as a lubricant between the aggregate particles, particularly during compaction, and also, as a waterproofing and bonding agent. A softer binder grade than rolled asphalt can therefore be specified because it is not contributing in the same way to the overall strength. Although Dense Bitumen Macadam may be used for wearing courses it is generally used for basecourses in the U.K. because it is not as impervious or dense as a rolled asphalt. Its lower bitumen content gives it an economic advantage but it is more difficult to compact.

2.2.1.3 Open Textured Macadam

This uniformly graded material also relies upon granular interlock for stability but has a significantly lower fines and bitumen content to that of dense macadams. The coarse aggregates are therefore not protected by a filler-binder matrix and consequently must have high resistance to abrasion and crushing where used as a wearing course on lightly trafficked roads. Although permeable and susceptible to the detrimental effects of air and water it has the ability to drain surface water through the voids in the material and is economical.

2.2.2 Bituminous Material Properties

A wide range of mechanical characteristics must be displayed by bituminous surfacing materials if they are to resist deterioration caused by traffic and the environment. It must be sufficiently stiff to reduce the stresses induced by traffic in the lower layers of the pavement structure to an acceptable level and yet be capable of resisting fatigue cracking. A high level of compaction is required to prevent air and water penetration and resist permanent deformation due to traffic, while proving a workable mix at the time of laying.

The selection of the most appropriate characteristics for any given circumstance requires that the mechanical properties of the mix be optimised with respect to the range of loading and environmental conditions anticipated. A compromise has to be sought as modification of these properties to limit any individual distress mechanism, such as reflection cracking, may be detrimental to the overall pavement surfacing requirements.

2.2.2.1 Stiffness Characteristics

Bituminous mixes display elastic, visco-elastic and viscous behaviour. Their behaviour depends on the mix temperature (T) and the time of loading (t). The stiffness (S) is a measure of the material's response to an applied stress and is defined as:

$$S(t,T) = \frac{\text{Stress}}{\text{Total Strain}} \qquad \text{- Eq.(2.1)}$$

Bituminous materials are viscous at high temperatures or long loading times and elastic at low temperatures or short loading times exhibiting visco-elastic behaviour under intermediate conditions.

The elastic mix stiffness (S_{me}) can be derived from numerical procedures but the prediction of the visco-elastic stiffness (S_{mv}) is more complex and requires laboratory testing appropriate to the loading conditions. S_{me} is a function of volumetric composition of the mix and the bitumen stiffness (S_b) while S_{mv} is also a function of aggregate type, grading shape and texture of the aggregate, confining conditions within the pavement and method and state of compaction.

2.2.2.2 Bitumen Stiffness

The viscous properties of a mix are governed by the rheology of the binder which is measured in the U.K. in terms of its penetration value at 25°C[10] and its ring and ball softening point[11]. These values can be used to define the stiffness of the binder for any given loading time and temperature using Van der Poels nomograph[13] as shown in fig. 2.1. The estimation of stiffness for all commercial penetration grade bitumens under a range of service conditions is possible to within a factor of two through the use of this nomograph. The input data required is:

1) $T_{800} - T$ where T_{800} is the ring and ball softening point of the bitumen (SP)°C (ASTM)[110] which in the nomograph is designated as the temperature at which the bitumen has a penetration of 800, and T is the pavement temperature in °C.
2) loading time (t), in seconds, which under a sinusoidal stress path is given by:

$$\frac{1}{\text{freq (Hz)} \times 2 \times \pi} \quad \text{or as} \quad \frac{1}{\text{Traffic Speed (Km/hr)}} \qquad \text{- Eq.(2.2)}$$

Alternatively, traffic loading time (t) for use with the nomograph may be determined from equation 2.3 which requires an estimate of pavement thickness (H)mm[27]:

$$\log(t) = 5 \times 10^{-4}H - 0.2 - 0.94\log V \qquad \text{- Eq.(2.3)}$$

where V = vehicle speed in Km/hr

3) Penetration Index (PI) which is a measure of the temperature susceptibility of the bitumen and is defined[27] by the expression:

$$PI = \frac{20(1 - 25A)}{1 + 50A} \qquad \text{- Eq.(2.4)}$$

$$\text{where} \quad A = \frac{\log(800) - \log(\text{penetration at } 25^{\circ}C)}{(SP)^{\circ}C\ (ASTM) - 25^{\circ}C}$$

Using this system the PI values of the bitumen vary between -2.5 and +8. Bitumens with low and negative PI values soften more readily than those with high values

Nomograms such as the one published by the Refined Bitumen Association[104] can be used to determine the PI of a bitumen when its softening point and penetration values are known.

Oxidization of the bitumen may occur during the mixing and throughout

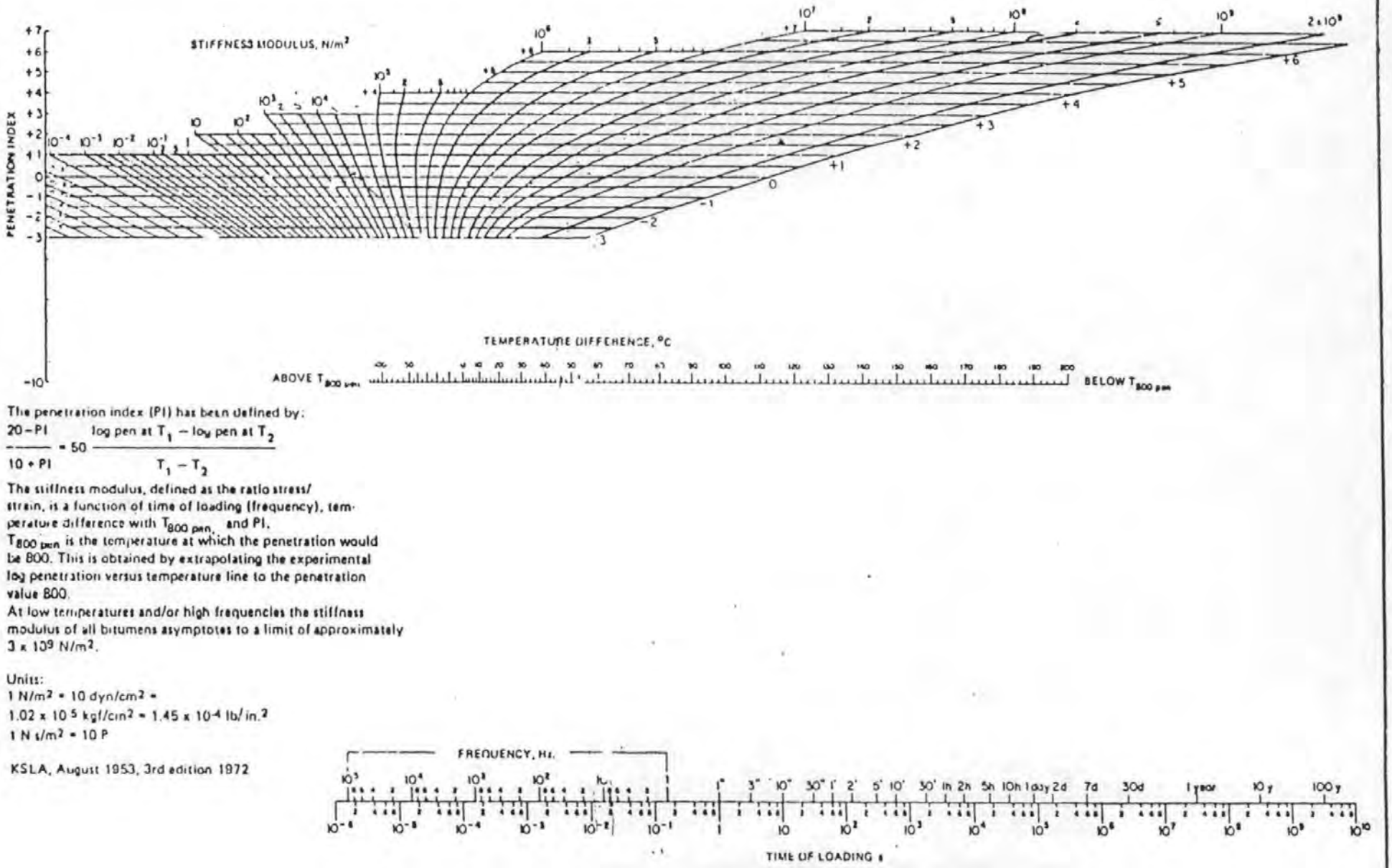

The penetration index (PI) has been defined by:

$$\frac{20 - PI}{10 + PI} = 50\,\frac{\log \text{pen at } T_1 - \log \text{pen at } T_2}{T_1 - T_2}$$

The stiffness modulus, defined as the ratio stress/strain, is a function of time of loading (frequency), temperature difference with $T_{800\ pen}$ and PI.
$T_{800\ pen}$ is the temperature at which the penetration would be 800. This is obtained by extrapolating the experimental log penetration versus temperature line to the penetration value 800.
At low temperatures and/or high frequencies the stiffness modulus of all bitumens asymptotes to a limit of approximately 3×10^9 N/m².

Units:
1 N/m² = 10 dyn/cm² =
1.02×10^{-5} kgf/cm² = 1.45×10^{-4} lb/in.²
1 N s/m² = 10 P

KSLA, August 1953, 3rd edition 1972

FIG.2.1 NOMOGRAPH FOR DETERMINING THE STIFFNESS OF BITUMENS (AFTER VAN DER POEL)[13]

the service life of the pavement. Therefore, the bitumen properties must refer to the condition in the road and take account of any hardening that has occured. This implies that the recovered binder parameters must be used. The relationships between Softening Point (SP), Penetration (P) and Penetration Index (PI) are given by equations 2.5 to 2.7[27]:

$$P_r = 0.65\ P_i \qquad \text{- Eqn.(2.5)}$$

$$SP_r = 98.4 - 26.4 \log P_r \qquad \text{- Eqn.(2.6)}$$

$$PI_r = \frac{1951 - 500 \log P_r - 20\ SP_r}{50 \log P_r - SP_r - 120.1} \qquad \text{- Eqn.(2.7)}$$

where suffixes 'i' and 'r' refer to the initial and recovered properties

For typical U.K. binders the bitumen stiffness within the pavement bituminous layers ranges from 1 x 10^2 to 1 x $10^6 N/m^2$ for the combination of daily and annual thermal cycles experienced in the U.K. Higher stiffnesses may, however , occur if excessive hardening has taken place as discussed in section 2.2.3.

The bitumen stiffness developed by traffic loading, because of the higher loading frequency is considerably greater and ranges from 1 x 10^7 to 5 x $10^9 N/m^2$.

As an alternative to using the nomograph, the following equation may be used to estimate, S_b, the bitumen stiffness[12]:

$$S_b = 1.157 \times 10^{-7} \times t^{-0.368} \times 2.718^{-PI_r} \times (SP_r - T)^5\ MN/m^2 \qquad \text{-Eqn.(2.8)}$$

The ranges of applicability of this equation are as follows:

PI_r = -1 to 1 $(SP_r - T)$ = 20 to 60°C and t = 0.01 to 0.1 sec.

2.2.2.3 Mix Stiffness

To enable the stresses and the strains induced into the bituminous layers of a pavement by the combination of traffic and environmental effects to be analysed, the respective values of mix stiffness must be defined. The value of stiffness is a function of material properties, loading time and temperature.

At bitumen stiffnesses of greater than 5 x $10^6 N/m^2$ bituminous mixes are predominantly elastic in character and their stiffness is primarily dependent upon the stiffness of the bitumen incorporated within the mix and the volumetric composition of the mix.

Extensive testing[14] of mixes has shown that the ratio between mix stiffness (S_m) and bitumen stiffness (S_b) depends on the aggregate fraction by volume (C_v) and is given by:

$$\frac{S_m}{S_b} = \left[1 + \frac{2.5}{n}\,\frac{C_v}{1-C_v}\right]^n \qquad \text{-Eqn.(2.9)}$$

where $n = 0.83\left[\frac{4 \times 10^4}{S_b}\right]$ and $C_v = \frac{\text{Volume of compacted Aggregate}}{\text{Volume of Aggregate and Bitumen}}$

These equations provide an estimate of the stiffness to an accuracy of ± 2. Stiffness values developed from them apply to well compacted mixes of less than 3% air voids. Van Draat and Sommer[15] have proposed a correction to C_v for mixes with air voids greater than 3% given in equation 2.9 as C_v^1

$$C_v^1 = \frac{C_v}{1 + (V_v - 0.03)} \qquad \text{- Eqn.(2.10)}$$

where V_v = fraction of air voids

Under low stiffness conditions the material approaches a viscous state and behaviour becomes more complex. The stiffness is now dependent upon additional factors such as aggregate and filler type and it is necessary to measure the actual material response under actual loading conditions. Various tests have been proposed to measure stiffness as a function of time. These include:-

(1) Creep under constant stress
(2) Stress relaxation
(3) Constant rate of strain
(4) Dynamic tests under sinusoidal stress or strain
(5) Dynamic tests under repeated step function pulse loading

The test selected is dependent upon pavement loading condition, controlling stress or strain characteristics, and the accuracy of results required. Hence, simulation of the dynamic response generated by traffic can be provided by measurement of resilient behaviour with short time intervals between sucessive pulses to allow for elastic recovery. However the permanent strain which accumulates under repeated loading, is essentially a creep phenomenon and therefore a constant stress creep test is more appropriate.

2.2.3 The Effect of Service Conditions on the Susceptibility of Bituminous mixes to Cracking

A range of complex changes take place within the surfacing under the influence of both weathering and traffic during the service life of the pavement. Discussion in this section will be limited to the changes in mix properties which affect crack propagation through the the surfacing of composite pavements. A predictive assessment of these modifications is required as an input at the design stage in any method for determining reflection crack growth.

2.2.3.1 Bitumen Hardening

An increase in bitumen stiffness occurs through oxidisation and evaporation of the volatile components of the binder. The rate of oxidisation is dependent upon the type of bitumen used, the degree of exposure of the bitumen to air and light and the pavement temperature regime.

Significant hardening through evaporation takes place during mixing and laying; maximum temperatures for both operations are specified to limit this effect[8,9]. Brown[17] has shown that the penetration value of bitumen reduces to 65% of its original value during the mixing and laying of bituminous surfacings.

For oxidixation of bituminous films to occur, air must be present and the process is accelerated if the films are also exposed to light. The extent of hardening will therefore be related to the void content of the mix. Data from the Colnbrook By-Pass Experiment in 1960 given in fig.2.2[18]shows that for a dense rolled asphalt with 40/50 pen bitumen little change occured either in void content or the properties of the the bitumen recovered after 8 years service. With 60/70 pen bitumen used for asphaltic concrete there were indications of some densification under traffic reducing the void content of the mix but only limited evidence of bitumen hardening. However, cores taken during this research from 15 year old sections of the M4 in Berkshire showed recovered bitumen penetration values as low as 7. The indication is that considerable hardening of the binder can occur in U.K. mixes under U.K. conditions.

Results from regions with more diverse climatic conditions also show significant hardening of the binder. Tests on a porous mix with

200/300 pen. bitumen used on the Zaca Wigmore Asphalt Test road in California shows a close relationship between hardening and void content; fig. 2.3.

Dickinson[20] investigated the relevance of void content and the use of antioxidants and types of filler on the hardening rates of dense surfacing mixes incoporating various grades of binder. His study covered samples obtained from pavements with up to six years service. The differential compaction of the surfacing layer under the action of traffic produced a range of bitumen exposure conditions corresponding to void contents from 4 to 10 per cent. Dickinsons' conclusions can be summarised thus:

(i) the rate of hardening over the service period was found to be signicantly influenced by the level of exposure,

(ii) trials with the antioxidant Zinc Diethyl Dithiocarbonate indicated that the additive decomposed after two years in service and therefore was ineffective,

(iii) laboratory tests showed the use of lime fillers to be effective in reducing the rate of bitumen hardening.

In a recent investigation into the performance of 60 experimental overlays constructed in different climatic regions in Kenya; Rolt, Smith and Jones[21] concluded that cracking was always associated with age hardening of the bitumen, especially in the top few millimetres of the surfacing. The cracking which began at the surface and propagated downwards was predominantly transverse across the carriageway resembling reflective cracking found on roads with cemented bases. However, sections which did not harden with age either did not crack at all or cracked only over a limited area. Therefore a superior performance can be expected if age hardening can be prevented.

A penetration decay function was derived in the exponential form of:-

$$P(t)' = A + (P_i' - A) \exp(-t/L) \qquad \text{- Eqn. (2.11)}$$

where P(t)' is a ratio of original penetration to a value of penetration at a time (t)

A is the asymptotic value

L is the time constant of decay

P_i' is the initial value of P(t)' at time = 0

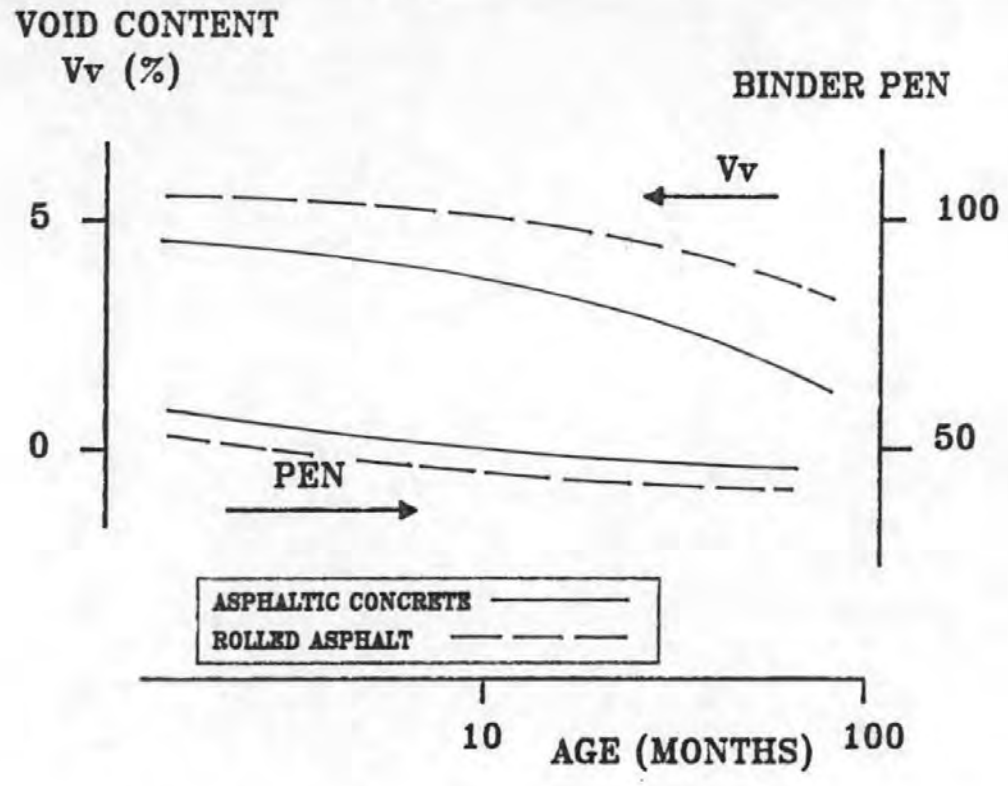

FIG.2.2 AGEING DATA FROM COLNBROOK BY-PASS EXPERIMENT[18]

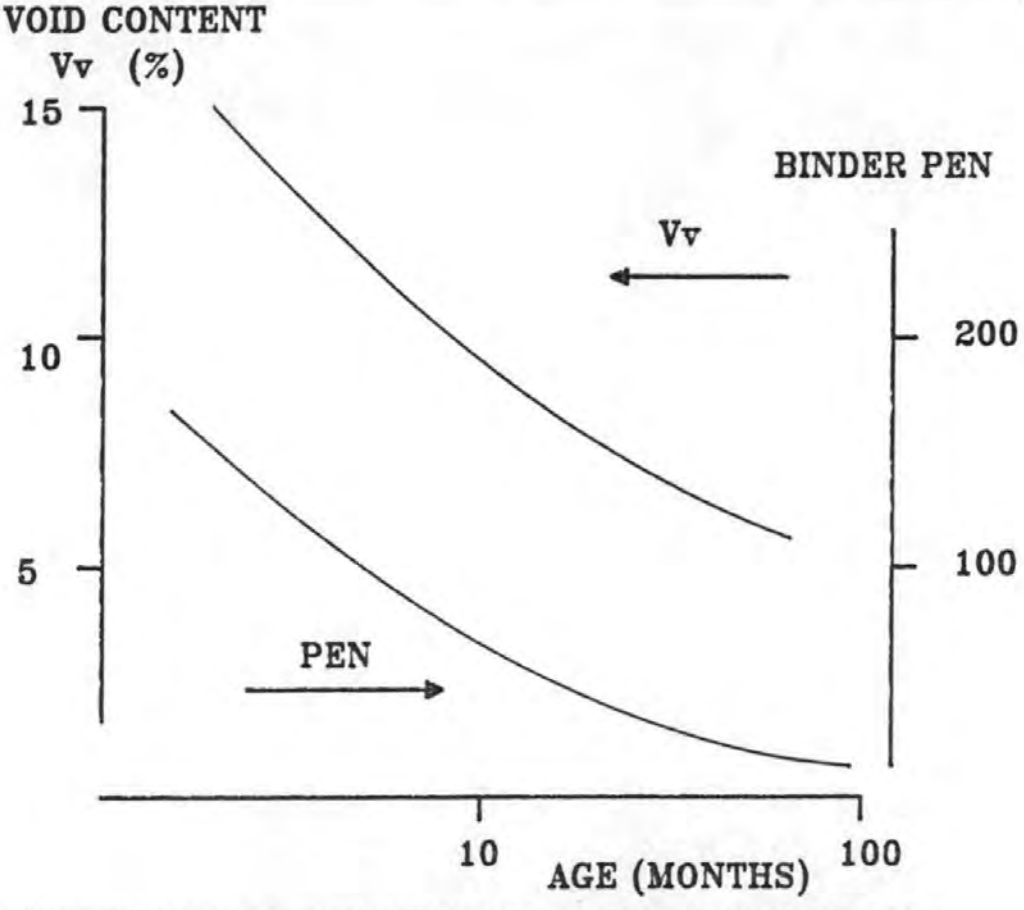

FIG.2.3 THE EFFECT OF VOID CONTENT ON BITUMEN HARDENING RESULTS OF THE ZACA-WIGMORE ASPHALT TEST ROAD[19]

The initial value of P_i' at time zero is the ratio of the binder penetration after mixing but before laying to its penetration value prior to mixing. P(t)' primarily relates to material taken from the top 50-70mm of the overlays but only a slight reduction in the age hardening effects were indicated from material taken from greater depths.

Empirical equations to predict the hardening of bitumen have been derived through regression analysis by Shahin and McCullough[22] from observations from four different areas of the United States on overlaid rigid pavements.

The equations predict the softening point, given as $SP_r(t)$, and the penetration value, given as $P_r(t)$, at a time (t) in months during the service of the pavement where:

$$P_r(t) = 0.4 + 0.716\ P_i - (0.193\ P_i - 9.1)\log_e t \qquad \text{- Eqn.(2.12)}$$

$$SP_r(t) = -\ 30.6 + 1.23\ SP_i + 10.5\ \log_e t \qquad \text{- Eqn.(2.13)}$$

where P_i and SP_i are the original penetration value and the softening point respectively.

The equations are based on both high and low penetration binders and assume an initial change in properties occuring during mixing and laying and, thereafter, followed by a time dependent change.

Large errors may however be expected on application of these equations to the U.K. situation. They were developed for surfacing mixes and temperature conditions relevant to the U.S.A. and do not allow for the variability of void content, mix grading, bitumen content and grade and filler type which have been shown to influence the hardening process.

Recent studies by Lund and Wilson[23] have identified the causes of bitumen oxidisation within a bituminous mix during manufacture and have provided a method by which the potential susceptibility of a particular bitumen to oxidisation may be predicted.

On the basis of Lund and Wilson's work, bitumen oxidisation appears to be as a result of one or more interrelated conditions. These are:-

i) the type of burner fuel used and its combustion during the heating of the aggregates prior to mixing,

ii) the temperature of the mixing operation and

iii) the origin and grade of the asphalt.

The hardening formula developed is based on:-

(i) viscosity measurements of the initial bitumen, A,

(ii) viscosity measurements of the bitumen recovered after mixing and laying, R and

(iii) the resultant value recored from the rolling film oven test[24], B.

It is given in the form:-

$$C = \frac{R - A}{B - A} \% \qquad \text{- Eqn.(2.14)}$$

Bitumen prone to excessive hardening would be denoted by a large positive ratio. Paving projects in Oregon with 'C' values over 50% showed distress linked to excessive hardening. Pavements with values from 30-50% showed minimal problems and pavements with values less than 30% showed signs of rutting, stripping and segregation in the surface associated with too soft a binder.

This formulation has since been adopted as a standard test by certain states in the U.S.A. to define the suitability of a particular bitumen and mixing process.

2.2.3.2 Void Content

The level of compaction of the mix influences the performance of the surfacing in several ways. These include:-

i) the resistance of bituminous material to in-service applied stresses is influenced by its ability to act as an integrated cohesive matrix,

ii) void coalescence can result in a mix being more susceptible to crack propagation,

iii) the mix must be sufficiently dense so as to prevent the ingress of water through the surfacing and into the lower layers of the pavement

iv) poorly compacted mixes are more prone to oxidisation[18,19,20].

Generally achieved void contents range from 7 to 10% for continuously

graded and 4–6% for gap graded mixes but vary with the number of roller passes, temperature, binder content and type and grading of aggregate. Guidance for compaction during construction in the current British Specifications[8,9] for all types of bituminous materials is limited to definition of the type and overall weight of the roller, permitted layer thickness and minimum material temperature.

Typically during construction fewer roller passes are made towards the edges of the pavement and compaction is not uniform across the laid material, resulting in the variability of its fatigue characteristics. This variability significantly influences the resistance of the surfacing material to reflection crack propagation, as demonstrated by the test results given in section 6.

3.0 PAVEMENT DESIGN

3.1 INTRODUCTION

The complexity of the factors involved in the thickness design of highway pavements resulted in the adoption of design methods based on experience. However, considerable advances in the understanding of pavement behaviour has allowed the development of analytical design methods[1,27]. These combine data collected from:

(i) the performance of existing pavements and materials

(ii) the results of research on mathematical modelling of pavement behaviour and

(iii) fatigue and stiffness tests on road materials.

The introduction of these methods allows pavement design to be undertaken in a similar manner to other structural elements in engineering.

3.2 U.K. EMPIRICAL DESIGN GUIDE

Experience from full scale experimental sites situated on lengths of normal in-service highways prior to 1969 provided the basis for the third edition of the design guide (RN29)[7]. The overall thickness requirements recommended by this design guide result from both pavement failure investigations and data extrapolated from those pavements which were performing satisfactorily.

RN29 considers only the number of commercial vehicles and their axle loadings as the structural damage caused by lighter traffic is insignificant. The traffic at the time of construction, and its growth rate, is estimated to enable the average daily flow to be calculated for each year of the pavement design life and summed to provide the cumulative traffic over this period. The average number of axles per commercial vehicle is taken to vary with the road classification. A factor given for each road classification is used to convert the cumulative number of commercial vehicles into an equivalent number of 80kN standard axles.

This approach was adopted due to the non uniform damage caused by axle loadings. AASHO road trials in the United States[28] indicated that the damaging power of any load L could be expressed in terms of an equivalent axle load factor F related to a standard axle, L_S where:

$$F = \left[\frac{L}{L_S} \right]^a \qquad \text{- Eq. (3.1)}$$

The value of 'a' was found to depend upon the thickness of pavement tested but a mean value of 4 has been widely adopted and subsequently verified, with limited variations, by recent analysis[30] and experimental results[29].

The roadbase and surfacing thicknesses are related to the anticipated design traffic loading defined in terms of standard axles while the sub-base thickness is related both to anticipated traffic loading and to sub-grade strength defined by a C.B.R. value. The recommendations permit the design of all pavement classifications for any combination of sub-grade and traffic conditions.

The thickness recommendations for the surfacing and soil cement, cement bound granular and lean concrete roadbase materials is illustrated in fig.3.1.

Suitable roadbase materials are rolled asphalt, dense coated macadam, lean concrete, soil cement, cement bound granular material, wet mix and dry bound macadam. The design curves presented provide thickness requirements up to 100 m.s.a. for all roadbase types except soil cement and cement bound granular material which are limited to 1.5 m.s.a. and 5 m.s.a. respectively. For traffic over 11 m.s.a. a composite roadbase may be formed which incorporates lean concrete, wet mix or dry bound macadam roadbase material. The composite roadbase shall comprise a minimum 100mm thickness of the roadbase material overlaid by an additional course of bituminous roadbase material to provide the total thickness required.

Various combinations of bituminous surfacing materials are included in the recommendations. Proven performance, economics and availability have resulted in the extensive use of Dense Bitumen Macadams[9] as a base course material overlaid by a 40mm wearing course of Hot Rolled Asphalt[8][31]. A comparison of construction thicknesses is given in Table 3.1 for the given roadbase types with a cumulative traffic flow of 10 m.s.a. during their design life.

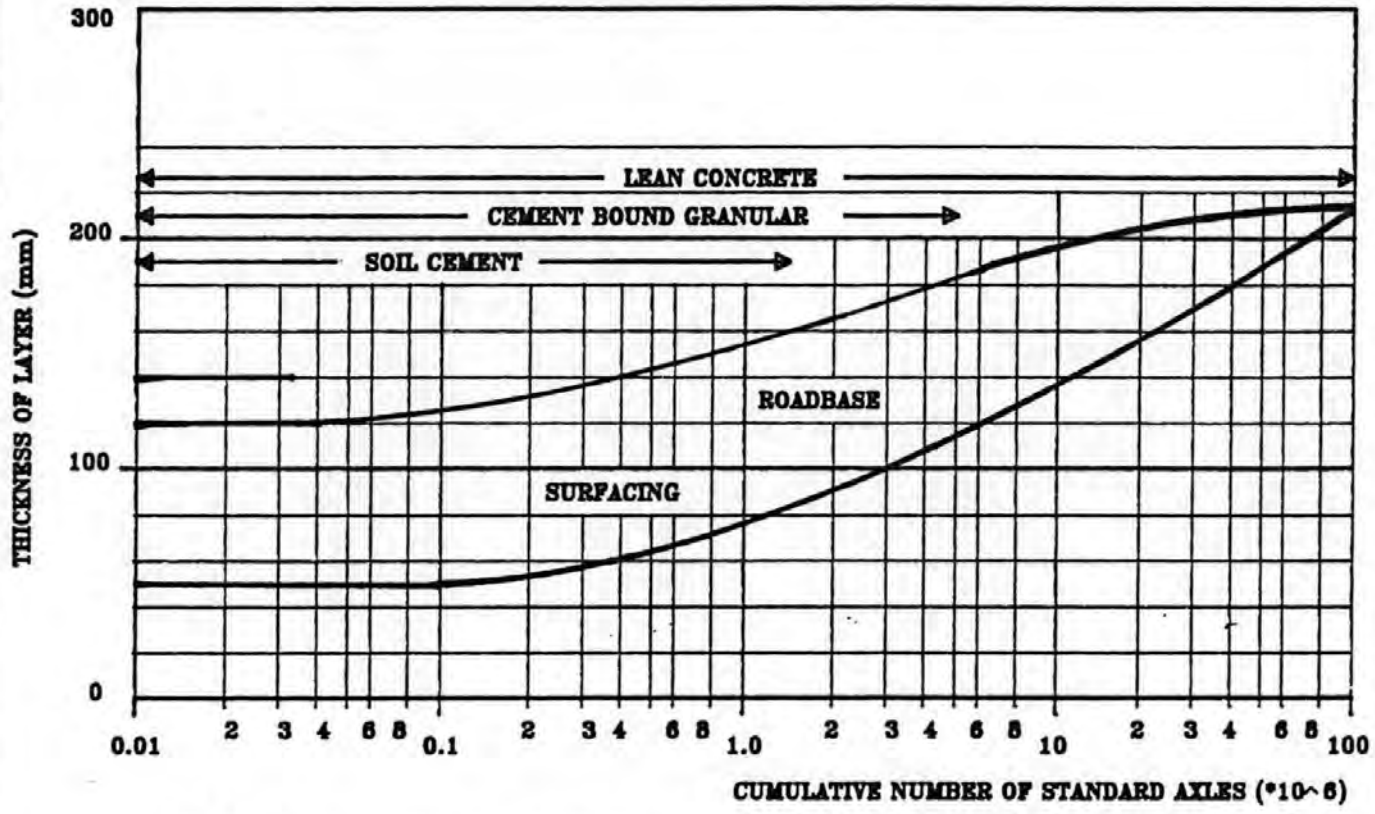

FIG.3.1 LEAN CONCRETE, SOIL CEMENT, AND CEMENT BOUND GRANULAR ROADBASES
MINIMUM THICKNESS OF SURFACING AND ROADBASE SPECIFIED BY R.N.29 (7)

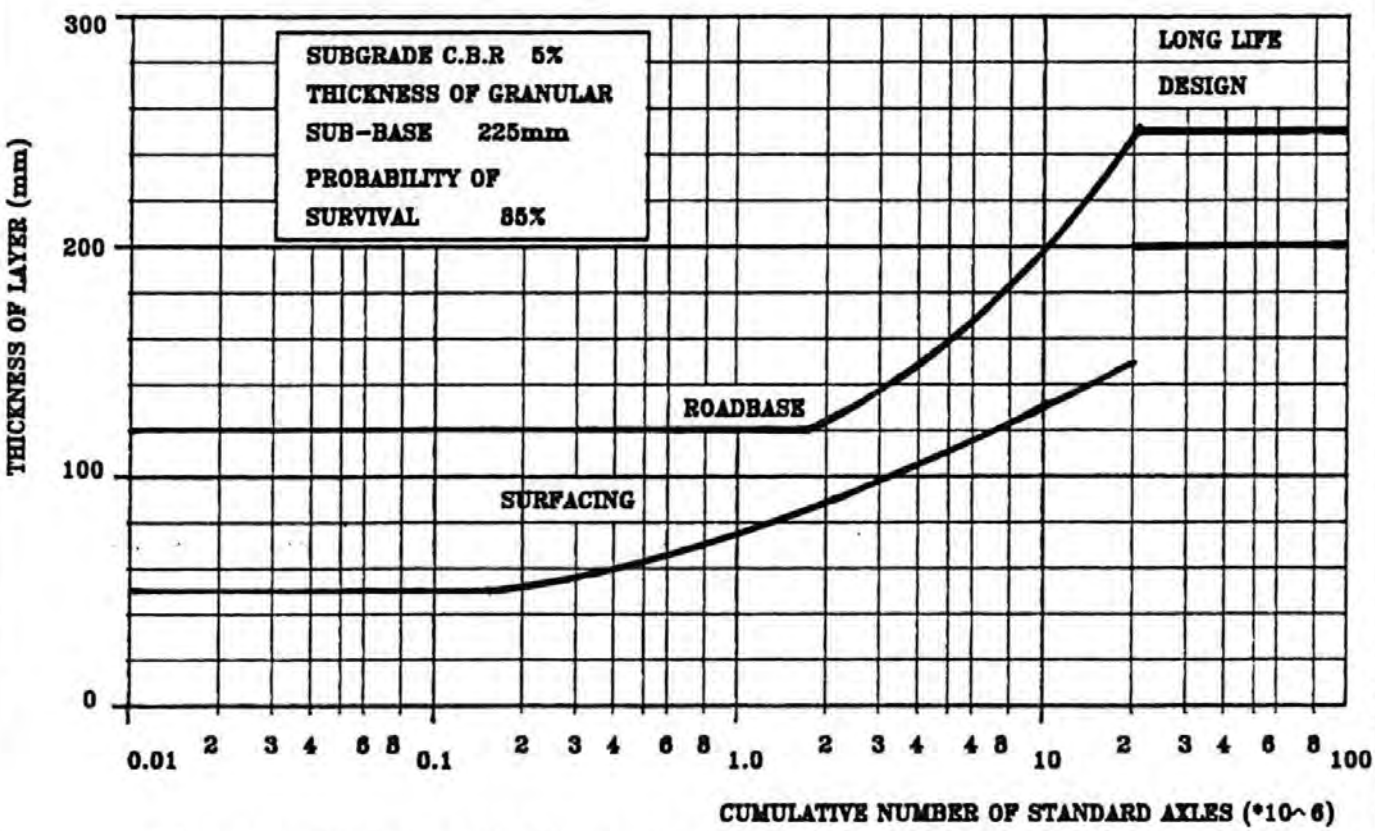

FIG.3.2 DESIGN CURVES FOR ROADS WITH LEAN CONCRETE ROADBASE
SPECIFIED BY LR.1132 (1)

TABLE 3.1 CONSTRUCTION THICKNESS FOR FLEXIBLE SEMI-FLEXIBLE AND RIGID PAVEMENTS (C.B.R.=5%) (10m.s.a.) [7]

ROADBASE TYPE	CONSTRUCTION DEPTHS (mm)
WET-MIX AND DRY BOUND GRANULAR MATERIAL	120mm SURFACING 220mm ROADBASE 260mm SUB-BASE
ROLLED ASPHALT ROADBASE MATERIAL	100mm SURFACING 120mm ROADBASE 260mm SUB-BASE
DENSE MACADAM ROADBASE MATERIAL	100mm SURFACING 140mm ROADBASE 260mm SUB-BASE
LEAN CONCRETE	120mm SURFACING 200mm ROADBASE 260mm SUB-BASE
STRUCTURAL CONCRETE	220mm SLAB 80mm SUB-BASE

Periodic reviews of the design guide have been required since its publication in 1970 to enable the inclusion of increased data from experimental road sections and change in traffic loading characteristics.

Technical Memorandum H6/78 issued in 1978[32] reviewed TRRL analysis of the increase in loading of axles of commercial vehicles and the number of axles/commercial vehicles. It also introduced more general use of capping layers on sub-grades with CBR values less than 5% to provide an improved foundation. The work of Currer and O'Connor[33] has been incorporated within the Memorandum to revise the damage factors for commercial vehicles on four categories of road. For the uppermost traffic category (above 2000 cvpd) the damage factor has been increased from 1.08 to 2.75 over the period 1969 to 1978. Tables are presented of the factors required for the design of a new road, for the prediction of the remaining life of an existing road and for the designing of strengthening measures for such a road. The Memorandum also rationalises the calculation of cumulative traffic volumes in terms of growth rate, pavement design life and initial traffic flows.

In addition, revised conclusions can now be drawn on the way in which commercial traffic is distributed between the left hand and overtaking lanes of motorways and trunk roads. Experience until 1974 did not go beyond the total flow of 7000 commercial vehicles per day, but observations by Currer[34] indicate that there would be an approximately equal distribution of commercial traffic between the lanes at a commercial flow of 10,500 vehicles per day. These observations indicate that the figures given in the 3rd edition of Road Note 29 will give an overestimate of the number of commercial vehicles in the left hand lane and lead to a measure of overdesign.

However a design procedure based on semi-empirical techniques confines the range of material types and loading conditions considered to those for which experimental evidence is available. The approach is unable to provide rapid evaluation of new materials and forms of construction. Furthermore, it does not include, as part of the design procedures, an analysis of the distribution of stress exerted on individual pavement layers or

materials. Consequently its application is limited to the combinations of material, thickness, traffic loading and environmental conditions obtained from the full scale experiments. Extrapolation of data beyond the limits defined by past experience has resulted in the inadequate design of pavements with a high intensity of commercial vehicles and their respective axle loading.

3.3 ANALYTICAL DESIGN GUIDES

The inadequacies of semi-empirical design techniques have resulted in the development of analytical design guides[1,27]. These include LR1132 published by the T.R.R.L.[1].

The performance criteria developed within these pavement design guides are :-

a) permanent deformation which is controlled by the permissible vertical strain in the sub-grade at formation, and

b) fatigue cracking which is controlled by the horizontal tensile strain at the bottom of the bound layer.

3.3.1 LR1132: General Design Considerations

In LR1132, the performance data from the full scale experiments have been used in a much more effective way. The primary function of the data is to provide the calibration necessary to establish practical material performance criteria from theoretical analysis of the pavement structure and laboratory testing programmes.

The most significant developments in pavement design methodology resulting from the publication of LR1132 are:-

(i) the introduction of a more fundamental approach to design which improves the accuracy of extrapolating pavement performance to very high traffic levels.

(ii) the definition of end of life is changed from a rut depth of 20mm adopted by RN29, to the need for reconstruction at a rut depth of 10mm, implying a need for overlay

strengthening. The consequence of this change is to increase design lives from 20 to about 30 - 35 years.

(iii) the recognition of the variability of pavement performance with the introduction of an 85th percentile probability of achieving the design life included in the design charts; the consequence of this is to increase the design life further to about 40 years.

(iv) the inclusion of the latest method of estimating traffic loading

(v) the introduction of new sub-base thickness design methodology; sub-base thickness is now controlled primarily by criteria related to the provision of an adequate construction platform for subsequent layers,

(vi) the introduction of greater design flexibility through the ability to convert thicknesses of granular material into equivalent thickness of bituminous materials; 10mm of bituminous roadbase macadam is equivalent to about 30mm of Type 1 sub-base [105] or 20mm of wet mix macadam.

(vii) the introduction of the estimation of sub-grade strength not just for equilibrium conditions, but, more importantly, in the construction phase as a result of adverse weather conditions.

3.3.2 LR1132: Lean Concrete Roadbase Design Considerations

The report recognises that transverse cracks can occur very early in the life of lean concrete pavements at a spacing of about 4m. Subsequent movement at the crack interfaces will induce cracking within the surfacing and result in general pavement deterioration.

Due to the expensive and time consuming operation of replacing the roadbase LR1132 proposes that it is more economical to design roadbases for heavily trafficked pavements (greater than 20 m.s.a.) to prevent general cracking, and provide a pavement of long, but indeterminate service life. The resistance of lean concrete roadbases to the combined effects of traffic and temperature is

estimated in terms of its flexural strength at 28 days. The recommended design thickness of 250mm of lean concrete is, however, based on results which give a wide scatter of values indicating that flexural strength is not the only parameter which governs crack resistance. Variation in aggregate types or grading are not considered.

The report acknowledges that while an increase in present 28 day compressive strength requirement from 11 to 15 MN/m^2 may permit a reduction in the required thickness of lean concrete there would be an associated increase in the frequency of transverse cracks.

LR1132 considers a surfacing thickness of 200mm will inhibit reflection cracking if the roadbase does crack. This thickness is significantly greater than that recommended to resist rutting and indicates the potential economic saving in material costs if a practical alternative to increasing the surfacing thickness was developed.

For lightly trafficked roads, (Cumulative traffic 1 - 20 m.s.a.), it is considered to be more economical to allow a reduced roadbase thickness to break up under the action of traffic providing only a limited life. The subsequent recommendations provided a design thickness for surfacing established primarily from the observation of cracking at the pavement surface whereas that for the lean concrete roadbase is derived from deflection measurements.

The revision of thickness requirements for both surfacing and lean concrete roadbases given in LR1132 is illustrated in fig.3.2.

Although thermal stresses within the roadbase have been considered, the related surfacing design curves are only given in terms of traffic levels, as in RN 29, whereas the damaging effect of such stresses is a time based parameter.

LR1132 does not include any revision of the types or characteristics of surfacing materials to be used with cement stabilized roadbases and therefore considers the recommendations in the previous code[7] to be satisfactory. However, the bituminous surfacing materials have not been designed specifically to inhibit

the initiation and propagation of reflection cracks and consequently there is a need to optimise the properties of these materials to resist this form of deterioration.

4.0 REFLECTION CRACKING

Reflection cracking is predominantly associated with composite pavement construction. The incidence of reflection cracking and its contribution to pavement deterioration on sites incorporating this form of construction, have been monitored as part of this investigation.

Plate 1 illustrates examples of transverse reflection cracking observed on two of these roads; the A30 Cambourne by-Pass, Cornwall and the M4 motorway, Berkshire.

4.1 THE EXTENT OF THE REFLECTION CRACKING PROBLEM

Composite pavement construction was used extensively throughout the U.K. in the 1960's and 1970's. However, its popularity has declined as a result of changing costs and the concern of some local authorities over reflection cracking. Lean concrete is the most extensively used cement stabilized roadbase material for flexible composite pavements. It is the only one permitted for relatively heavily trafficked roads with a design traffic loading in excess of 5 m.s.a.[7].

A quantitive indication of the use of lean concrete was given in 1972 by James[35] who analysed 60 successful tenders for new road construction started in 1969. The analysis related to a length of 422km and, of 60 schemes lean concrete was used in 26 instances. Brooks[36] reported that during this period lean concrete roadbases were the most common form of construction in most parts of the country.

4.1.1 Crack Surveys

Crack surveys have been undertaken frequently by local authority engineers, to ascertain the extent of the problem. The earliest extensive review was undertaken by Wright[37] on 41 sites in 1962 and was considered representative of road construction carried out using lean concrete over the previous 11 years. Of the 41 sites in England and Wales 6 were not examined after completion and of the remaining 35, 11 were classified as completely sound, a further 12 were sound except for the presence of transverse cracking which had

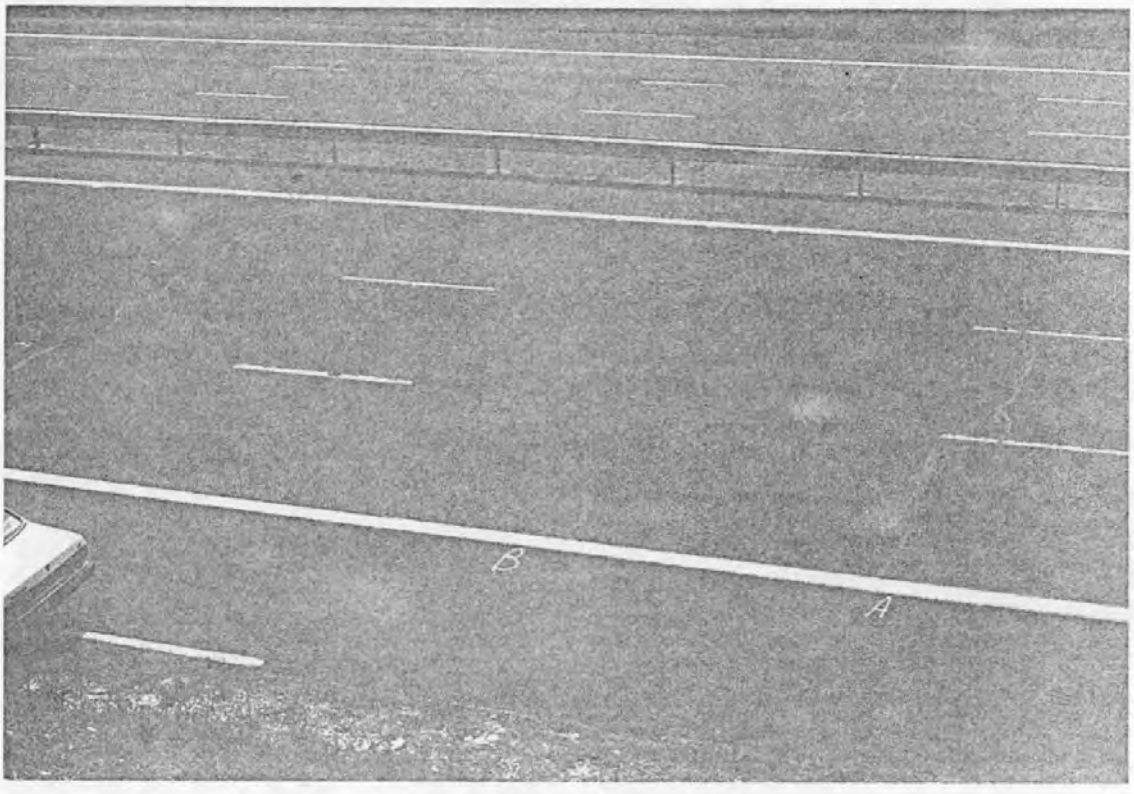

REFLECTION CRACKING ON A HEAVILY TRAFFICKED MOTORWAY (M4) AFTER 15 YEARS WITH A FULLY DEVELOPED PRIMARY CRACKING AT 9m SPACING AND SECONDARY CRACKS INITIATING AT 4.5m SPACING (175mm SURFACING)

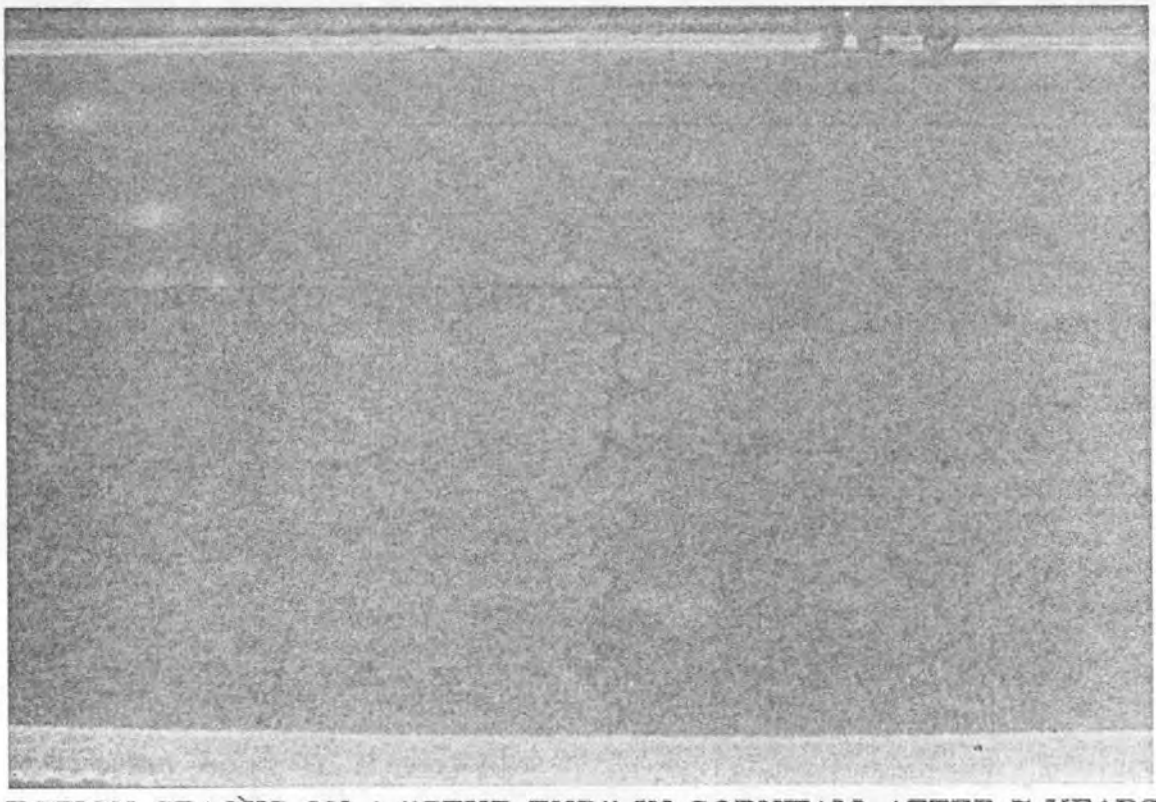

REFLECTION CRACKS ON A "STUB END" IN CORNWALL AFTER 7 YEARS WITH A CRACK SPACING OF 25m (90mm SURFACING)

PLATE 1 REFLECTION CRACKING ON M4 MOTORWAY AND A30 TRUNK ROAD

not developed to an extent necessitating repair work and were not at the time considered a serious defect. These pavements were of various ages but none, however, had reached half of their the 20 year design life. Of the 12 remaining sites where some defects other than reflection cracking were observed, in most cases the defects were of a minor nature. Resurfacing was necessary after 12 years service on only one site .

A more recent study undertaken by the 'Reflective Cracking Working Group' (TRRL)[2] carried out a survey on 340km of motorway and 145km of trunk road built with cement bound roadbases. The group selected schemes opened between 1960 and 1975 primarily to study the significance of changes to RN29 on crack frequency and severity. Each scheme was sub divided into 200m units. They reported only 5% of the total units had average crack spacing of less than 10m. There was no longitudinal cracking in the large majority of the units and only 8.5% of the units had cracking in the wheel tracks and 4% in other places . However, both the proportion of units exhibiting transverse cracks and the frequency of transverse cracks per unit increased with the age of the surfacing.

Kent County Council have used composite pavement construction extensively over the past 25 years and report that cracks of 6m spacing generally appear at the surface after only a fraction of their design life[39]. In extreme cases reflection cracks have appeared on the surface even before a road has been opened to traffic.

Correspondence with Local Authority engineers by the author has enabled the extent of reflection cracking to be established on a national basis. Of the 32 Local Authority engineers replying, 18% reported having a policy of not using cement bound roadbases in highway construction while 22% experienced only limited problems. However, in each case, this form of road construction only contributed a minor part of the total recent pavement construction within the County. Of the Counties with extensive use of cement stabilised roadbases 36% of the total reported the occurrence of reflection cracking which, to date had not caused major maintenance problems. The remaining 24% considered the phenomenon of

reflection cracking to be a significant source of pavement deterioration.

Pavement surveys undertaken as part of this investigation were primarily concerned with collection of data on the frequency of cracks, the results of which are discussed in Section 6. Therefore, the survey was limited to roads constructed with lean concrete roadbases with over 10 years service and predominantly in the South West of England. Reflection cracking was observed on the majority of these pavements. Crack spacing and general deterioration associated with reflection cracking differed greatly from site to site. It varied from isolated hair line cracking in the centre and edges of the carriageway to open transverse cracks of over 5mm in width at a spacing of 3m. The open cracks were often associated with spalling of the pavement surface adjacent to the crack face with 'secondary' cracking parallel to the main cracks.

4.1.2. Overlaid Rigid Pavements

Reflection cracking has also occurred, particularly in the U.S.A., on rigid pavements overlaid with asphalt layers. Problems associated with reflection cracking within this pavement classification will become increasingly relevant to those sections of Britain's motorway network of rigid construction as their ultimate design lives are exceeded and require strengthening through bituminous overlays.

Although reference will be made to overlaid rigid pavements, this work is limited to considering composite pavements under U.K. conditions.

4.2 THE EFFECTS OF PAVEMENT DETERIORATION THROUGH REFLECTION CRACKING

Reflection cracks are fractures in the surfacing layers that are the result of crack movement in the underlying layer. They are characteristic of pavements incorporating bituminous surfacing on cement stabilized layers and overlaid concrete roads. They occur both as transverse cracks across the width of the carriageway and as longitudinal cracks over strip joints. Initially, they take the

form of hair line cracks at the surface but can, in cold weather or after the deposition of debris into the crack over long periods of time, open to over 5mm reducing the riding quality of the pavement.

This form of deterioration can allow the ingress of water into the surfacing material which, as a result of freezing, will induce spalling of the material on either side of the crack face.

The ingress of water into the lower layers of the pavement can cause local sub-grade failure resulting in the settlement of the roadbase. If the cracks are not sealed effectively then initially the interlock between individual slabs will be reduced. Once the roadbase has been reduced to unconnected blocks, high differential movements will occur between them and, as illustrated in LR833[3], rapid failure of pavement will occur.

4.3 CAUSES OF REFLECTION CRACKING

Reflection cracking in composite pavements can be related directly with the construction technique and materials used for this type of pavement. During the initial curing period the cement bound roadbase is reduced to a series of interconnecting slabs which are subsequently overlaid by a continuous layer of bituminous surfacing. Due to this continuity any movement within the pavement structure will induce concentrations of stress in the surfacing above the roadbase cracks irrespective of loading condition.

Previous researchers have identified five conditions under which stresses, induced in the surfacing material, contribute to reflection cracking. They include:-

(i) roadbase thermal movement
(ii) thermal warping of the structural layers
(iii) traffic loading
(iv) differential slab settlement
(v) long term shrinkage of the surfacing

The occurrence of one or more or these conditions may induce the operation of crack mechanisms within the surfacing layer above the cracked cement bound roadbase. Three forms of crack mechanism have been identified which may combine or act independently.

The mechanisms, shown diagrammatically in fig.4.1, have been termed:

(i) tensile fatigue
(ii) tensile yield
(iii) shear fatigue

Therefore, to alleviate this form of pavement deterioration an overall solution must account for the complex interaction between them with an understanding of the predominant mechanism in each circumstance.

4.3.1 Tensile Fatigue

Under this mechanism stresses within the surfacing layers are induced through horizontal movement in the roadbase caused by daily and annual cycles of temperature; fig.4.1. These stresses are focused at the cracks between the roadbase slabs. Their magnitude, therefore, is related to the width to which the roadbase cracks open during the thermal cycle.

The crack opening width is dependent upon the temperature range, the thermal properties of the roadbase material and length of the slab. The probability of reflection cracks resulting from this mechanism increases as the slab length increases. Initial crack growth occurs at flaws within the surfacing, at its interface with the roadbase. On successive stress cycles a crack propagates to the surface.

The transmission of stress across the interface relies upon a good shear bond between the layers. This bond has been shown to exist generally through the inspection of cored samples, although limited debonding between the layers in the vicinity of the crack is common. Where debonding occurs reflection cracks formed through this mechanism may be offset from directly above roadbase cracks to the end of the de-bonded area.

The rate of crack development is governed by the crack opening width and the ability of the surfacing material to resist this form of fatigue. It is further influenced by the depth of surfacing material. The crack tip stress decreases exponentially with the

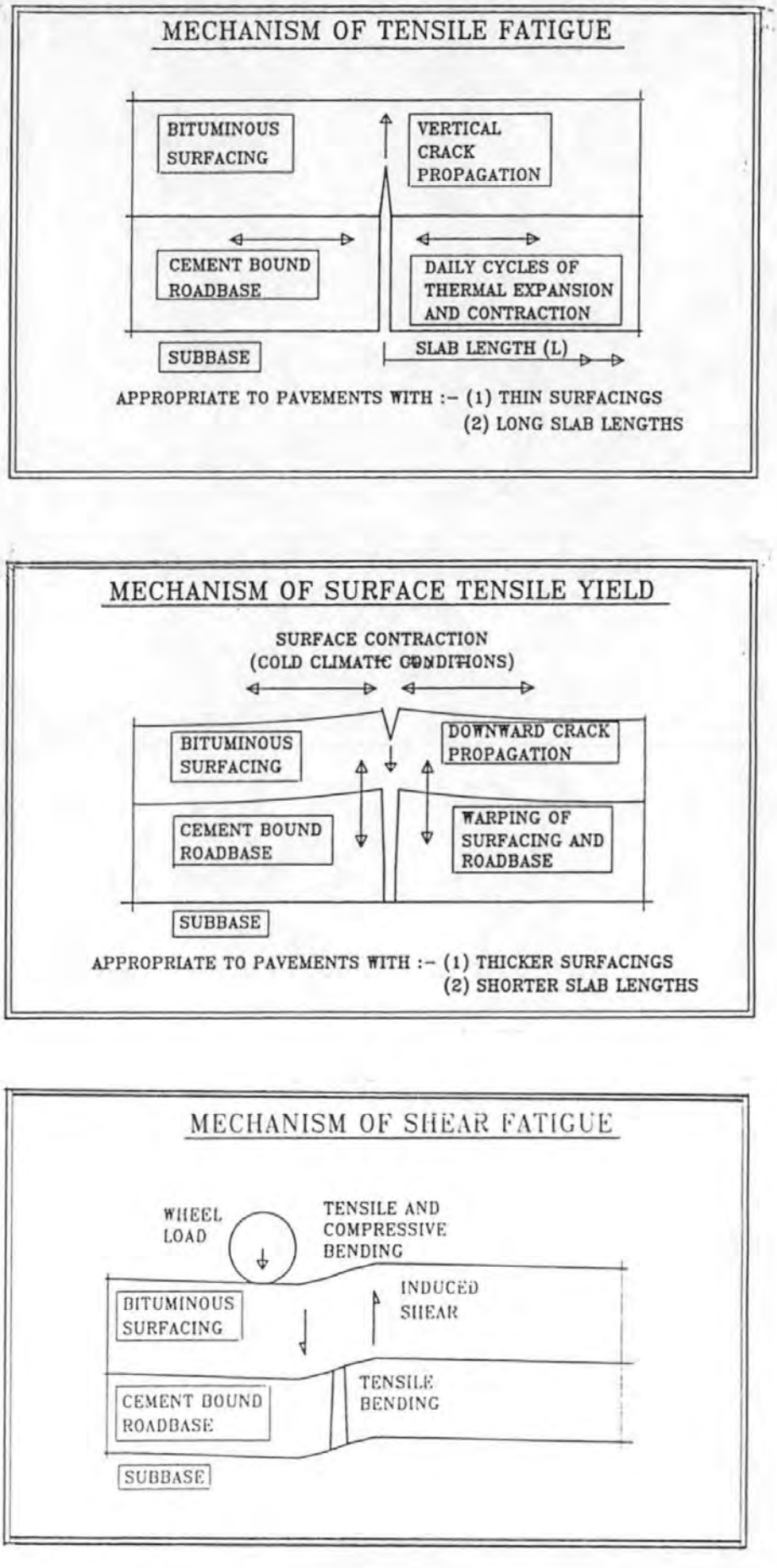

FIG.4.1 DOMINANT REFLECTION CRACKING MECHANISMS

crack length as the crack propagates to the surface. Therefore, by increasing the surfacing depth, the potential crack path is lengthened resulting in an extended fatigue life. Additionally, the surfacing material tends to insulate the roadbase reducing thermal temperature cycles and thereby reducing slab movement.

4.3.2 Tensile Yield

If the occurrence of reflection cracking initiated at the surface of the bound layer is related to the tensile properties of the surfacing material, the conditions of thermal warping and contraction and long term shrinkage may be considered as contributing to this crack mechanism. The mechanism is illustrated in fig.4.1.

4.3.2.1 Influence of Thermal Warping

Under extreme cycles of temperature thermal gradients are formed across the pavement structure. An increase in temperature with depth will produce a concave surface with an upward curling at the slab ends inducing tensile stresses at the surface. This condition is not solely dependent upon the thermal gradient, but is also influenced by the self weight of the structure and frictional restraint between the slabs. It is largely independent of slab length except in very short slabs. Analysis may be carried out either by considering the slab as a beam on an elastic foundation[39] or through a finite element model of the condition. This mechanism cannot be controlled however simply by increasing the thickness. In some circumstances this may be detrimental and lead to an increase in surface tensile stress.

These tensile warping stresses may be further aggravated through a rocking motion induced by the passage of traffic especially on slabs of shorter length. However, embedment of the slab within the lower layers may reduce this effect, especially on a weak sub-grade.

Downward warping of the slab ends through a decrease in temperature with depth could also influence reflection cracking, but this effect will be restrained by the sub-base and sub-grade. Furthermore, this effect occurs when the pavement surfacing directly above cracks within the roadbase is in compression, rather

than subjected to tension and therefore any cracks will be closed.

4.3.2.2 Influence of Long Term Shrinkage

The tensile yield of the surfacing material is also influenced by the occurrence of long term shrinkage of this layer.

Observations of county engineers provides an increasing volume of evidence that currently specified wearing course material is prone to this effect. This form of pavement deterioration is not confined to composite pavements, but also affects full depth bituminous construction[20]. Transverse cracking initiates at the surface and propagates downwards and, although shrinkage is not directly responsible for cracking through the lower layers of the surfacing, these regions become a focus of stress due to other mechanisms.

The influence of this condition is dependent upon the pavement age, mix characteristics and the susceptibility of the binder to oxidization. The end result of long term shrinkage and warping are similar and the contribution made by either is difficult to determine for pavements of composite construction.

4.3.3. Shear Fatigue

Shear stresses are induced into the surfacing material through vertical differential movements between adjoining slabs as traffic crosses a roadbase crack; the mechanism is illustrated fig.4.1. However, from the results of deflectograph surveys[38] it is apparent that the mechanism is complicated through simultaneous bending within the pavement producing tension in the underside of the surfacing.

Whereas horizontal movements associated with temperature fluctuations are relatively large but slow, the vertical movements due to traffic are usually small and rapid. They are also normally partially restrained through granular interlock between the slabs. Therefore the displacement may vary according to the freedom of the joints. These are at their largest when the temperature is low and the joint is open or when the slabs are warped concavely at night. Furthermore, at low temperatures, the asphalt stiffness is high which reduces deflection but also increases its susceptibility to

reflection crack propagation. Thicker surfacing layers also provide additional restraint to differential vertical movement through the transfer of traffic stresses from one slab to the next.

A breakdown of interlock may occur if the roadbase is constructed from poor quality material or through general deterioration during the service life of the pavement. If breakdown occurs the shearing action increases as the pavement is deemed to be in a critical condition with a subsequent overstressing of the sub-grade. Under these circumstances, the shear stresses within the surfacing would be significant and form the predominant crack mechanism.

Initially, the mechanism is stress controlled, but as the effective restraint decreases through crack propagation within the surfacing and breakdown of interlock between the slabs it will change progressively to a strain controlled condition.

4.3.4 Differential Settlement

Differential settlement of adjacent roadbase slabs may occur on a long term basis across areas of cut and fill or on sections of variable sub-grade. Although not a common occurrence it may account for longitudinal reflection cracking observed on sections of embankment, but not commonly in cuttings.

As the problem is associated with sub-grade condition it cannot be considered within the context of surfacing crack mechanisms and it is not investigated within this study.

4.4 A REVIEW OF METHODS USED TO INHIBIT REFLECTION CRACKING

A wide variety of methods have been used to inhibit reflection cracking both in new pavement construction and in the maintenance of existing pavements. In reviewing the results the following categories have been defined:

A. Pavement Construction

4.4.1 Aggregate type and mix characteristics of lean concrete roadbase

4.4.2 Depth of bituminous surfacing.

4.4.3 Bituminous mixes.

4.4.4 Modified binders.

4.4.5 Bond breaking layers.

4.4.6 Stress Absorbing Layers.

4.4.7 Cushioning layers.

4.4.8 Cracking and Seating of concrete pavements.

B. Maintenance procedures

4.4.9 Scarifying and recycling or overlaying

4.4.10 Overbanding

4.4.11 Surface dressing

4.4.12 Overlays

4.4.13 Reconstruction

4.4.1. Aggregate Type and Mix Characteristics of Lean Concrete Roadbase

The type of aggregate used in a lean concrete roadbase affects the magnitude of horizontal movement resulting from thermal expansion and contraction.

Bonnell and Harper[40] have shown that by using limestone rather than a flint or quartzite aggregate the coefficients of thermal expansion can be halved, thus effectively reducing the horizontal crack opening width in the lean concrete roadbase by a similar magnitude. Similar conclusions are reached by Wright[37] in a field survey of 41 UK sites which were considered representative of most of the road construction thickness incorporating a lean concrete roadbase used up to 1963.

From experimental pavement sections on the Wheatley By-pass, Croney[41] notes that high strength cemented roadbases were liable to thermal cracking appearing at about 5m intervals while with weaker cemented roadbases the crack spacing was smaller and therefore less likely to develop significant thermal movement. An optimum 28 day compressive strength of about $10N/mm^2$ is recommended.

Weak concrete incorporating aggregate with low thermal expansion will reduce the incidence of reflection cracking.

4.4.2. Depth of Bituminous Surfacing

Based on crack propagation studies in the mid 1960's Croney[41]

suggests that a two course bituminous surfacing of 90-100mm thick will control reflection cracking within the surfacing for a life of 5 m.s.a. and that a thickness of 120-130mm will inhibit cracking for at least 10 m.s.a.

From data collected by the TRRL in 1962[42] it was concluded that at least 100mm of surfacing was required to increase the thermal insulation of lean concrete roads sufficiently to substantially control reflection cracking.

Survey data correlated by the 'Reflective Cracking Working Group', T.R.R.L. 1985[2] showed the frequency of transverse cracking decreased with an increased thickness of bituminous cover. No correlation was found between the frequency of transverse cracking and cumulative traffic or design life on the sections which exhibited reflection cracking.

However, Korfhage[43] reports observations of test sections of concrete pavements on US interstate highways overlaid by 100mm, 125mm, 150mm and 225mm of bituminous surfacing. After 5 years, the 225mm surfacing showed a decrease in transverse cracking of only 40% over the 100mm layers.

From an extensive programme of coring and observation of surface cracking of experimental roads, TRRL Report 1132[1] concludes that for pavements designed to carry over 20 m.s.a., under UK climatic conditions, 200mm of bituminous surfacing over 250mm of lean concrete should be sufficient to resist reflection cracking provided that the current minimum average compressive strength requirement of 11 N/mm^2 for the lean concrete is met.

The thickness of bituminous surfacing may therefore inhibit reflection cracking but the importance of its influence cannot be determined from the literature.

4.4.3 Bituminous mixes

General experience and surveys in the UK prior to 1962[42] suggests that a dense rolled asphalt with a low stone content is usually the most suitable surfacing to inhibit the growth of reflection cracking.

The Iowa Highway Department[44] experimented with asphalt stiffness by using two different grades of binder. The softer bitumen (115 pen. at 25°C) reduced reflection cracking to approximately one half of that of the stiffer (80 pen.) bitumen after 51 months service.

Similarly, conclusions drawn from the NEEP-10 project in 1972[45] showed that binder viscosity at the time of laying was a significant factor in retarding reflection cracking. The temperature susceptibility of the bitumen, the climate, the binder content and its ability to resist hardening all affect the rate of crack propagation. It was found that the penetration value of 45 was critical to crack initiation and the longer the binder can maintain a penetration above this value, the longer it will be before reflection cracks appear. It is important, therefore, to use the lowest viscosity bitumen in the design of a surfacing that is compatible with stability requirements.

Additional evidence concerning the effect of asphalt viscosity is given by studies conducted in Saskatchewan, Canada[46] which indicates that the use of air blown bitumens will improve viscosity-temperature characteristics, allowing the use of harder grades of bitumen in cold climates, while still satisfying the viscosity requirements for cold weather. These bitumens may be less susceptible to reflection cracking under thermally induced tensile stresses.

Furthermore, dense mixes with low air void contents have been shown[47] to reduce the rate of bitumen hardening which will also reduce the risk of reflection cracking early in the life of the pavement.

A theoretical study by Chang, Lytton and Carpenter[48] adopting fracture mechanics to study the crack propagation in flexible pavements due to thermal expansion and contraction concluded that the ideal surfacing design consisted of:-

> "a thin layer with soft asphalt and low modulus of elasticity to serve as a stress relieving layer overlaid by a layer of slightly less soft asphalt and higher modulus of elasticity to

provide a surfacing."

A fracture mechanics based model has been developed by Lytton and Shanmugham[49] to predict the occurrence of transverse cracking in bituminous overlays in terms of the number of daily thermal cycles. This model shows that hardening of the binder under service conditions is a significant factor in the development of reflection cracking.

To summarise, dense mixes with softer grades of binder will inhibit reflection cracking although a compromise is required to ensure mix stability criteria are satisfied. Bitumens refined through an airblown process are reported to have superior visco-thermal characteristics.

4.4.4 Modified Binders

Throughout the 1950's and 60's numerous field tests were carried out with rubberised binders exhibiting tougher and more resilient properties than normal asphalts to reduce asphalt cracking. Bone, Crump and Roggeveen[50], however, concluded from tensile tests that although rubberised asphalts stretched more than unrubberised ones they would not accommodate, without cracking, movements of the order required over cracked sections of concrete road subjected to thermal movement.

From full scale tests conducted in the United States[51] using various types of rubber compounds, proportioned 5-7% by weight of bitumen, it was noted that there was no marked difference between sections with additives and those without. A similar study by the Road Research Laboratory in England[52] also indicated that a rubberised asphalt did not reduce cracking.

Nevertheless, products under current investigation contain significantly higher proportions of rubber (20% to 30% by weight of binder) than the earlier materials as reported by Jimenez[53]. These new products utilize recycled tyre rubber and are therefore more economic. Morris and McDonald[54] reviewed the performance of a number of full scale field trials using asphalt-rubber as the binder both for a chip-seal coat over the surface of cracked pavements and as an interlayer between the existing pavement and an

asphalt overlay. These pavements have been in service for up to 9 years in Arizona. In summarising their results, Morris and Macdonald observe that the full scale projects have shown that when placed as a seal coat the system will effectively control the reflection of fatigue-cracking and that when placed as an interlayer the system will control effectively the reflection of all types of cracking.

On the basis of these positive results the use of a sand-rubber-bitumen emulsion is being investigated on several projects in North America[55].

Several polymer-modified asphalts have recently come on the market, for example Asphapol, manufactured by the Associated Asphalt Company. Initial laboratory and field tests[56] tend to verify manufacturers' claims that a two layer system consisting of a cushioning course overlaid by a H.R.A. surfacing, both incorporating the modified binder, will absorb the stresses which induce reflection cracking. The cushioning course comprises a 0/3 sand mix with 12.6% of penetration grade bitumen/asphapol additive composite binder. This material is laid as a thin screed to be overlaid by a conventionally graded H.R.A.. It is claimed that the resultant layer thickness required is only 60% of that required by standard materials giving a net cost benefit while providing a surfacing of conventional stiffness and skid resistance.

An increasing number of modified binders are being marketed but the results from field tests have yet to verify their long term advantages, although initial results indicate they do inhibit reflection cracking.

4.4.5 Bond Breaking Layers

The concept of placing bond breaking layers in the vicinity of a crack between the concrete roadbase and overlaid bituminous surfacing has been under investigation since the 1960's, both in the United Kingdom and America. Theoretically such layers should reduce the strains exerted in the narrow band of bituminous surfacing adjacent to the crack by allowing the longitudinal roadbase slab movements to be absorbed over a greater length of

surfacing material.

Early tests by both the T.R.R.L. and American Highway Authorities[57] used thin layers of sand roofing felt and building paper to prevent a bond between the roadbase and base course for a width of up to 1m either side of the crack. The results were largely inconclusive because the thickness of the bituminous layer was reduced at the same time to make the process economically viable.

More recently (1977) heavy duty waterproof membranes have been employed by the Georgia Highways Authority[58]. The use of the waterproofing strips over the concrete pavement joints and cracks prior to the application of a 50mm asphaltic overlay prevented reflection cracks from occurring after 15 months service. A corresponding control section without the waterproofing strips had 88 per cent of the concrete joints reflected through the overlay in the same period.

However, the results from other field trials in the U.S.A.[59] indicated that the treatment of existing cracks in pavements prior to overlay has been of limited success only. Overlay construction difficulties, concern over possible lateral displacement of the overlay and the introduction of stress relieving interlayers have all combined to reduce the emphasis placed on incorporating bond breaking layers and agents as a method of controlling reflection cracking.

4.4.6 Stress Absorbing Layers

The earliest experiments using reinforcement in bituminous surfacings were reported in the 1940's both in the United States and the United Kingdom. The work in the UK[42] consisted of expanded metal strips laid over joints in concrete pavements prior to overlaying with a single 50mm thickness of asphalt. Cracking was found to be merely transferred from the joint to the edge of the reinforcing strips.

Several States in North America[60,61] have experimented with the use of wire mesh both in short strips laid over the joints and

continuous reinforcement. The degree of success reported in their use to prevent reflection cracking is variable, although it has been shown to generally delay the appearance of the cracks on the surface if a continuously laid, large mesh fabric was employed with a dense, cohesive asphaltic concrete.

Steel reinforcement has recently been used on the M6 motorway reconstruction and strengthening in Staffordshire but performance data is not yet available. The lean concrete roadbase was overlaid by steel mesh with bars at a spacing of 125mm and bedded in with a 60 mm thick layer of bituminous base course. The uppermost courses consisted of a 125mm thick layer of 28mm nominal sized H.R.A.[8] and 40mm of H.R.A. surfacing.

The last decade has seen the advent of various types of material for use as stress absorbing membrane interlayers; literature on the performance of these materials is limited but some have displayed promising initial results. These materials may be categorised into three specific types:-

1) Non woven fabric,
2) Woven fabric,
3) Geogrid of predominantly two differing materials
    a) Polypropylene based with a variety of additional synthetic fibres such as polyester and nylon,
    b) fibre glass yarn.

These materials are biologically and chemically resistant. Although both grids and fabrics provide a tensile member within the pavement surfacing, they rely upon differing restraining mechanisms. The geogrids rely on a mechanical interlock with the aggregate above while offering a lateral restraint to the underlying layers. The fabrics depend upon the friction gained by their increased surface area and the adhesion offered by a bituminous tack coat. The continuity of the fabrics also provides an additional impermeable layer to prevent water from entering the subgrade.

The promotion of geogrids in the U.K. has led to laboratory and field tests. Nottingham University have recently published a report on a 50mm x 50mm stretched polypropylene mesh 'Tensar ARI'[62] manufactured by Netlon Ltd, which was subjected to laboratory testing to simulate fatigue and traffic induced

reflection cracking. The inclusion of Tensar ARI in four different asphalt mixes (HRA and DBM base and wearing courses) increased the resistance to rutting substantially while a layer of grid placed immediately over a roadbase discontinuity prevented the development of a reflection crack in the overlaying asphalt. The inclusion of the grid within the overlay inhibited the crack growth and limited the crack width.

Conclusive results from early field use of this type of material, laid above a cracked concrete roadbase at Canvey Island in Essex, are still pending, but reflection cracks have not appeared at the surface of the flexible layer after four years of service[63].

In the U.S.A. widespread testing and field trials incorporating engineering fabrics have shown promising results although a laboratory study by Texas University[64] concluded that the amount of benefit gained by adding fabric layers depends upon a great many variables. The type of fabric, of those investigated, appeared to be of secondary importance compared with the influence on crack resistance of the application rate of tack coat with which the fabric was saturated prior to laying the bituminous overlay. The location of the fabric within the overlay also has a significant effect.

The optimum performance was shown by:-

a) placing the fabric layer near the bottom of the overlay rather than near the top
b) using high tack coat rates
c) using heavier fabrics
d) using flexible fabrics

Laboratory tests by Majidzadeh[65] to investigate the use of 'Petromat' fabric found that under simulative field testing the reinforced samples showed at least a 1000% improvement in fatigue life. The most effective position of the fabric was found to be in the lower third of the overlay.

The performance of a polypropylene non-woven fabric as a stress relieving layer has been investigated by Gulden[66] on test sections of the I-85 in Georgia, U.S.A. The fabric was overlaid by

a range of thicknesses of bituminous surfacing. After 15 months service, 25% of the original reflection cracks were visible on the road surface on sections incorporating the fabric and a 50mm overlay. In the same time period, over 80% of the cracks had propagated through control sections of similar surfacing thickness. Sections incorporating the fabric and 100mm and 150mm of overlay were free from reflection cracking whereas 30% of the original cracks had propagated through the control sections.

However, McGhee[55] in summarising methods used in Virginia, USA, to reduce reflection cracking of bituminous overlays on concrete pavements concludes that high strength fabrics can delay the onset of reflection cracking, but such cracking will eventually develop under repeated wheel load application. Several projects are cited in his investigation. These include the use of a non woven polypropylene fabric to span the reflective cracks of a previously overlaid concrete pavement on US-460. The fabric was laid using a cationic bitumen emulsion tack coat in 0.9m wide strips centred on the cracks prior to overlaying with bituminous material. After three months under traffic many of the joints were reflected through the second overlay although there was somewhat more cracking in an adjacent section where no fabric was used. The survey of a similar project on the I.95 highway, conducted 2½ years after resurfacing using a similar material and construction procedure to that on the US-460 highway, showed 52% of the fabric treated cracks had reflected through to the surface. 100% of the original cracks had reflected through an untreated control section. For both projects, cores showed that the cracks were directly above cracks in the concrete base and that the fabric was still intact with no signs of distress.

North Carolina Highways Department[67] laid similar test sections on the US-70 highway investigating the viability of four types of engineering fabric, namely Mirafi, Structors, Petromat and fibreglass laid both continuously and in strips centred on the cracks. After five years of service, survey reports showed that the joint cracking appeared to vary far more with location along the highway than with the different overlay treatments used in the experiment.

It is difficult to assert whether the majority of the materials have been effective as they have not been accompanied by a control section; even on those that have, the initial results are variable.

4.4.7 Cushioning Layers

The use of a crushed rock or slag layer as a cushioning course laid over the concrete base prior to overlaying with asphaltic surfacing has been used in the United States for many years[68]. The generally accepted layer thicknesses consisted of 100 -150mm of stable granular material with 50 to 100mm of surfacing. It has been shown to be an effective remedy but raising the final road surface level makes the treatment expensive and only suitable for roads in open country.

The use of a similar technique is well established in South Africa for the construction of pavements for all traffic classifications. The main load bearing element consists of a cement treated base layer. The design of this layer accepts that it is susceptible to fatigue cracking and makes provision for calculating the number of load repetitions that will induce cracking . Thereafter, the elastic modulus will be reduced and the layer will act as a granular material. The cement treated base is overlaid by crushed stone material and a thin layer (50-70mm) of asphalt surfacing.

The untreated granular layer ensures that differential movement between the interconnected sections of the cement treated layer does not result in reflection cracking through the bituminous surfacing. However, if the untreated layer is too thick it acts as a 'sponge' between the stiffer asphalt and cement-treated sub-base. Experience and analytical design has shown its optimum thickness to be between 70-100mm

4.4.8 Cracking and Seating of Concrete Bases

Cracking the concrete base into sections is a practice used extensively in the United States on concrete highways prior to bituminous overlaying and has been shown to be a highly effective method of preventing or delaying reflection cracking. The United States National Asphalt Pavement Association[69] have standardised the procedure and stress that the correct cracking techniques are essential to produce fine cracks that run through the complete

depth of the slab. Destructive techniques will lead to spalling and loss of structural strength. Impact hammers or modified pile hammers are employed to break the concrete base into 500mm to 1000mm square sections. Seating of the cracked pieces into the subgrade using a pneumatic tyred roller prior to surfacings is also vital to prevent rocking.

The material costs of maintenance are minimised by the milling of the original overlay and stockpiling it prior to recycling.

4.4.9 Scarifying and Recycling or Overlaying

The traditional method of restoring a surface, that has suffered surface deterioration is to overlay with a new asphalt. However the processes of surface planing and either recycling the existing surfacing material or overlaying with new material provide viable alternatives.

These methods have a significant advantage when applied to pavements which require resurfacing due to reflection cracking, but which contain construction thicknesses in excess of their actual structural needs. The uppermost 40 to 70mm of surfacings hardened through bitumen oxidization and therefore susceptible to initiation of cracking at the surface may be adequately treated or replaced.

The success of recycling in providing a rejuvenated mix resistant to reflection cracking is dependent upon a high standard of quality control. Reclaiming the material increases the fines content of the old material and therefore involves a blending of both new clean aggregates and additional bitumen, softening agents or additives with the original material to produce a hot cycled mix with the required gradation, air voids and stability.

The extensive use of heater scarification [70] has been made in the U.S.A. prior to overlay construction as a means of eliminating existing crack patterns, restoring flexibility to aged and brittle pavements and creating a positive bond between the old pavement and the new overlay. The existing pavement is scarified to a depth of 20mm and this material is treated with a bitumen emulsion or other rejuvenating agent designed to combine with the original bitumen. After application of the agent the scarified material is

recompacted and the overlay applied. This method has been successfully used on both airfield and highway pavements. The Arizona Department of Transportation concluded that this method was the most effective means of retarding the appearance of reflection cracks of twenty different pavement treatments investigated [45]. Recycling of the bituminous surfacing at regular intervals could provide a cheap solution to reflection cracking in urban areas.

4.4.10 Overbanding

Overbanding is carried out extensively throughout the U.K. as a temporary treatment to prevent water entering through a cracked pavement and weakening the subgrade. The cracks are cleaned of all foreign matter and a sealant poured into the crack. The sealant must adhere to the bituminous material, remain in position and retain its flexibility under the extremes of climate.

Secondary cracking in the vicinity of original cracks and spalling of the surfacing material at the crack face will render this treatment ineffective under continued trafficking.

The properties of sealants currently used, methods of test and permissible limits of performance are given in BS 2499 [71].

4.4.11 Surface Dressings

Surface dressings, using conventional materials and methods, have been used in the South West of England to provide a temporary seal to cracks and improve the riding quality of the pavement adjacent to the cracked areas. However, periodic surveys have shown the treatment to be ineffective with the road surface deteriorating to its original condition in under six months.

4.4.12 Overlays

Overlays have been used extensively in the U.K. to extend the service life of composite pavements, providing both a strengthened road structure and an effective seal on reflection cracks[3].

As periodic overlaying is generally carried out to treat other forms of pavement deterioration, the additional control of reflection cracking is an economic bonus. However, it is only a temporary expedient. The time taken for the reflection cracks to

propagate through the overlay is dependent upon the thickness of the layer and overall structural condition of the pavement.

4.4.13 Reconstruction

Reflection cracks which have not been effectively sealed will allow the ingress of water into the pavement sub-layers with subsequent loss of support and failure of the pavement structure. In this condition reconstruction of the pavement is the conventional solution. However, if failure is limited to sections of the pavement adjoining the cracks local reconstruction techniques may be applicable. Although expensive, a reconstructed pavement is unaffected by the previous crack pattern.

4.4.14 Conclusions

Pavement construction techniques used to inhibit reflection cracking include the use of aggregates with low coefficient of thermal expansion within the lean concrete base, increasing the surfacing thicknesses, employing dense bituminous surfacings with softer, rubberised or polymer additive binders, the use of bond breakers, stress absorbing or cushioning layers and the cracking and seating of the concrete base. Methods used to maintain existing cracked pavements include scarifying and the recycling or replacing of surfacing material, overbanding, surface dressing, overlays and reconstruction.

The crack opening widths between slabs of lean concrete roadbase maybe reduced through the use of aggregates with low coefficient of thermal expansion. Therefore, stresses induced through temperature fluctuations within the roadbase are less likely to result in an overstressing of the bituminous surfacing.

The design life of both semi-flexible and rigid pavement structures may be achieved if a sufficient thickness of conventional bituminous surfacing is used to prevent reflection cracking. However, the thickness of 200 mm suggested by the current design recommendations[1] is excessive when related to other forms of pavement deterioration and is an uneconomic solution.

Thermal reflection cracking can be inhibited by a dense macadam or rolled asphalt with a soft binder as an upper roadbase or base

course.

The recent advent of polymer bitumen binders has shown promising initial results but they have yet to be proven in full scale field tests on semi-flexible pavements in the UK.

The use of thin bond breaking layers has been inconclusive although theoretically they should reduce the rate of crack growth by increasing the gauge length over which the induced strains develop. This treatment, however, adds no increased structural capacity to the pavement and provides no improvement to existing problems concerning voids under the slab ends or reducing differential deflections. Some benefit may be gained where used on existing pavements of rigid construction prior to a structural concrete overlay.

Mild steel mesh is currently being employed in the UK on the M6 motorway as a bituminous surfacing reinforcement using a 175mm mesh. Earlier case studies have shown these larger meshes to be more effective than expanded metal and smaller mesh fabrics. Although field tests on polypropylene materials such as Petromat have failed to inhibit reflection cracking, stretched polypropylene meshes have, under laboratory conditions, been successful in preventing cracking and reducing rutting.

The inclusion of cushioning layers of crushed rock or gravel between roadbase and surfacing or overlay has proved to be successful as a maintenance technique for structural concrete pavements prior to overlaying. A water conduit or reservoir is however introduced between the two major structural layers of the pavement to the detriment of its long term stability. The critical stresses induced within the surfacing or overlay may be increased, dependent upon the modulus and thickness of the cushioning course, leading possibly to earlier failure through fatigue. The technique is expensive due to the large quantity of aggregate required it also increases the elevation of the pavement. Use of this method is limited to open, rural pavements.

The use of a granular base layer overlying a cement bound base with a thin bituminous surfacing is a viable form of pavement

construction and is not susceptible to reflection cracking.

The technique of 'cracking and seating' is regarded as an effective method of crack prevention on overlaid concrete pavements in the United States. This method relies upon good intergranular reaction between the cracked pieces to resist differential vertical deflections. A loss of structural integrity within the concrete slab may, however, require an increased thickness of overlay. Furthermore, the low strength lean concrete roadbases in the United Kingdom would not display the same intergranular reaction as structural concrete pavements and, therefore, could make this method ineffective.

The sealing of cracks using proprietary overbanding products may temporarily prevent moisture from entering the base but does not prevent horizontal or vertical movement, it is expensive and provides only a very brief period of protection.

Surface dressings provide a temporary seal and improve the riding quality of the pavement for a very limited period.

Overlaying or recycling the surfacing material could, if linked to the regular maintenance of surface and structural pavement deficiencies, also provide a cheap solution to reflection cracking, particularly in urban areas.

4.5 AN APPRAISAL OF ANALYTICAL METHODS TO PREDICT THE RATE OF CRACK GROWTH THROUGH BITUMINOUS SURFACINGS

Reflection cracking is one of the most difficult pavement maintenance problems to solve. This form of deterioration is associated with bituminous surfacing overlaying concrete or cement bases of composite pavements. Considerable research has failed to produce a single all-embracing sub-system to design against reflection cracking regardless of its cause and this is a weakness of current design procedures. The requirements of such a cracking sub-system must include analysis of stress concentrations resulting from both temperature associated movements of the cemented layers and traffic loading.

A concensus exists among researchers that these cracks develop from the bottom of the asphalt layers directly above built in expansion

joints or cracks in the cement bound layer. The failure criteria adopted correspond to the appearance of a crack on the surface of the pavement, the crack length in the asphalt being equal to the thickness of that layer.

Most analyses are concerned with either traffic loadings or thermal effects, although several recent research reports combine the two conditions. The Texas Transportation Institute commenced a programme of analysing reflection cracking due to daily thermal cycles in the early 1970s. Schapery [72] developed the theory of fracture mechanics to relate material properties to the two material controlled fatigue constants required to solve Paris' equation:

$$dc/dN = A(\Delta k)^n \qquad \text{- Eqn.(4.1)}$$

where dc/dN = rate of crack growth

Δk = stress intensity amplitude, $\Delta k = k_{max} - k_{min}$ ($\Delta k = k_o$ where $k_{min} = 0$)

A and n = fatigue constants of material (see section 6)

To alleviate the need for complex cyclic testing, Schapery sought to produce the constants from static loading on representative bituminous samples. The material properties used in his theory were creep compliance, tensile strength, and fracture energy, resulting in the development of the expression:

$$A = \frac{\pi}{6\sigma_m^2 I_1^2} \left[\frac{(1 - \nu^2)D_2}{2r} \right]^{1/m} \left[\int_0^{\Delta t} w(t)^{2(1 + 1/m)} dt \right] \qquad \text{- Eqn.(4.2)}$$

and $n = 2(1+1/m)$ - Eqn.(4.3)

where Δt = time period for the cycle (1 day)

r = fracture energy

σ_m = failure tensile stress in the plastic zone ahead of the crack tip

m and D_2 = respectively the slope and the intercept log t = o of the bitumen creep compliance plot

$w(t)$ = the wave shape of the stress-intensity factor

I_1 = a shape function of the plastic zone ahead of the crack tip

ν = Poisson's ratio

The complexities of the mathematical formulae associated with the theory render it impractical for general use in conjunction with a design sub-system.

Experimental investigation of this concept was carried out by Germann and Lytton and published in 1979[73]. Bituminous beams of 25,50 and 75mm deep were subjected to crack propagation tests on an 'overlay tester'. This machine was built specifically to simulate the displacements resulting from temperature changes in cracked or jointed cement bound roadbase materials beneath a bituminous overlay. Overlay samples investigated included samples with fabric known as "Petromat" and those composed of different grades of bitumen, open graded, dense graded and hot sand mixes.

For all mixes, the fracture constants A and n for use with Paris' Law were evaluated both experimentally and using Schapery's theory. Ultrasonic techniques utilizing piezoelectric crystals embedded in the ends of the test samples were used for measurement of crack length. These values were related to a function of stress intensity factor (k), material modulus (E) and crack opening width (u) for a range of overlay thicknesses (d) in the form 2k/Eu versus c/d from the output of a finite element program developed by Barenblatt[74].

The results of the investigation showed poor correlation between experimental and theoretical values of the fracture constants, except for soft grades of bitumen. The experimental values of A were found to be affected by bitumen content and mix grading but were not related to the thickness of the bituminous layer. Bitumen content and the grade of bitumen were the only variables affecting n. However, Germann and Lytton demonstrated a method by which fracture mechanics can be used to predict the fatigue life of bituminous surfacings but this requires complex laboratory testing of representative samples to derive the material constants, A and n.

A further development of this work was carried out by Lytton and Shanmugham [49] who presented a theoretical model based on fracture mechanics but included field data to validate the model and to

account for the change in fracture parameters due to bitumen hardening with time.

Schapery's theory was used for deriving n. (Eqn.4.3), but corrected by dividing by a factor of 2.5. The parameter A was determined directly from n using the relationship:

$$n = - 0.69 - 0.511 \text{ Log.} A. \qquad \text{- Eqn.(4.4)}$$

The poor correlation between theoretical and experimental values of A and n given in the earlier report[73] and somewhat arbitrary factorising of the values of n and hence A, throws doubt on the accuracy of the model.

The effect of hardening of the bitumen when calculating A and n were accounted for by empirical equations relating the change in softening point and penetration to the life of the pavement. The stress intensity factor k, (Eqn.4.1) was determined from the resultant stress levels at the crack tip of predefined cracks (length Yc), from the output of a finite element pavement model and presented in the form:-

$$K = a\,(Yc)^b \qquad \text{- Eqn.(4.5)}$$

where k = stress intensity factor

Yc = crack length

and a and b were derived as best fit coefficients dependent upon the asphalt stiffness, the thickness of the asphalt layers and the change of air temperature below an assumed stress free temperature of 24°C, (75°F).

The model determines the time required for a specified initial crack length to propagate through the total thickness of the asphalt by integrating the Paris equation (Eqn.4.1) for each daily temperature cycle.

The model was run for parameters relevant to thirty two pavements in Michigan; deriving for each a cumulative damage factor, "c", defined as the time for the first crack to appear in the surface. The parameters investigated included material types and properties, layer thickness, temperature variations and pavement life. This last factor was subsequently related to observed cracking and

through application of regression analysis to form a mean cracking index I, given as the sum of the number of transverse cracks per 150m of road.

The model developed is not directly applicable to design but could be used to determine the regression equations required to suit local pavements and conditions.

An analytical study by Ramsamooj[75] applied fracture mechanics to combine the effect of thermal and traffic induced stresses on transverse crack propagation. Both the theory of linear elastic fracture mechanics and that of delayed fracture in visco-elastic materials were used to formulate a method of solution.

The rate of crack propagation due to traffic loading was obtained from the elastic crack growth law given in Equation 4.6 which is an extension of Paris' Equation 4.1.

$$\frac{dc}{dN} = A_1(k_1)^4 + A_2(k_2)^4 \qquad \text{- Eqn.(4.6)}$$

where k_1 and k_2 are the stress intensity factors and A_1 and A_2 are material constants for mode 1 and mode 2 fractures. Mode 1 fracture is induced by a 'tearing' action within the bituminous surfacing and mode 2 by a shear developed within this layer. The various fracture modes are more fully described and discussed in section 6.10.

The problem was simplified by Ramsamooj who only considered the tearing fracture (mode 1) which was suggested to be the more important mode. A further simplification was made by assuming that for the stress intensity factor (k), which is given in Paris' Equation (Eqn.4.1) raised to the power n; n is equal to 4.

The response of a pavement to stresses produced by temperature variations was considered to be visco-elastic in nature and visco-elastic analysis is used in the evaluation. The rate of crack growth with respect to time (t) is given by:-

$$\frac{dc}{dt} = \Delta \psi^{-1} (k_{1c}/k_1)^2 \qquad \text{- Eqn.(4.7)}$$

where $\Delta = \frac{\pi}{8(1-\nu^2)} (k_1/\sigma_y^2)$ - Eqn.(4.8)

ψ^{-1} = inverse compliance function

σy = tensile yield stress of the asphalt

k_1 = stress intensity factor due to temperature stresses for crack length c

k_{1c} = the critical value of k_1 at which rapid growth occurs resulting in catastrophic failure

ν = Poissons ratio

Laboratory testing is required to determine the parameters relating to both traffic and temperature induced cracking.

Complete experimental and field verification is required although a worked example of the model was provided which appears to give reasonable results. The complexity of the theoretical derivations and the assumptions made in the calculations of crack propagation rates induced by traffic exclude it from use in a simple design procedure. Furthermore, Ramsamooj reports $k_1 = 0$ when $c = 0$ for temperature induced stresses. This is incorrect since, for reflection cracking, the crack in the cement bound layers would induce stress concentrations in the overlay even before crack initiation.

Based on a two dimensional finite element model, BIFIS, Marchand and Goacolou[76] provide a theoretical study into the influences of the parameters governing the behaviour of a pavement subjected to reflection cracking.

The model uses fracture mechanics with a conventional finite element grid to represent the structure remote from the crack, together with a special crack tip element. The investigation includes three loading conditions, thermal movement of the roadbase, vehicle loading offset from the crack and vehicle loading centred on the crack. A design method using the model is proposed in which the crack propagation times are calculated taking into account the most probable crack path. Three possibilities are considered as shown in fig. 4.2. A stress intensity factor versus the number of load applications (N) is plotted for each case, and used to integrate Paris' law (Eqn.4.1). However, no values of

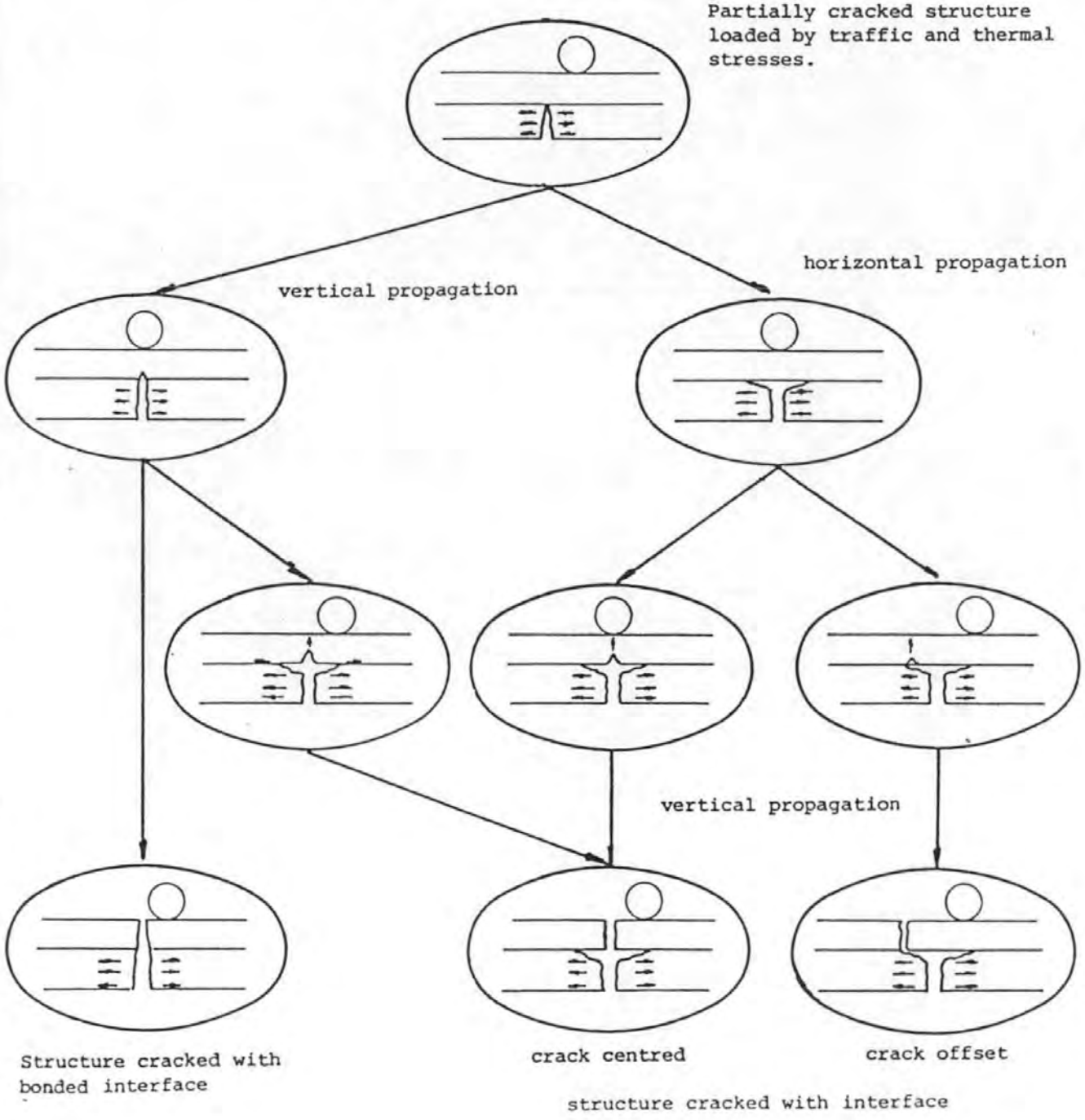

FIG.4.2 PROGRESSION OF HORIZONTAL AND VERTICAL CRACKING (AFTER MARCHAND AND GOACOLOU) [76]

fracture parameters are presented.

A simple application of the model is described in which the deflection and radius of curvature response of cracked and uncracked pavement are compared. The BIFIS model, with an uncracked roadbase, was initially matched to a conventional linear elastic multilayer programme. Increments of crack length were then introduced into the roadbase and comparisons made between the uncracked and cracked state for various bituminous layer thicknesses, with respect to surface deflection and radius of curvature. These values were subsequently plotted against layer thickness for a given crack length. In general, deflection was found to increase by about 28%, and radius to decrease by about 65% of the uncracked values.

A field calibration of an overlay design procedure to prevent reflection cracking is given by McCullough and Seeds[77] providing simple analysis in the form of a computer program (RFLCR). The programme basically consists of two failure modes for reflection cracking:-

1. an opening mode due to horizontal movements of the existing pavement due to temperature changes.
2. a shearing mode resulting from inadequate load transference across a joint or crack.

In developing the model a number of simplifying assumptions have been made. These include the static equilibrium of all forces acting on the pavement, linear elastic behaviour of all materials, uniformly distributed temperature variations in the cement bound slab and considering concrete slab movement to be continuous with slab length and uniform with depth. The basic outputs are the shear strain in the bituminous surfacing due to to traffic loading and tensile strains caused by thermal movement.

Input data of temperature and slab length are determined from observed field measurements of the horizontal slab movements which account for the frictional forces between the cement bound layer and granular sub-base. The method, however, only defines the pavement performance due to a single fall in temperature. In reality, the pavement will be subjected to both seasonal and daily

variations with the majority of damage being concentrated into periods of the most adverse temperature conditions.

Differential movements across the cracks caused by traffic are determined from field measurements using conventional methods. The movements are used to defined the load transfer across the crack. Formulae are presented which allow the shear strains developed in the overlaid pavement to be calculated for particular design loads. These strains are given as a function of the design wheel load and its width, and the dynamic stiffness, thickness and Poisson's ratio of the overlay. The number of load applications that will produce a level of 50% reflection cracking is determined from a fatigue relationship.

A sensitivity analysis presented indicates the influence of the dynamic stiffness of the overlay material on the shear strain. The determination of overlay performance from a single estimate of stiffness, for a given temperature, represents a weakness of the method.

Researchers have generally assumed that reflection cracking initiates at the base of bituminous layer and propagates upward. However, Majidzadeh and Suckarieh [78] suggest that reflection cracks appear in the surface of bituminous surfacing shortly after construction and propagate downwards. The reflective cracks are therefore considered to be mainly caused by horizontal temperature movement and vertical curling of the slabs after surfacing. Their study of the temperature distribution within the cement bound layer showed a steep thermal gradient to exist for some five to nine hours after overlaying with asphalt. Subsequent cooling induces contraction of the slabs, crack openings and tensile stresses in the bituminous surfacing.

Using a two dimensional finite element programme, they[78] presented nomographs relating the joint or crack width, surfacing thickness and modulus to stresses in top and bottom of the bituminous overlay (figs. 4.3 and 4.4) for the horizontal movements. A similar approach was adopted with the warping stresses inducing a vertical movement. A stress distribution was subsequently derived for various crack opening widths and overlay

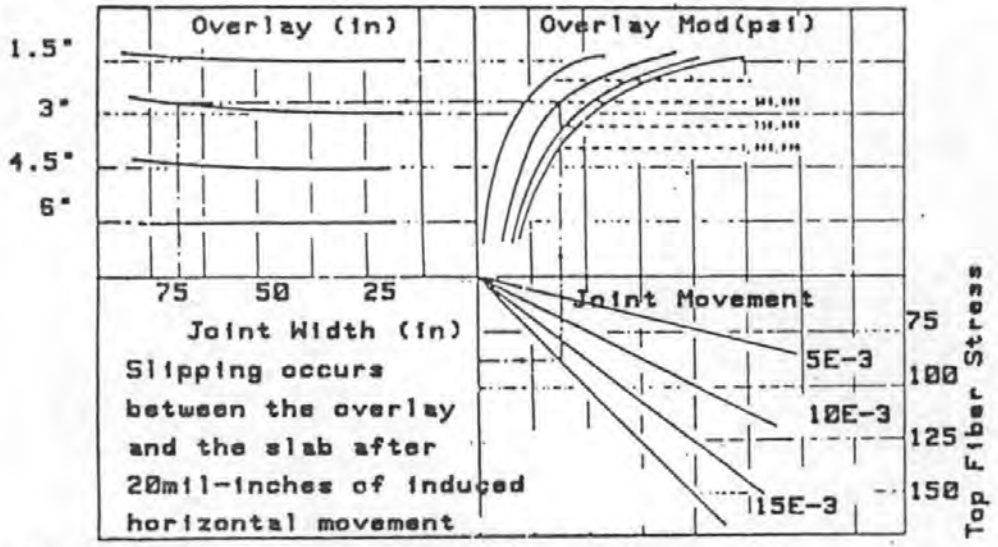

FIG.4.3 TOP FIBRE STRESS IN OVERLAY DUE TO J.R.C.P. JOINT MOVEMENT

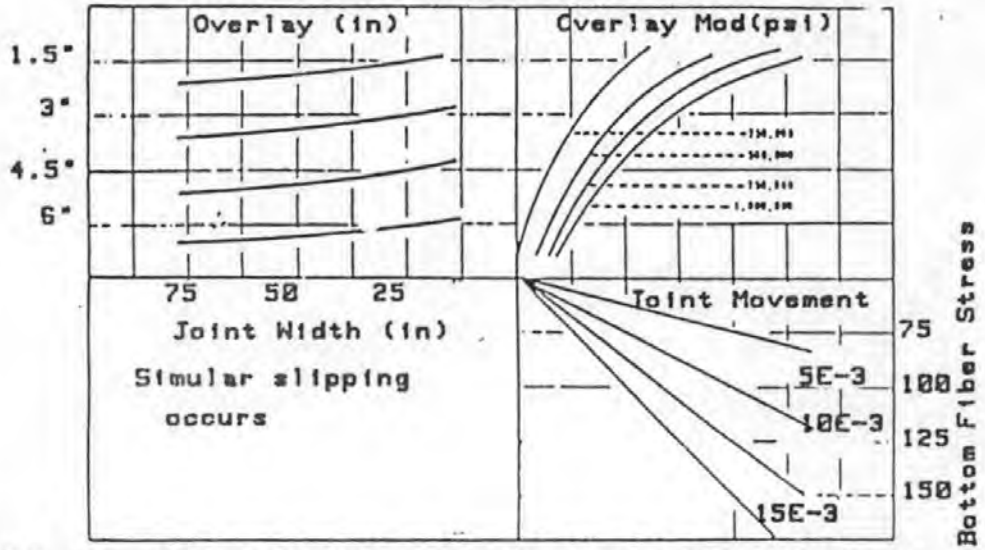

FIG.4.4 BOTTOM FIBRE STRESS IN OVERLAY DUE TO J.R.C.P. JOINT MOVEMENT

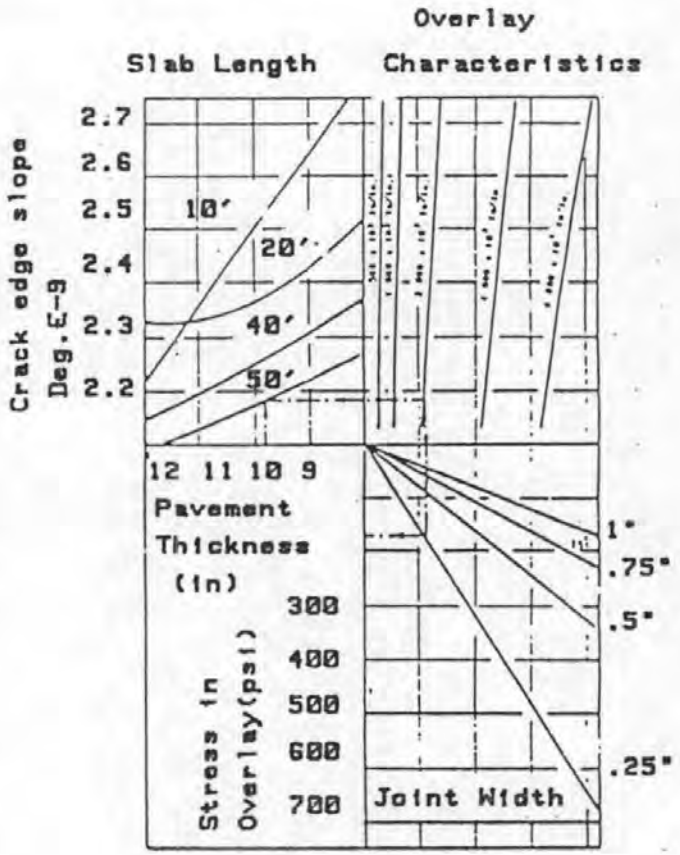

FIG.4.5 MAXIMUM STRESS IN OVERLAY DUE TO 1 DEG. F TEMPERATURE DIFFERENTIAL IN A RIGID PAVEMENT

(AFTER MAJIDZADEH AND SUCKARIEH) [78]

thicknesses (fig.4.5) and the following conclusions made:-

1. the effect on the stress in the overlay of changing the modulus of elasticity and the thickness of the concrete slabs is negligible,
2. horizontal movement of the joint and induced stresses in the surfacing are directly related,
3. the maximum shearing stresses (τmax) in the asphalt tack coat varies from 42 - 70 kN/m^2 (6 -10 psi) for a range of temperatures.

Therefore, it was assumed that if the stresses in the bonding layer exceed 70kN/m^2 (10psi), horizontal joint movement will transfer no more stress to the overlay but slipping will occur between the pavement and the overlay.

Elastic analysis used in the finite element program cannot model relaxation of the bituminous surfacing which tends to reduce the tensile stresses derived. Furthermore Majidzadeh and Suckarieh imply that compression occurs in the bottom of asphalt layers due to warping but the temperature differential across the slab will induce tension across the entire depth of overlay. The suggestion that cracking initiates in the surface based on curling of pavement slabs is not substantiated by stress distributions derived by other researchers [76,77,79]. It is feasible, however, that more than one mechanism operates which may cause cracking to either propagate upwards or downwards depending upon the predominant mechanism.

4.5.1 Conclusions

The majority of analytical methods described cannot be applied easily as a design procedure.

The series of reports from Texas A and M University[48,49,64] offer some interesting and original ideas concerning the application of fracture mechanics but display both the strength and weakness of the concept. Lytton and Shanmugham[49] show how fracture mechanics need not be limited to the consideration of a single crack in a pavement, but may be applied in a wider form to describe the cracking in entire highway projects. The inability to satisfactorily predict the fatigue constants, however, remains a disadvantage with the use of fracture mechanics.

Opinions differ as to the relative importance of the different fracture modes although both the opening and shearing modes are included in the models presented by McCullough and Seeds[77] and Marchand and Coacolou[76] but only the latter considers the possibility of debonding between cemented layers and surfacing.

Although analysis of differing facets of the reflection cracking phenomenon have been outlined there is still no proven method of analysis which allows an accurate prediction of the life of bituminous surfacing or bituminous overlay.

5.0 AIMS AND OBJECTIVES OF THE INVESTIGATION

An understanding of the mechanisms involved in the development of reflection cracking is essential to allow predictive analytical models to be established for this form of deterioration.

Analytical models provide a method for estimating reliably the fatigue life of surfacings overlying cement bound roadbases. Use of such models will also allow comparisons to be drawn as to the effectiveness of using differing structural designs, mix designs and material types, to inhibit the deterioration associated with the development of reflection cracking.

Present design codes do not predict this form of cracking and guidelines are limited simply to increasing the depth of surfacing material. Although this approach may prove to be successful, the resulting pavement may be overdesigned with respect to other design parameters and is also unlikely to represent the cheapest solution to prevent reflection cracking.

The objective of this research is to build upon the groundwork provided by previous studies [76,77,78,79,80] and define design criteria to inhibit reflection cracking.

These studies have defined three mechanisms which cause reflection cracking in composite pavements; their significance is discussed in section 4.3. They are:

i) Tensile fatigue of the bituminous layer through daily and annual thermally induced movements within the roadbase.

ii) Tensile yield of the bituminous surfacing caused by a combination of thermal contraction and warping of the uppermost structural layers.

iii) Shear fatigue induced from shear stresses in the surfacing materials generated by vertical differential movements between adjoining slabs under the action of traffic.

The design method and criteria defined are based on the results from laboratory simulation of the three mechanisms evaluated using fracture mechanics theory supported by field data. A finite element model has been used to enable the laboratory based study to

be extended to predict full scale pavement behaviour. In addition, the influence of individual mix parameters on the overall performance of the asphalt under the action of the three mechanisms has been determined. This allows the design method to be presented in a format that can be easily implemented.

The versatility of the design system will be enhanced by incorporating the results within a computer package to allow the effects of a large number of mix design variables to be assessed quickly and easily.

The investigation considers these mechanisms acting both in combination and isolation. A mix design of a bituminous surfacing to inhibit reflection cracking may therefore be a compromise between the requirements of the various mechanisms.

In addition to developing a design method for conventional asphalt mixes an investigation has been made into the use and benefits of incorporating (i) polymer based bitumen additives to modify the elastic properties of asphaltic materials and therefore increase their resistance to tensile fatigue, and (ii) geogrids as a stress relieving interlayer. This extension of the investigation has been made as the use of these new materials may produce an alternative and cost effective solution to the reflection cracking problem.

6.0 MECHANISM OF TENSILE FATIGUE

6.1 INTRODUCTION

Although extensive research programmes have been carried out to investigate the phenomenon of reflection cracking a method has yet to be derived that enables the fatigue life of the bituminous surfacing layer to be predicted under conditions which produce reflection cracking. The development of a comprehensive method has been restricted by the complexity of the phenomenon which involves three separate mechanisms. The only practical approach is to investigate and analyse each mechanism separately to define the circumstances under which each occurs and assess their relative significance. This section describes the laboratory/library investigation of the tensile fatigue mechanism.

6.1.1 The Mechanism

Tensile fatigue cracking occurs in the bituminous surfacing as a result of thermal fluctuations within the lean concrete roadbase. Cracking initiates at the roadbase/surfacing interface and propagates upwards to the surface.

The roadbase, laid continuously without joints, cracks into slabs during curing and prior to being overlaid by a bituminous surfacing. Crack opening, between adjacent slabs, occurs as a result of thermal contraction.

The magnitude of the crack opening may be calculated as the product of the length of slab, coefficient of contraction of the cement bound material and temperature change within the roadbase. It is assumed that the adjacent slabs are equal in length and that each roadbase slab will expand and contract about its centre. Furthermore, it is assumed that the roadbase cracks never close, which is valid for roadbases laid in the summer or for roadbases that undergo some shrinkage either during curing or in the longer term.

Expansion and contraction of the roadbase slabs will induce tensile and compressive stresses within the overlaid surfacing which forms, at least initially, a continuous layer over the roadbase discontinuities. A bituminous emulsion is usually applied to ensure a bond between the bituminous and cement bound layers which is

assumed to remain intact right to the cracks. However, debonding of the layers may occur if the emulsion yields with a consequent reduction in the stresses transmitted between them.

In the analysis of this mechanism it is assumed that the stiffness of the surfacing under daily cyclic loading is so low that it is does not restrain the thermal contraction of the roadbase. However, contraction may be partially restrained by the sub-base.

6.1.2 Development of a Predictive Model

Under the mechanism of tensile fatigue the thermal stresses can be characterised by a daily cycle of horizontal crack opening movement between roadbase slabs. This condition may be simulated by applying horizontal displacements to the base of the asphalt beams in the laboratory rather than by the use of temperature differentials. The surfacing adjacent to the roadbase crack is of major interest and laboratory simulation may be confined to this region for modelling purposes.

The thermal cycle of 24 hours can be accelerated by using the concept of bitumen stiffness as a reduced parameter to combine the influence of asphalt viscosity and loading time. Using this concept, the stress level induced in the laboratory surfacing material is consistent with that induced under thermal loading in the full scale pavement[73]. These stresses may be determined precisely, and subsequent crack growth monitored, to provide the input data for finite element analysis of the crack tip stress. This approach has been combined with Paris' fracture theory[81] to expand the laboratory fatigue results and provide an estimation of fatigue life for various conditions of temperature regime, roadbase slab length, depth of surfacing and material characteristics.

The influence of these parameters on surfacing mixes currently specified in the U.K. has been investigated and the extension in fatigue life which may be derived from modifications in mix design and compaction levels has been quantified.

In developing a predictive model of the tensile fatigue mechanism, practical and theoretical considerations detailed by other researchers have been considered and where appropriate, combined with

test and field data relevant to U.K. conditions and pavement construction.

6.2 LABORATORY SIMULATION OF THE TENSILE FATIGUE MECHANISM

6.2.1 Tensile Fatigue Test Rig

The test rig, shown in fig.6.1 and plate 2, was developed to simulate the daily and annual horizontal displacements of a cracked cement bound roadbase overlaid by a bituminous surfacing under variations of cyclic ambient temperature.

Cyclic sinusoidal movements are induced in two base plates simulating two adjacent slabs of a cracked roadbase section. These produce a crack opening between the butted slab ends which represents the crack opening produced by thermal changes in the roadbase. Adoption of the theory of equi-bitumen stiffness (described in section 6.5) allows the input cycle to be accelerated so that an amplitude equivalent to an annual cycle is provided at a frequency of reasonable time period (10^{-5} to 10^{-3} Hz). Superimposed on this annual cycle are 365 cycles equated to daily temperature fluctuations. An example of the combined wave form is illustrated in fig.6.2 with details of the maximum frequency and maximum peak to peak amplitude of the individual wave forms.

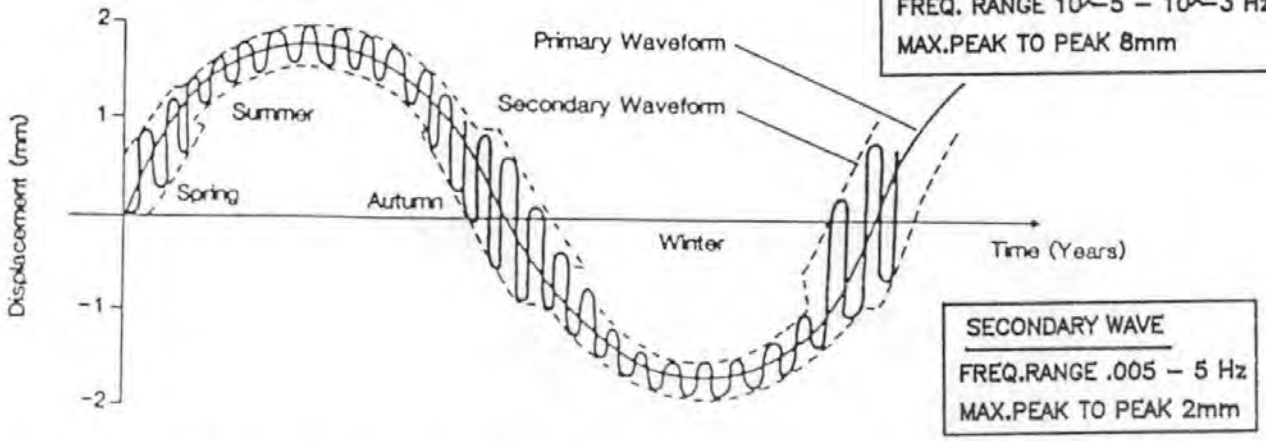

FIG.6.2 INPUT DATA SIMULATING BOTH DAILY AND ANNUAL EXPANSION AND CONTRACTION OF THE ROADBASE DUE TO THERMAL VARIATIONS

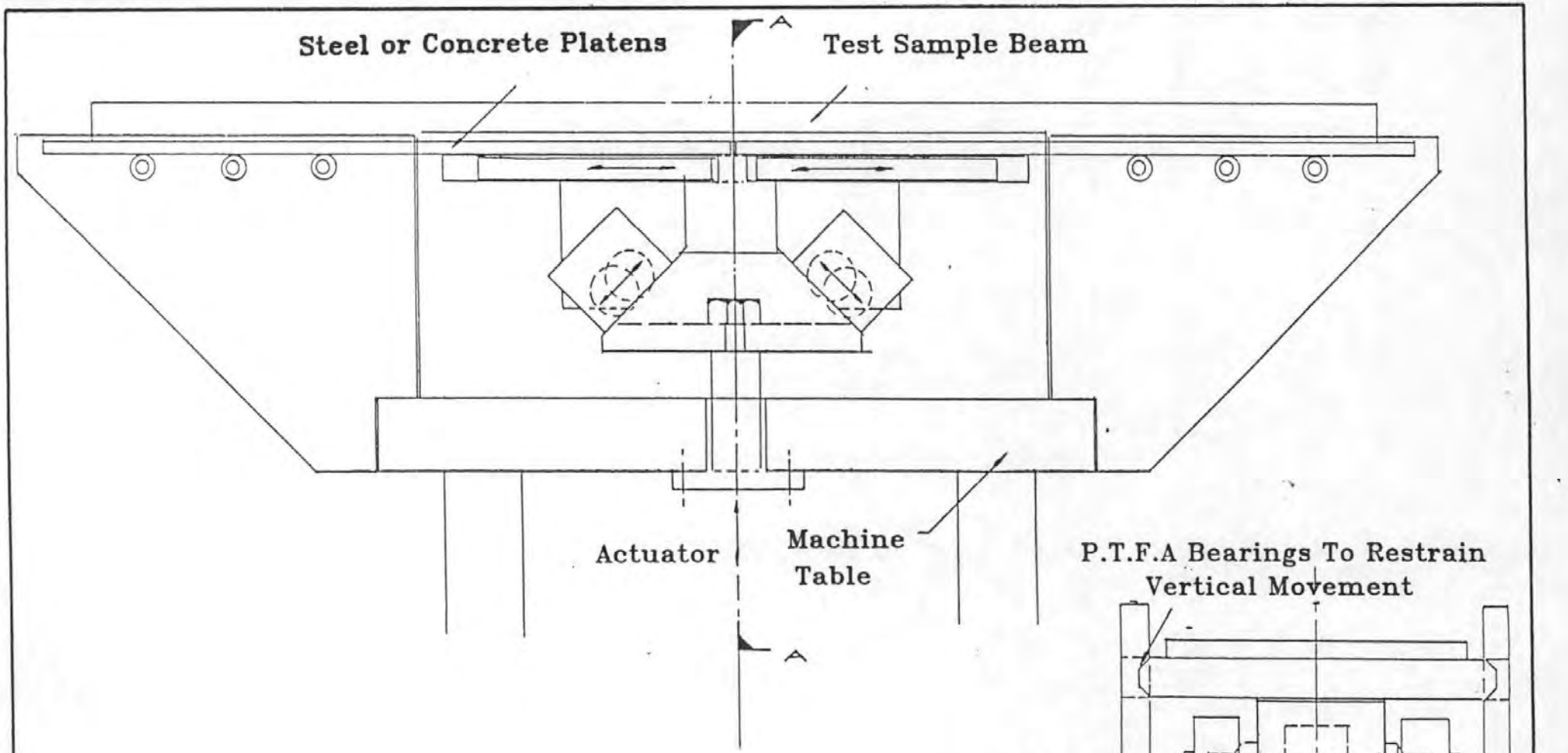

FIG.6.1 ELEVATION ON THERMALLY INDUCED REFLECTION CRACKING SIMULATION RIG

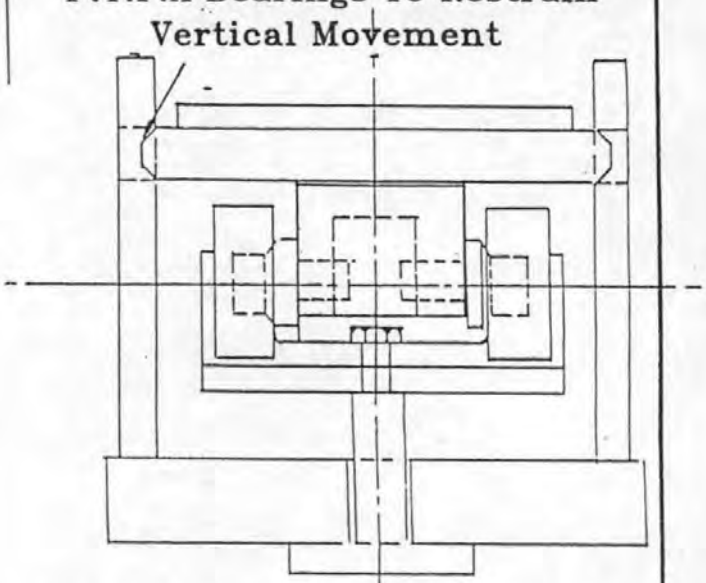

SECTION A–A WEDGE SYSTEM

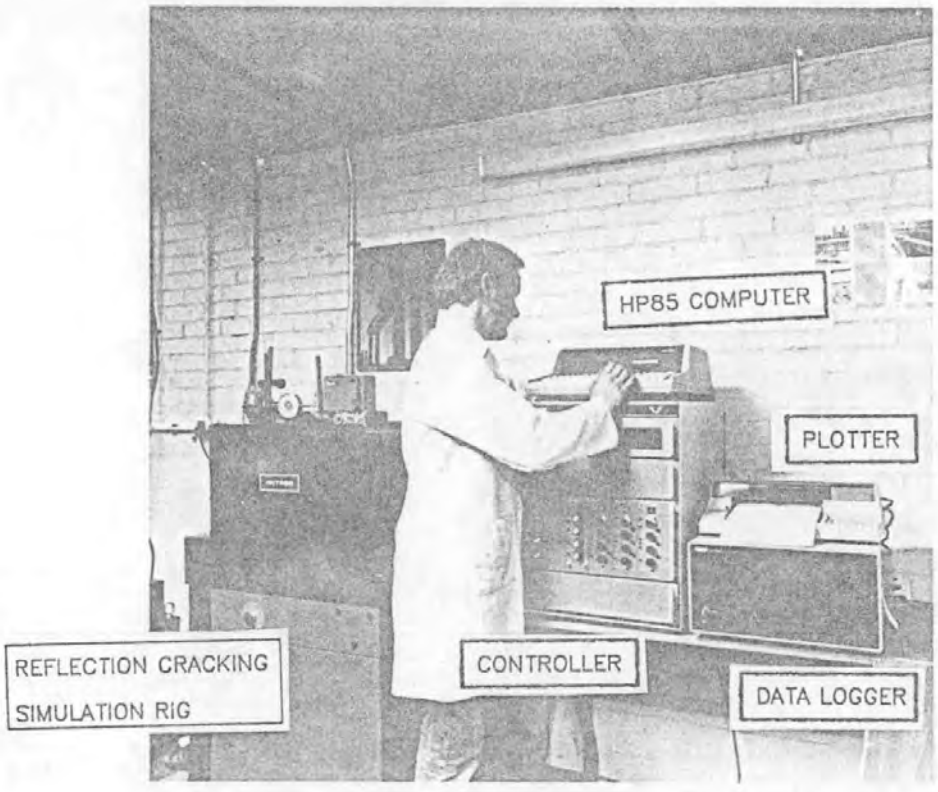

DATA LOGGER AND RIG CONTROL SYSTEM

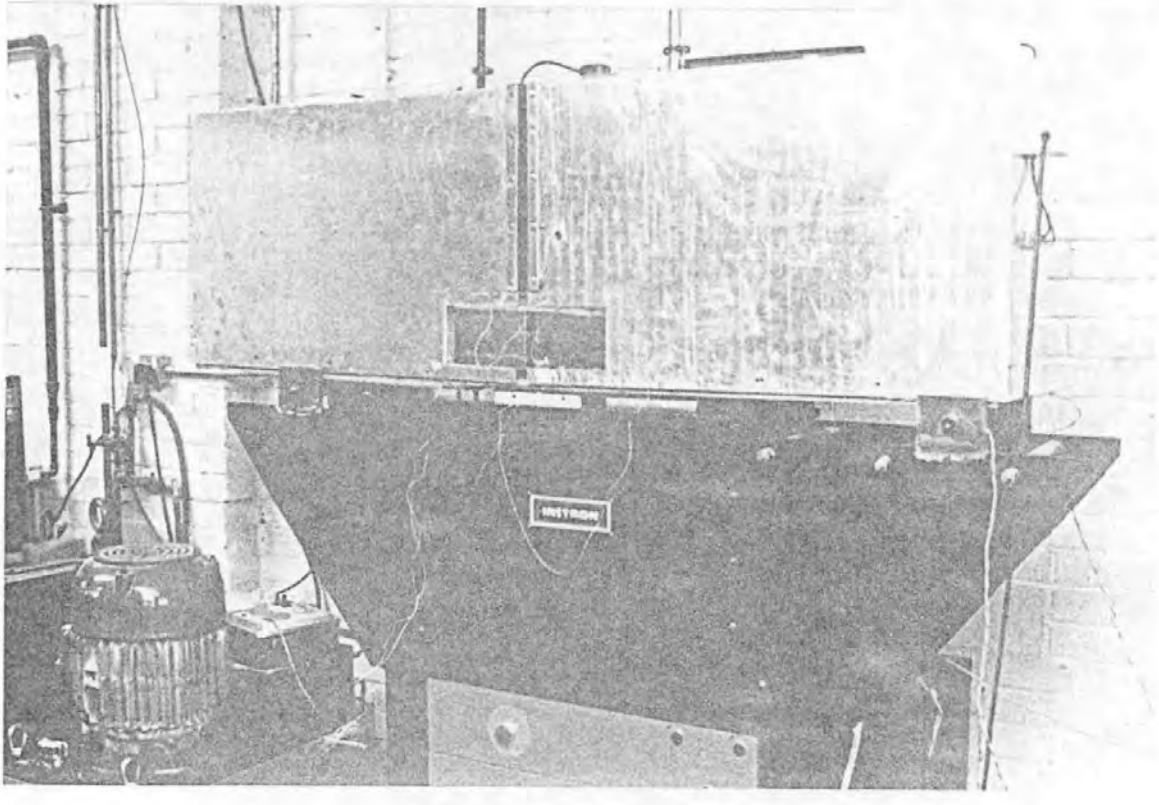

TEMPERATURE CONTROL CABINET

PLATE 2 TENSILE FATIGUE TEST RIG

The horizontal displacements are generated by a 10kN capacity hydraulic actuator mounted vertically below the modified worktop of a standard fatigue testing frame. The actuator head or ram acts upon the base of a wedge arrangement which converts its vertical stroke to a horizontal displacement. The uppermost surface of the wedges are vertically restrained through PTFA bearing plates at the sides of the assembly which effectively prevented upward movement while allowing horizontal freedom. A load cell is mounted between the bearing plates and calibrated to a maximum load of 10 kN. This cell measures the shear force between the wedges and steel platens and is unaffected by frictional losses within the actuator, wedges or the PTFA bearing plates.

A hydraulic actuator controlled through a servo valve was incorporated to ensure a constant crack opening width regardless of crack length. The initial loading on the first cycle before any cracking had been induced into the beam was found to be approximately 3kN. The exact value depended upon the stiffness of the bituminous mix, but in all cases was well below the 10kN maximum load available.

6.2.2 Control System

The test frequency and amplitude of crack opening are controlled by an HP 85 computer linked through a data logger which serves also as a digital to analogue converter, plate 2. The computer facility allows the frequency (Hz) and amplitude (mm) of the primary wave form (annual cycle) to be defined with a subsequent input of 365 secondary wave forms (daily cycles) to be superimposed on it.

The HP control program is written in such a way that the primary wave form is sub-divided into a maximum of 122 step increments with a smooth transition between each step. A minimum of three secondary cycles are then completed at each step prior to progressing to the subsequent one. The amplitude and frequency of these secondary cycles are confined to four levels corresponding to the seasons.

The control program was produced originally by the manufacturers of the system but amended subsequently to suit the individual requirements of the test regime. A copy of the final program is given in Appendix 6.

6.2.3 Test Arrangement

The test arrangement simulates a cracked roadbase section overlaid by a bituminous surfacing into which horizontal cyclic strains can be induced through sinusioidal displacement of platens. The platens, constructed from 12 mm steel plate, are butted together prior to testing and bolted to the uppermost surface of the test rig wedges; as illustrated in plate 3. Epoxy resin (Araldite 2005) is used to adhere sample beams of bituminous surfacing material to the plates.

To enable two tests to be carried out on each beam three platens are used. These are labelled in plate 3 as platens A and B (end platens), and C (mid platen). While testing is in progress using one end platen and the mid platen, (position 1; plate 3) the remaining end platen is clamped rigidly to the mid platen to prevent differential displacement between them. On completion of the first test the platen clamping system is reversed, releasing the originally clamped end platen. The entire platen system is moved, adjusted and bolted to allow a further test on the beam at position 2; plate 3.

Evidence from cores taken through composite pavements indicates that a good bond normally occurs between the roadbase and the surfacing. However, the use of steel platens and epoxy resin creates a perfect, rather than a good bond, which may not accurately simulate field conditions. The effect on the fatigue life of using a perfect bond was evaluated by including control tests in which the steel plates and epoxy resin were replaced with concrete platens and a layer of bitumen emulsion.

The concrete platens, consisting of a high strength concrete mix and reinforced with wire mesh, received a coat of cathodic bitumen emulsion applied at a rate of 1.3 lts/m^2 prior to being butted together and forming the base of the compaction mould on which the beam samples were prepared in the normal way.

6.3 INSTRUMENTATION AND DATA LOGGING

6.3.1 Introduction

To enable test results to be analysed using the theory of fracture mechanics it is necessary to define the rate of crack growth per

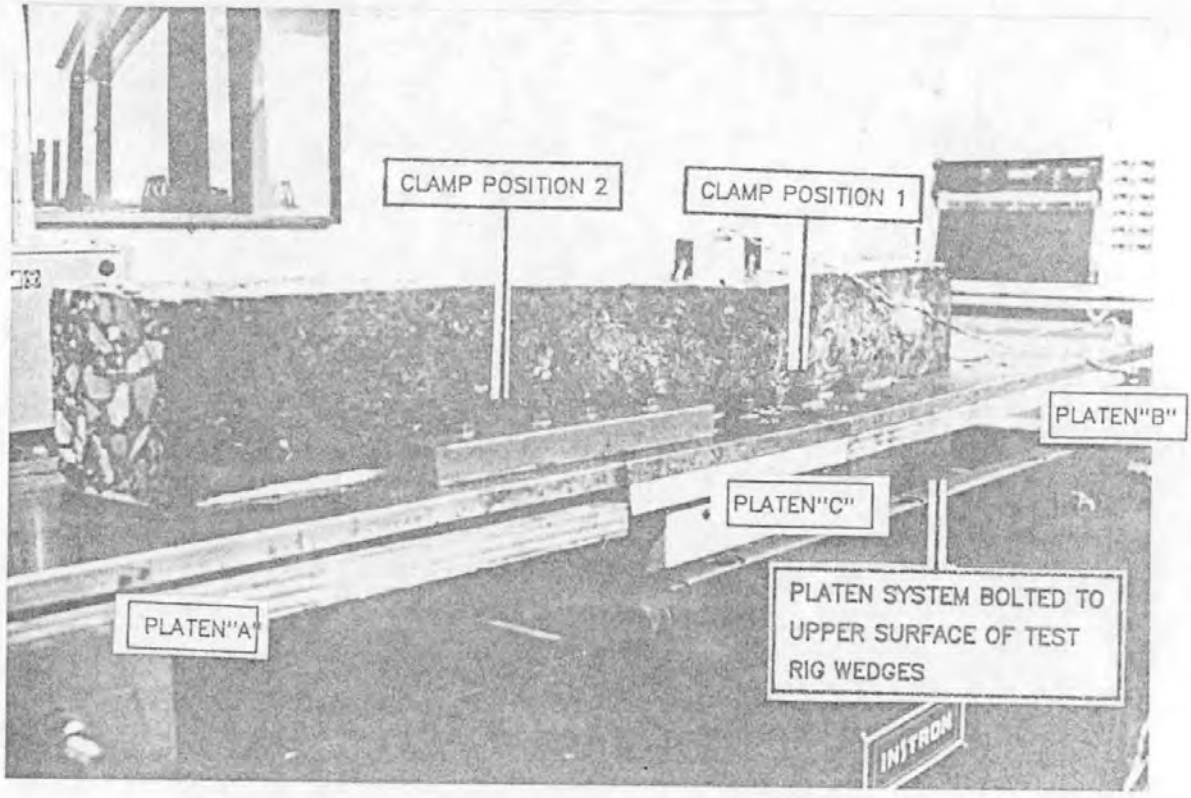

SAMPLE BEAM MOUNTED ON STEEL PLATENS

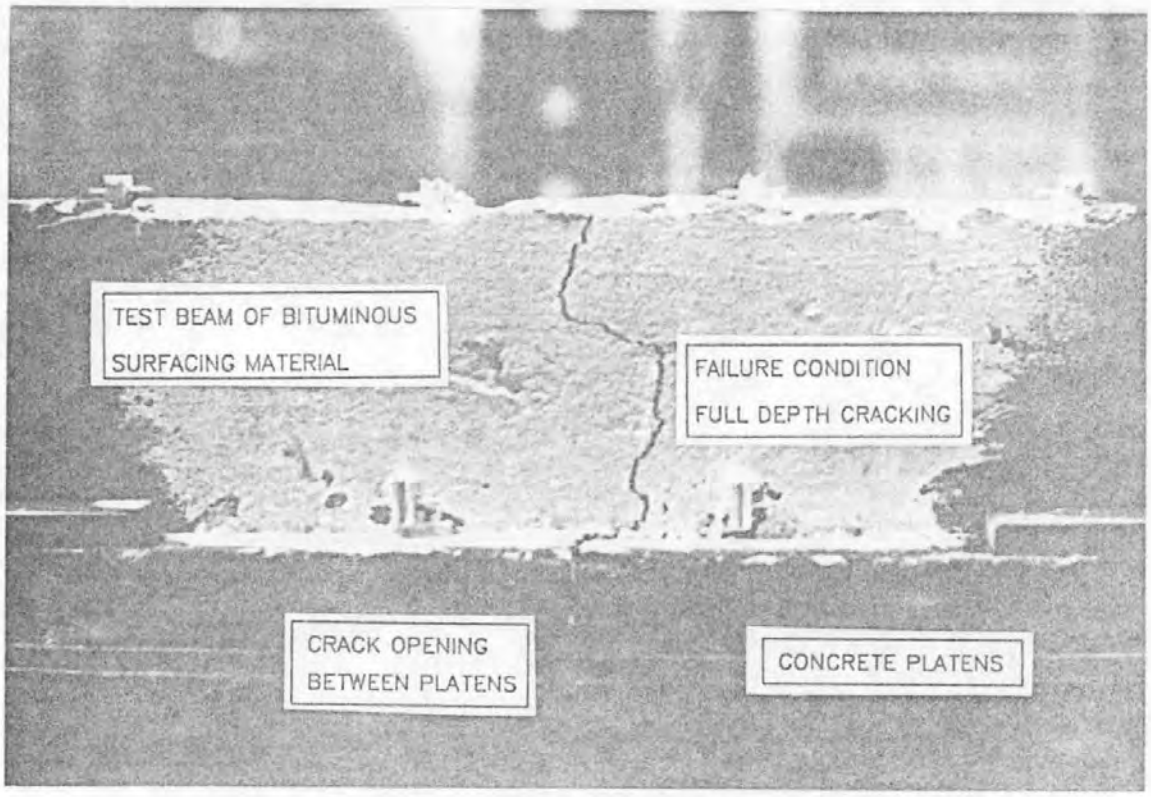

FULL DEPTH CRACKING OF BITUMINOUS TEST BEAM

PLATE 3 TENSILE FATIGUE TEST RIG

stress cycle within the bituminous test beam. Instrumentation has been developed [82] to monitor continuously the position of the crack within the beam throughout the test.

Fatigue testing of the asphalt beams involves long term testing with individual tests lasting for up to 3 days. To produce an efficient testing regime an automatic data logging system has been developed.

6.3.2 Instrumentation of the Sample Beams For Crack Growth

Two independent systems have been developed[82] to monitor crack growth.

Direct crack measurement was obtained by adhering to the surface of the sample a gauge of many foil strands backed on suitable paper, Plate 4. The strands were secured horizontally across the induced crack path and each strand wired as an individual circuit to a switch logic gate. The output of each gate was connected to a resistor bank so that the failure of a strand resulted in a step voltage decrease. The failure of a given strand therefore located the crack tip.

The gauge was of simple construction and easily wired prior to testing, using a spring loaded connector strip with the system powered by a standard D.C. supply.

The second system developed was used in conjunction with the displacement output of a finite element simulation of the asphalt beam. The procedure is described in section 6.3.4. The instrument, shown in fig.6.3 and plate 5 was designed for the measurement of horizontal displacements. It incorporates four 120 ohm strain gauges adhered to a thin copper portal frame. Under the normal test procedure two frames are used, one mounted on the uppermost surface of the test beam, the other across the crack opening between the steel or concrete platens. The mountings consisted of aluminium 'feet' notched out to receive the portal frame and provide a simple support connection. The base of these mountings was adhered rigidly to both the beam surface and platens by use of epoxy resin. These frames absorbed a negligible stress in comparison to the stresses being transmitted to the beam throughout the test.

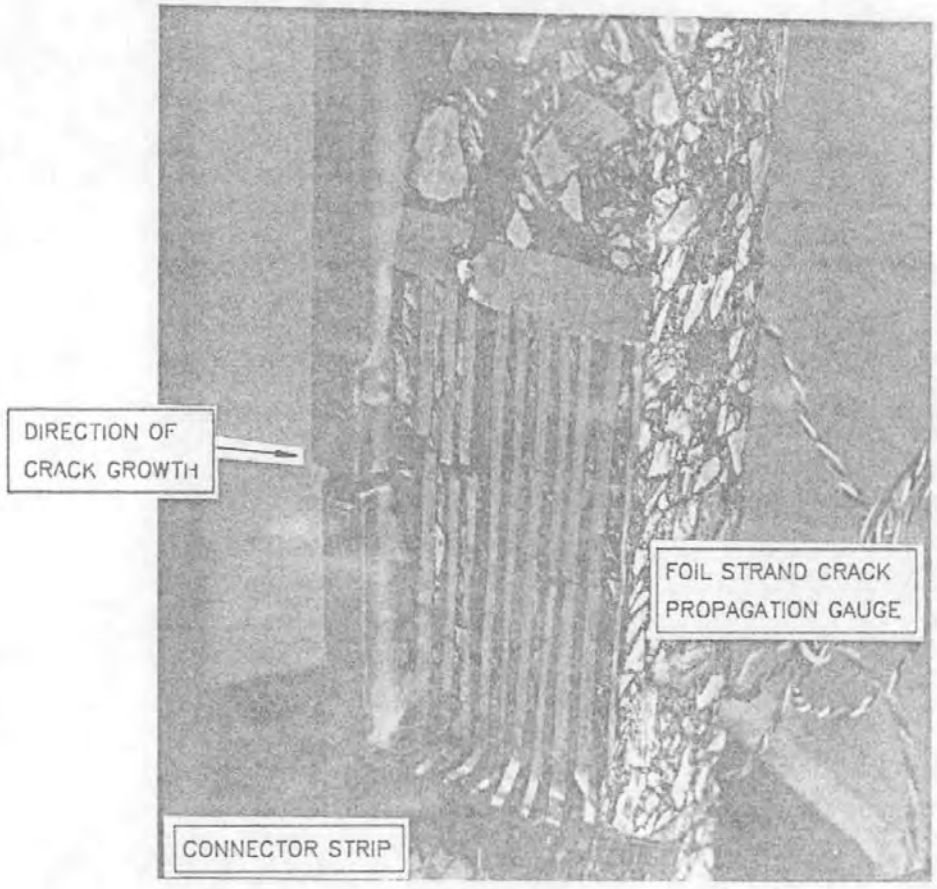

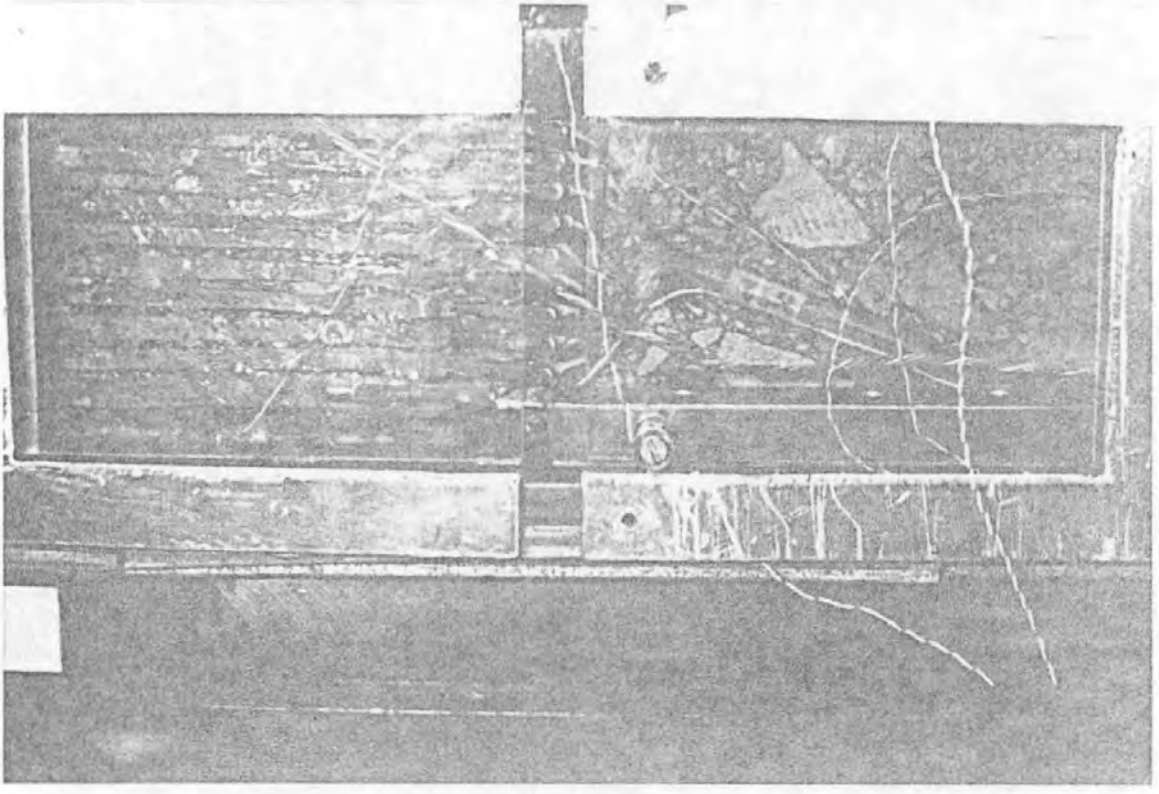

FAILURE OF FOIL STRANDS LOCATING CRACK TIP

PLATE 4 CRACK PROPAGATION GAUGES

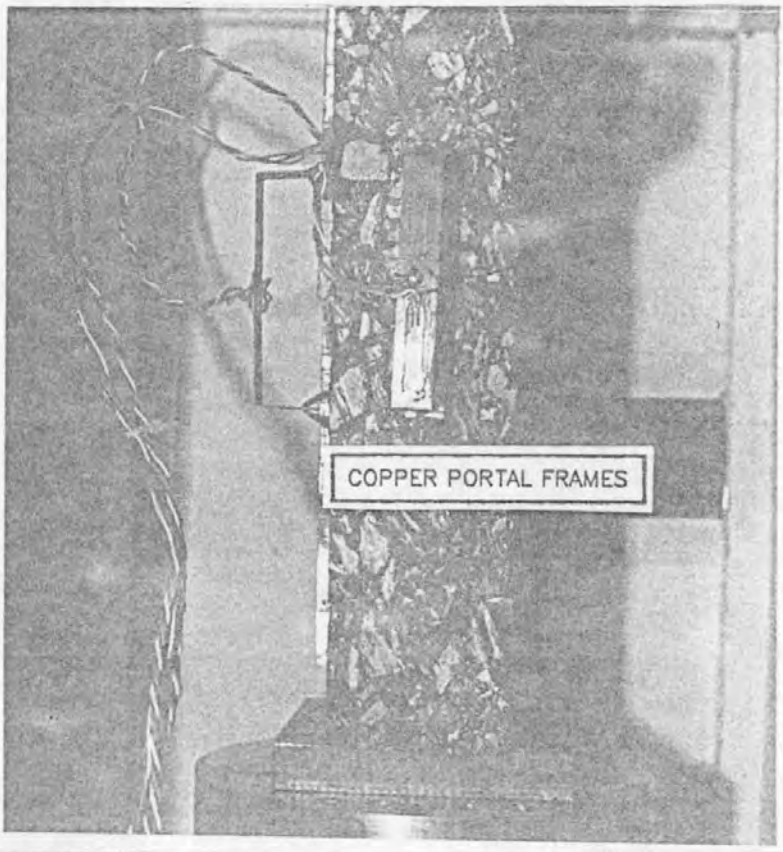

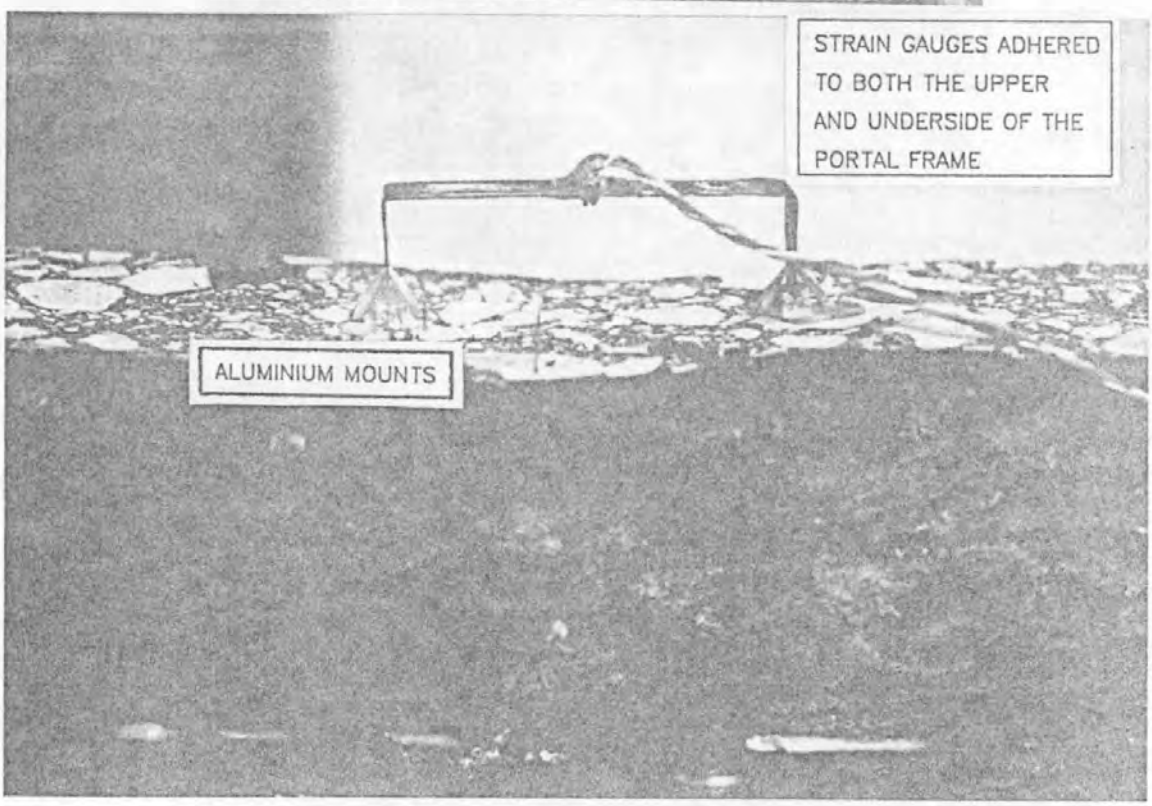

STRAIN GAUGES ADHERED TO COPPER PORTAL FRAMES TO MONITOR CRACK GROWTH

PLATE 5 PORTAL FRAME GAUGES

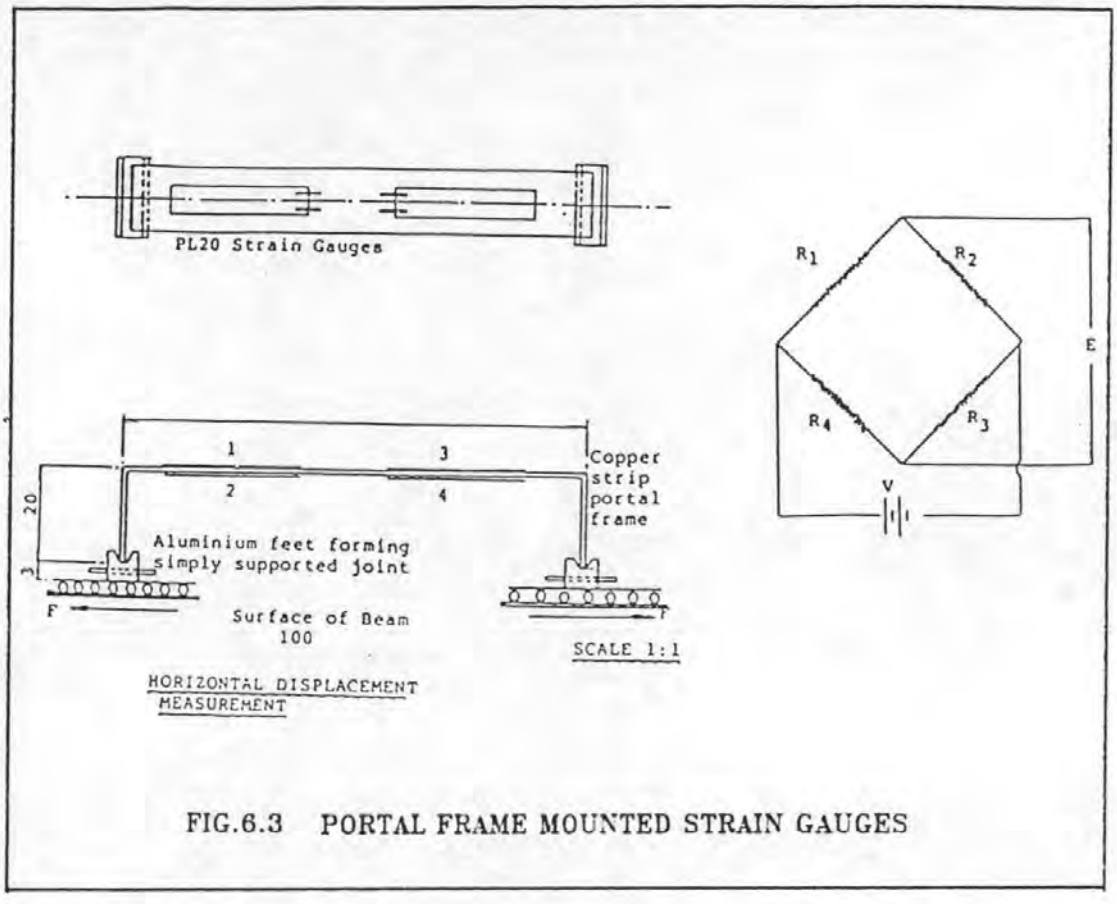

FIG.6.3 PORTAL FRAME MOUNTED STRAIN GAUGES

The four arm bridge used for these gauges was adopted principally for the level of sensitivity it achieved but also because it allowed automatic temperature compensation between the gauges. The amplified output allowed displacements to be measured to an accuracy of 0.1mm.

The test procedure induced strains into the test beam which displaced the frame mountings and produced a voltage change across the Wheatstone Bridge. The trace output from the gauge on the beam surface was compared with that from the gauge across the two platens, for which the horizontal displacement was known. This allowed the displacement on the beam surface to be calculated. Hence, the output from the gauge on the beam surface was automatically calibrated against the output of a similar gauge of known displacement. Periodic checks were made on the gauges to ensure compatible displacement/voltage output characteristics.

6.3.3 Automatic Data Logging

Two alternative methods have been established to record the output

from the crack propagation gauges.

The first method involved a Solartron 'Orion' data logging unit to record the output from the strain gauges, applied cycles and loading. To reduce the quantity of data, the strain from the initial 100 crack opening cycles was recorded and thereafter strain was logged at a set interval of cycles, programmable prior to the start of the test sequence. Programme control was achieved through the HP85 computer; the computer was used also to analyse collected data at the end of a test.

The second method relied upon strain gauge excitation through a bank of amplifiers with the output voltages being recorded graphically on a time base multi- channel plotter. This latter method was adopted for the majority of the tests and recorded the strain from every cycle. The calibrated output voltage from the load cell was also recorded on the plotter.

6.3.4 The Derivation of Crack Length

Data relating crack length to the horizontal displacement on the uppermost surface of the test beam was obtained from the displacement output phase of a finite element model simulating the test arrangement . These displacements, recorded for defined increments of crack length, were used in conjunction with the data derived from the surface mounted strain gauge to locate the crack tip throughout a test. The output for an elastic analysis is given in fig.6.4 for a bituminous sample beam of 100mm depth. However, the linear elastic approach to crack measurement is over simplistic as plasticity ahead of the crack tip is neglected. The effect of viscous flow, modelled by Dugdale[106], is shown in fig.6.5. His work provided the basis for a corrective procedure to allow for the yielded plastic region ahead of the crack tip.

For each increment of crack length the strain,(Er), at nodes ahead of the crack was obtained from the output of the finite element model. Fig.6.6 shows the strain ahead of the crack plotted against various crack lengths within a 100mm surfacing layer. A plastic zone was defined as the distance ahead of the crack which exhibited a strain greater than that of the yield strain of the bituminous mix; fig.6.7. Yield strain of the mix was established from tensile creep testing,

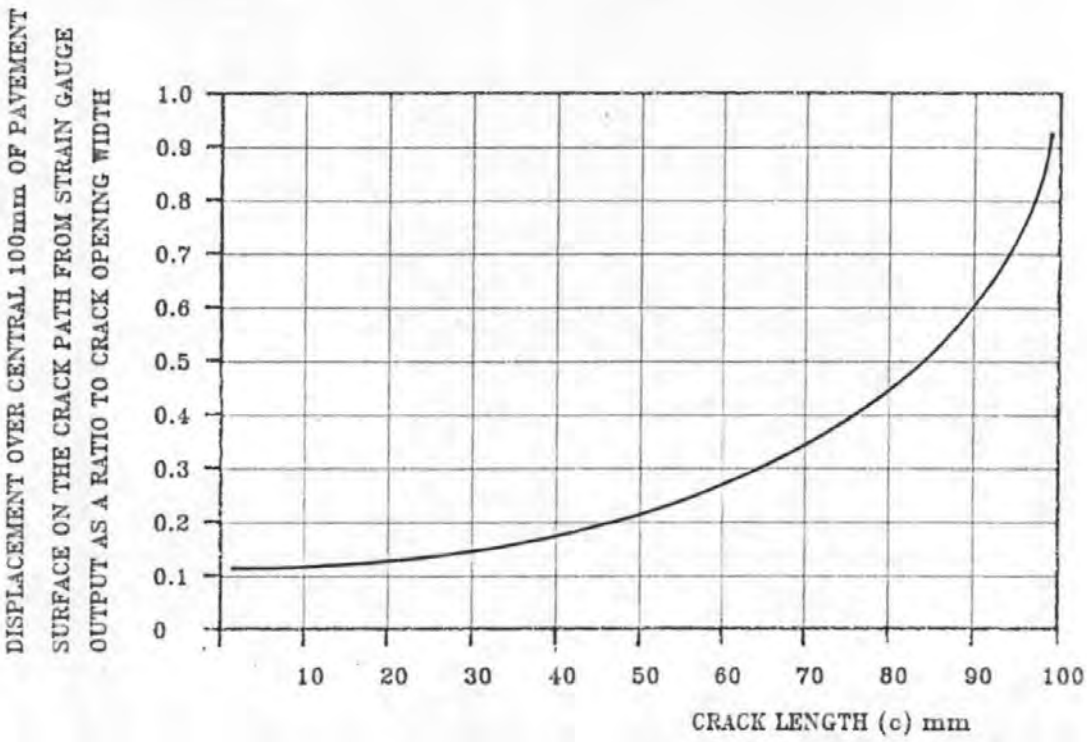

FIG.6.4 PLOT OF PAVEMENT SURFACE DISPLACEMENT VERSUS CRACK LENGTH FROM LINEAR ELASTIC FINITE ELEMENT MODEL OUTPUT

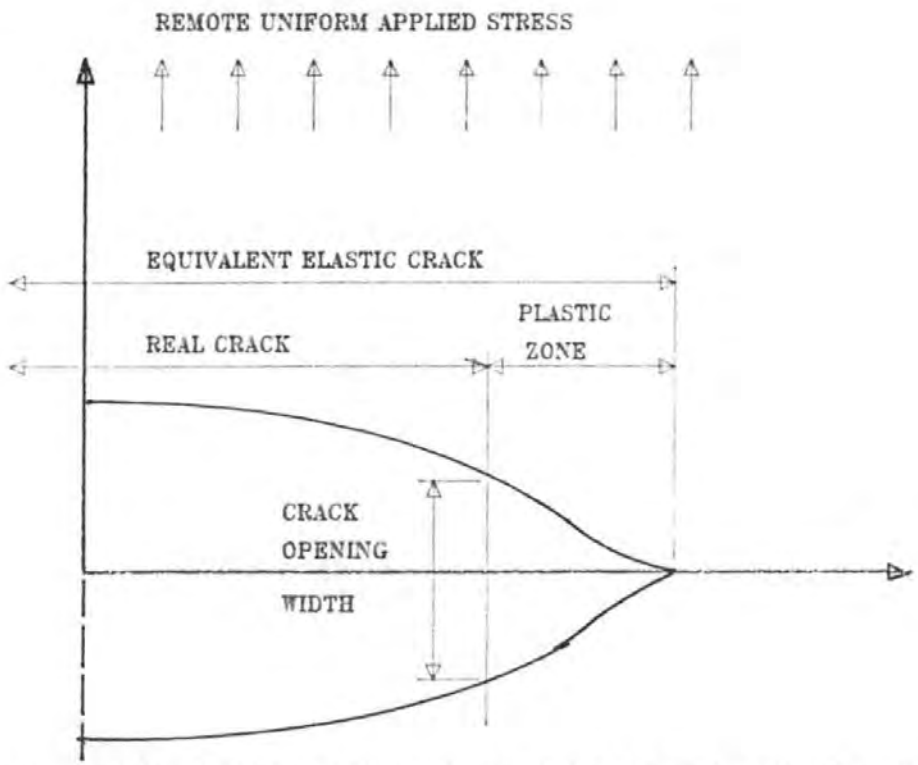

FIG.6.5 THE "DUGDALE" MODEL FOR CRACK TIP PLASTICITY (106)

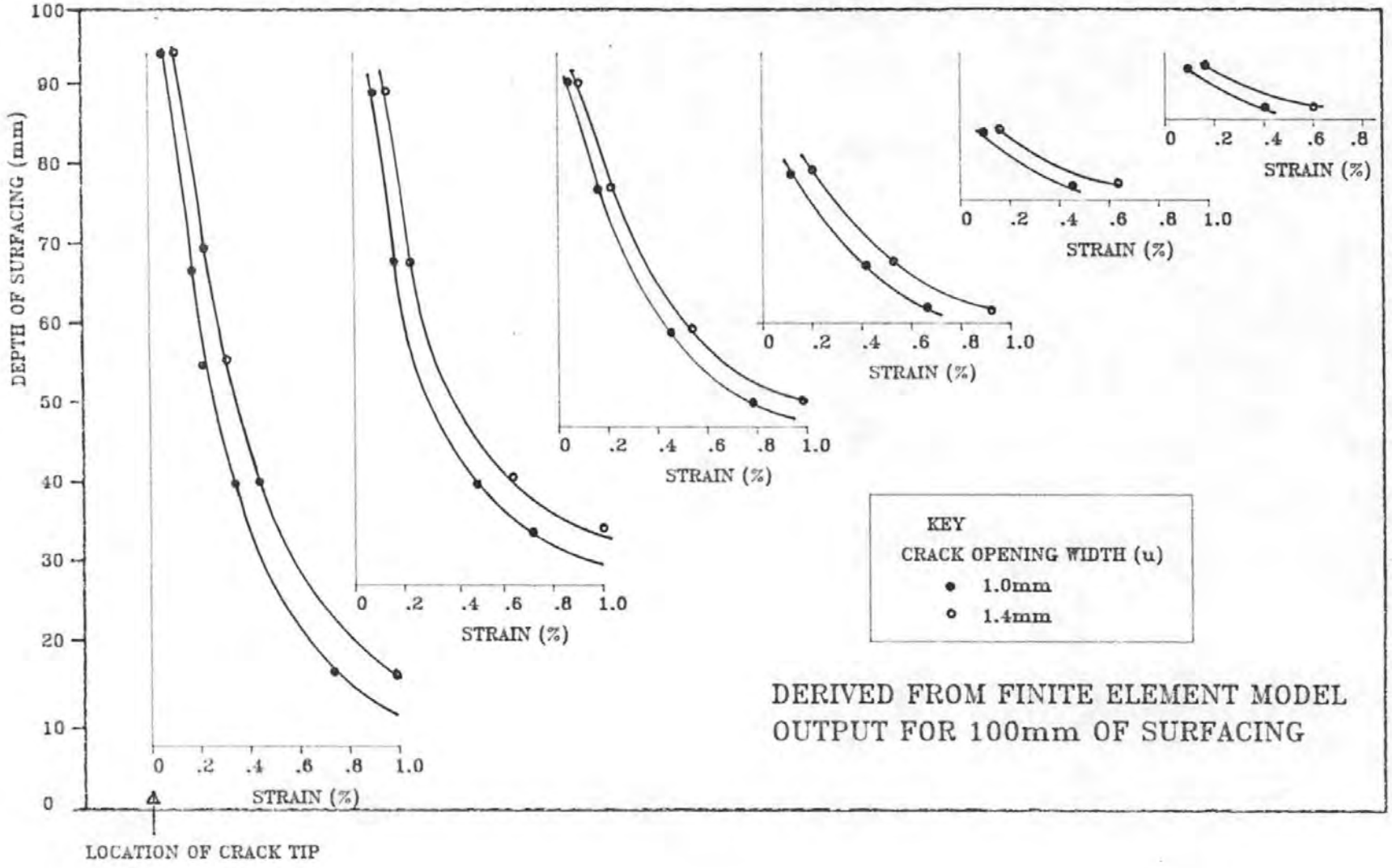

FIG.6.6 STRAIN AHEAD OF GIVEN INCREMENTS OF CRACK ON THE CRACK PATH FOR CRACK OPENING WIDTHS OF 1.0 AND 1.4mm

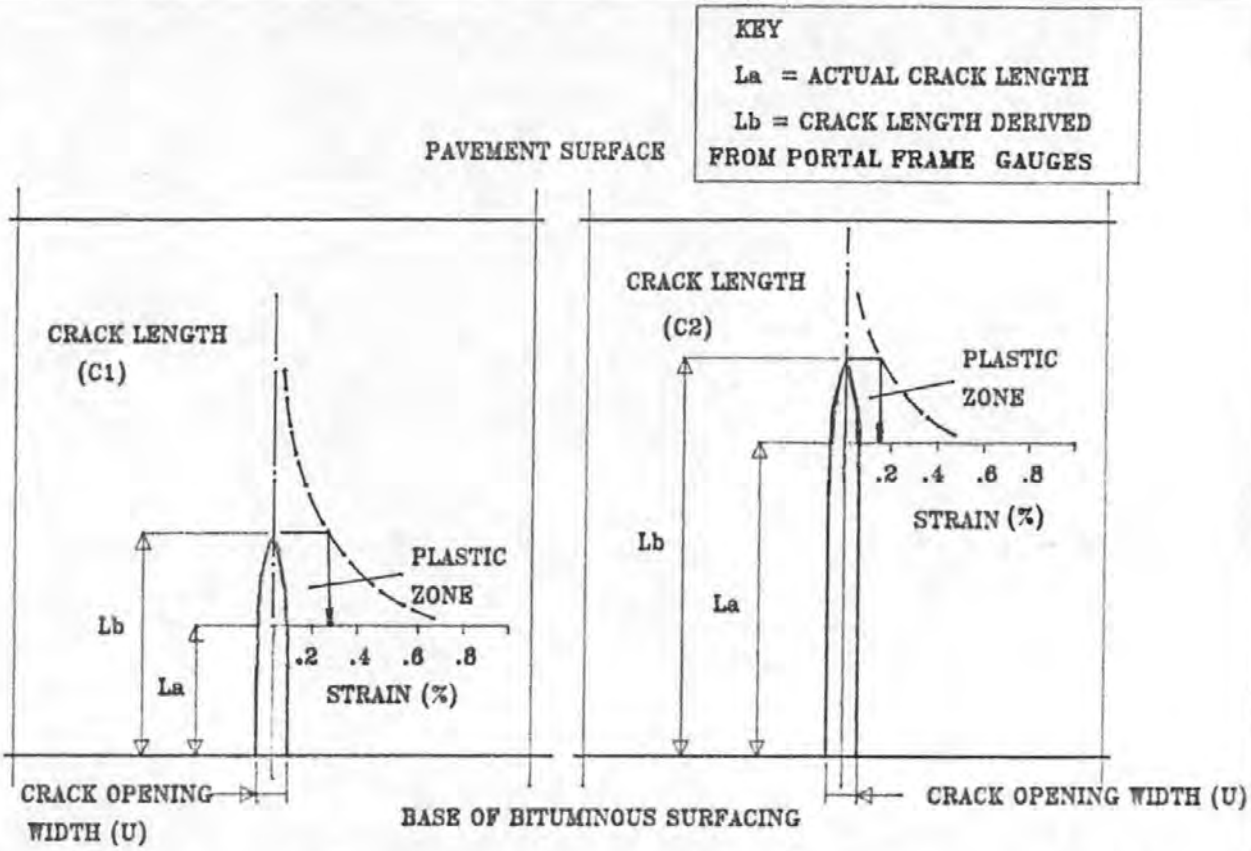

FIG.6.7 DIAGRAMMATIC PRESENTATION OF THE PLASTIC ZONE AHEAD OF THE CRACK TIP

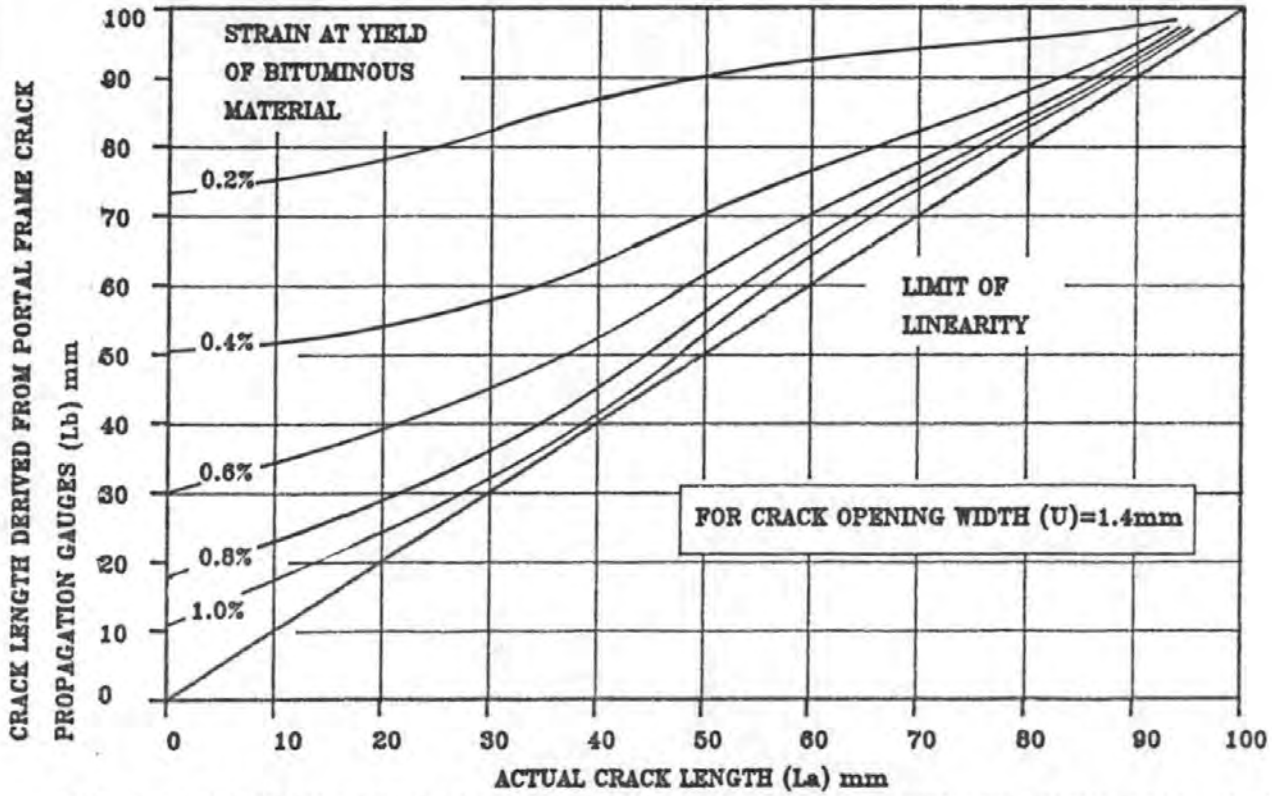

FIG.6.8 CORRECTION TO CRACK LENGTH GIVEN BY ELASTIC ANALYSIS RELATED TO STRAIN YIELD OF BITUMINOUS SURFACING FOR U = 1.4mm

described in section 6.9. Using this approach it was possible to define a relationship between actual crack length and crack length derived from combining the output readings from the portal frames with the finite element analysis. This relationship is shown in fig.6.8 for a crack opening width of 1.4mm with respect to a range of yield strains.

This procedure was used to correct 20-30 readings throughout each test sequence so as to provide an accurate plot of crack length versus crack opening cycles. An additional check on the accuracy of the method was obtained by the visual recording of the crack length at intervals throughout each test.

6.4 ASPHALT TEST MIXES

6.4.1 Introduction

The test programme was concentrated on one particular mix type; Dense Bitumen Macadam[9] . However, a limited number of tests have also been conducted on Hot Rolled Asphalt[8] and Open Textured Macadams[9]. The primary aim of the programme has been to investigate the influence of mix proportions (aggregate grading and bitumen grade and content) and compaction level on the rate of crack growth.

6.4.2 Mixes

A DBM incorporating a 20mm nominal aggregate size, 4.2% bitumen content and 3% void content with a 100 pen binder was adopted as a standard mix to provide the control against which all other mix types and gradings could be compared. The resistance to crack growth of conventional bituminous surfacings has been investigated through the variation of five parameters:-

1) Bitumen content
2) Bitumen grade
3) Void content
4) Nominal aggregate size
5) Grading curve

Two further factors of bitumen type of manufacture and aggregate type may be significant as they affect the cohesive properties of the mix and although their possible influence is discussed, they were not included in the experimental investigation.

6.4.2.1 Aggregates

The aggregate for all tests and all grading sizes was a crushed oolitic limestone from EEC quarries, Chipping Sodbury. Prior to use the aggregate was dried and sieved to provide material of 11 single size categories.

This procedure allowed subsequent accurate batching of each mix by weight. The grading curves are given in Appendix 5.

6.4.2.2 Binder

The bitumen of nominal 50, 100 and 200 pen with softening point values of 54.5, 47.5 and 42.5 °C respectively was obtained from a local supplier. A sample was taken before the mixing of each test beam to ensure the binder had not undergone significant oxidization through repeated heating and cooling.

6.4.2.3 Mix Preparation

Both aggregate and binder were heated to the maximum temperature permitted within the relevant specification [8,9] for a period of 16 hours before mixing. Mixing was carried out in a 0.0075m^3 capacity Hobart mixer for at least five minutes to ensure complete coating of aggregate by the binder. To maintain the specified mix temperature (110-165°C dependent upon binder grade) the mixer bowl was preheated and periodic checks carried out to ensure it remained within the specified temperature limits.

The mix was compacted in three layers in a 1800mm x 125mm x 125mm timber mould by a vibrating hammer sequentially moving along the length of the mould. Experience gained during the manufacture of test beams indicated that a variation in compactive effort from 2-10 minutes for each layer resulted in the void content varying from 11-3% respectively. Specification temperature limits for laying were adhered to throughout the compaction procedure.

Prior to testing, the beams were trimmed to 100mm deep by 100mm wide. This provided a clean smooth surface on which to observe crack growth and minimise edge effects caused by manufacture in a mould. After testing the void content of each beam was calculated using the method described in BS 598[83] from 100 x 100 x 40mm sections cut from the beam. Four similar sized blocks were also cut for subsequent creep

tests.

6.4.3 Test Beams

The experimental investigation has been based on thirty-four beams of various types of bituminous material. Although the platen arrangement, described in section 6.2.4, allowed two tests per beam, this facility was not always used. Furthermore, occasional problems with the control of the test rig resulted in the premature failure of eight tests, leaving a total 52 tests from which the results presented in Section 6.12 are based. Details of the test mixes are given in Table 6.1.

6.5 THE CONCEPT OF ACCELERATED TESTING

6.5.1 Introduction

To enable the test programme to be carried out in a practical time period, testing must be accelerated from a daily, 24 hour, cycle in the pavement to within the range of 0.001 to 0.1 Hz.

With an elastic material acceleration of testing is straightforward, but with a visco-elastic material some consideration of time and temperature is necessary because of stress relaxation effects. These become more significant at higher temperatures and slow loading rates. The reduced stress relaxation associated with an acceleration of test frequency would normally decrease the fatigue life. The aim of accelerated testing is to balance the reduced stress relaxation at a higher frequency, with increased stress relaxation by using a higher test temperature, or a softer grade of bitumen.

Thermal reflection cracking resulting from thermal movements in a cracked cement-bound roadbase, occurs under low frequency loading, and therefore at lower stiffness than in conventional fatigue testing to simulate traffic loading[107,108]. Under these low stiffness conditions, previous researchers[72,109] have shown that brittle fracture does not occur and crack growth is a result of severe localised deformation at the crack tip. Fracture or deformation of the aggregate particles is unlikely and as tensile fracture occurs within the bitumen. it is assumed that the crack growth rate is related to bitumen stiffness.

TABLE 6.1

TEST MIX DETAILS

Ref.	Spec. (BS)	CL	Mix Type	Nominal Agg.Size (mm)	Bitumen Content (%)	Filler Content (%)	Bitumen Grade (Pen)	Void Content %	Comments
1	4987	2.2.4	DBM	40	4.2	7	100	3.2	
2	4987	2.2.5	DBM	28	4.2	7	100	3.0	
3	4987	2.2.6	DBM	20	4.2	7	100	3.1	
4	4987	2.3.1	DBM	14	4.2	7	100	2.7	
5	4987	2.3.2	DBM	10	4.2	7	100	3.0	
6	4987	2.2.4	DBM	40	4.2	15	100	2.5	
7	4987	2.2.4	DBM	40	4.2	5	100	3.3	
8	4987	2.2.4	DBM	40	4.2	0	100	4.1	
9	4987	2.2.6	DBM	20	4.2	7	50	3.3	
10	4987	2.2.6	DBM	20	4.2	7	200	3.1	
11	4987	2.2.6	DBM	20	4.7	7	200	2.9	
12	4987	2.2.6	DBM	20	5.2	7	200	3.0	
13	4987	2.2.6	DBM	20	4.2	7	200	3.1	Granite Aggregate
14	4987	2.2.6	DBM	20	6.2	7	200	2.7	
15	4987	2.2.1	Open Mac	40	4.2	-	200	-	
16	4987	2.2.2	Open Mac	20	3.8	-	200	-	
17	4987	2.2.2	Open Mac	20	4.2	-	50	-	

TABLE 6.1(Cont)

Ref.	Spec. (BS)	CL	Mix Type	Nominal Agg.Size (mm)	Bitumen Content (%)	Filler Content (%)	Bitumen Grade (Pen)	Void Content %	Comments
19	4987	2.2.4	DBM	40	4.2	7	100	11.2	
20	4987	2.2.4	DBM	40	4.2	7	100	7.8	
21	4987	2.2.4	DBM	40	4.2	7	100	6.2	
22	4987	2.2.4	DBM	40	4.2	7	100	4.7	
23	4987	2.2.6	DBM	20	4.2	7	127 (S.B.S.)	2.6	
24	4987	2.2.6	DBM	20	4.2	7	100	3.1	Ref. 24 geotextile grid type 1 at 1/3 dept
25	4987	2.2.6	DBM	20	4.2	7	100	3.2	Ref. 25 geotextile grid type 1 at base
26	4987	2.2.6	DBM	20	4.2	7	100	3.4	Ref. 26 geotextile grid type 2 at 1/3 dept
27	4987	2.2.6	DBM	20	4.2	7	100	3.3	Ref. 27 geotextile grid type 2 at base
28	4987	2.2.6	DBM	20	4.2	7	100	2.9	Ref. 28 welded mesh reinforcement ½ depth
29	594	F	HRA	20	6.5	10	200	4.3	
30	594	F	HRA	20	6.5	10	100	4.1	
31	594	F	HRA	20	6.5	10	44	3.9	
32	594	F	HRA	20	6.5	10	35	4.3	
33	594	F	HRA	20	6.5	10	26	4.8	
34	594	F	HRA	20	6.5	10	17	4.2	

where CL.NO is the clause number of the appropriate British Standard

The validity of accelerated testing at low values of bitumen stiffness was investigated experimentally.

6.5.2 Experimental Verification

The test sequence used to test the validity of the equi-bitumen stiffness concept at low stiffness, high temperature conditions consisted of two series of tests conducted on a standard DBM mix. The format was similar to that described in section 6.2, but consisted of smaller samples mounted and loaded vertically, as illustrated in the top photograph of plate 5.

The bitumen stiffness was maintained at $10^5 N/m^2$ for the initial tests, while the temperature was increased for each test in 5°C increments from 15°C to 40°C. The corresponding test frequency was determined by the Van der Poel's nomograph[13]. The second series of tests were carried out at bitumen stiffnesses ranging from 5×10^4 to $5 \times 10^6 N/m^2$. A 1mm cyclic crack opening width was maintained for all tests. The number of crack opening cycles required to produce full depth cracking through the bituminous sample was recorded and defined as the fatigue life.

6.5.3 Results

The fatigue lives recorded for the initial tests, fig.6.9, show remarkably little variation. The variations exhibited may be attributed to minor differences between the mixes or test control. The results show a mean of 12,600 cycles and a standard deviation of 866 cycles, assuming a normal distribution. 95% confidence limits between 10,500 and 14,500 cycles demonstrate the accuracy obtainable through crack opening fatigue testing at low bitumen stiffness using the Van der Poel nomograph.

However, a degree of temperature susceptibility was evident as the testing approached within 15°C of the bitumen softening point. This enabled an upper test temperature limit to be defined for all subsequent testing with the bitumen grade and type used here.

The relationship between the load transmitted to the beam through the platens and fatigue cycles is given in fig.6.10. The resultant gradient characterises the individual mix in terms of bitumen stiffness.

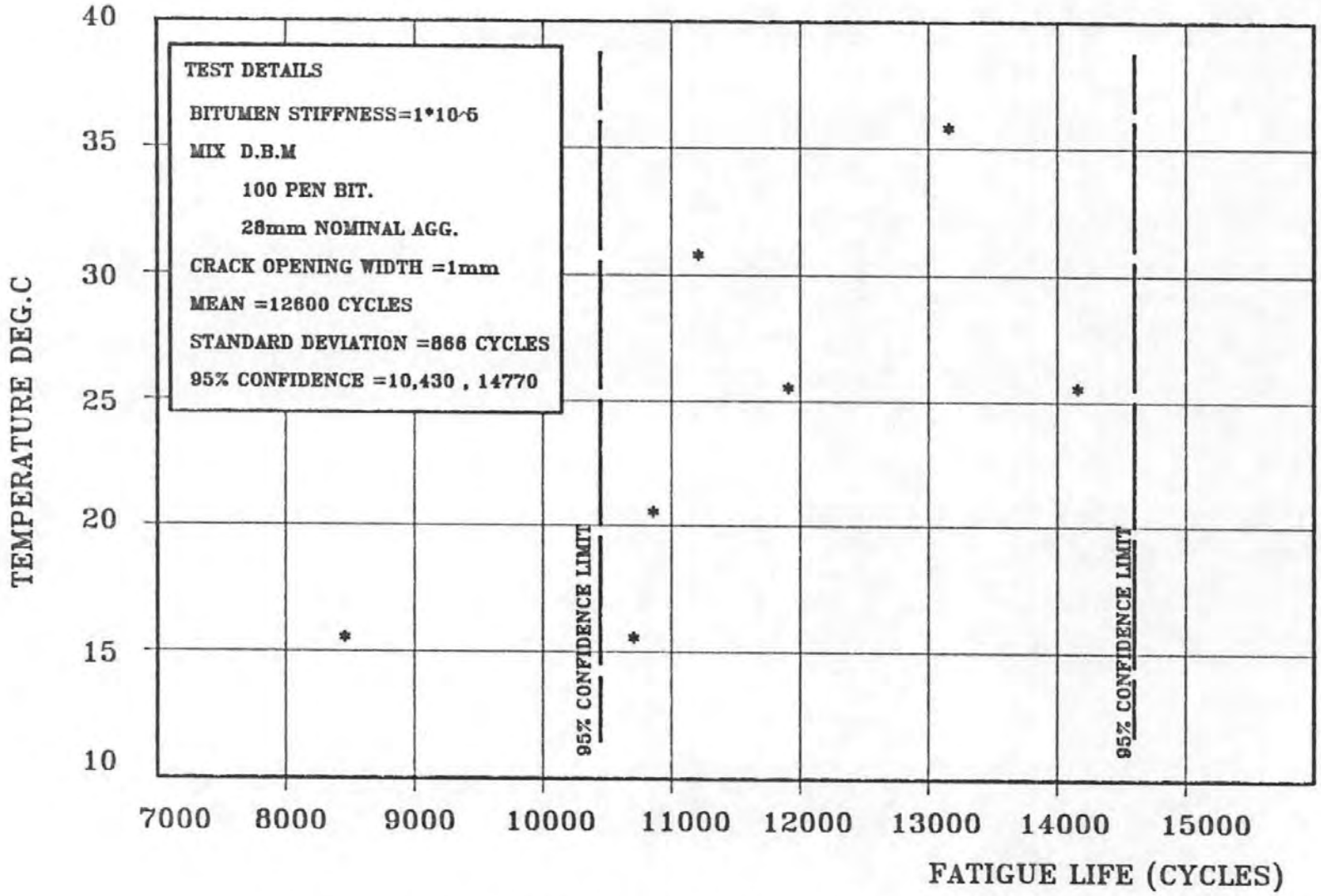

FIG.6.9 VERIFICATION OF CONCEPT OF ACCELERATED TESTING

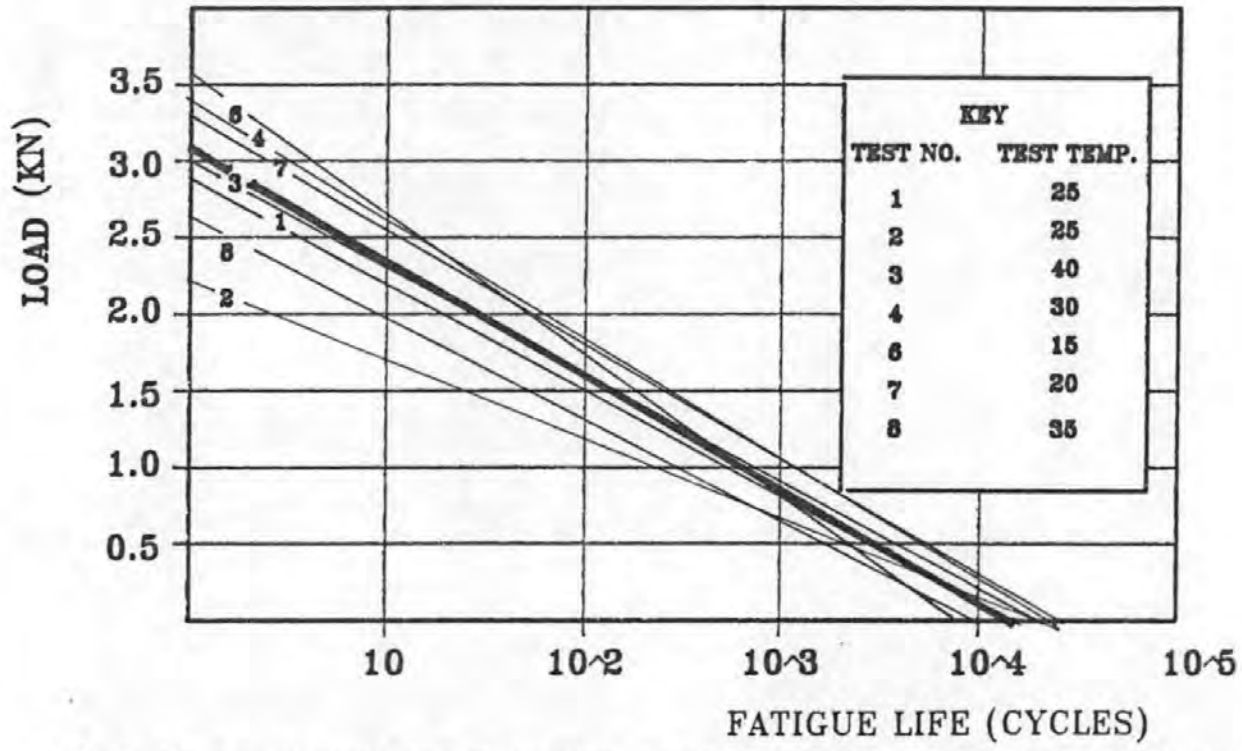

FIG.6.10 LOAD VERSUS FATIGUE CYCLES PRODUCING CHARACTERISTIC GRADIENT FOR TEST CONDITIONS AND SAMPLE GEOMETRY

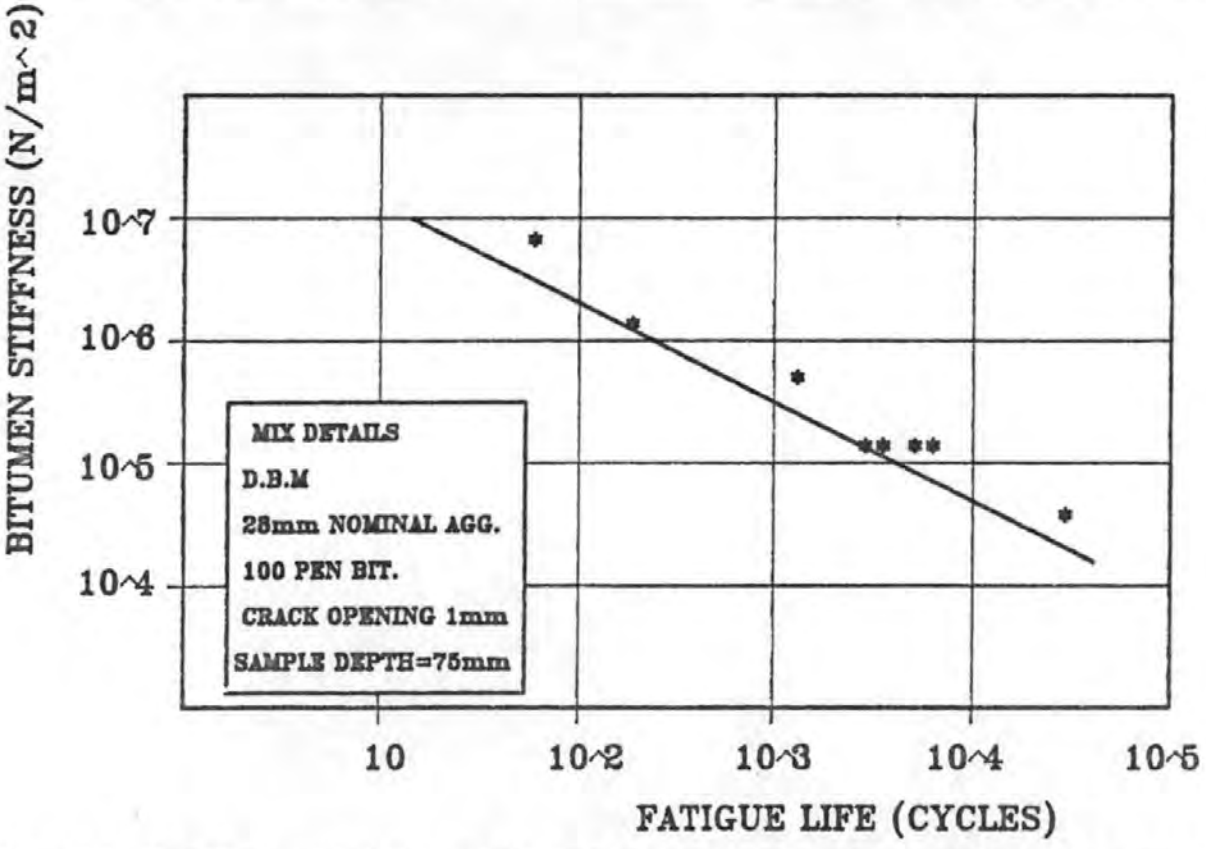

FIG.6.11 VERIFICATION OF RELATIONSHIP BETWEEN BITUMEN STIFFNESS AND FATIGUE LIFE FOR CRACK OPENING FATIGUE TESTING

Subsequent tests on the same asphaltic mix but with a variation in bitumen stiffness are plotted in fig.6.11. A relationship is shown between fatigue life and bitumen stiffness for a given crack opening width of the form:-

$$\log S_b = -m\log Nf + c \qquad \text{-Eqn.(6.1)}$$

where S_b = Bitumen stiffness (N/m^2)

Nf = Fatigue life (cycles)

m and c = gradient and the intercept on the Y-axis

These series of tests therefore verified the concept of accelerated testing while indicating the level of accuracy obtained through repeated tests. Furthermore a strong correlation was shown to exist between bitumen stiffness and crack opening fatigue life.

6.6 FRACTURE MECHANICS APPROACH

Fracture mechanics explains the failure of structural members at lower stresses than the ultimate design load under cyclic loading. It describes this process in terms of flaws in the structures around which stress concentrations are produced which result in crack propagation and eventual failure. In the present application to reflection cracking the analysis focuses on those stress concentrations induced through movement between adjoining cracked roadbase slabs and considers their effect on the overlying surfacing material.

Previous analysis of pavement damage associated with repeated loading has been based on the principle of Miners Law[85] which states that:

$$D = \sum_{i=1}^{j} \frac{n_i}{N_i} \qquad \text{- Eqn.(6.2)}$$

where D = total cumulative damage having a value of 1 at failure

j = No. of strain levels,

n_i = No. of applications at level i

N_i = No. of applications to cause failure at level i

However, Miners Law does not satisfactorily account for the influence of geometry and inhomogeneties, and can only be applied to a pre-defined critical cracking condition to estimate the onset of cracking.

The advantage of applying fracture mechanics to predict the rate of

crack growth through the bituminous surfacing is that the interactive effects caused by both environmental and traffic stresses can be evaluated and combined to determine the life of the pavement. Failure can be defined as either a specific crack length or other predefined critical crack criteria.

The validity of applying the fracture mechanics approach to analyse the performance of bituminous surfacings has been verified by a number of researchers [49,72,76,77,78] and the basic theory is well documented. It is reviewed in section 4.5.

The loading times induced by traffic loads moving at 15mph or greater will, according to Ramsamooj[75], induce an essentially elastic response in bituminous material so that elastic analysis is applicable. Furthermore, by incorporating elastic analysis, a reasonable engineering solution has been shown to exist[79] even under low stiffness conditions produced by slow moving traffic and daily cycles of temperature.

Visco-elastic analysis applied by Chang [48] provides a more accurate description of the crack mechanisms caused by slow moving traffic and daily cycles of temperature. However its complexity confines it to a theoretical level and it is not readily applicable to practical situations.

The two methods differ with regard to the derivation of material modulus. The visco-elastic approach adopts a creep compliance modulus, although previous researchers[48,72,73] disagree on the method of measurement. Elastic analysis incorporates an estimate of bitumen stiffness in terms of loading time and ambient temperature using the nomograph developed by Van der Poel [13]. A corresponding value of mix stiffness is derived from a bitumen stiffness versus mix stiffness relationship determined from laboratory tests appropriate to the loading conditions.

The flow mechanisms within the bituminous material prevent rapid unstable fracture but failure may still occur under the action of slow stable crack growth. The rate at which this crack growth occurs will determine the time required for the crack to propagate through the surfacing. Crack growth laws[79] relate the rate of crack growth

with respect to the number of load applications to the stress level associated with each cycle. Although these laws have been proposed in many forms the power law proposed by Paris[81] (Equation 4.1) is adopted by this study.

The Paris equation has been successfully applied to cracking through bituminous materials by Salam[86], Majidzadeh[78] and others for the analysis of laboratory tensile tests under fatigue loading. However, in later publications Majidzadeh et al [78] report that the crack growth relation between log (dc/dN) and log(k), is not generally linear because fatigue constant n is partially dependent on loading conditions. They conclude that a four term model gives a more precise description of the experimental data in the form:

$$\frac{dc}{dN} = A_1\Delta k + A_2\Delta k^2 + A_3\Delta k^4 + A_4\Delta k^6 \qquad \text{Eqn.(6.3)}$$

where $\frac{dc}{dN}$ = rate of crack growth

Δk = stress intensity amplitude

A_1, A_2, A_3, A_4 = fatigue constants of the material

However, it seems unlikely that this degree of sophistication is necessary to derive crack growth resulting from daily temperature fluctuations. Satisfactory use of the simple Paris Equation has been confirmed by Schapery[72].

Although other researchers [49,75,76] have applied the concepts to existing pavements as described in section 4.5, an effective design process has not yet been derived.

The crack propagation rate derived from Paris' equation[81] is a function of the amplitude of the stress intensity factor (Δk) and material fatigue constants (A and n). These parameters have unique values dependent upon the basic fracture mode as defined in fig.6.12. However, the three fracture modes can operate independently or in combination depending upon the loading configuration.

Thermal movements within the road base induce mode I cracking in the surfacing layers due to tensile stresses. This form of cracking can be described adequately by the Paris' Equation.

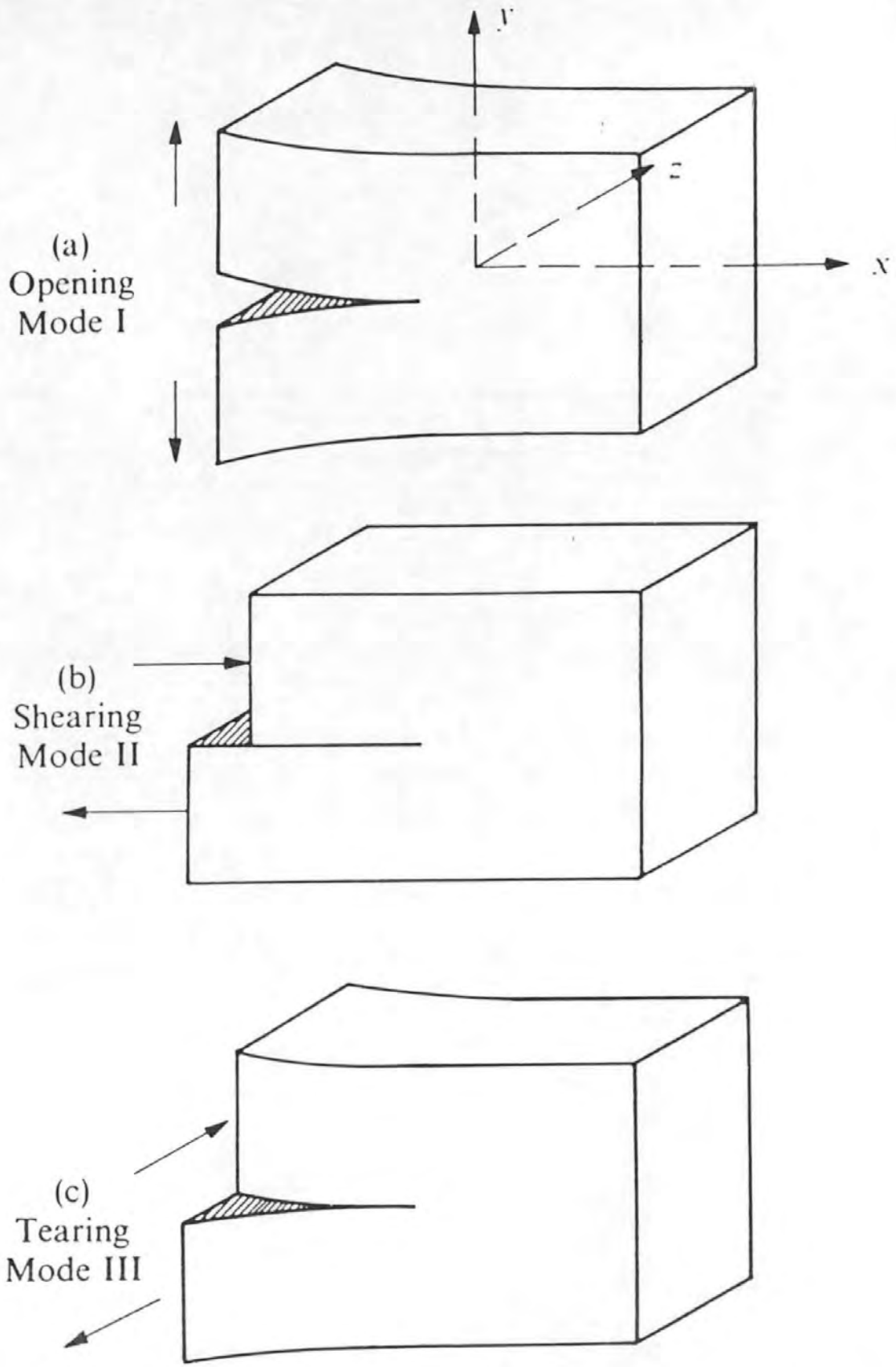

FIG.6.12 FUNDAMENTAL MODES OF FRACTURE: (a) OPENING MODE 1 (b) SHEARING MODE 11; (c) TEARING MODE 111

Traffic loads produce a combination of mode I and mode II due to shear stresses induced in the surfacing by differential roadbase movement and due to tensile stresses induced at the base of the surfacing. The crack will therefore propagate in two modes; the opening mode and the in-plane sliding mode. For cycles of a constant wheel load the rate of crack propagation is then given in an expanded form of the Paris Equation:

$$\frac{dc}{dN} = A_1(\Delta k_1)^{n_1} + A_2(\Delta k_2)^{n_2} \qquad \text{- Eqn(6.4)}$$

where Δk_1 and Δk_2 are the amplitudes of the stress intensity factors for these two modes of cracking, and n_1, n_2 and A_1, A_2 are the material fatigue constants unique to mode 1 and mode 2 fracture and determined from laboratory tests which simulate the individual configurations.

Roberts and Erodogan [97] give the following formula for use with variable wheel loads:

$$\frac{dc}{dN} = A_1(1 + \beta)^2(\Delta k)^{n_1} \qquad \text{- Eqn.(6.5)}$$

for stable crack growth where

$\beta = (k_{max} + k_{min})/2\Delta k$

k_{max} and k_{min} are the maximum and minimum values of stress intensity factor during the passage of a wheel load

and $\Delta k = k_{max} - k_{min}$

6.7 THE PREDICTION MODEL

6.7.1 Introduction

The tensile fatigue prediction model, defined in fig 6.13, calculates the stress induced into the surfacing layers by daily cycles of roadbase movement. The stress, considered in terms of a stress intensity factor, is related to the resistance of the bituminous surfacing to crack growth, considered in terms its material fatigue constants. This relationship allows an estimation of the fatigue life of the surfacing material. The fatigue life is defined as the number of stress cycles required to cause a flaw in the base of the surfacing layer to propagate to the surface.

6.7.2 Roadbase Movements

The roadbase movements are defined in terms of the opening width or

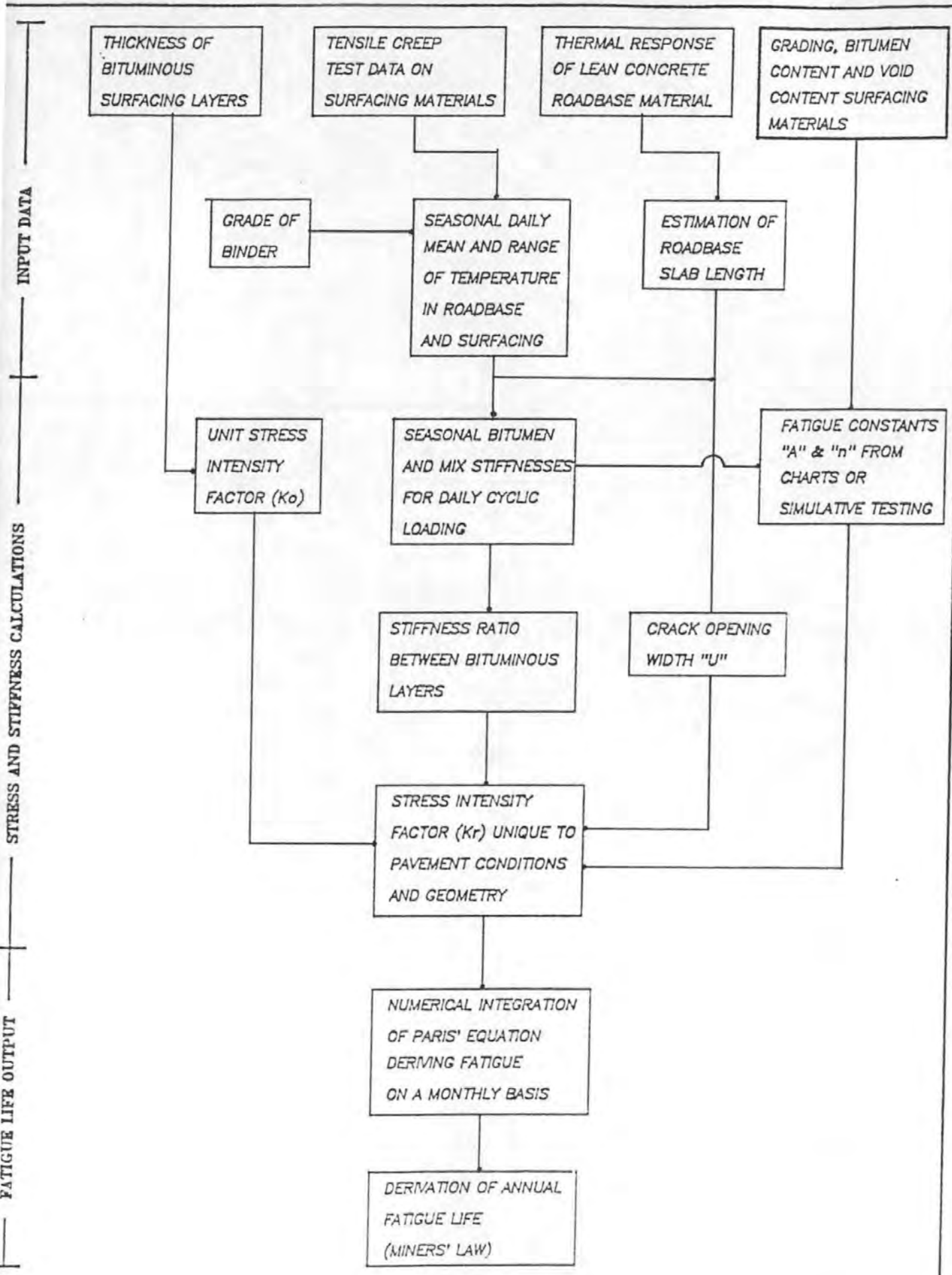

FIG.6.13 FLOW CHART DEPICTING METHOD OF TENSILE FATIGUE MODEL

amplitude (u) between the ends of adjacent roadbase slabs. This width is dependent upon the temperature range within the roadbase, the coefficient of thermal movement of the roadbase material, length of slab and the restraint offered by the underlying sub-base. The influence of these parameters on the crack opening width is discussed in sections 6.8.1. to 6.8.5.

6.7.3 Stress Intensity Factors

The stress, induced in the surfacing material by roadbase movements, is related to the amplitude of the cyclic stress intensity factor, k_r, which characterises the magnitude of the crack tip stress field under defined conditions.

The magnitude of the stress intensity factor (k_r) is dependent upon:-

i) the unit stress intensity factor, k_o, (where $k_o = \Delta k$ for $k_{min} = 0$)
ii) the crack length within the surfacing layer
iii) the stiffness of the surfacing layer
iv) the crack opening width

The significance of (iii) and (iv) are discussed in sections 6.9 and 6.8.1 respectively and the derivation of the stress intensity factor by finite element techniques is described in section 6.10.

6.7.4 Material Fatigue Constants

Using linear elastic fracture mechanics, the restraint to crack propagation of a material can be evaluated in terms of its fatigue constants, A and n. Direct simulation of crack mechanisms in the laboratory allows the constants to be determined and applied directly to similar material within the pavement. The procedure used to define these constants from the results of laboratory testing is described in section 6.11.

6.7.5 Fatigue Life

Integration of Paris' Law (equation 4.1) over limits defined as the thickness of each layer of bituminous surfacing, provides an expression for the fatigue life, Nf,:

$$Nf = \int_{o}^{c_1} \frac{dc}{A_1 k_r^{n_1}} + \int_{c_1}^{c_2} \frac{dc}{A_2 k_r^{n_2}} \qquad \text{- Eq. (6.6)}$$

where suffixes 1 and 2 relate to the basecourse and wearing course, and c is the layer thickness. The pavement surfacing layer/roadbase interface is the lower limit; o.

Using Equation 6.6, a value of fatigue life may be evaluated for the total depth of surfacing. As the parameters A and k are temperature dependent and related to the mean monthly pavement temperature the fatigue life derived is a multiple of individual months. The equivalent annual fatigue life may be calculated by using Miners Law (85) to accumulate the damage within the surfacing which occurs in each month of the year and is given by Equation 6.2.

6.7.6 Results

The results from the model, presented in section 6.12, are based on the bituminous mixes described in section 6.4. A numerical example incorporating these results is given in Appendix 3.

6.8 STRESS INDUCED THROUGH ROADBASE MOVEMENTS

6.8.1 Crack Opening Widths

Cracks in a cement bound roadbase will tend to become wider due to shrinkage and will fluctuate in width due to temperature change. The width of cracks between the adjoining roadbase slabs may be calculated assuming linear elastic thermal movement of the lean concrete partially restrained by sub-base friction so that

$$u = C' * L * \Delta T - SR \qquad \text{- Eqn.(6.7)}$$

where u = crack opening width

C' = coefficient of thermal movement of the roadbase material

L = roadbase slab length

ΔT = temperature range

SR = term relating to sub-base restraint

The crack opening widths derived for use with the tensile fatigue model are given in table 6.2. They incorporate the data relating to pavement temperature, the coefficient of thermal movement of lean concrete, roadbase slab length and sub-base restraint described in sections 6.8.2 to 6.8.5

TABLE 6.2

DAILY CYCLIC CRACK OPENING MOVEMENTS IN THE ROADBASE, CORRECTED FOR SUB-BASE FRICTION RESTRAINT EFFECTS

The values of cyclic crack opening (mm) are for lean concrete with thermal coefficient, $C' = 10^{-5}/°C$; for other values of C' the cyclic crack opening will be proportionally greater.

	JAN	FEB	MAR	APR	MAY	JUN	JUL	AUG	SEP	OCT	NOV	DEC
slab length (m)	COMPOSITE PAVEMENT, 100mm SURFACING											
5	.11	.17	.27	.45	.52	.57	.48	.40	.34	.25	.18	.13
10	.22	.33	.53	.87	1.00	1.09	.91	.78	.64	.48	.34	.24
15	.32	.48	.78	1.25	1.45	1.59	1.31	1.12	.93	.69	.50	.36
20	.42	.63	1.00	1.63	1.87	2.07	1.71	1.47	1.22	.90	.65	.47
	COMPOSITE PAVEMENT, 150mm SURFACING											
5	.08	.12	.22	.34	.38	.41	.37	.31	.27	.19	.14	.09
10	.15	.24	.43	.65	.72	.79	.70	.60	.50	.37	.26	.16
15	.22	.34	.64	.96	1.05	1.15	1.01	.86	.72	.54	.39	.24
20	.29	.45	.82	1.22	1.35	1.50	1.31	1.13	.95	.70	.50	.32
	COMPOSITE PAVEMENT, 200mm SURFACING											
5	.05	.08	.16	.24	.28	.27	.27	.23	.20	.14	.11	.07
10	.10	.16	.31	.47	.53	.51	.51	.45	.37	.27	.20	.12
15	.14	.23	.45	.69	.77	.75	.73	.65	.53	.39	.30	.19
20	.18	.30	.58	.88	.99	.98	.95	.85	.70	.51	.39	.24

6.8.2 Temperature Profiles within Composite Pavements under U.K. Conditions

The results from a previous investigation by Brooker [90] which determined the temperature profiles within composite pavements have been adopted for use with this study. Although previously documented[88], a summary is given of the objectives and the method used to derive the resultant data (tables 6.3 and 6.4).

The aims of Brooker's investigation included development of procedures to estimate:

1) the mean monthly temperature at varying depths within the structure of the pavement and therefore provide the data required to calculate the surfacing mix stiffness.
2) the daily variation in temperature within the roadbase, for each month of the year, to enable the corresponding crack opening width between adjoining roadbase slabs to be calculated.

Initially a temperature model was formed for composite pavements from limited T.R.R.L. survey data [89]. Air temperature and pavement temperature at various depths were recorded at two sites of similar climatic conditions; one comprising a concrete and the other a bituminous pavement. The data was logged at two hourly intervals for one month in each season during a particular year; 1969. This information was initially extended by extrapolation to cover all twelve months of the year; fig.6.14.

The temperature model is based on characteristic hourly temperature profiles for each month of the year produced by combining the daily cycles of pavement temperature from both sites, in terms of their isochrome distribution, i.e. temperature profile at defined times of the day. The distributions were crudely fitted together, the profiles from the bituminous pavement provided the surfacing data and those from the concrete pavement related to the roadbase of the composite pavement.

To enable an accurate fit to be made a heat balance equation was formed to relate the heat gain of both pavement types through surface absorption to the convection loss effects. This analysis provided an estimated daily temperature profile for composite pavements related to specified months of the year.

TABLE 6.3

MONTHLY MEAN AND EQUIVALENT VALUES FOR THE DAILY TEMPERATURE RANGE IN THE SURFACING FOR DETERMINATION OF BITUMEN STIFFNESS[80]

MEAN TEMPERATURE IN SURFACING (°C)													
MONTH		JAN	FEB	MAR	APR	MAY	JUN	JUL	AUG	SEPT	OCT	NOV	DEC
SURFACING THICKNESS (mm)	100	3.7	4.3	7.0	11.2	16.1	21.7	22.8	20.3	16.3	10.0	6.8	4.6
	150	4.2	4.7	7.5	11.7	16.7	22.4	23.4	20.6	16.6	10.4	7.2	5.0
	200	4.5	5.0	7.8	12.1	17.1	22.9	23.7	20.7	16.7	10.6	7.4	5.3
EQUIVALENT MEAN CONSTANT TEMPERATURE FOR A SINUSOIDAL CYCLE (°C)													
SURFACING THICKNESS (mm)	100	7.0	6.7	8.0	10.5	15.1	19.7	20.3	19.5	16.9	12.7	8.5	7.9
	150	7.5	7.1	8.5	11.0	15.7	20.4	20.9	19.8	17.1	13.1	8.9	8.3
	200	7.8	7.4	8.8	11.4	16.1	20.9	21.2	19.9	17.2	13.3	9.1	8.6

TABLE 6.4

MONTHLY MEAN AND EQUIVALENT VALUES FOR DAILY TEMPERATURES AT THE TOP OF THE ROADBASE FOR CALCULATION OF DAILY CRACK OPENING MOVEMENTS (°C)[80]

MEAN DAILY TEMPERATURE RANGE AT THE TOP OF ROADBASE (°C)													
MONTH		JAN	FEB	MAR	APR	MAY	JUN	JUL	AUG	SEPT	OCT	NOV	DEC
SURFACING THICKNESS (mm)	100	2.3	3.5	5.5	9.1	11.5	12.7	10.8	9.0	6.8	4.9	3.5	2.5
	150	1.6	2.5	4.5	6.8	8.3	9.2	8.3	6.9	5.3	3.8	2.7	1.7
	200	1.0	1.7	3.2	4.9	6.1	6.0	6.0	5.2	3.9	2.8	2.1	1.3
TEMPERATURE RANGE FOR CALCULATION OF CRACK OPENING MOVEMENTS (°C)													
SURFACING THICKNESS (mm)	100	2.2	3.3	5.2	8.3	9.7	10.6	8.7	7.5	6.3	4.6	3.4	2.3
	150	1.4	2.3	4.2	6.3	7.0	7.6	6.8	5.8	4.9	3.5	2.6	1.6
	200	1.0	1.5	3.0	4.6	5.4	5.4	5.3	4.3	3.6	2.6	2.0	1.2

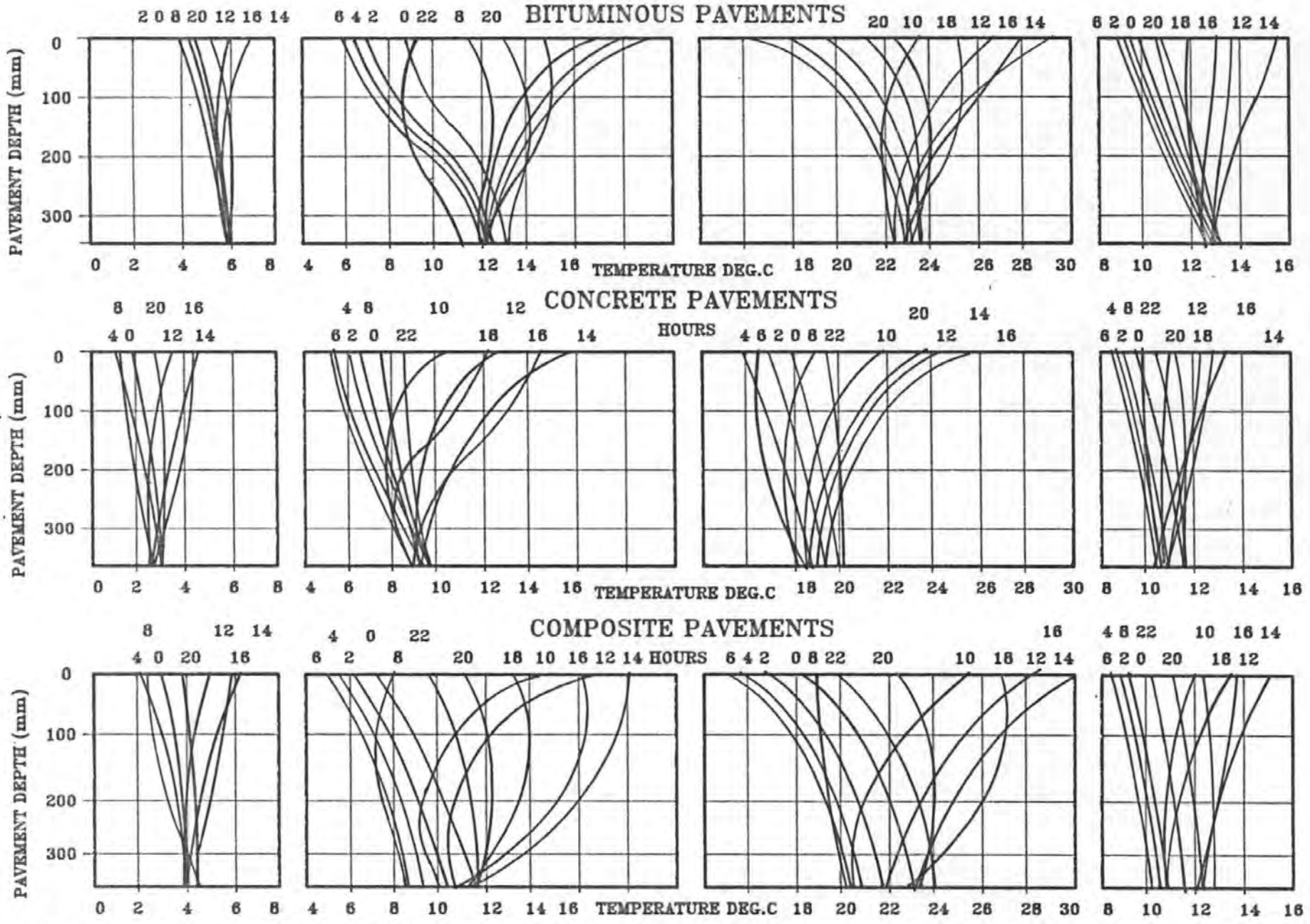

FIG.6.14 BI-HOURLY TEMPERATURE/DEPTH PROFILES FOR BITUMINOUS,CONCRETE AND COMPOSITE PAVEMENTS FOR JANUARY,APRIL,JULY,AND OCTOBER

A subsequent relationship between pavement and air temperature allowed the model to be extended, in such a way that it may be applied to any site in the U.K.

Both the mean daily temperatures and the temperature ranges calculated from the model required modification before they could be used to calculate the surfacing stiffnesses and roadbase crack opening widths.

The mean temperatures had to be adjusted to allow for the difference between the mean of the irregular cycles of pavement temperature and the mean of sinusoidal cycles used with laboratory modelling of tensile fatigue cracking. A procedure was established whereby the 24 hour temperature cycle for each month of the year was analysed in terms of the relaxation modulus of the surfacing material corresponding to the temperature at hourly time intervals. The stress level at the peak temperature value of the actual temperature range was used to determine an equivalent sinusoidal cycle. The mean temperature was taken as the mean of this sinusoidal cycle.

Equivalent sinusoidal temperature cycles at the top of the roadbase were also required for the calculation of crack opening amplitude. Cycles of pavement temperature calculated by the model were plotted and superimposed by 'best fit' sine curves. These curves were further modified to correct for the disproportionate damaging effect caused by occasional extremes of temperature. Crack growth rate has been shown to be proportional to the sixth power of crack opening [90] for a linear increase in daily temperature range. The above average daily temperature ranges in each month were tabulated and the crack opening amplitudes increased accordingly.

The modified values of both daily mean and range of temperature calculated from the model are given in tables 6.3 and 6.4. The values given in these tables also illustrate the insulation given to the roadbase by increasing the thickness of bituminous surfacing material.

6.8.3 Coefficient of Thermal Expansion and Contraction of Lean Concrete

The magnitude of the coefficient of thermal expansion and contraction of concrete depends upon:-

(i) the cement content of the mix and its coefficient of thermal expansion and contraction,

(ii) the aggregate content of the mix and its coefficient of thermal expansion and contraction and

(iii) the hygral state of the mix at the time of the temperature change.

The coefficient of thermal expansion and contraction of cement paste varies between 11 x 10^{-6} and 20 x 10^{-6} per °C and is higher than the coefficient of aggregate. Lean concretes, with a low cement content, will be influenced predominantly by aggregate type. Shacklock [91] provides a useful summary of the coefficients of linear expansion of 6:1 aggregate/cement ratio concretes made with different aggregates and this is reproduced in Table 6.5. These values demonstrate that thermal movement within a roadbase slab may be halved through the use of a limestone aggregate with a coefficient of 7.3 x 10^{-6} per °C compared with the use of aggregates with a high coefficient of thermal expansion such as gravel or quartzite.

Although information is not readily available for lean concretes the difference in coefficient values between paste and aggregate suggests that the coefficient for these concretes would be slightly reduced from those for a structural mix. This assumption is reinforced by Meyers [92] investigation into variations on sand/cement ratios for mortars given in table 6.6.

The moisture content influences the paste component of the overall concrete coefficient. When saturated paste is warmed, the moisture diffusion from gel to capillary pores at constant gel water content is partially offset by contraction as gel loses water so that the apparent coefficient is smaller [93]. A similar but opposite effect occurs on cooling. The curing regime can vary the coefficient by 20%. The effect of curing on the coefficient of concretes incorporating limestone and gravel is given in table 6.7.

TABLE 6.5

THE INFLUENCE OF AGGREGATE TYPE ON THE COEFFICIENT OF THERMAL EXPANSION OF CONCRETE[91]

Aggregate (Geological group)	Coefficient of Thermal expansion (per°C x 10^{-6})	
	Range	Mean
Chert	11.4-12.2	11.8
Quartzite	11.7-14.6	13.2
Quartz	9.0-13.2	11.1
Sandstone	9.2-13.3	11.3
Marble	4.1- 7.4	5.8
Siliceous limestone	8.1-11.0	9.6
Granite	8.1-10.3	9.2
Basalt	7.9-10.4	9.2
Limestone	4.3-10.3	7.3
Gravel	9.0-13.7	11.4

TABLE 6.6

THE INFLUENCE OF AGGREGATE/CEMENT CONTENT ON THE COEFFICIENT OF THERMAL EXPANSION[92]

Sand/cement ratio	Coefficient of Thermal expansion (per°C x 10^{-6})
neat cement	18.5
1:1	13.5
3:1	11.2
6:1	10.1

TABLE 6.7
THE INFLUENCE OF CURING CONDITION ON THE COEFFICIENT OF THERMAL EXPANSION[93]

Aggregate	Curing Condition		
	Weathered per °C x 10^{-6}	Air Cured per °C x 10^{-6}	Water Cured per °C x 10^{-6}
Gravel	13.1	12.2	11.7
Limestone	7.4	6.1	5.9

Lean concrete roadbases in the South-West of England predominantly contain crushed limestone aggregates. The data presented in this section indicates that lean concrete incorporating this aggregate has a mean coefficient of thermal expansion and contraction of 1 x $10^{-5}/^{o}C$

6.8.4 Crack Spacings in Cement Bound Roadbases

6.8.4.1 Introduction

Cement bound roadbases are laid without expansion joints or reinforcement, a construction method which is both continuous and economic. Cracking of the roadbase is inevitable and is produced by thermal and curing effects during the early life of the material before the tensile strength is fully developed. This cracking tends to be transverse across the full width of the carriageway.

Prolonged moist curing delays the advent of shrinkage, but the effect of curing on the magnitude of shrinkage is small. However rapid drying out does inhibit stress relief by creep and leads to more frequent cracking.

6.8.4.2 Theoretical Considerations

A predictive model of crack spacing is provided by Taylor and Williams [94] and has been adopted for use with this work. The model assumes that cracking will occur in continuously laid cement bound roadbases, within the 7 days curing period. Furthermore, traffic loading will induce secondary cracking in poorly designed roadbases early in the service life of the pavement.

The following effects are considered to influence crack spacing early in the life of the roadbase;

(i) shrinkage,
(ii) heat of hydration,
(iii) temperature differentials and
(iv) restrained thermal movement.

As lean concrete contains little cement paste it is unlikely that the relationship between concrete shrinkage and reduced volume of cement gel accounts for early cracking. It is considered to be more probable that shrinkage would increase the intensity of the cracks at a later stage in the life of the roadbase.

The tensile stresses induced through the heat of hydration are likely to be dissipated through radiated and convected heat losses. Temperature differential causing warping within the slab is a significant factor although under normal ambient temperatures such warping is restrained by the self-weight of the slab. However, on the first night after laying, warping and thermal stresses combine to produce tension in the surface.

The restraint to thermal movement is also considered to be significant in producing cracking. Thermal stresses induce tensile stresses into continuously laid roadbases and, if the roadbase is substantially restrained by the underlying sub-base, the tensile stresses can accumulate and cause the lean concrete to crack.

For the condition of non-uniform sub-base restraint, which occurs in practice, the critical parameters are defined as:

i) Coefficient of thermal contraction of the lean concrete
ii) the frictional coefficient between sub-base and roadbase (μ)
iii) tensile strength of the material (f)
iv) the unit self weight of the material (γ)

The resultant crack spacing (L) is given by

$$L = \frac{3f}{\mu\delta\gamma} \qquad \text{- Eqn.(6.8)}$$

where $\mu\delta = 3.03 \log (1 + 4000\delta)$

δ = crack width (mm)

Crack spacings were derived using this equation in conjunction with laboratory based measurements of tensile strength on a gravel aggregate lean concrete with a cement content of 122 kg/m^3. The crack

spacings, given in Table 6.8, are in terms of the temperature fall of the roadbase material in the first night after laying.

A minimum crack spacing of 9.6m is predicted.

TABLE 6.8

CALCULATED CRACK SPACINGS FOR GRAVEL AGGREGATE LEAN CONCRETE ROADBASE ON CLINKER SUB-BASE AS A FUNCTION OF TEMPERATURE FALL[94]

Age hours/day	Tensile Strength MN/m^2	Elastic Modulus GN/m^2	Crack Spacing L(m) for stated temperature fall in C° 2	3	4	5	6
16 –	0.12	9.0	16.3	12.9	11.5	10.3	9.6
1	0.31	18.4	31.0	21.1	21.2	19.4	18.0
2	0.56	23.1		37.6	32.7	29.8	27.6
7	1.12	30.3		67.7	56.4	50.6	47.1
28	1.45	34.1			70.6	62.0	57.9

6.8.4.3 Crack Spacing Surveys

With some variations the published results from field studies of fully developed reflection cracking [95] tend to confirm the predictions of the model proposed by Taylor and Williams[94].

A crack survey undertaken as part of the current study on six sites in Devon and Cornwall on pavements constructed predominantly from limestone aggregates showed crack spacings to vary by a factor of 4 from a scatter band of 5.8 to 21.8m with a mean value of 13.5m. The construction depths of the 6.2 km of carriageway surveyed were all similar with a thickness of roadbase slab between 110mm and 140mm.

A greater variation in slab lengths than those indicated in table 6.8 may be attributed to the wide range of critical material properties permitted by the relevant specifications, prevailing environmental conditions and occurrence of secondary cracking on roadbase slabs greater than the characteristic length, particularly where laid on sub-grades offering poor restraint.

6.8.5 Sub-base Restraint

Either compressive or tensile stresses are induced into the roadbase

dependent on whether temperatures increase or decrease. In both cases a partial restraint to thermally induced movement of the roadbase is provided by frictional forces between this layer and the underlying sub-base. These frictional forces, considered in terms of a restraining stress, increase linearly with roadbase displacement up to a maximum stress and thereafter remain constant for greater displacements.

Relationships presented by Sparks [96] and Stott [97] show that the type and smoothness of the foundation have a marked effect on the restraint stress. On the basis of his test results, Sparks suggested that the restraint stress increased linearly to 6 kN/m^2 at a longitudinal displacement of 1.4mm and thereafter remained constant for all sub-base types. However, Stott proposed a linear relationship increasing from zero to 1.7 kN/m^2 at 7mm displacement for the crushed limestone sub-base material used predominantly in the South West of England. Both sets of results indicate that the restraint must be considered as varying with the width of crack opening (displacement) and hence with the length of slab. Thermal movements predicted through elastic analysis must therefore be reduced by a factor related to slab length and frictional restraint.

The method adopted to calulate this factor was originally developed in 'Concrete Roads' [98]. The restraint to roadbase movement at a point x in a slab of length (l) is integrated within the limits of 0 to $l/_2$ to provide an expression for the slab end. The crack opening width is the product of two slabs and therefore the expression must be doubled to take account of both adjacent slab ends.

$$\Delta c = 2 \left[\frac{Q}{Eh} \frac{l^2}{12} \right] \qquad \text{- Eq.(6.9)}$$

where Δc = reduction in roadbase movement at the slab end in metres
Q = frictional restraint stress per unit area of foundation
E = Elastic Modulus of lean concrete
h = roadbase thickness
l = roadbase slab length

Adopting the relationships between Q and roadbase displacement proposed by Stott and Sparks, fig.6.15 shows the correction in millimetres for a range of roadbase slab lengths and crack opening widths.

The following assumptions are made:-

(i) roadbase thickness = 150mm,

(ii) elastic modulus of lean concrete = 34.16×10^9 N/m^2.

As the restraint stresses proposed by Stott represent the worst case they are used to correct the crack opening widths adopted by the tensile fatigue model and presented in Table 6.2.

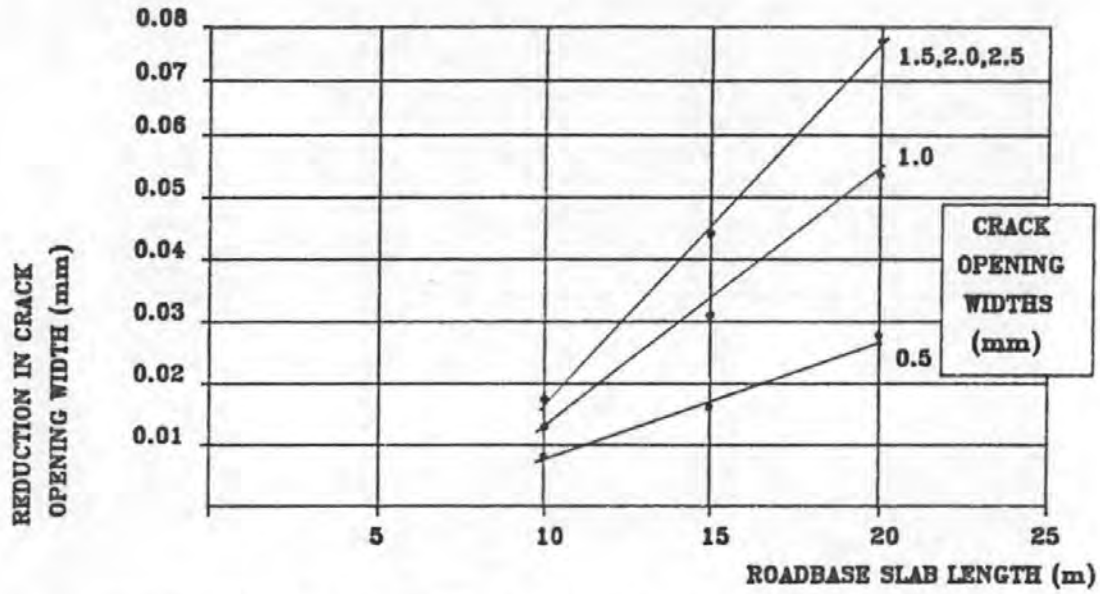

REDUCTION IN CRACK OPENING WIDTHS BASED ON THE ANALYSIS OF SUB-BASE RESTRAINT FROM THE RESULTS OF SPARKS (96)

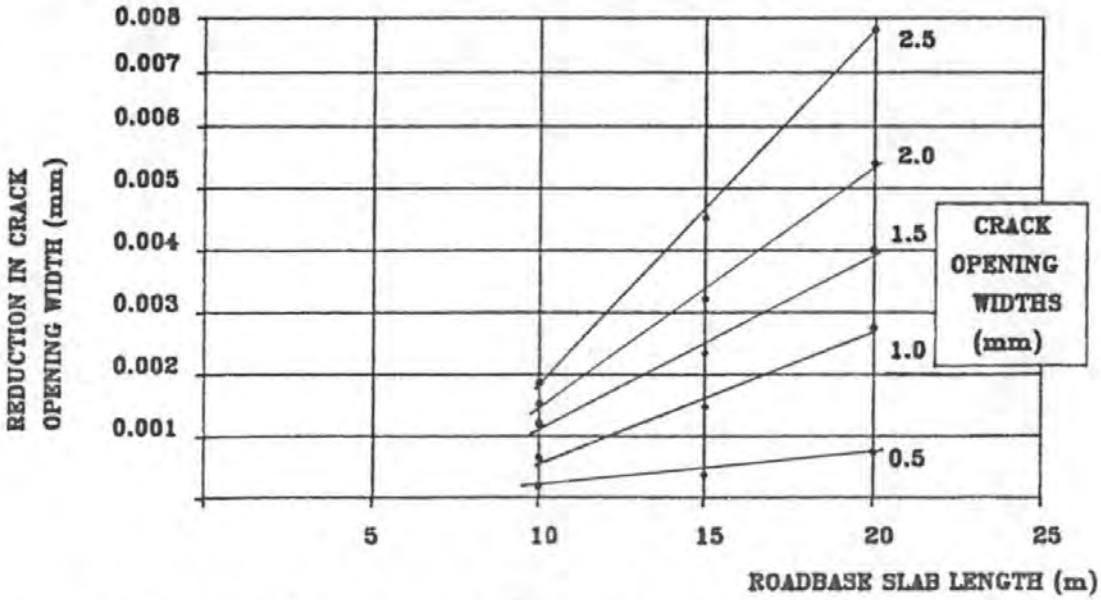

REDUCTION IN CRACK OPENING WIDTHS BASED ON THE ANALYSIS OF SUB-BASE RESTRAINT FROM THE RESULTS OF STOTT (97)

FIG.6.15 EFFECT OF SUB-BASE RESTRAINT ON ROADBASE MOVEMENT

6.9 MIX STIFFNESS OF BITUMINOUS SURFACINGS RELEVANT TO TENSILE FATIGUE

6.9.1 Introduction

The magnitude of the stress intensity factor required for the application of the Paris Equation is dependent upon the stiffness of each individual layer of bituminous surfacing and the stiffness ratio between them. Therefore, a method of measuring the response of asphaltic material in terms of its loading time and temperature was required that was both easy to perform and would provide consistent results.

A combination of simple experimental procedures, supplemented for high bitumen stiffnesses by the use of published data, provides a system for the measurement of mix stiffness (S_m) under cyclic loading conditions exerted by:

(i) thermally induced stresses (S_b less than $1 \times 10^5 N/m^2$) and

(ii) traffic loading (S_b greater than $1 \times 10^5 N/m^2$)

6.9.2 Calculation of Creep Stiffness

Deterioration of bituminous surfacings due to the mechanism of horizontal crack opening occurs during the tensile phase of the displacement cycle. Thus the tensile rather than compressive creep modulus is relevant.

A simple creep test procedure has been developed. 100 x 100 x 40mm blocks of test material are bonded to rectangular steel platens with epoxy resin and mounted horizontally in series on a greased slide way [95]; (plate 6). The end platens are designed so that one may be secured while the other is fitted with an eye bolt through which the samples may be loaded by the application of weights via a steel strop. A direct tensile stress of 7.3×10^3 N/m^2 was found to be the optimum stress level to allow manual recording of results and is applied by attaching a 30kg mass to the strop. This loading method allows manual readings of the tensile displacements to be taken at set time intervals from a dial gauge mounted across the samples. The stress/strain relationship derived allows the tensile creep stiffness to be calculated for each time interval and to be plotted against the corresponding values of bitumen stiffness derived from Van der Poels nomograph [13]. The values of bitumen softening point and penetration index necessary for use with the nomograph are either derived from tests [10,11] on binders recovered from the specimens,

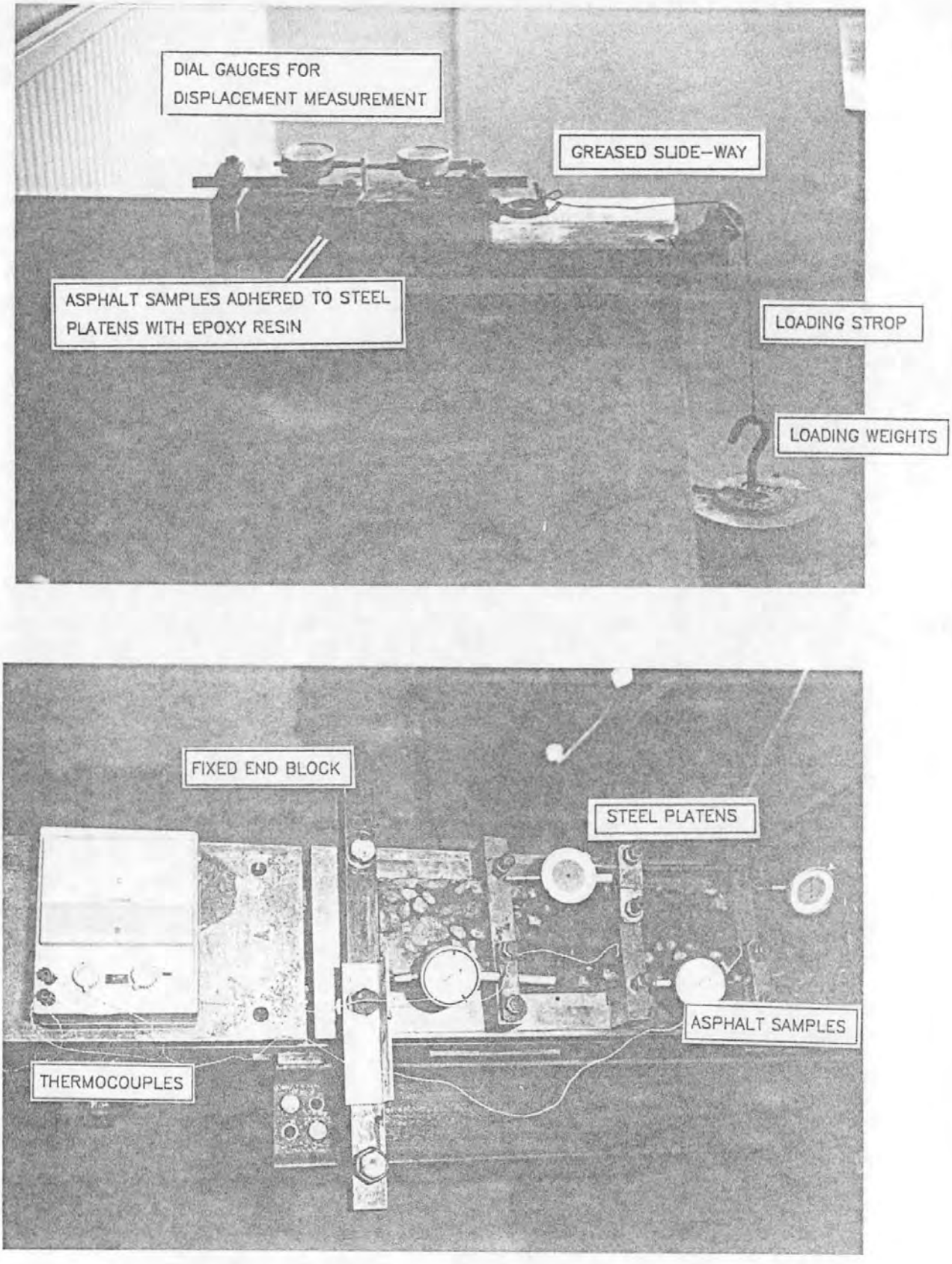

TEST CONFIGURATION WITH DIAL GAUGES TO MONITOR STRAIN

PLATE 6 TENSILE CREEP TEST

or determined from an empirical relationship for recovered properties which estimates hardening of the binder during the mixing process; Eqns 2.5 and 2.6. A program, C.R.P.100, written in 'basic' and listed in Appendix 6 allows the test results to be plotted in a standard format. The manual data recording system limits the use of the test to bitumen stiffness (S_b) values within the range 1 x 10^{-2} N/m^2 to 1 x 10^5 N/m^2 at ambient temperature. For higher values of bitumen stiffness, the mix stiffness can be calculated directly from relationships between S_m, S_b and volume of compacted aggregate and binder derived by Van der Poel [13] and modified by Henkelom and Klomp [14], (see section 2.2.2).

Tensile creep tests have been carried out on each of the test samples listed in Table 6.1. The recovered bitumen properties used in conjunction with the mean monthly pavement temperatures, fig.6.3, allows the bitumen stiffness to be calculated from the nomograph[13] for a daily loading cycle. The sinusoidal loading cycle is modified to convert it into an equivalent static loading time; Eqn.2.2. A corresponding value of mix stiffness, S_{md}, has been recorded from the S_m / S_b plot of each mix and is used in the derivation of its annual fatigue life, (section 6.13).

The effectivness of the simple tensile creep test procedure can be demonstrated by comparing mix stiffnesses obtained from the test with those obtained from the more conventional method of three point bending under an applied cyclic load, fig 6.16. However, the non-uniform application of stress must be considered as a criticism of the test which is an over-simplification to provide a practical test to give comparitive data only.

6.9.3 Tensile Yield Strain

The creep test described in the previous section can, by continuing the test to failure of the sample blocks, provide an indication of the yield strain of the material. The yield point is defined from the plot of mix stiffness versus bitumen stiffness, fig.6.17, as the point at which the characteristic curve diverges from that described by the yielding material. The corresponding strain value is taken from the experimental data of measured strain.

A relationship between yield strain (Ys) and the plastic zone ahead of the crack tip; provides a correction to the elastic analysis used

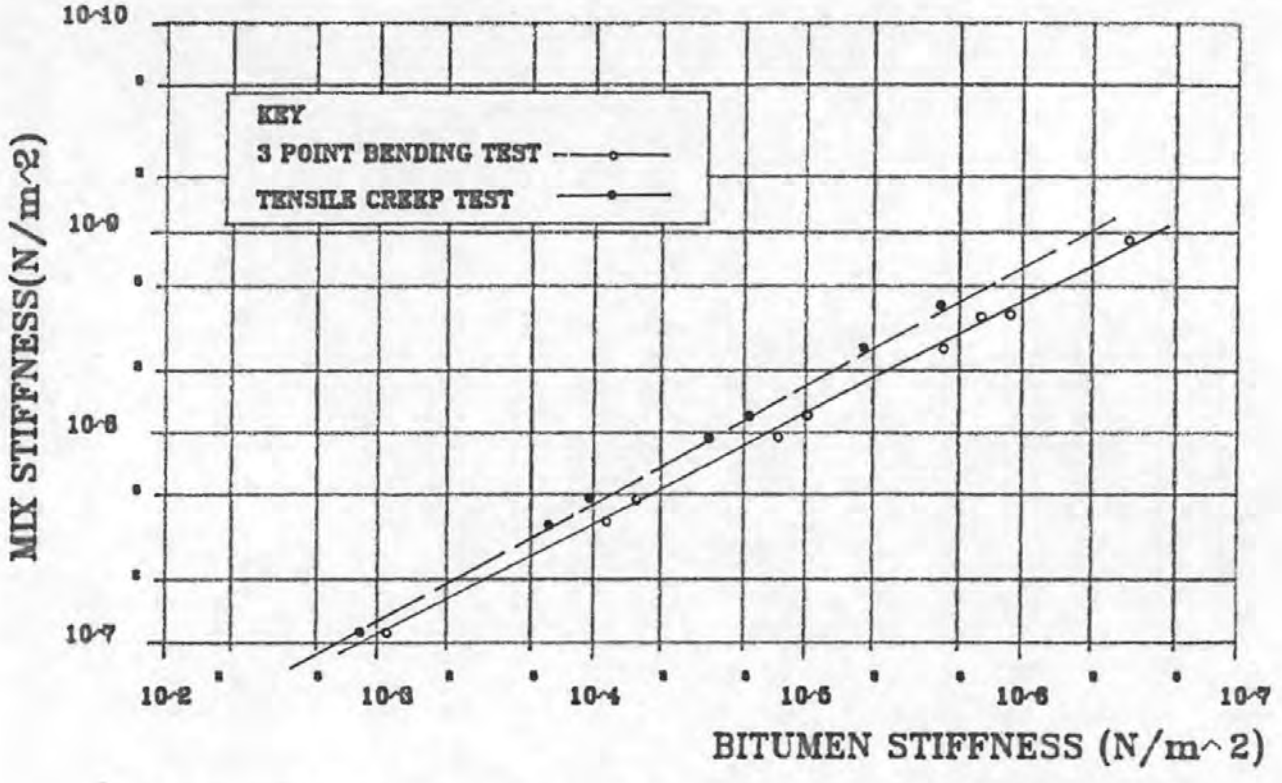

FIG.6.16 COMPARISON OF STIFFNESS VALUES FOR MATERIAL TESTED BY TENSILE CREEP TEST AND 3 POINT BENDING

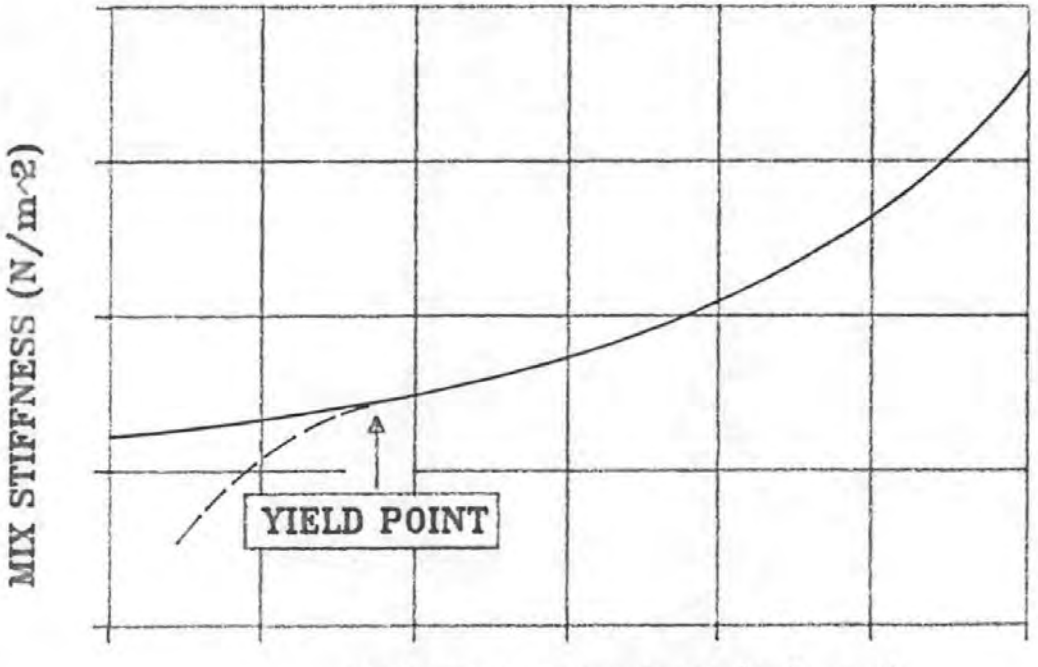

FIG.6.17 DEFINITION OF TENSILE YIELD POINT (DIAGRAMMATIC ONLY)

to evaluate the crack length, described in section 6.4.3 and shown in fig.6.8. Furthermore, it gives an indication of the resistance exhibited by bituminous materials to the mechanism of tensile yield, described in section 7.

6.10 STRESS INTENSITY FACTORS

6.10.1 Introduction

An interpretation of the fracture phenomena which occur near the crack tip is provided by applying fracture mechanics theory. This approach, originally developed by Irwin [99], noted that the stresses in the vicinity of a crack tip could be expressed in the following form:

$$\begin{vmatrix} \sigma xx \\ \\ \sigma yy \\ \\ \tau xy \end{vmatrix} = \frac{k \cos \phi/2}{\sqrt{2\pi r}} \begin{vmatrix} 1 - \text{Sin } \phi/2 \text{ Sin } {}^{3}\phi/2 \\ \\ 1 + \text{Sin } \phi/2 \text{ Sin } {}^{3}\phi/2 \\ \\ \text{Sin } \phi/2 \text{ Cos } {}^{3}\phi/2 \end{vmatrix} \qquad \text{- Eqn. (6.10)}$$

where r, ϕ are the cylindrical polar coordinates of a point with respect to the crack tip, k is the stress intensity factor and σxx and σyy are the normal stress and τxy is the shear stress shown in fig.6.18.

Therefore, for a characteristic spatial distribution of stress, each case may be characterised by the stress intensity factor k, which describes the mechanical environment as a whole.

The magnitude of k controls the rate of crack propagation during the condition of stable crack growth. The upper limit of this magnitude is defined by the critical stress intensity factor k_c at which unstable brittle fracture occurs. However, previous research has shown[72] that this value is not reached and crack growth remains stable within the bituminous layers.

The three possible cracking modes are depicted in fig.6.12. Their associated stress intensity factors are given the subscripts I, II and III. The subscript 'I' refers to the case where the in-plane loading is symmetric with respect to the crack plane; subscript 'II' refers to the case where the in-plane loading is skew-symmetric with respect to the crack plane, and subscript III refers to the case where the loading is anti-plane shear (shear loading in x-z and y-z

Using The Coordinate System:-

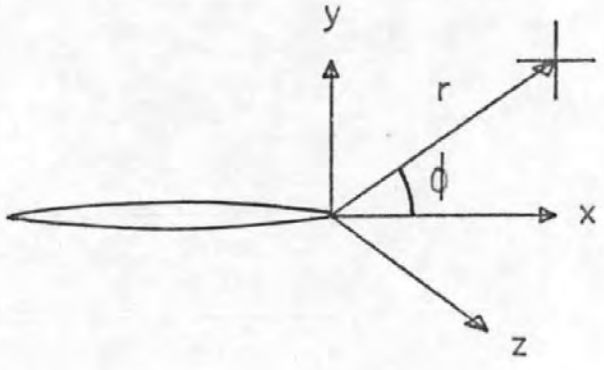

And Mode 1 Cracking

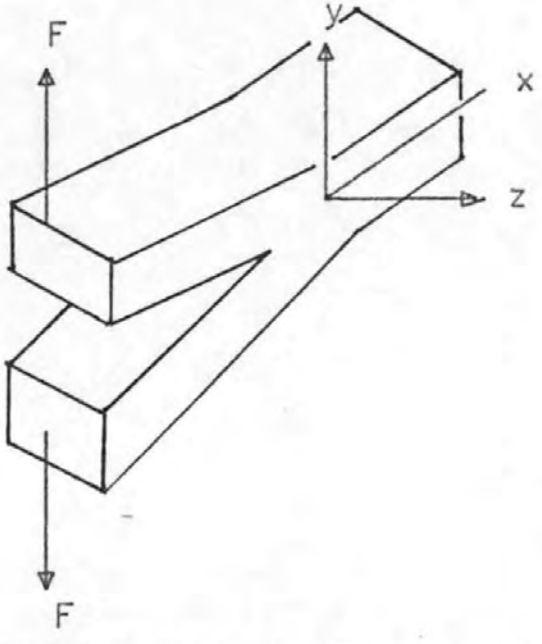

FIG.6.18 *DEFINITION OF THE PRINCIPAL STRESSES FOR DERIVATION OF THE STRESS INTENSITY FACTOR FROM EQUATION (6.12)*

planes).

The loading condition associated with the mechanism of tensile fatigue is in-plane and therefore the value of the stress intensity factor is given by k_I. However, this value refers to static loading and requires modification for use with cyclic loading conditions. For a sinusoidal loading cycle that incorporates a tensile and compressive phase the stress intensity factor relating to the phase difference must be considered and is given by:

$$\Delta k = k_{max} - k_{min}$$

The relaxation mechanisms in bituminous materials will reduce the stress in the compressive phase to zero. Furthermore, it is assumed that crack initiation occurs in the surfacing during the initial contraction of the slabs after construction. Crack growth occurs in the tensile phase of subsequent cycles of expansion and contraction. Therefore, Δk equals the maximum stress intensity factor k_{max} which is represented by k_o throughout this thesis.

6.10.2 Derivation of the Stress Intensity Factors using Finite Element Techniques

The finite element approach requires the structure to be reduced to a skeletal form consisting of individual members (elements) connected at their ends (nodes). Analysis of the skeletal form is carried out initially by considering the independent behaviour of individual elements and then by assembling the elements together so that the following three conditions are satisfied at each nodal point.

(1) equilibrium of forces
(2) compatability of displacements
(3) laws of material behaviour

Accurate modelling of a pavement structure may be achieved by its subdivision into geometrically simple elements with the mesh refinement dictated by the proximity of the crack tip.

This modelling technique provides a method by which the stress (σ)(Equation 6.10) adjacent to the crack tip may be defined for structures of unique geometry and loading conditions for input increments of crack length. It has been shown [100] that for isoparametric elements the most accurate results are given by displacement extrapolation to the crack tip along the radial line

$\phi = 180^{\circ}$, fig. 6.18. Equation 6.10 may therefore be simplified to:-

$$k = \sigma xx\sqrt{2\pi r} \qquad \text{- Eqn.(6.11)}$$

where σxx is the stress at a distance r ahead of the crack tip as r tends to zero.

and $k = k_{max}$, $(k_{min} = 0)$

Values of normal stress at nodes ahead of the crack tip are substituted into Eqn.6.11 to provide a plot of k versus their respective distance from crack (r) enabling k_o to be defined at the point where r tends to zero, fig.6.19.

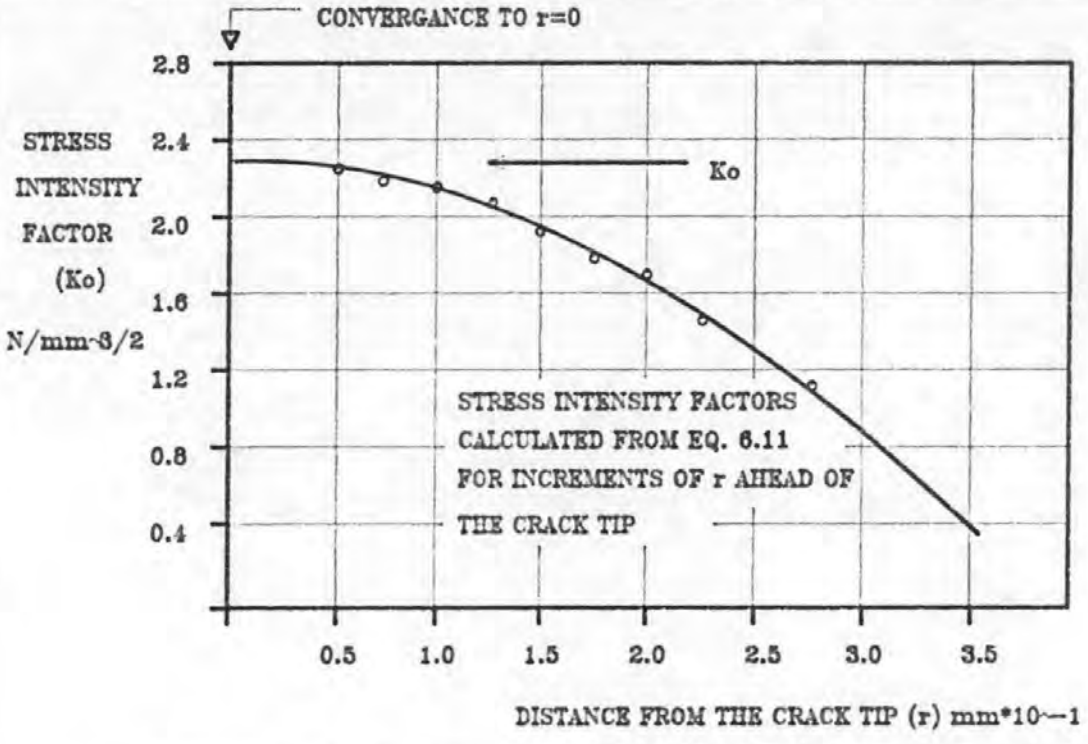

FIG. 6.19 DERIVATION OF STRESS INTENSITY FACTOR (Ko) FROM THE STRESS OUTPUT OF THE F.E MODEL

The accuracy attained by this method is therefore dependent upon the geometry and size of the element mesh adopted in the vicinity of the crack tip. It is necessary that the elements immediately adjacent to the crack tip be very small in proportion to the crack length with an optimum size of about 0.005c [101], where c is the crack length. The most efficient mesh results from a smooth progressive increase in element size radiating in all directions from the crack tip. However, beyond a distance of one crack length from the crack tip there is no limitation on element size. Furthermore, very slender elements

anywhere in the mesh produce errors in the results. These errors are negligible if the element length to width ratio is confined to a maximum of 15.

6.10.3 Description of Finite Element Model, F.E.1, used to Define the Stress Intensity Factor

The finite element package 'PAFEC'[102] has been used to analyse the stresses within the surfacing layers of a pavement structure resulting from thermally induced roadbase displacements. It is a commercially available program, which provides for a range of input modules. These modules allow a wide variety of engineering problems with differing material characteristics and loading regimes to be evaluated.

Analysis of the composite pavement has been confined to a two-dimensional model and assumes that plane strain conditions prevail. This assumption is violated only near the edge of the pavement, elsewhere the bulk of the pavement material prevents Poisson contraction under applied displacements. The model, F.E.1, shown in fig.6.20 is constructed of eight noded isoparametric curvilinear quadrilateral elements and adopts the guidelines relating to mesh generation in the region of the crack tip described in the previous section. The stiffness, mesh and loading matrices are all computed by the program by transforming the curved shape into a square using an isoparametric method.

Bending and twisting effects acting on the plane of the element are ignored and materials are defined as linear elastic and isotropic. Although the use of elastic analysis is an approximation it is overcome by considering the mix stiffness, S_{md}, as an elastic modulus. Furthermore, the plastic zone ahead of the crack tip is assumed to have negligible influence upon the stress intensity factor and the crack configuration is idealised with no irregularities or permanent deformation within the surfacing.

The mid-side nodes of the two eight node isometric elements which meet at the crack tip are moved from the half to the quarter positions. This element distortion increases the linearity of the relationship between $k/\sigma xx(2\pi r)^{\frac{1}{2}}$ versus distance ahead of the crack tip and therefore adds a greater accuracy to the displacement method

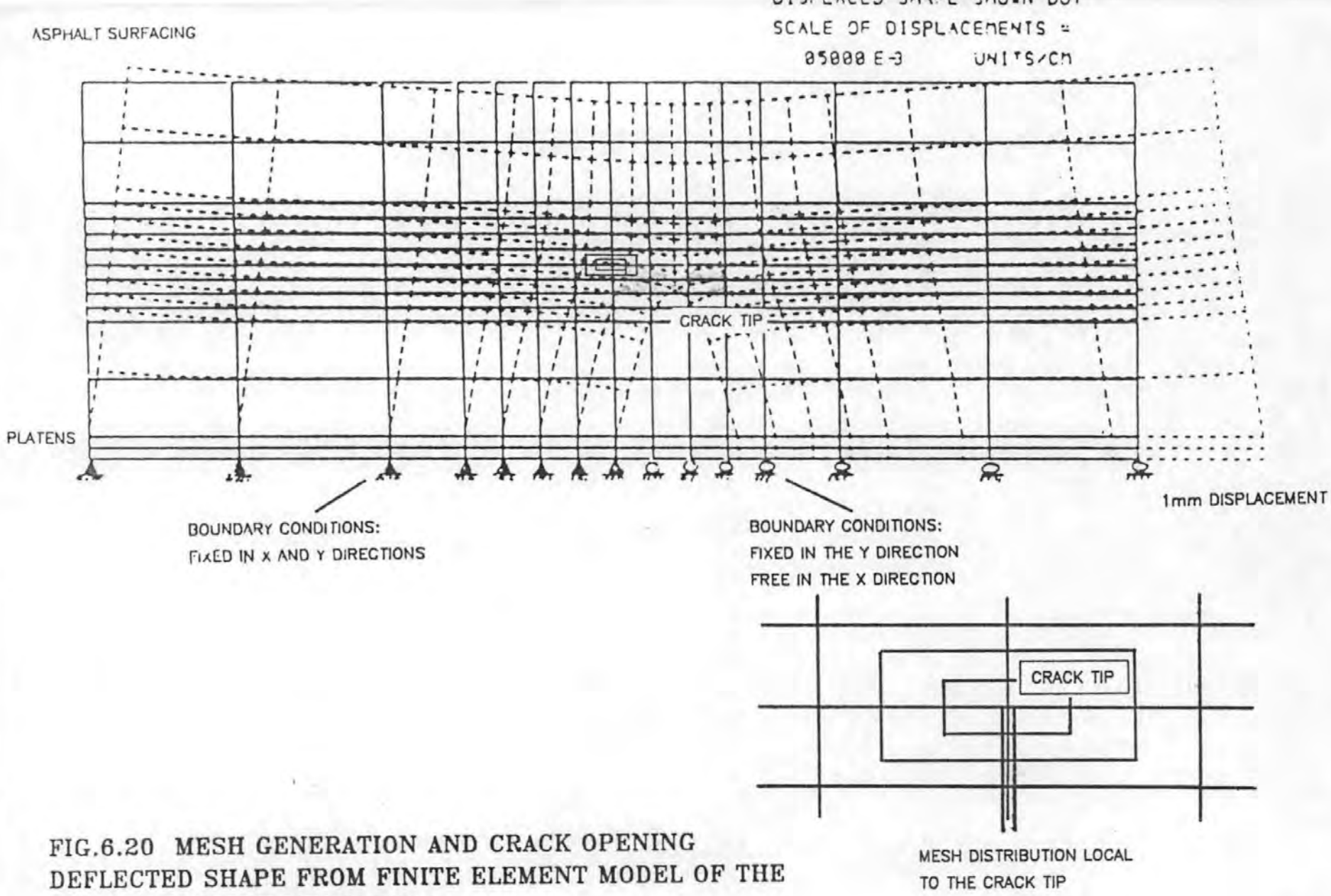

FIG.6.20 MESH GENERATION AND CRACK OPENING DEFLECTED SHAPE FROM FINITE ELEMENT MODEL OF THE TENSILE FATIGUE MECHANISM

of stress intensity calculation.

The boundary conditions at the base of the structure are defined as a restraint in the y (vertical) direction but freedom of movement in x (horizontal) direction with the sides and surface given total freedom of movement and rotation. Various lengths of pavement section have been analysed to ensure that the stress field and boundary conditions remote from the crack on the final model did not influence the accuracy of the subsequent values of stress intensity factor.

Thermal movement within the roadbase is simulated by displacing each side of the crack a nominal displacement of 0.5mm. The resultant 1mm crack opening width (u) induces tensile stresses within the surfacing.

The output listing phase of the program gives the principal stresses at each of the eight nodes and at a central point for each element. Each corner node occurs in the output listing of four elements. Slight variations generally occur between the estimation of stress for each of these nodes. The similarity of these values is a measure of the overall accuracy of the analysis. The averaged stresses at nodes are also listed. At nodes ahead of the crack tip these values are defined as σxx in equation 6.11 and are used to evaluate the stress intensity factor.

The model assumes an idealised rigid bond between the surfacing and roadbase. However, a modification has been made to allow an investigation of the reduction in stress magnitude which would result from any debonding between these two layers.

6.10.4 Modified Stress Intensity Factors in Terms of Input Strain Parameters

The stress intensity factor is a function of stress within a cracked material, as described in section 6.10.1. Therefore, for any given crack length, it may further be defined in terms of the magnitude of the crack opening width and the stiffness of the material. The elastic linearity of material assumed throughout the analysis allows stress intensity factors derived for unit conditions, fig.6.21, to be expanded to incorporate any condition of crack opening width, ratio of stiffness values between layers and pavement geometry.

The unit values are defined as:

1) crack opening width of 1mm
2) depth of surfacing of 100mm
3) surfacing stiffness of $1 \times 10^8 N/m^2$

Further runs of the finite element model allowed the stress intensity factor to be determined for various ratios between the stiffnesses of the wearing course and the basecourse, shown in fig.6.21.

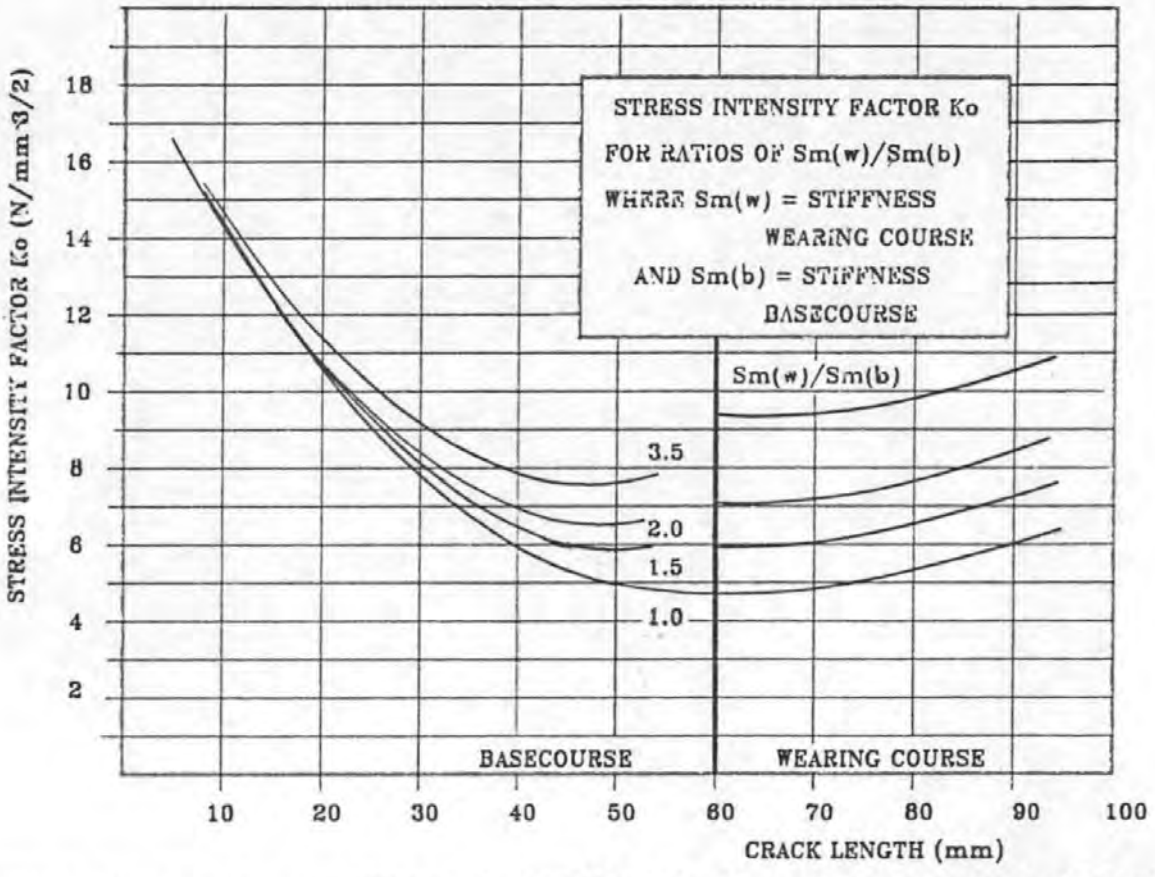

FIG.6.21 STRESS INTENSITY FACTOR Ko VERSUS CRACK LENGTH FOR GIVEN RATIO OF WEARING COURSE/BASECOURSE STIFFNESSES

As the stress intensity factor, k_o, is directly proportional to the crack opening width (u) it may be combined with the ratio of stiffness values to provide an expression for the modified stress intensity factor, k_r, for any specified crack opening width and stiffness value of the wearing course:

$$k_r = \frac{k_o \times u \times S_{md(w)}}{10^8} \qquad \text{- Eqn.(6.12)}$$

where k_o = stress intensity factor from fig.6.19

u = crack opening width

$S_{md}(w)$ = stiffness of the wearing course due to daily cyclic loading at a specified mean monthly temperature

The pavement geometry is considered in terms of the depth of surfacing through which the crack propagates. The stress intensity factor is a function of the square root of distance ahead of the crack tip given by equation 6.12 and therefore is proportional to $\sqrt{h/h_o}$, where;

h = the depth of surfacing material and

h_o = 100mm (the surfacing depth used for calculating the unit stress intensity factor k_o).

Equation 6.12 may therefore be expanded to incorporate this term giving:-

$$k_r = \frac{k_o \times u \times S_{md}(w)}{10^9} \sqrt{\frac{h}{h_o}} \qquad \text{Eqn.6.13}$$

The analysis is limited by the assumption of a bond over the entire length of roadbase/surfacing interface. The stress intensity factor at the crack tip is reduced if debonding occurs along this interface, as strains exerted by roadbase movement on the surfacing act over a finite length rather than at a point. The greater the debonded length the greater the reduction in the value of the crack tip stress intensity factor.

This condition is illustrated in fig.6.22 with a plot of stress intensity factor versus debonded lengths of 100mm and 200mm along the roadbase/surfacing interface adjacent to vertical cracks within the surfacing.

The significance of this condition on the extention to the fatigue life of the pavement surfacing is discussed in section 6.13.

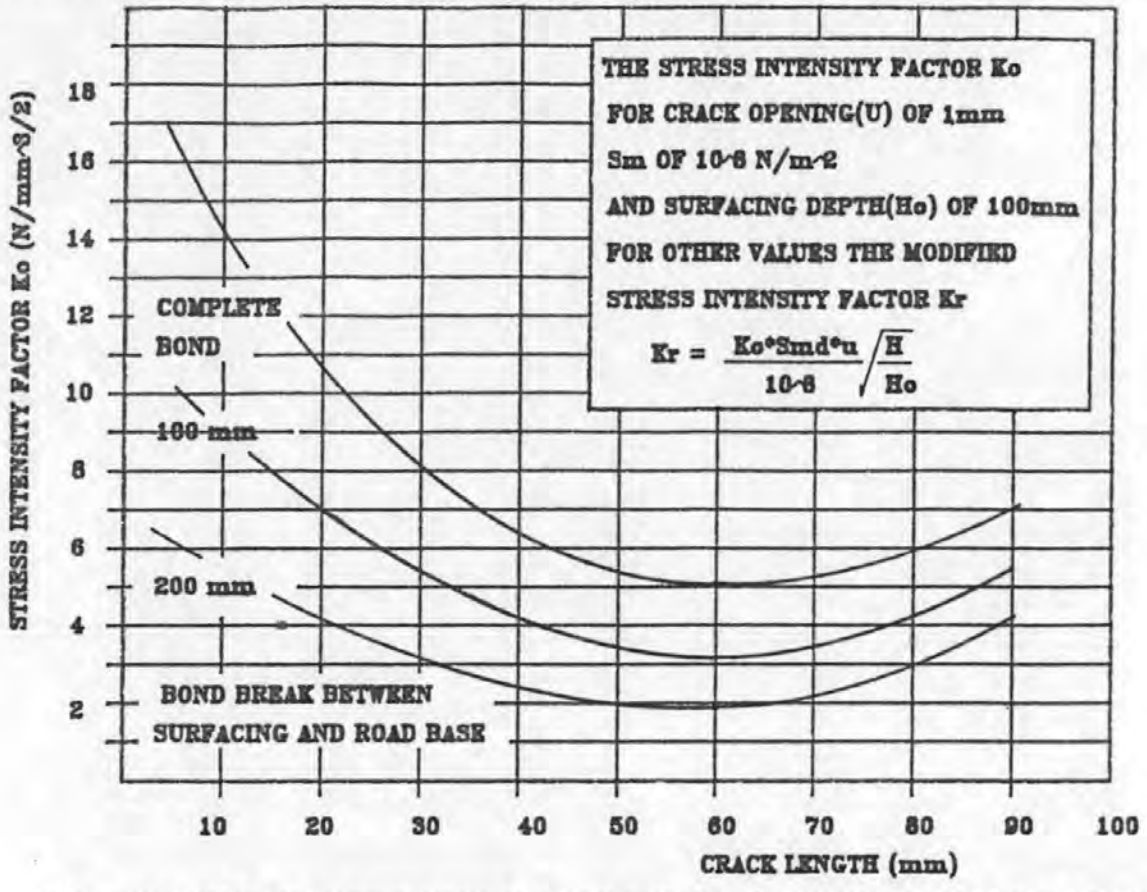

FIG.6.22 STRESS INTENSITY FACTOR (Ko) VERSUS CRACK LENGTH FOR BOND BREAK BETWEEN SURFACING AND ROAD BASE

6.11 DETERMINATION OF FATIGUE CONSTANTS A AND n

6.11.1 Introduction

The material constants in Paris' Equation[81] provide a measure of the susceptibility of bituminous material to crack propagation. The influence of both constants on the fatigue life of the surfacing is illustrated in fig.6.23. This presents a graphical solution of Paris' Equation; the plot is obtained by numerical integration of the equation with a unit value of stress intensity factor k. For a constant value of n the fatigue life will increase as the value of constant A decreases. A similar increase in fatigue life exists for a constant value of A with an decreasing value of n. However this applies only to a single value of mix stiffness.

The gradient and location of the parallel lines of constant n are governed by the magnitude of the stress intensity factor. However,

for conditions of constant crack opening width (u) and for a defined pavement geometry the value of k varies solely with the stiffness of the mix. For constant values of A and n the location of the lines moves to the right as the stiffness of the mix is reduced and the fatigue life increases.

Laboratory testing to determine A and n and hence produce a plot of the format shown in fig.6.23 for every mix and design situation is both complex and time consuming. An alternative and more practical approach is to evaluate the fatigue life directly either through manual calculation, numerical integration or an appropriate computer program.

6.11.2 Experimental Procedure

The crack opening simulator was used to test beams of asphaltic material and provide a plot of crack length (c) versus the number of strain cycles (N). The correction procedure described in section 6.4 is applied to the elastic analysis to allow for plastic yield ahead of the crack tip. Using an appropriate routine a polynomial function is fitted to the corrected c/N plot in the form of $c = A_1 N^{A_2}$. Differentiation of this equation gives an expression that defines the rate of crack propagation dc/dN.

For each increment of crack length (c) the unit stress intensity factor (k_o) has been evaluated from the output of the finite element model, described in section 6.10. These values are subsequently modified to satisfy the test conditions of crack opening width (u) and material stiffness (S_m).

The calculated values of dc/dN are then plotted against the corresponding values of the modified stress intensity factor (k_r) to give the material constants A and n, fig.6.24. An example of this procedure is given in Appendix 2 for a 20mm D.B.M.

6.12 TEST RESULTS

6.12.1 Introduction

Daily fluctuations of temperature under typical U.K. conditions provide a range of bitumen stiffness from 1×10^3 to $5 \times 10^5 N/m^2$ for binders used in conventional surfacing mixes. Therefore, the bitumen

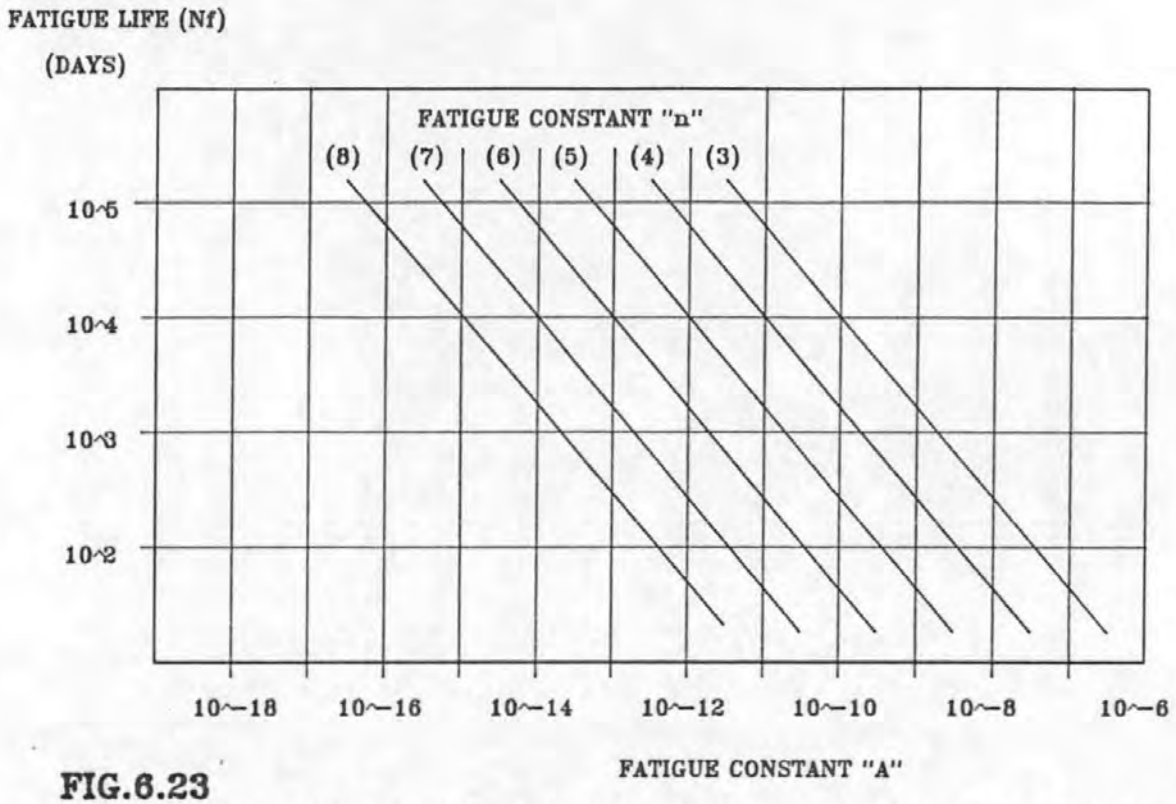

FIG.6.23
EXPANSION OF PARIS' EQUATION THROUGH NUMERICAL INTEGRATION

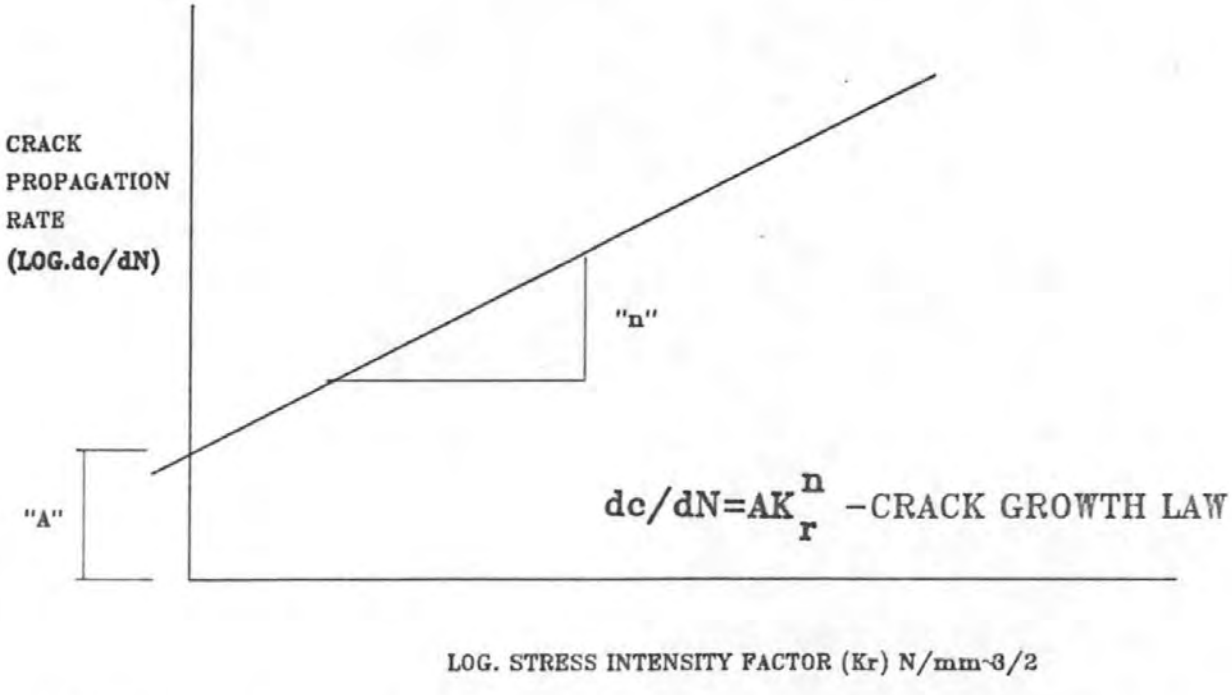

FIG.6.24 DERIVATION OF FATIGUE CONSTANTS "A" AND "n"

stiffness of the laboratory tests was restricted to a similar range by regulating the test frequency and temperature. However, tests undertaken with bitumen stiffness values below 1 x $10^4 N/m^2$ failed through plastic deformation rather than cracking. The mechanism of tensile fatigue is unlikely, therefore, to operate under low stiffness conditions.

To enable a comparison to be made between test results the crack opening width (u) was standardised at 1.4mm. This value is typical of that generated between slabs of length 10-20m under typical U.K. temperatures.

6.12.2 The Effect of Mix Parameters on Fatigue Constants A and n

The fatigue constants derived from the laboratory tests related to bitumen content, void content, bitumen grade, nominal aggregate size and material type are given in tables 6.9 to 6.13. To enable the effect of each parameter to be assessed each table contains all the results carried out within the specified test sequence, although this has resulted in some repetition of results. The results from these tables are presented graphically in figures 6.25 to 6.27. The influence of bitumen stiffness and bitumen content on fatigue constant A is demonstrated in fig.6.25. An increase in bitumen stiffness and a reduction in bitumen content reduces the value of parameter A. Larger nominal aggregate size and greater compaction, shown in fig.6.26 and 6.27 respectively, also reduce the value of A.

The mix variations produced values of A ranging from 10^{-10} to 10^{-1}. An error in A leads directly to a proportional error in the reflection cracking fatigue life. A high degree of accuracy is required when determining the magnitude of A.

Bitumen grade has been shown to have a major influence on the value of n and a mean value has been derived for each grade. Although this involves a simplification, the effect of this on the calculated annual fatigue life can be shown to be negligible.

6.13 DERIVATION OF ANNUAL FATIGUE LIFE

6.13.1 Introduction

The method outlined in Section 6.7 and the data provided in sections 6.8 to 6.10 have been combined with laboratory test results (fatigue

TABLE 6.9

RESULTS FROM TESTS INVESTIGATING THE INFLUENCE OF BITUMEN CONTENT ON THE CYCLES TO FAILURE AND FATIGUE CONSTANTS

Test Sample Thickness = 100mm

Sample No. (Table 6.1)	Nominal Agg. Size (mm)	Material Type	% Bitumen	Bitumen Grade (Pen)	Void Content (%)	Test Conditions			Test Results		
						Crack Opening Width u(mm)	Bitumen Stiffness (N/m^2)	Mix Stiffness (N/m^2)	Cycles to Failure (No.)	Fatigue Constant A	Fatigue Constant n
10	20	DBM	4.2	200	3.1	1.4	1×10^4	8×10^6	24,500	5×10^{-4}	4.3
10	20	DBM	4.2	200	3.1	1.4	5×10^4	1.7×10^7	11,200	4×10^{-5}	4.2
10	20	DBM	4.2	200	3.1	1.4	1×10^5	3×10^7	3,600	9×10^{-6}	4.6
10	20	DBM	4.2	200	3.1	1.4	5×10^5	8×10^7	1,250	1×10^{-6}	4.7
11	20	DBM	4.7	200	2.9	1.4	1×10^5	5×10^7	8,100	4×10^{-5}	4.7
12	20	DBM	5.2	200	3.0	1.4	1×10^5	2×10^7	17,280	8×10^{-5}	4.7
14	20	DBM	6.2	200	2.7	1.4	5×10^4	8×10^6	121,650	3×10^{-4}	4.8
14	20	DBM	6.2	200	2.7	1.4	1×10^5	1×10^7	24,580	1×10^{-4}	5.0
14	20	DBM	6.2	200	2.7	1.4	5×10^5	3×10^7	7,120	2×10^{-5}	4.9

TABLE 6.10

RESULTS FROM TESTS INVESTIGATING THE INFLUENCE OF VOID CONTENT ON THE CYCLES TO FAILURE AND FATIGUE CONSTANTS

Test Sample Thickness = 100mm

Sample No. (Table 6.1)	Nominal Agg. Size (mm)	Material Type	% Bitumen	Bitumen Grade (Pen)	Void Content (%)	Test Conditions			Test Results		
						Crack Opening Width u(mm)	Bitumen Stiffness (N/m^2)	Mix Stiffness (N/m^2)	Cycles to Failure (No.)	Fatigue Constant A	Fatigue Constant n
19	40	DBM	4.2	100	11.2	1.4	1×10^4	1.1×10^7	1,468	1.7×10^{-1}	6.2
19	40	DBM	4.2	100	11.2	1.4	1×10^4	1.1×10^7	1,970	1.3×10^{-1}	6.4
20	40	DBM	4.2	100	7.8	1.4	1×10^4	2.3×10^7	4,680	1.3×10^{-3}	6.5
21	40	DBM	4.2	100	6.2	1.4	1×10^4	2.6×10^7	10,700	4.6×10^{-4}	6.6
21	40	DBM	4.2	100	6.2	1.4	1×10^4	2.6×10^7	8,400	7.0×10^{-4}	6.7
22	40	DBM	4.2	100	4.7	1.4	1×10^4	3.2×10^7	12,511	6.7×10^{-6}	6.5
1	40	DBM	4.2	100	3.2	1.4	1×10^4	4.0×10^7	23,400	6.0×10^{-9}	6.9
1	40	DBM	4.2	100	3.2	1.4	1×10^4	4.0×10^7	26,100	5.5×10^{-9}	6.8

TABLE 6.11

RESULTS FROM TESTS INVESTIGATING THE INFLUENCE OF BITUMEN GRADE ON THE CYCLES TO FAILURE AND FATIGUE CONSTANTS

Test Sample Thickness = 100mm

Sample No. (Table 6.1)	Nominal Agg. Size (mm)	Material Type	% Bitumen	Bitumen Grade (Pen)	Void Content (%)	Test Conditions			Test Results		
						Crack Opening Width u(mm)	Bitumen Stiffness (N/m^2)	Mix Stiffness (N/m^2)	Cycles to Failure (No.)	Fatigue Constant A	Fatigue Constant n
10	20	DBM	4.2	200	3.1	1.4	1×10^4	8.0×10^6	24,300	5.0×10^{-4}	4.3
3	20	DBM	4.2	100	3.1	1.4	1×10^4	6.3×10^7	14,760	5.0×10^{-7}	6.9
3	20	DBM	4.2	100	3.1	1.4	1×10^5	2.5×10^8	8,340	4.0×10^{-9}	6.7
3	20	DBM	4.2	100	3.1	1.4	5×10^5	7.0×10^8	3,260	4.0×10^{-11}	6.8
3	20	DBM	4.2	100	3.1	1.4	1×10^6	3.0×10^9	810	1.5×10^{-13}	6.5
9	20	DBM	4.2	50	3.3	1.4	1×10^4	8.2×10^7	9,100	1.0×10^{-7}	8.2
9	20	DBM	4.2	50	3.3	1.4	1×10^4	8.2×10^7	12,250	7.0×10^{-7}	7.9
9	20	DBM	4.2	50	3.3	1.4	5×10^5	9.2×10^8	2,820	9.0×10^{-15}	7.4
9	20	DBM	4.2	50	3.3	1.4	1×10^6	4.2×10^9	630	2.0×10^{-17}	7.5

TABLE 6.12

RESULTS FROM TESTS INVESTIGATING THE INFLUENCE OF NOMINAL AGGREGATE SIZE ON THE CYCLES TO FAILURE AND FATIGUE CONSTANTS

Test Sample Thickness = 100mm

Sample No. (Table 6.1)	Nominal Agg. Size (mm)	Material Type	% Bitumen	Bitumen Grade (Pen)	Void Content (%)	Test Conditions			Test Results		
						Crack Opening Width u(mm)	Bitumen Stiffness (N/m^2)	Mix Stiffness (N/m^2)	Cycles to Failure (No.)	Fatigue Constant A	Fatigue Constant n
1	40	DBM	4.2	100	3.2	1.4	1×10^4	4.7×10^7	23,400	6.0×10^{-9}	6.9
1	40	DBM	4.2	100	3.2	1.4	1×10^4	4.7×10^7	26,100	5.5×10^{-9}	6.8
2	28	DBM	4.2	100	3.0	1.4	1×10^4	4.0×10^7	19,600	7.0×10^{-9}	7.0
2	28	DBM	4.2	100	3.0	1.4	5×10^4	9.0×10^7	11,310	4.0×10^{-10}	6.9
2	28	DBM	4.2	100	3.0	1.4	5×10^5	1.1×10^9	4,200	2.1×10^{-13}	6.6
3	20	DBM	4.2	100	3.1	1.4	1×10^4	6.3×10^7	14,760	5.0×10^{-7}	6.9
4	14	DBM	4.2	100	2.7	1.4	1×10^4	7.2×10^7	10,600	2.0×10^{-8}	7.2
5	10	DBM	4.2	100	3.0	1.4	1×10^4	7.0×10^7	8,950	1.8×10^{-6}	6.8
5	10	DBM	4.2	100	3.0	1.4	5×10^5	3.5×10^8	2,470	8.0×10^{-11}	6.7
5	10	DBM	4.2	100	3.0	1.4	5×10^6	8.5×10^8	330	1.0×10^{-14}	6.5

TABLE 6.13

RESULTS FROM TESTS INVESTIGATING THE INFLUENCE OF MATERIAL TYPE ON THE CYCLES TO FAILURE AND FATIGUE CONSTANTS

Test Sample Thickness = 100mm

Sample No. (Table 6.1)	Nominal Agg. Size (mm)	Material Type	% Bitumen	Bitumen Grade (Pen)	Void Content (%)	Test Conditions			Test Results		
						Crack Opening Width u(mm)	Bitumen Stiffness (N/m^2)	Mix Stiffness (N/m^2)	Cycles to Failure (No.)	Fatigue Constant A	Fatigue Constant n
29	20	HRA	6.5	200	4.3	1.4	1×10^4	2.0×10^7	83,500*	8×10^{-4}	5.2
30	20	HRA	6.5	100	4.1	1.4	5×10^4	5.0×10^7	52,000*	1×10^{-4}	4.6
31	20	HRA	6.5	44	3.9	1.4	1×10^5	1.5×10^8	21,600	4×10^{-6}	5.0
32	20	HRA	6.5	35	4.3	1.4	5×10^5	6.0×10^8	1,760	6×10^{-9}	6.2
33	20	HRA	6.5	26	4.8	1.4	5×10^6	2.5×10^9	840	1×10^{-11}	8.0
34	20	HRA	6.5	17	4.2	1.4	5×10^7	8.5×10^9	127	4×10^{-10}	7.3
15	40	open	4.2	200	-	1.4	1×10^4	6.2×10^6	8,120	2×10^{-5}	4.2
16	20	textured	3.8	200	-	1.4	1×10^4	5.4×10^6	7,840	9×10^{-5}	4.6
17	20	bitumen	4.2	50	-	1.4	1×10^4	9.0×10^6	5,324	7×10^{-4}	8.5
17	20	macadam	4.2	50	-	1.4	1×10^4	9.0×10^6	4,130	4×10^{-4}	8.1

* Estimated fatigue life

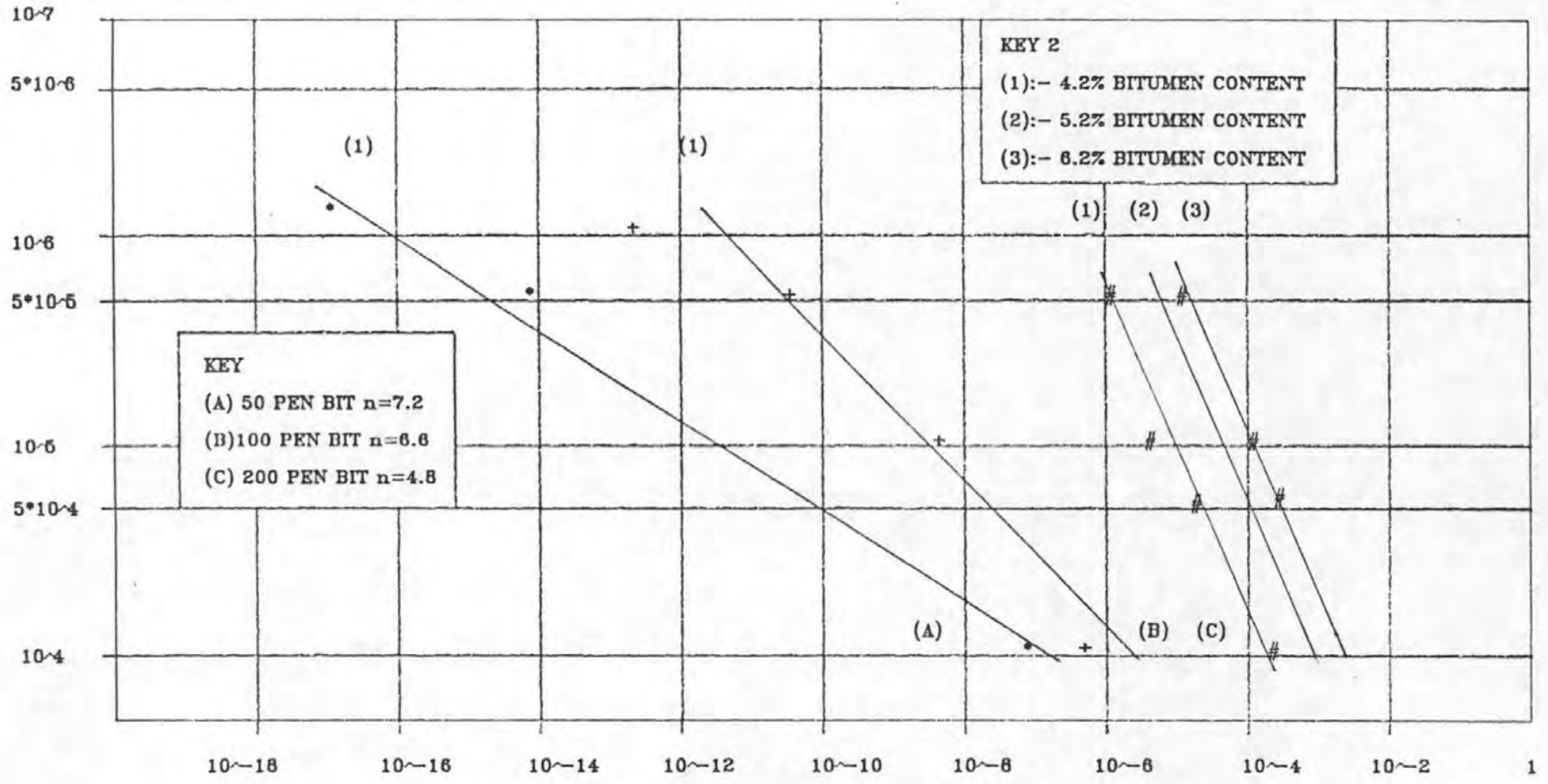

FIG.6.25 BITUMEN STIFFNESS VERSUS FATIGUE CONSTANT "A" FOR D.B.M. MIXES (1)

AGGREGATE GRADING:- 20mm BITUMEN CONTENT:- AS GIVEN

VOID CONTENT:- 3%

DENSE BITUMEN MACADAMS

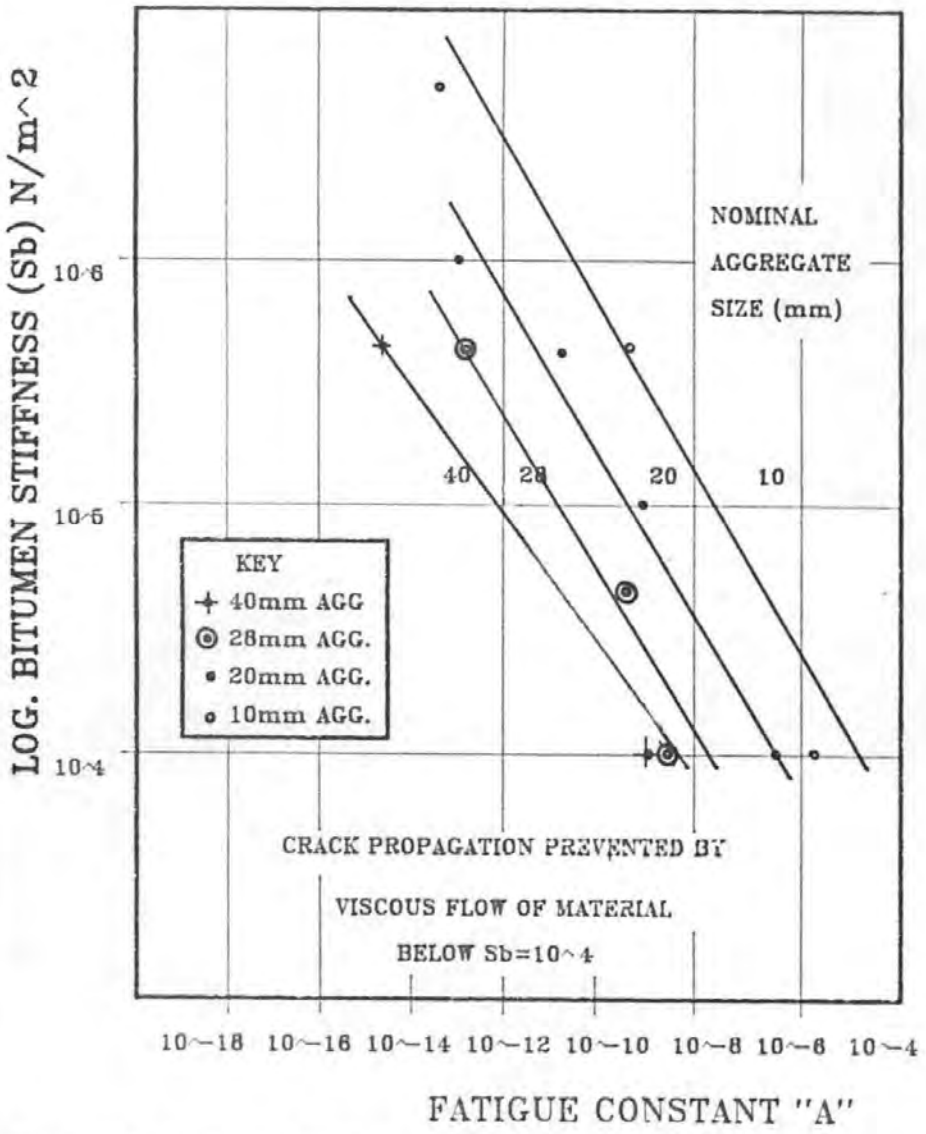

FIG. 6.26 BITUMEN STIFFNESS VERSUS FATIGUE CONSTANTS "A" FOR D.B.M. MIXES(2)Pi =100pen. BITUMEN CONTENT=4.2% VOID CONTENT=3%

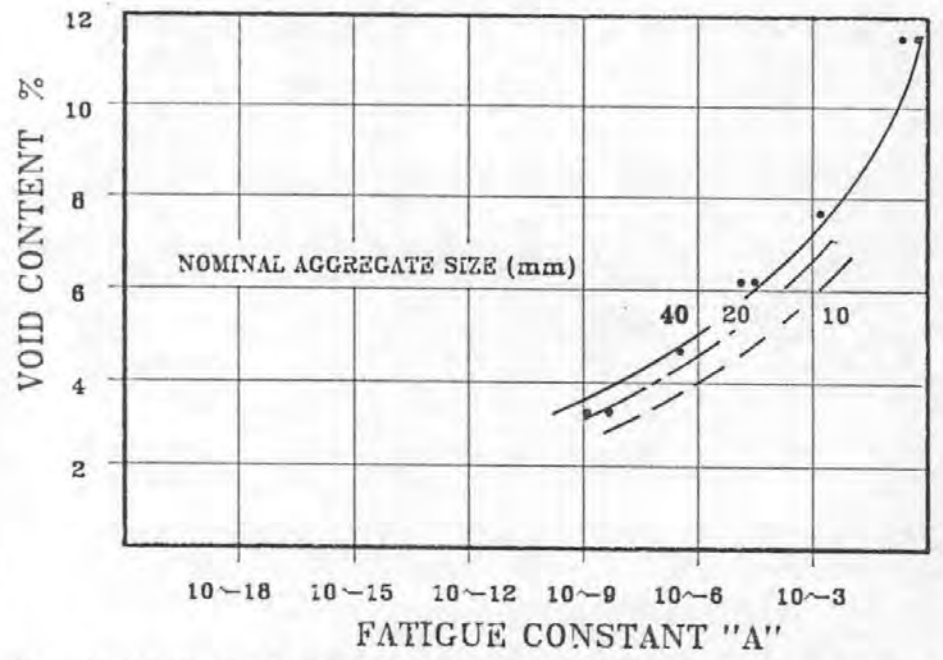

FIG. 6.27 VOID CONTENT VERSUS FATIGUE CONSTANT "A" FOR D.B.M. **MIXES** B.S.4987 Sb=10^4N/m^2

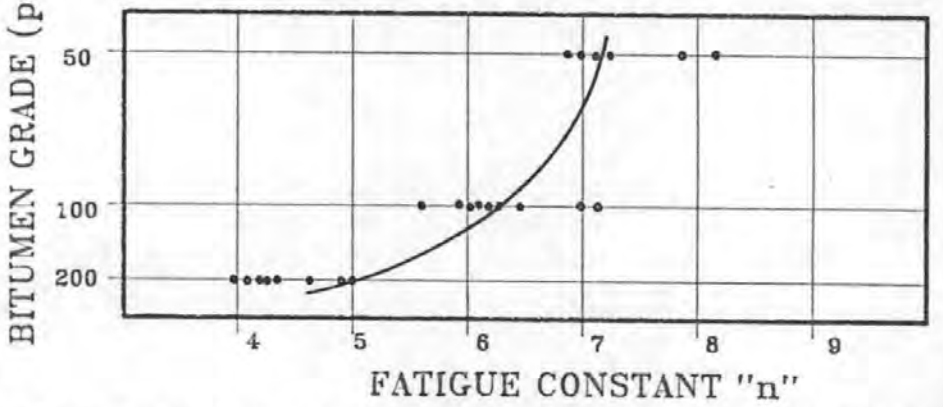

FIG. 6.28 BINDER GRADE VERSUS FATIGUE CONSTANT "n" FOR D.B.M. **MIXES** B.S.4987

lives and fatigue constants), on the 29 bituminous mixes, specified in section 6.4, to evaluate their annual fatigue life under the tensile fatigue crack mechanism. The annual fatigue life is defined as the time, in days, for a crack to initiate at the roadbase/surfacing interface and propagate through the bituminous material to the surface of the pavement under environmental conditions typical of a U.K. annual cycle.

The annual fatigue life is derived by solving Paris' equation (Eq.4.1); an example calculation is provided in Appendix 3. The complexity of the calculations limit the number of alternative design options that may be considered manually. Therefore, a computer program (R.F.T.100) has been written which allows the annual fatigue life to be derived for a range of roadbase slab lengths and surfacing material types. Input data includes monthly pavement temperatures under U.K. conditions, stress intensity factors and laboratory derived material fatigue constants. The program allows the derivation of the annual fatigue life for a wider range of pavement conditions than those modelled within the laboratory through extrapolation of tests results.

6.13.2 Program R.F.T.100

This program has been written in 'Basic' language, to solve Paris' equation (Eqn 4.1) and provide an estimation of fatigue life (in days) due to crack propagation initiating at the base with subsequent upward crack growth to the surface; the mechanism of tensile fatigue.

The program incorporates;

(i) the values of crack opening widths given in table 6.2 for composite pavements,

(ii) the temperature data for typical U.K. temperature conditions; tables 6.3 and 6.4,

(iii) the relationships between the stress intensity factors and crack length given in figs. 6.21 and 6.22 and

(iv) the relationships between bitumen stiffness, bitumen content and void content versus fatigue constant A presented in figs. 6.25 to 6.27. Mean values of the fatigue constant n have been taken as 4.8, 6.6 and 7.2 for 200 pen, 100 pen and 50 pen bitumens respectively.

Data, input by the user, includes;

(i) the roadbase slab length,

(ii) the type of coarse aggregate used for the construction of the lean concrete roadbase,

(iii) the depth of the bituminous layer and

(iv) mix characteristics of the bituminous material.

The program evaluates the reflection cracking fatigue life of standard U.K. surfacing materials (D.B.M. and H.R.A.)[8,9]. Within these mix types the four predominant factors that influence the fatigue life may be varied:-

1) Compaction level
2) Bitumen content
3) Bitumen grade
4) Aggregate grading

Limits have been set on each of these factors and are as given in table 6.14.

TABLE 6.14
LIMITS TO MIX INPUT VARIABLES FOR PROGRAM R.F.T.100

Factor	Limits
Compaction level	3% to 11%
Bitumen content (D.B.M. mixes)	4.2%, 4.7%, 5.2% 6.2%
Bitumen grade (D.B.M. Mixes)	200 pen, 100 pen, 50 pen
(H.R.A. Mixes)	45 pen, 35 pen, 25 pen
Nominal aggregate grading	40mm, 28mm, 20mm, 10mm

A two layered surfacing (wearing course and base course) is assumed and any two materials or a single material of specified depth may be defined. The program is limited to the bituminous mixes tested and to their respective creep stiffness values. Additional crack opening fatigue data from appropriate tests (described in section 6.3) is required prior to the evaluation of surfacing mixes outside the limits specified in Table 6.14.

The results from the investigation into the debonding at the roadbase/surfacing interface are included in the form of options for a perfect bond or a debonded length of 100mm or 200mm either side of the crack path.

To provide a solution to Eqn.4.1 R.F.T.100 calculates:

i) the mix stiffness, S_{md}, and hence the modified stress intensity factor, k_r,

ii) the fatigue constant A,

for each month of the year. The fatigue constant n is read from the value of bitumen grade input by the user. A value of fatigue life is derived for each month and the damage caused during each month is summed to provide the annual fatigue life. A flow chart illustrating the logic steps and options available is provided in fig.6.29 and a listing of the program is given in Appendix 6.

6.13.3 Results

The results presented in this section are from the standard output of program R.F.T.100. This demonstrates the influence of mix and compaction variables and material classification types on the annual fatigue life of bituminous surfacing layers of composite pavements.

Assumptions made in the analysis are:

(i) the use of a limestone aggregate for the roadbase,

(ii) the use was made of limestone aggregate for all grading sizes in the bituminous test mixes. Other aggregate types may exhibit differing absorption properties which may influence the proportion of free binder, aggregate/binder bond and therefore the ultimate fatigue life. No evidence exists, however, to indicate that this would have a major effect on the results obtained,

(iii) the crack is assumed to propagate vertically as occurred in the majority of tests. An increase in fatigue life was shown to occur if the cracks propagated at an angle to vertical, due to an increase in the subsequent length of the crack path,

(iv) allowance is not made for in-service hardening of the binder other than the slight oxidization which occurs during the preparation of the beams.

The effect of hardening is investigated in a series of five tests on beams which incorporate a binder of differing oxidization levels. A method which accounts for in-service hardening, using the results from this study in conjunction with models for predicting the rate of binder hardening is included as appendix 4.

The reflection cracking annual fatigue life of bituminous surfacings incorporating a single material type is given in figs. 6.30 to 6.33 with respect to void content, bitumen grade, grading and bitumen content respectively. These are based on a D.B.M. mix incorporating

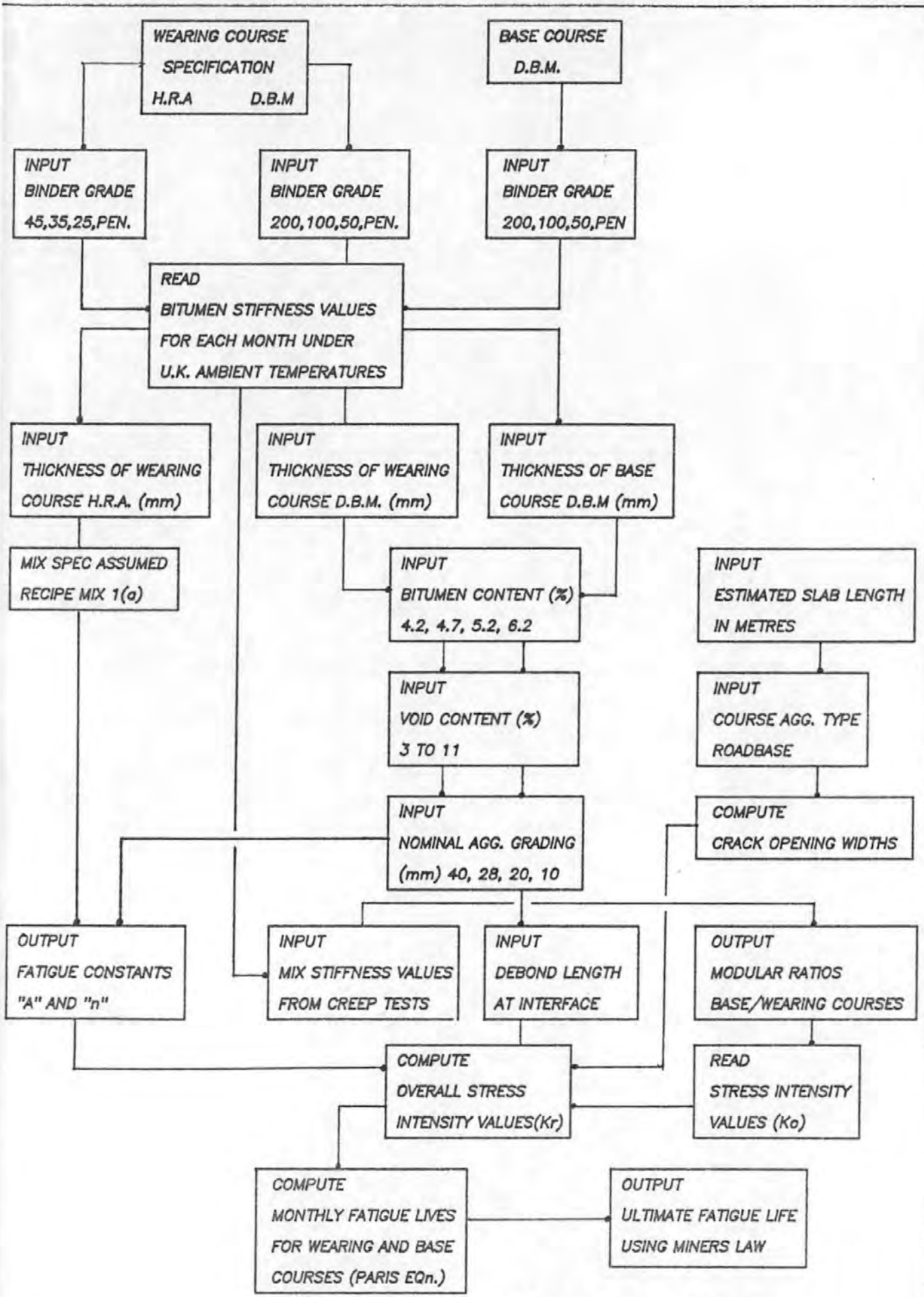

FIG.6.29 FLOW CHART OF PROGRAM R.F.T.100

FIG.6.30 FATIGUE LIFE (DAYS) VERSUS AGGREGATE GRADING(mm)
FOR 100mm DEPTH OF D.B.M MATERIAL OF MID GRADING(B.S.4987)
4.2% BINDER CONTENT 3% VOID CONTENT 100 PEN.BINDER
FOR GIVEN SLAB LENGTHS(m)

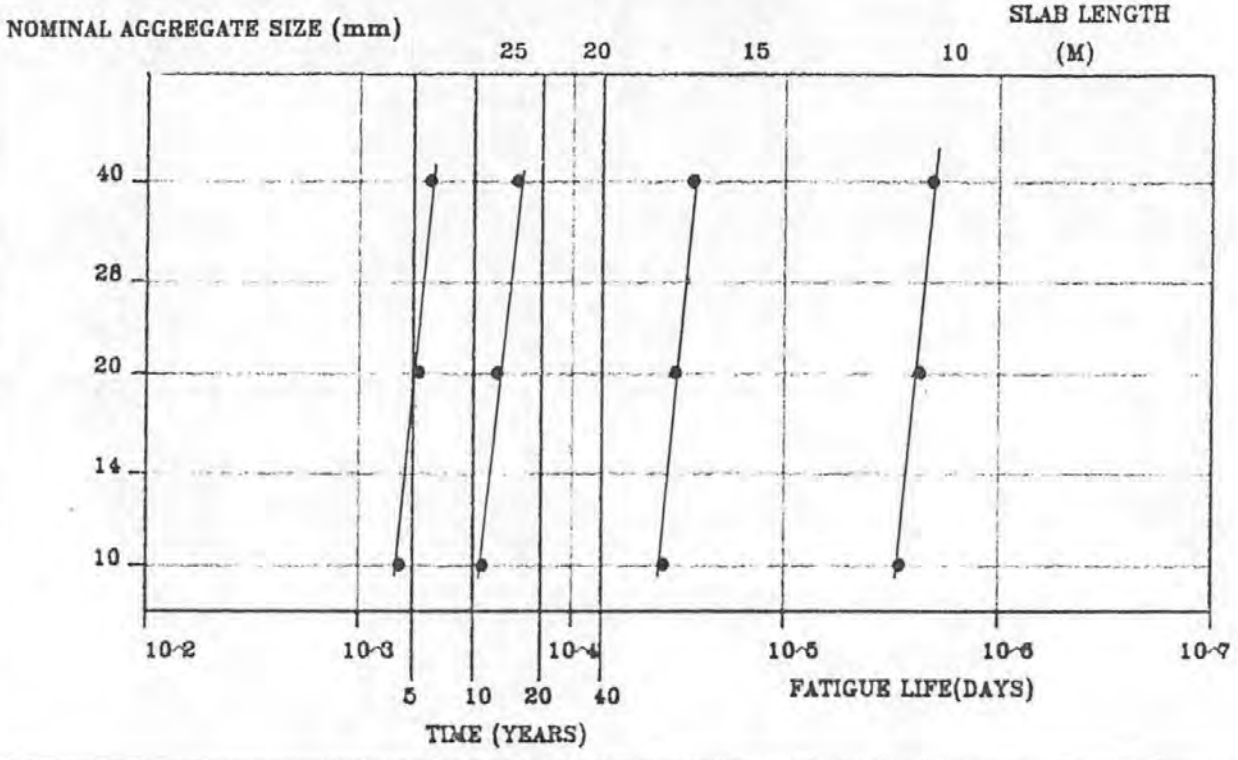

FIG.6.31 FATIGUE LIFE (DAYS) VERSUS BINDER CONTENT (%)
FOR 100mm DEPTH OF 200 PEN. D.B.M. MID GRADING(B.S.4987)
3.0% VOID CONTENT 20mm AGGREGATE GRADING
FOR GIVEN SLAB LENGTHS(m)

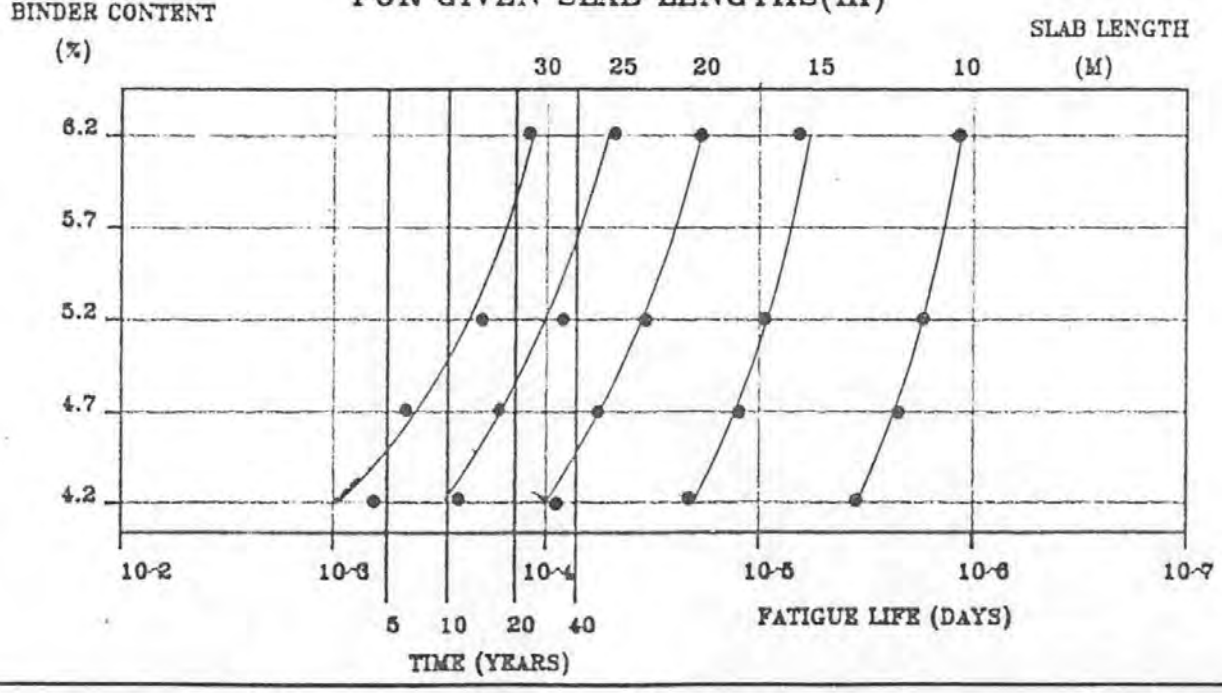

FIG.6.32 FATIGUE LIFE (DAYS) VERSUS PENETRATION GRADE FOR 100mm DEPTH OF D.B.M MATERIAL OF MID GRADING(B.S.4987) 4.2% BINDER 3% AIR VOIDS 20mm AGGREGATE GRADING FOR GIVEN SLAB LENGTHS(m)

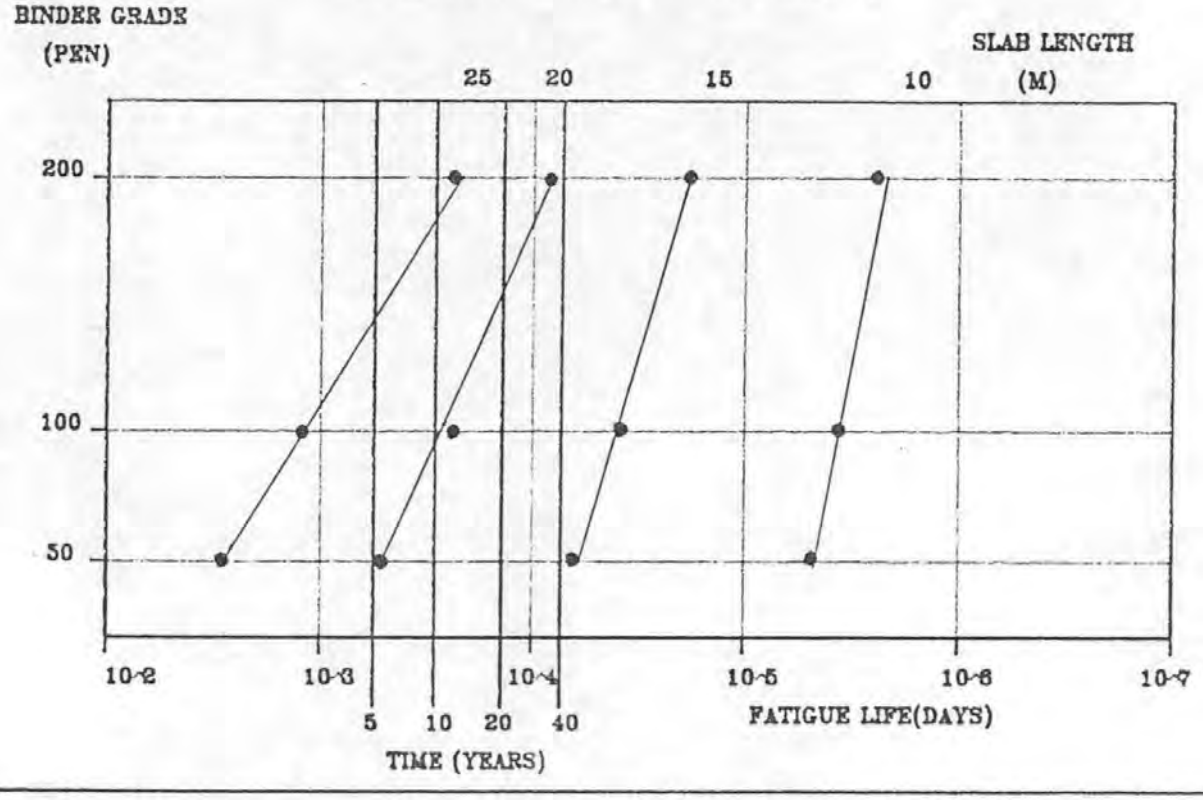

FIG.6.33 FATIGUE LIFE (DAYS) VERSUS VOID CONTENT (%) FOR 100mm DEPTH OF 100 PEN. D.B.M. MID GRADING(B.S.4987) 4.2%BINDER CONTENT 28mm AGGREGATE GRADING FOR GIVEN SLAB LENGTHS(m)

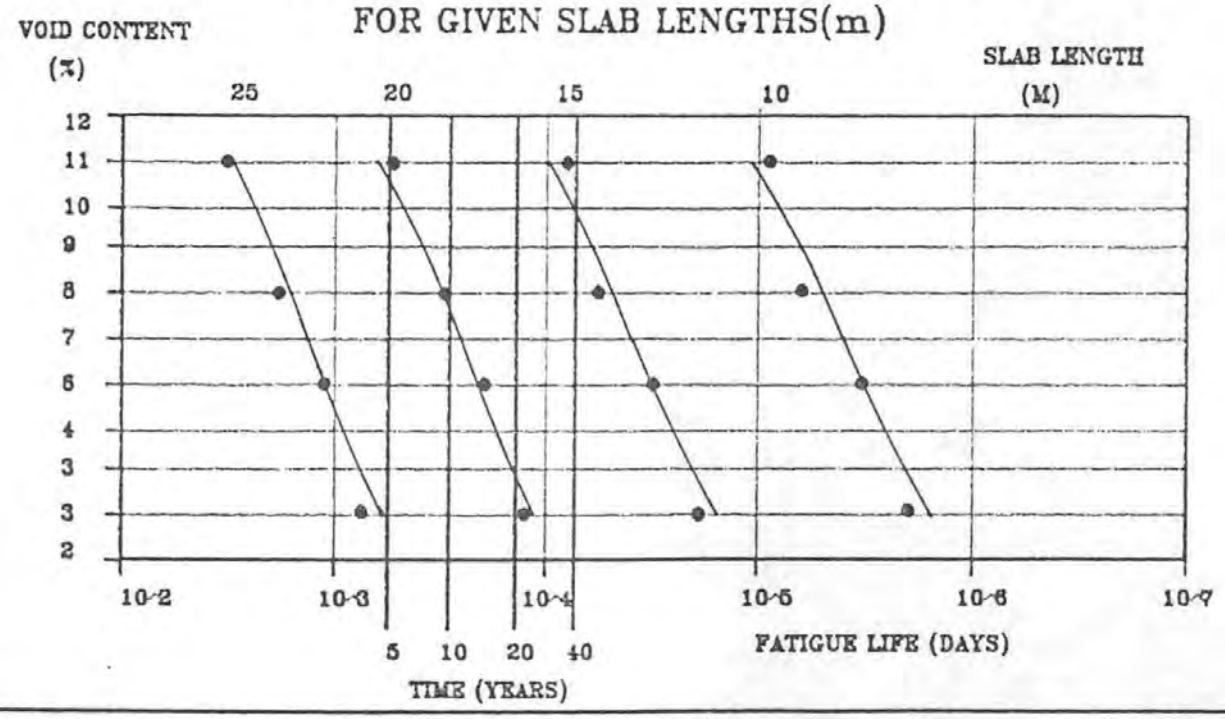

a nominal aggregate size of 20mm, 100 pen binder grade, 4.2 bitumen content and with a compaction level of 3%, on which the mix parameters and compaction level has been varied. The plots indicate an extension in annual fatigue life may be achieved through the use of larger size nominal aggregates, an increase in the binder content of the mix, the use of softer grade bitumens or an increase in compaction of the bituminous layer.

The effect of bitumen content on the fatigue life was investigated by tests on four beams of 20mm nomimal sized D.B.M. material with a 200 pen binder. An eight fold increase in fatigue life was obtained by increasing the specified[9] bitumen content from 4.2% to 6.2%. As surfacing mixes excessively rich in bitumen are susceptible to permanent deformation under the action of traffic and therefore a compromise is required. A limited increase in bitumen content from 4.2% to 4.7% did improve the fatigue life by a factor of 2 while providing a mix of superior stiffness.

The void content of the standard D.B.M. material was varied by differing the compactive effort exerted on the beams during their manufacture. Compaction of dense coated macadams carried out to the relevant specification, BS 4987[9], results in void contents of between 6-8%. The test results show that reducing the void content by 50 per cent doubled the fatigue life.

The results from fig.6.11 and fig.6.32 indicate that the fatigue life of the test mixes increased as the stiffness of their bituminous binders decreased. At a constant temperature, therefore, softer grades of binder will exhibit lower stiffnesses with an improved resistance to crack propagation through the mechanism of tensile fatigue.

Fig. 6.30 shows that though the nominal aggregate size of the D.B.M. mixes have only a slight influence in the fatigue life, the coarser mixes exhibit greater resistance to reflection cracking. Crack propagation was observed to occur around the aggregate and therefore, in mixes incorporating larger aggregate, this formed a longer and more irregular crack path.

Figs. 6.34 to 6.42 indicate the extension in fatigue life that may be

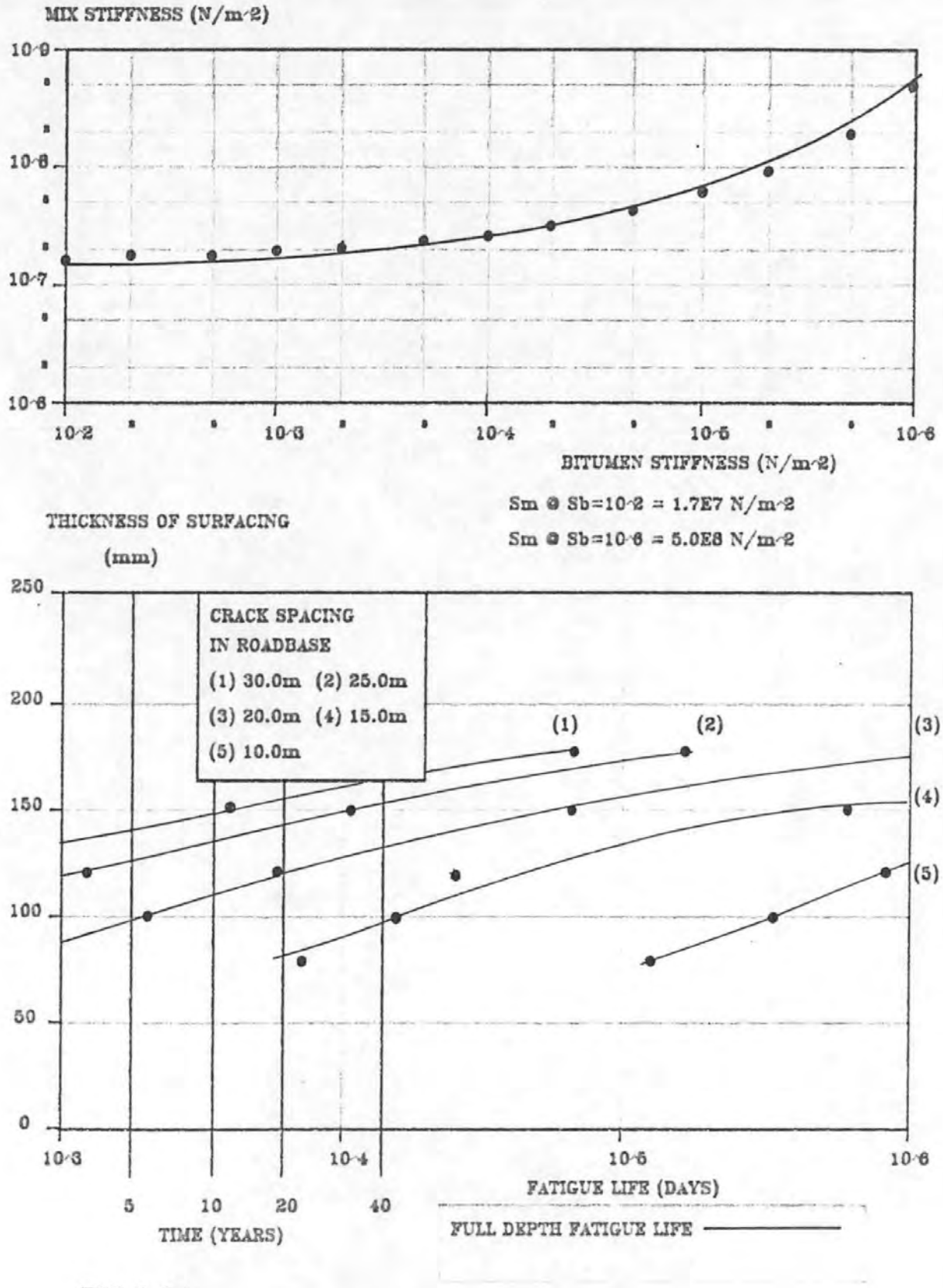

FIG.6.34

MIX STIFFNESS AND FATIGUE LIFE DATA

MIX:-D.B.M BINDER PEN:-50 AGGREGATE GRADING:-20mm

VOID CONTENT:-3% BINDER CONTENT:-4.2%

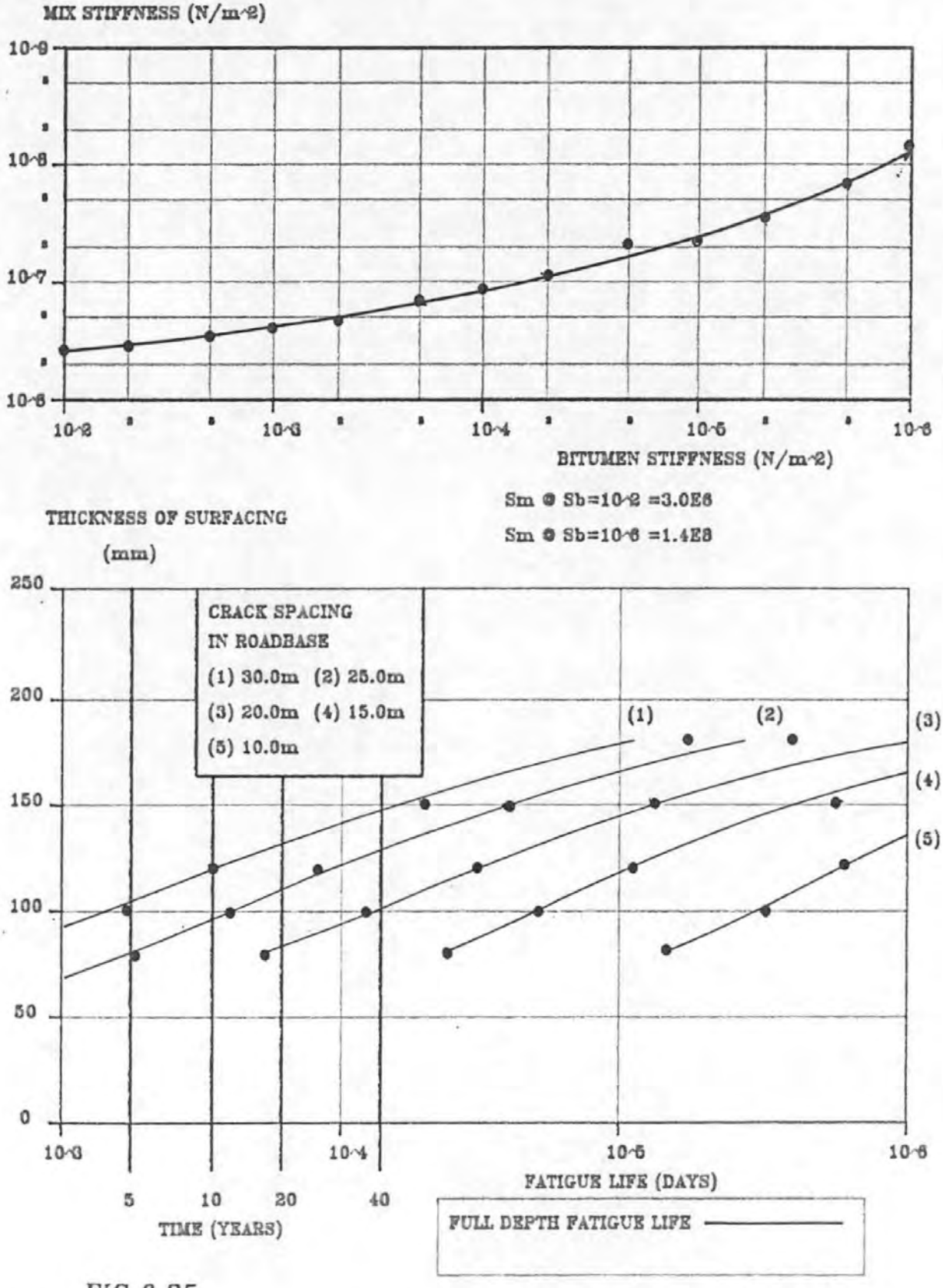

FIG.6.35

MIX STIFFNESS AND FATIGUE LIFE DATA

MIX:-D.B.M BINDER PEN:-200 AGGREGATE GRADING:-20mm

VOID CONTENT:-3% BINDER CONTENT:-4.2%

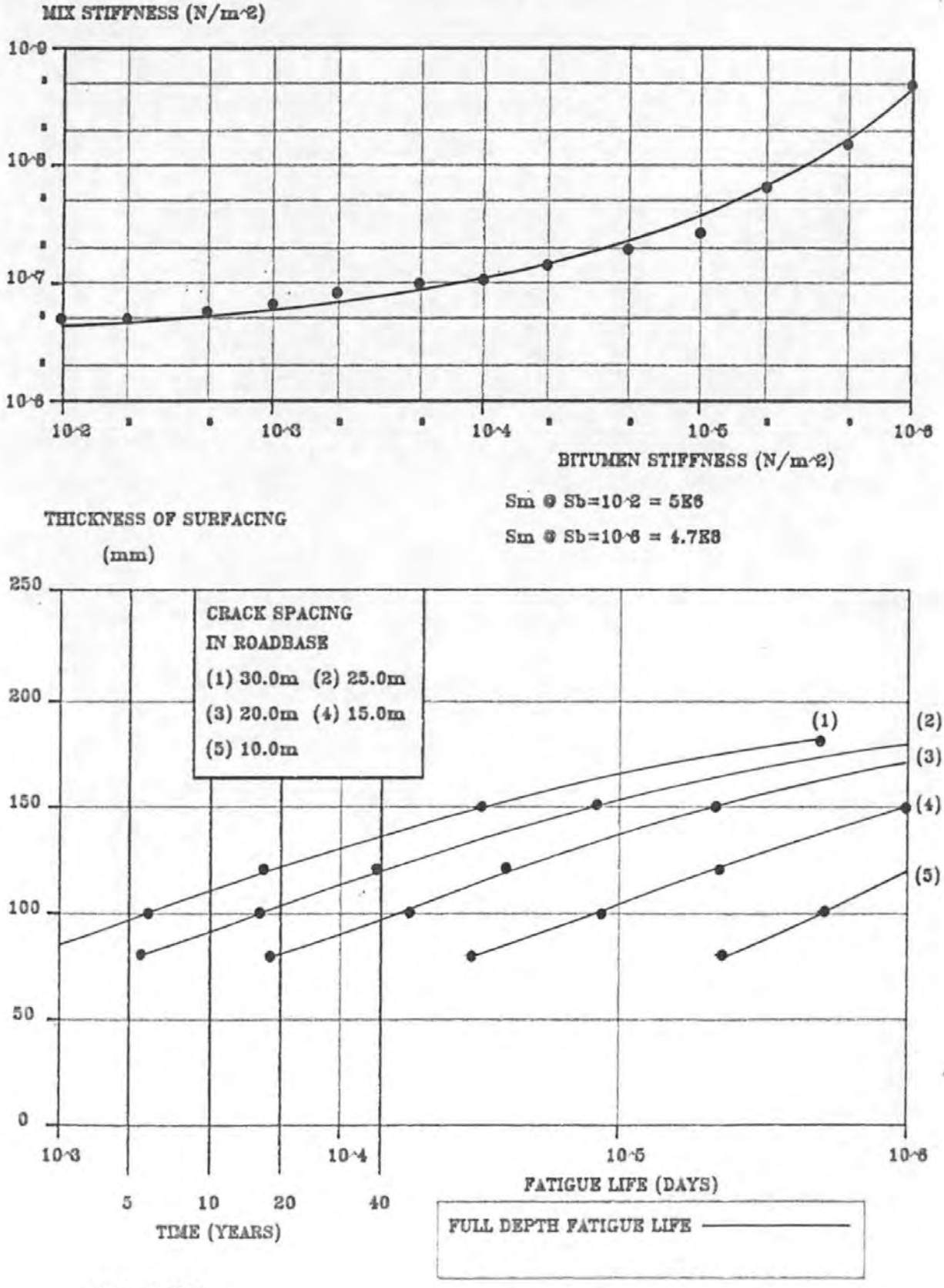

FIG.6.36

MIX STIFFNESS AND FATIGUE LIFE DATA

MIX:-D.B.M. BINDER PEN:-200 AGGREGATE GRADING:-20mm

VOID CONTENT:-3% BINDER CONTENT:-4.7%

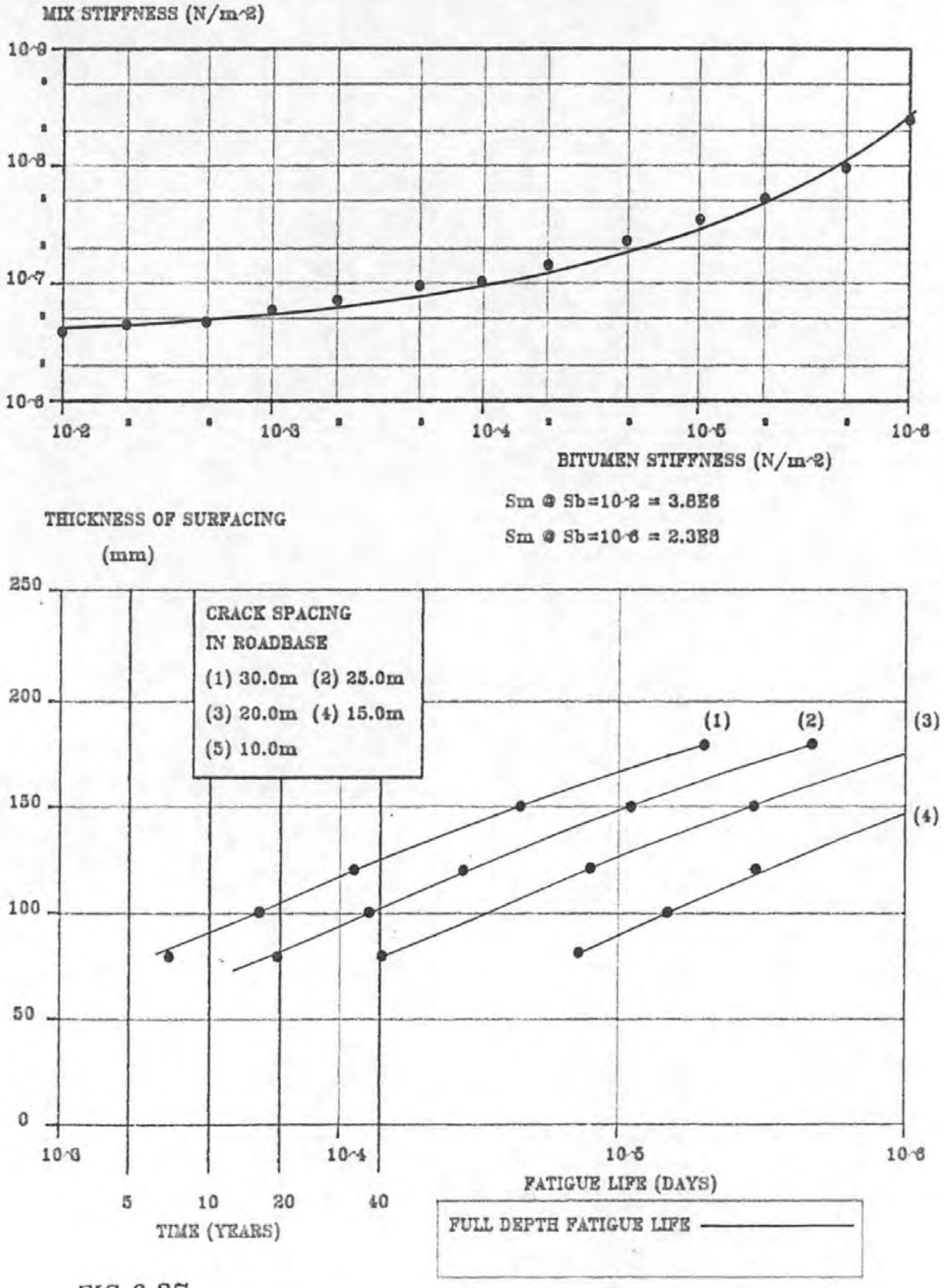

FIG.6.37

MIX STIFFNESS AND FATIGUE LIFE DATA
MIX:-D.B.M BINDER PEN:-200 AGGREGATE GRADING:-20
VOID CONTENT:-3% BINDER CONTENT:-5.2%

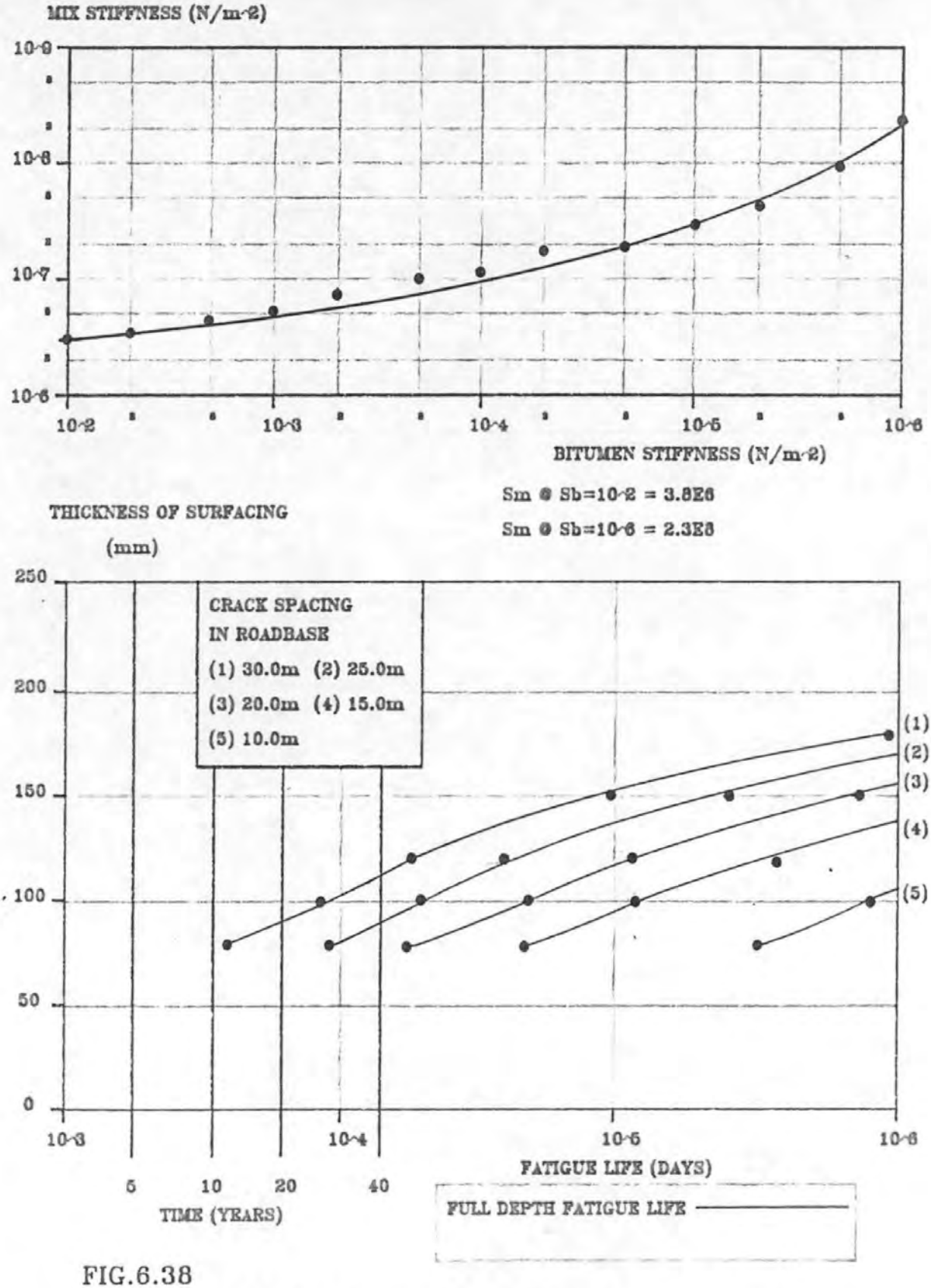

FIG.6.38

MIX STIFFNESS AND FATIGUE LIFE DATA
MIX:-D.B.M BINDER PEN:-200 AGGREGATE GRADING:- 20mm
VOID CONTENT:-3% BINDER CONTENT:-6.2%

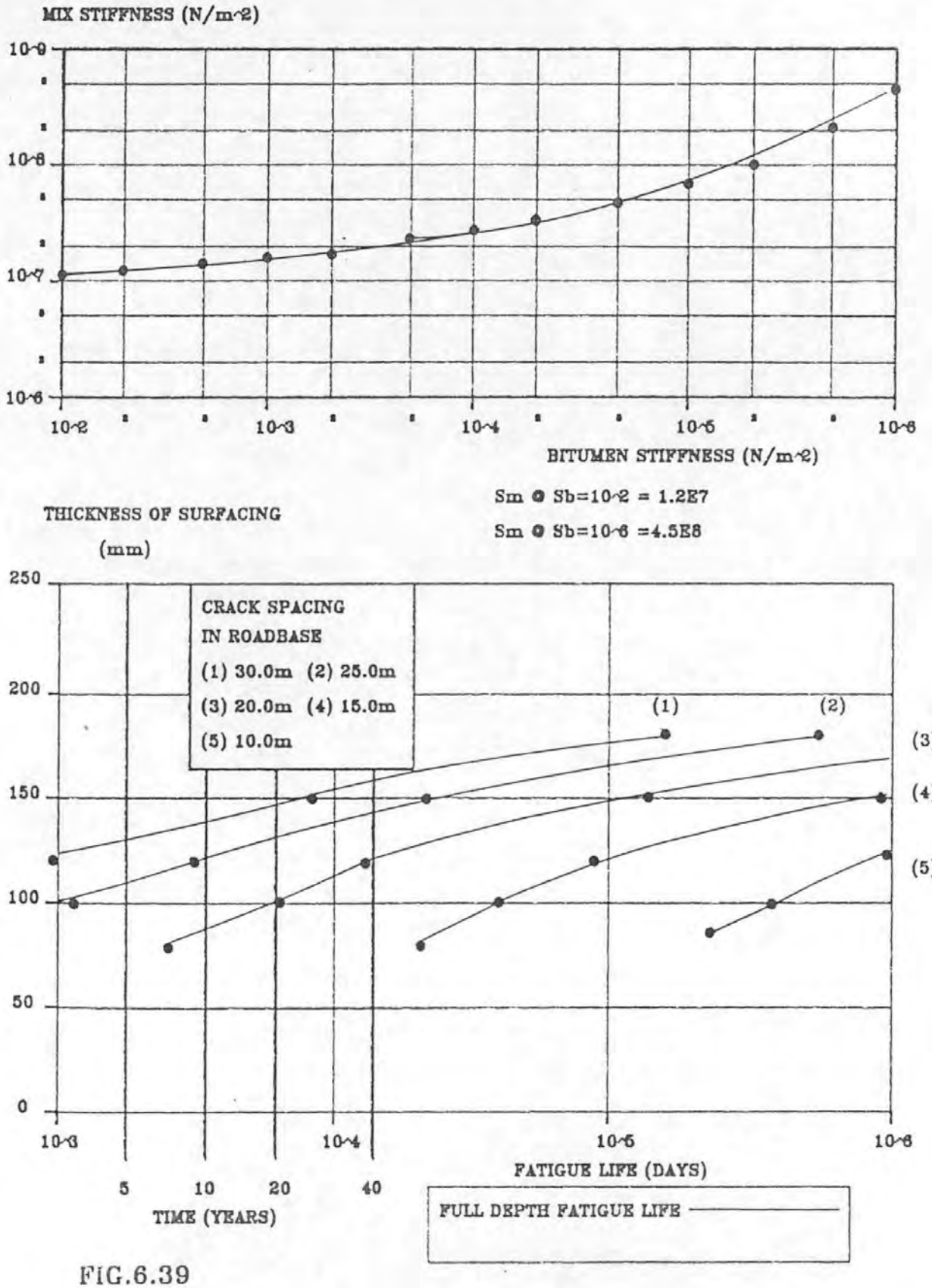

FIG.6.39

MIX STIFFNESS AND FATIGUE LIFE DATA
MIX:-D.B.M BINDER PEN:-100 AGGREGATE GRADING:-40mm
VOID CONTENT:-3% BINDER CONTENT:-4.2%

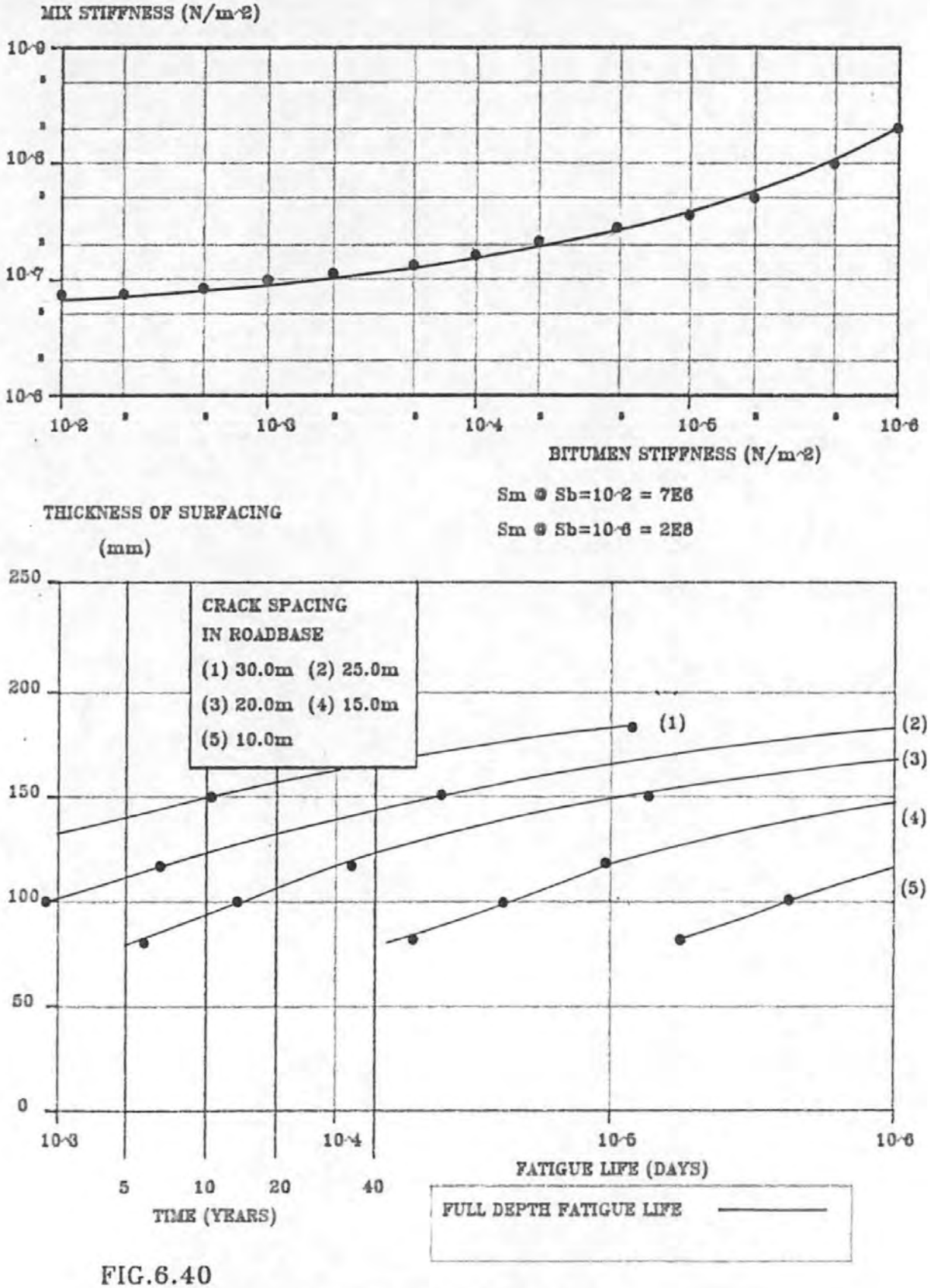

FIG.6.40

MIX STIFFNESS AND FATIGUE LIFE DATA
MIX:-D.B.M. BINDER PEN:-100 AGGREGATE GRADING:-40mm
VOID CONTENT:-6% BINDER CONTENT:-4.2%

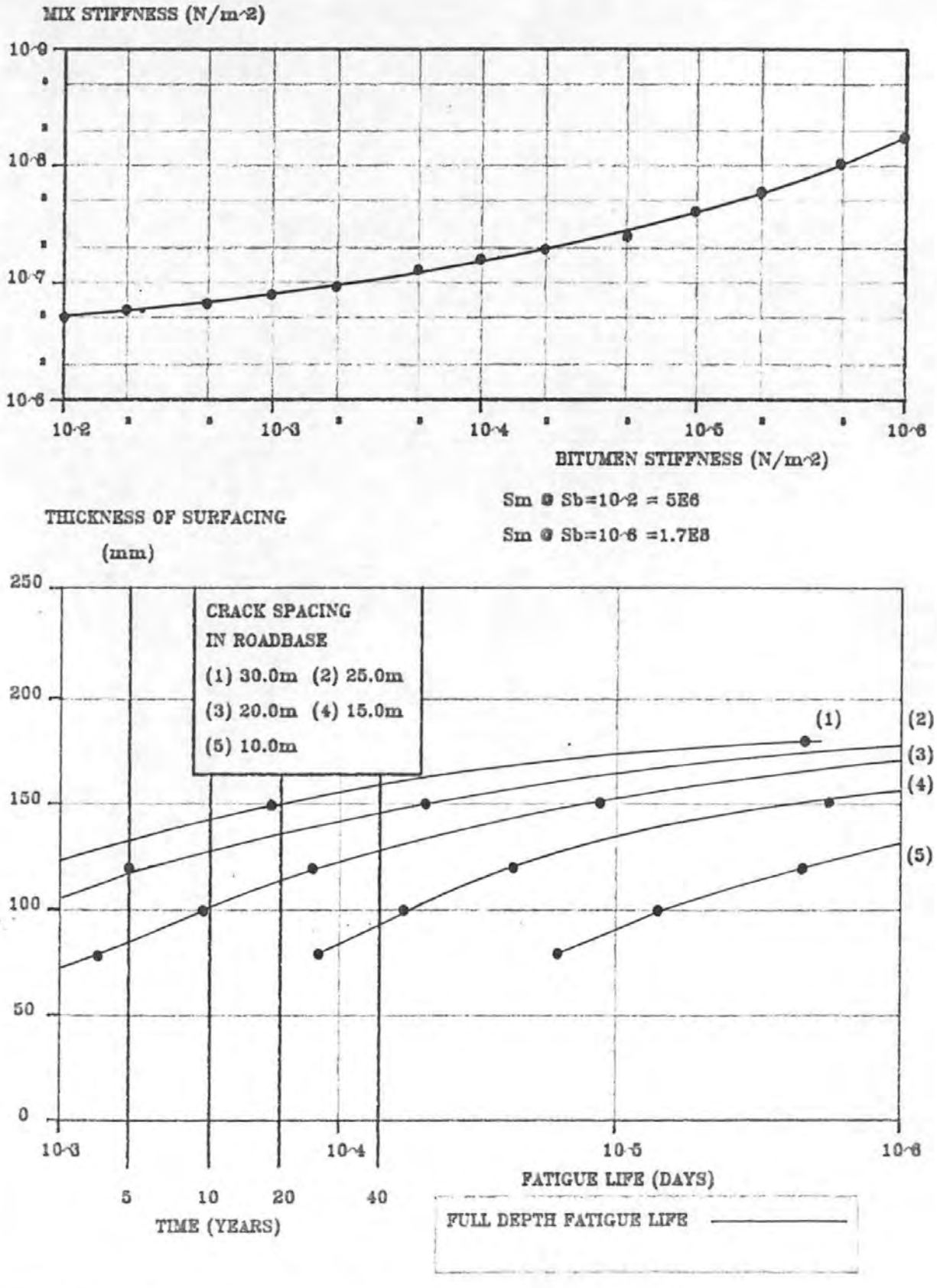

FIG.6.41 STIFFNESS AND FATIGUE LIFE DATA
MIX:-D.B.M BINDER PEN:-100 AGGREGATE GRADING:-40mm
VOID CONTENT:-8% BINDER CONTENT:-4.2%

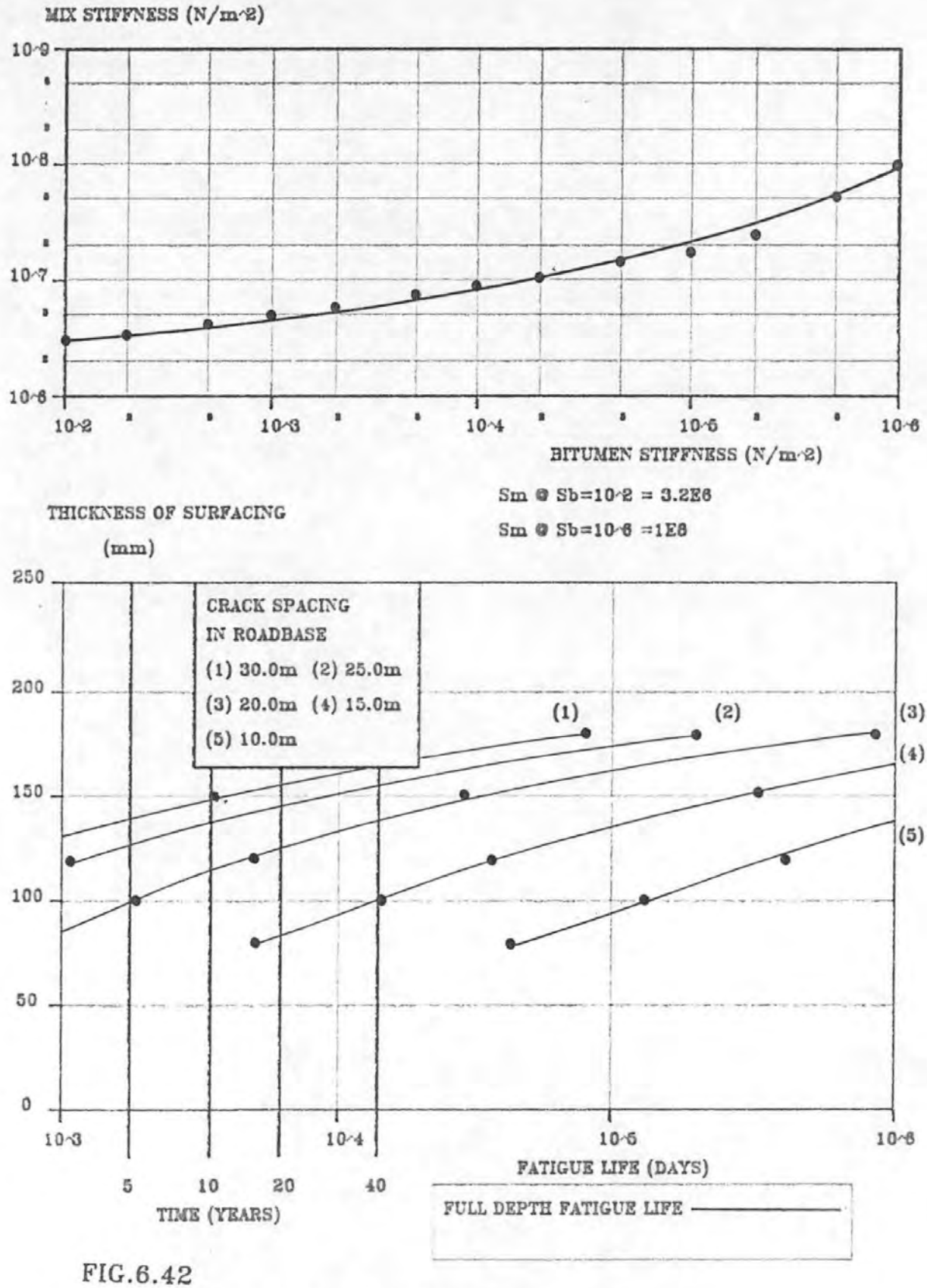

FIG.6.42

MIX STIFFNESS AND FATIGUE LIFE DATA
MIX:-D.B.M. BINDER PEN:-100 AGGREGATE GRADING:-40mm
VOID CONTENT:-11% BINDER CONTENT:-4.2%

Figs. 6.34 to 6.42 indicate the extension in fatigue life that may be achieved through a reduction in slab length and an increase in layer thickness. Each plot also includes the stiffness characteristics derived from tensile creep tests.

The results from the model extended to incorporate a two layered pavement surfacing is given in fig.6.43. The resultant life for a D.B.M. base course is indicated and a comparison drawn between an H.R.A. wearing course incorporating a binder of differing oxidization levels and a D.B.M. wearing course with a 50 pen binder. The D.B.M. wearing course is shown to be superior to a H.R.A. mix with a 25 and 35 pen binder, but inferior to a H.R.A. with a 45 pen binder. Therefore a H.R.A. mix is superior to a D.B.M. mix incorporating a similar grade of binder. The increased resistance to cracking of the H.R.A. is due to its higher bitumen content and a greater mix density obtained during manufacture of the material.

The influence on the annual fatigue life of a limited length of debonding at the roadbase/surfacing interface using a single thickness of the standard D.B.M. mix is shown in fig.6.44. Debonding at this interface tends to reduce the stresses induced into the surfacing layer by displacements of the roadbase slabs. The stresses act over a finite length rather than at a point as with a crack tip. Therefore, the increase in fatigue life is related to the length of the debonded zone.

Two tests were also carried out on a 20mm open textured macadam with a 50 pen binder. Although insufficient results were available to establish the fatigue life in detail, the laboratory results show the control mix of dense macadam to have a fatigue life of 2.5 times greater than that provided by the open textured mix.

To summarize, this work has predicted the magnitude and effect of:-
(i) tensile fatigue cracking which can be inhibited by using mixes with softer binders, higher binder contents, better compaction and coarser aggregate gradings, by increasing the thickness of the bituminous layer or by placing a viscous layer between the roadbase and surfacing,
(ii) using poorly compacted 'dry' mixes which incorporate a hard or oxidized binder and offer a reduced resistance to crack propagation.

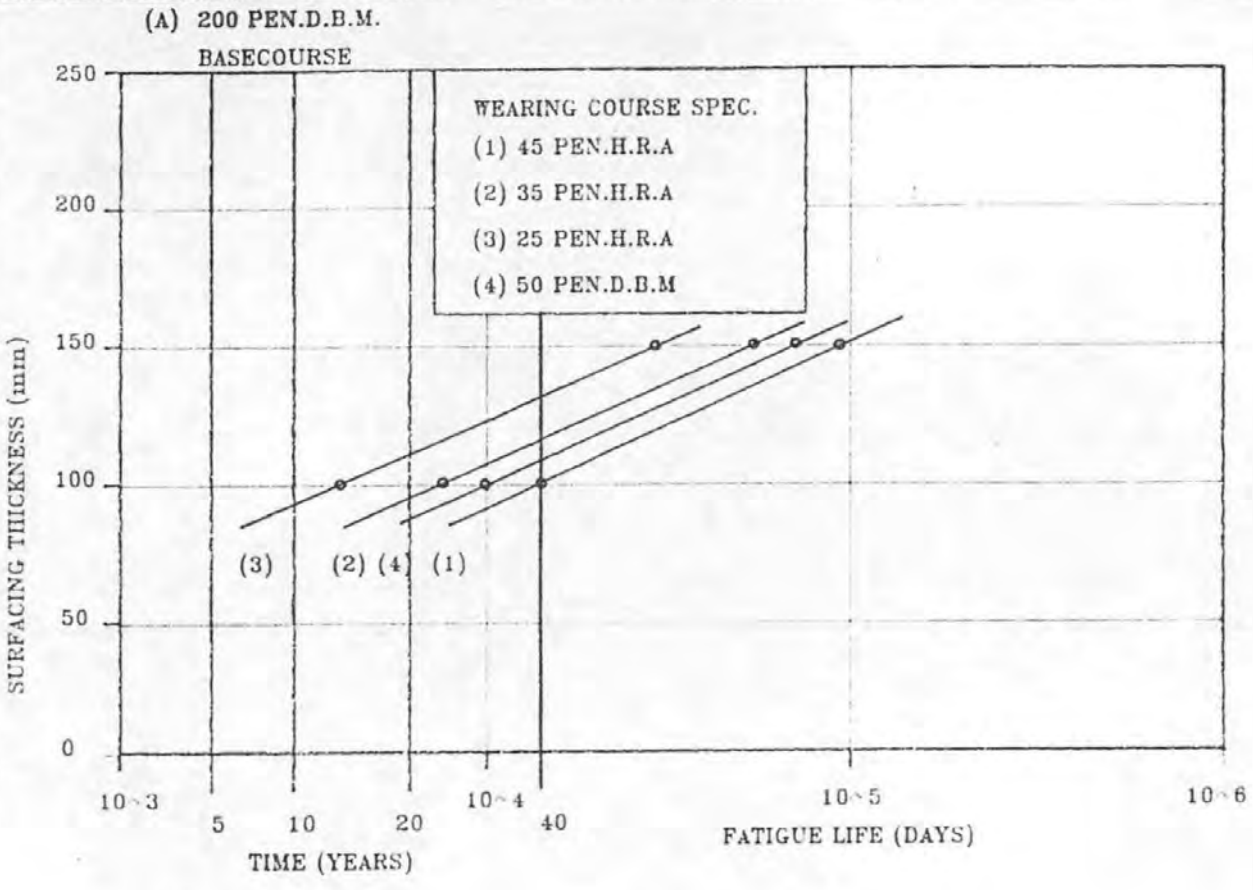

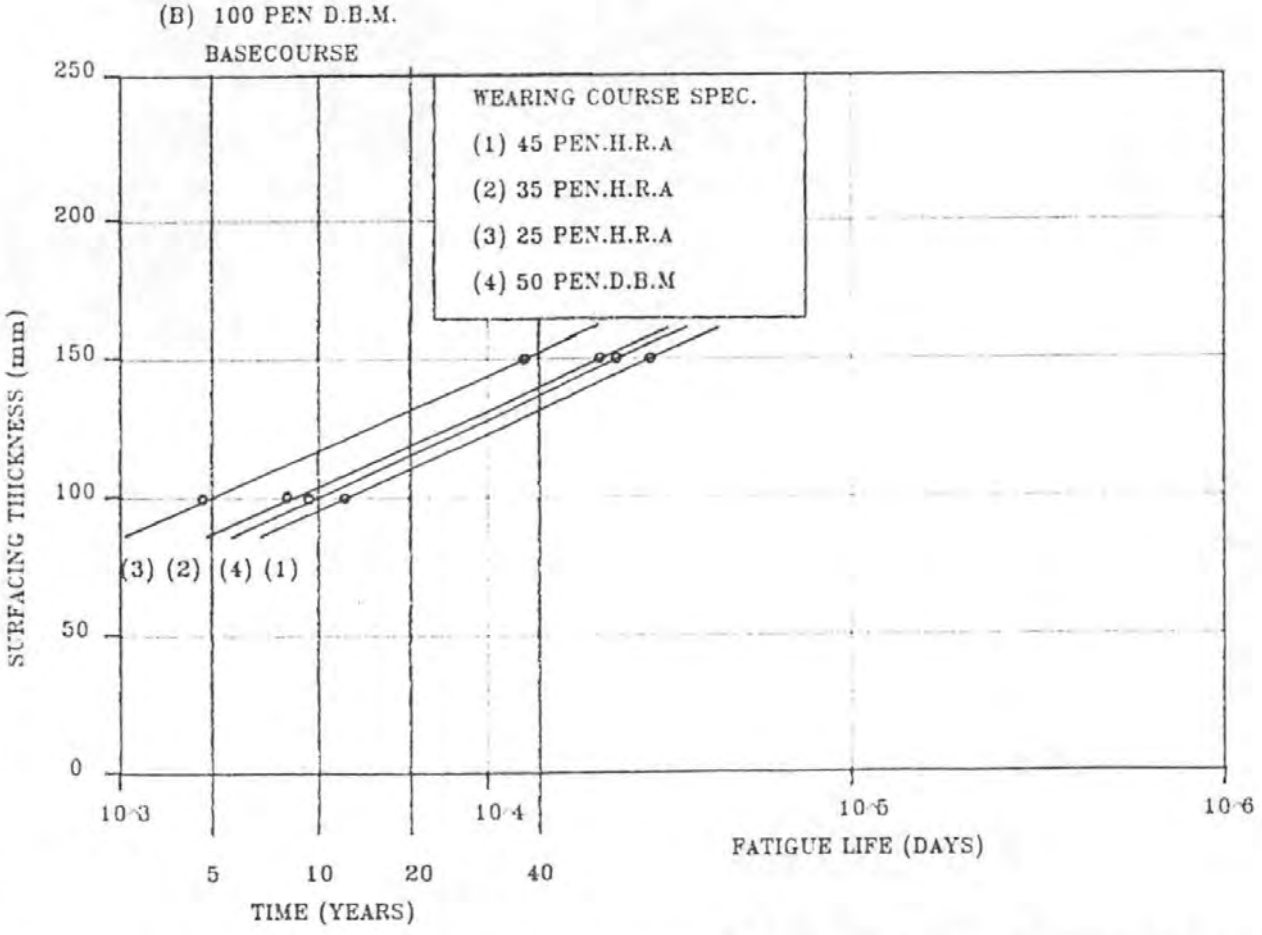

FIG.6.43 FATIGUE LIVES FOR OXIDIZED H.R.A. AND D.B.M WEARING COURSES WITH 100 AND 200 PEN.D.B.M.BASECOURSES 20m SLAB LENGTH

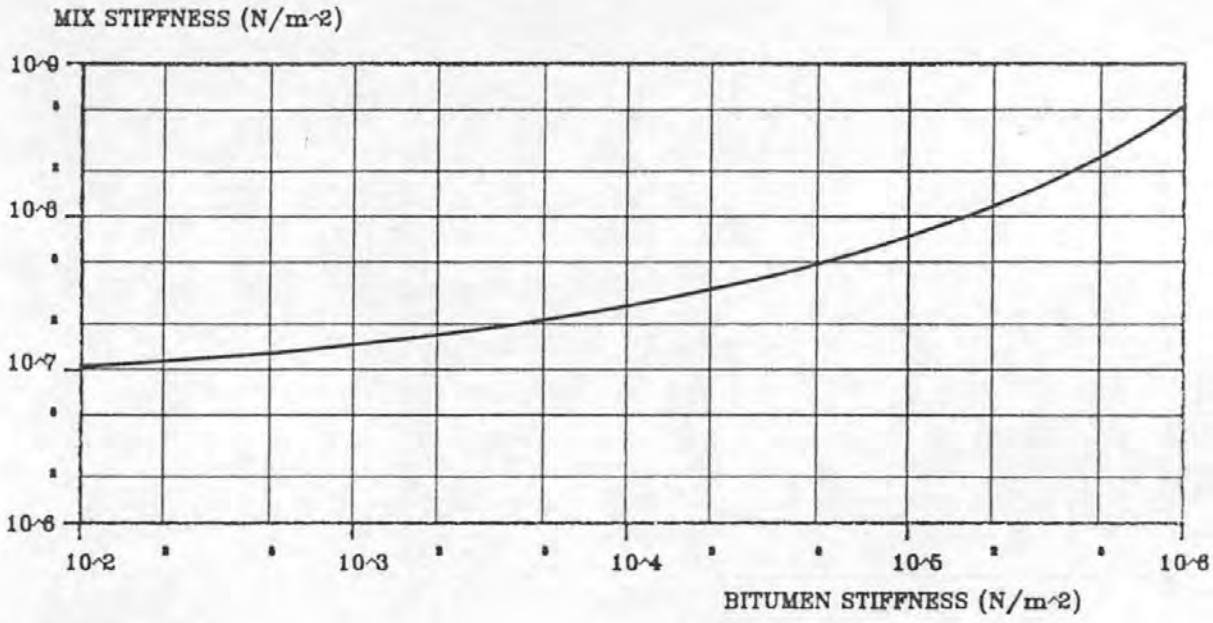

Sm @ Sb=10^2 = 1.2E7 N/m^2

Sm @ Sb=10^6 = 4.5E8 N/m^2

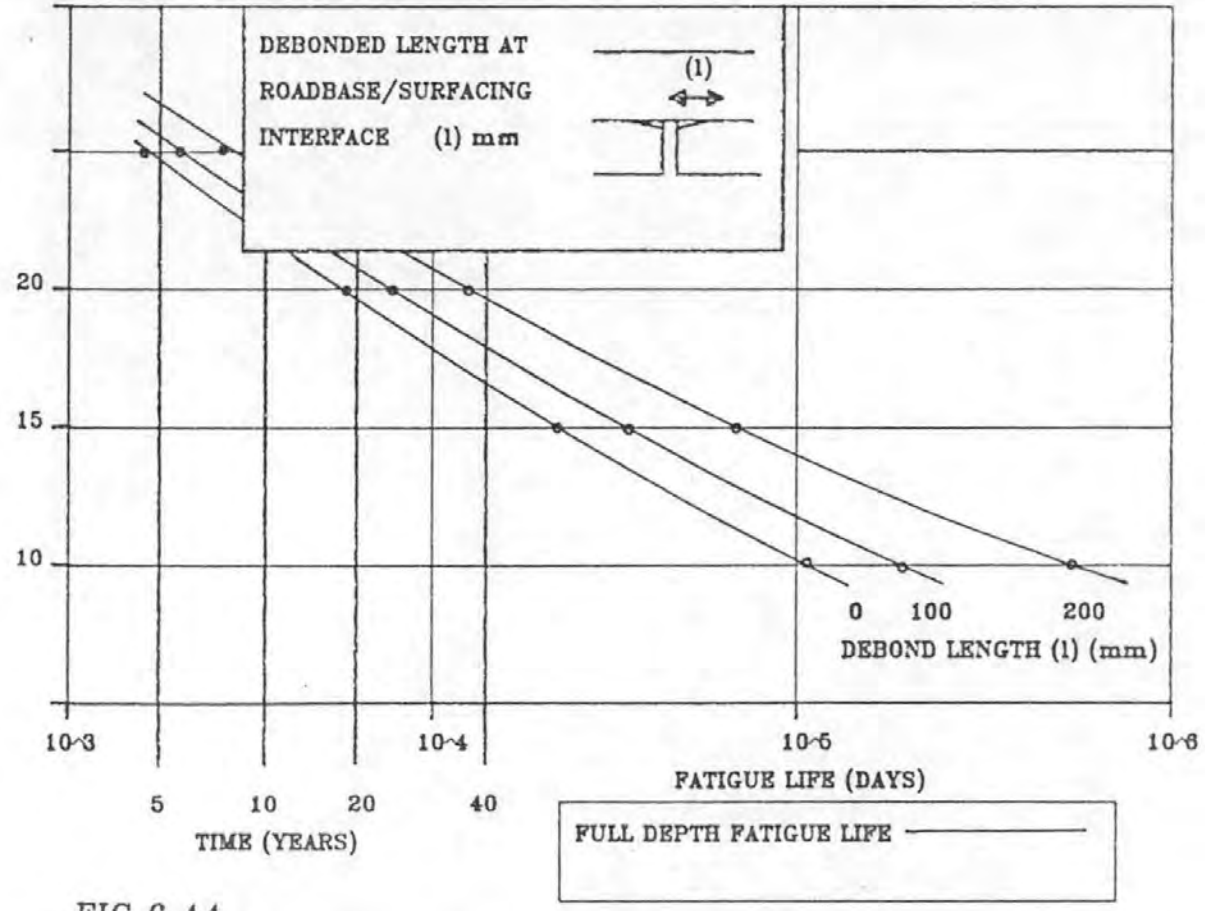

FIG.6.44

MIX STIFFNESS AND FATIGUE LIFE DATA DUE TO DEBONDING
MIX:-D.B.M. BINDER PEN:-100 AGGREGATE GRADING:-40mm
VOID CONTENT:-3% BINDER CONTENT:-4.2% SURFACING:-100mm

7.0 MECHANISM OF TENSILE YIELD

7.1 INTRODUCTION

The mechanism of tensile yield initiates reflection cracks at the pavement surface, normally above cracks in the underlying roadbase, which propagate downwards through the bituminous layers. This mechanism, described in section 4.3 and illustrated in fig.4.1 results from tensile strains induced in the asphalt by a combination of thermal warping of the lean concrete slab and thermal contraction, warping and long term shrinkage of the surfacing layer. The warping and contraction are associated with cold weather conditions while long term shrinkage is related to fluctuating extremes of temperature and asphalt mix and binder characteristics.

Investigation of this mechanism is based on a combination of field data (from cores and observations), laboratory testing and computer analysis. Extensive coring of several sites indicates that this mechanism is dominant in pavements incorporating substantial thicknesses of asphalt surfacing and with a roadbase crack frequency of less than 15m; a combination of conditions which would not lead to cracking from tensile fatigue.

Field observations carried out during extended periods of cold weather have shown that this mechanism can create surface cracks in excess of 5mm in width, which reduce to hairline width on subsequent moderation of weather conditions. Dramatic crack growth, both transversely across the pavement and downwards through the pavement surfacing, was observed during these periods of cold temperature.

Initial field data was provided from an investigation of the M4 motorway in Berkshire and data from subsequent investigations on other sites was used to validate conclusions drawn from the M4. The conditions under which this mechanism will occur are defined by equating tensile yield characteristics of the surfacing material, derived from laboratory tests on cored samples, to the strain levels generated in the pavement, obtained from a finite element model of the structure.

7.2 STUDY OF M4 REFLECTION CRACKING

The investigation into the mechanism of tensile yield was instigated as a result of a field survey report on the structural condition of the M4 in Berkshire[103]. This comprehensive study provided evidence that transverse cracking initiates at the surface and propagates downwards in composite pavements of a thickness required under the 1970 edition of RN29 for motorway loading specifications.

The evidence in support of downward propagation was drawn from extensive coring adjacent to the cracks and supported by the findings of visual survey of the pavement surface. Inspection of the cores showed that the reflection cracks formed in the surfacing vertically above cracks in the underlying lean concrete roadbase. Although in most cases, the cracks were still retained within the wearing course, examples were found to demonstrate the various phases of crack development including the 'failure' condition where the crack has propagated through the full depth of the surfacing.

This 80km length of M4 motorway built in 1970/71 provided a unique opportunity to study the mechanism of tensile yield through four sections which exhibited differing degrees of deterioration. Each of these sections represent a construction contract numbered 3 to 6. The deterioration of each contract was monitored by the local authority and the data compiled presented as the 'M4 Structural Condition Survey (1984)'[103]. It provides a detailed history, including field observations of crack initiation, development and spacings and also includes details of the thickness and material type of the pavement layers and traffic flows.

The facts contained within this document and considered relevant to the investigation are summarised in the next section where the results of an evaluation of the tensile characteristics of the surfacing are also presented.

7.3 VARIATIONS IN THE MATERIAL PROPERTIES OF THE M4

The surfacing of the composite pavement construction consists of a 40mm thickness of H.R.A.[8] wearing course with pre-coated chippings. Between junctions 8/9 and 15 the basecourse consists of 65mm of

DBM[9] overlying a 70mm layer of DBM upper road base. The high strength of cores taken from the dry lean road base suggest that it acts as a 'rigid slab' except for a short length on contract 6. Details of the development of transverse cracking and material properties for each contract are summarised below.

7.3.1 Contract 3

The earliest reflection cracking occurred on this section producing regular and constant crack spacings throughout the length of the contract. They are transverse across the width of the carriageways at an interval of 26m.

The wearing course appears uniformly hard and brittle with the binder exhibiting penetration values as low as 7. The lean concrete road base is constructed using a crushed limestone aggregate with core samples giving an average compressive strength of 16N/mm^2 (the only one of the three contracts to use limestone aggregate). This section of motorway is subjected to the lowest traffic flow of the four contracts at 2,700 cvpd.

7.3.2 Contract 4

Reflection cracking has occurred more recently on both this contract and contract 5. Although lengths of this section are heavily cracked, wide variations in crack spacing exist, with several kms virtually free from cracks. There is little variation between individual traffic lanes but the east bound carriageway is twice as badly cracked as the west bound. On the most badly cracked sections the spacing between cracks is reduced to 4.5m. The roadbase is constructed of a flint gravel dry lean concrete giving a mean cube strength of 12N/mm^2. Traffic levels on both contracts 4 and 5 are approximately 3000 cvpd

7.3.3 Contract 5

Contract 5 is currently the most heavily cracked section but, as with contract 4, shows wide variations in crack spacings along the length of the contract and also across the individual lanes. An aggregate similar to that used in contract 4 was used for the roadbase giving similar compressive strengths.

7.3.4 Contract 6

This contract is virtually free from transverse cracking but prone to

rutting. The penetration value of the wearing course binder is generally high indicating a soft asphalt. The lean concrete utilizing a gravel aggregate has a low compressive strength with a mean value of 13N/mm^2. Daily traffic flow on this section is 3,200 cvpd.

7.4 DISCUSSION ON THE LOCAL AUTHORITY REPORT

The continuous method of construction employed when laying the lean concrete roadbase results in transverse shrinkage cracks occurring at regular intervals during curing. The heat of hydration generated during this phase suggests that the coefficient of thermal contraction (C') of the aggregate to be a major factor governing the spacing between successive cracks. The limestone aggregate used in Contract 3 exhibits a low value of C' (4×10^{-6}/°C) while the flint gravel incorporated into the dry lean mix on the other contracts is characterised by values exceeding 12×10^{-6}/°C. The difference in the spacing of the cracks on these contracts is related directly to their respective coefficients of thermal contraction.

The regularity of the crack spacing on contract 3 shows that propagation through the surfacing is likely to be fully developed at its present interval of 26m. The wide variation in crack spacings on contracts 4 and 5 indicate that propagation may be delayed by differences both in surfacing material characteristics and crack mechanism. Initially, crack spacing was at a frequency of 9m, but with the occurrence of secondary cracking, these sections are progressively exhibiting a crack frequency of 4.5m. The soft binder characteristics of each of the layers on contract 6 would appear to have prevented transverse crack propagation through the surfacing.

A visual survey of the pavement surfacing shows the transverse reflection cracks to initiate in any of the three lanes or even the hard shoulder, indicating a relationship with material composition of the bituminous surfacing rather than traffic levels.

The traffic levels on all four contracts are of similar magnitude at approximately 3000 cvpd. Traffic loading tends to accelerate cracking induced by a thermally controlled mechanism but if traffic stresses were a significant factor in the cracking observed then longitudinal as well as transverse cracking would be expected and the nearside lane would have the highest frequency of cracks.

Numerous instances were noted where transverse cracks appeared in the surface between the lanes but not in the wheel paths. Subsequent monitoring of these cracks by the local authority showed that, in time, crack development extended across the full width of each carriageway. The surfacing material in the traffic lanes where the crack was not fully developed were therefore at the point of yield. Cores, taken ahead of the transverse development of the crack, provided material from which yield values were derived and used to define the strain at which cracking initiated.

The void content of the wearing course material and the hardness of the binder contained in this layer has been shown to vary across the carriageway in areas where the cracking was confined to the lane lines. A typical example of the variation in compaction is given in fig.7.1 which indicates that a reduction in the void content from approximately 3% in the lane lines to 1.5% in the wheel tracks provides a significant increase in the resistance to reflection cracking.

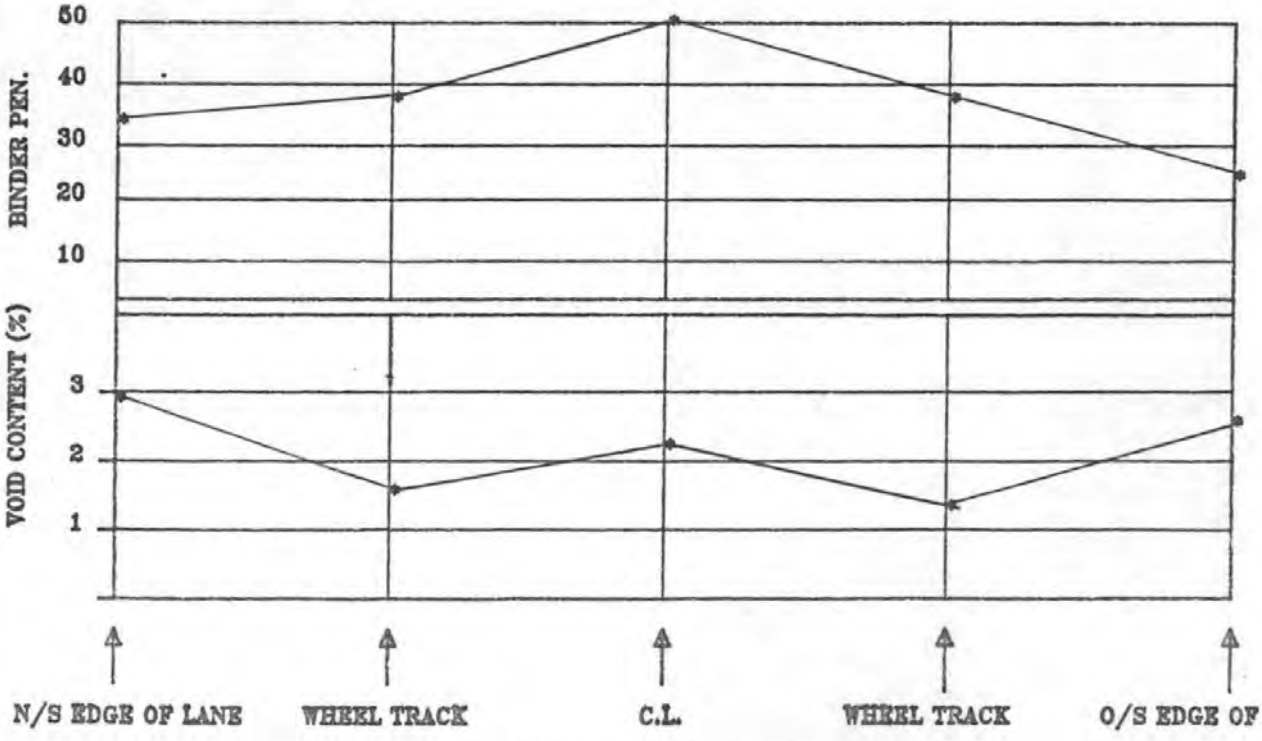

FIG.7.1 VOID CONTENT AND BINDER PEN.
NEARSIDE LANE CONTRACT 3 M4 MOTORWAY (AFTER A.BURT) (103)

7.5 AIMS OF THE INVESTIGATION

The aims of the investigation into this form of transverse cracking were:-

i) to use field data to provide an input into a finite element model of a pavement section with material characteristics and geometry similar to the M4 motorway and subjected to both moderate and severe temperature gradients.

ii) to form an understanding of this crack mechanism.

iii) to predict the conditions under which the relevant mechanisms will operate.

7.6 PAVEMENT MODELLING

7.6.1 Introduction

Cores were taken from the nearside lane of each of the four contracts under investigation. The location, individual layer thicknesses and crack frequency within the 100m length of pavement from which they were cored is given in Table 7.1. It is assumed that the cores are representative of the respective contracts.

7.6.2 Stiffness Data

Tensile creep tests were conducted on each of the bituminous layers and provided stiffness data which is given in Table 7.2 for the wearing courses.

The stiffness of all three bituminous layers of contract 3 are significantly higher than the material from the other contracts. The stiffness of the wearing course is a factor of ten greater than that found on either contracts 4 or 5 and a factor of 50 greater than that found on contract 6 at 0°C.

TABLE 7.2

WEARING COURSE - MIX STIFFNESS DATA
FROM CORES TAKEN ON CONTRACTS 3-6

		SURFACE TEMP 0°C		SURFACE TEMP. -10°C	
CONTRACT	SP_r(°C)	S_b(N/m²)	S_m(N/m²)	S_b(N/m²)	S_m(N/m²)
3	61.2	4×10^5	5×10^9	1.2×10^7	4.3×10^{10}
4	57.9	2.5×10^5	6.4×10^8	4×10^6	5.9×10^9
5	56.2	2×10^5	4.6×10^9	2.8×10^6	3.8×10^9
6	47.2	4×10^4	1.0×10^8	3.0×10^5	8.0×10^8

TABLE 7.1
LOCATION, PAVEMENT CONSTRUCTION DEPTHS AND CRACK SPACING DETAILS FOR CORES TAKEN FROM M4

CONTRACT 3 - MILE POST NO.102 AVERAGE TRANSVERSE CRACK SPACING = 26m
PAVEMENT CONSTRUCTION

LAYER	MATERIAL	THICKNESS(mm)
Wearing Course	HRA	39
Base Course	DBM	55
Upper Roadbase	DBM	85
Roadbase	D/Lean	160
Upper Sub-Base	Type 1	Variable
Sub-Base	Granular	Variable

CONTRACT 4 - MILE POST NO.81 AVERAGE TRANSVERSE CRACK SPACING = 6m
PAVEMENT CONSTRUCTION

LAYER	MATERIAL	THICKNESS(mm)
Wearing Course	HRA	38
Base Course	DBM	65
Upper Roadbase	DBM	90
Roadbase	D/Lean	190
Upper Sub-Base	CBGM	Variable
Sub-Base	Type 2	Variable

CONTRACT 5 - MILE POST NO.69 AVERAGE TRANSVERSE CRACK SPACING = 6m
PAVEMENT CONSTRUCTION

LAYER	MATERIAL	THICKNESS(mm)
Wearing Course	HRA	39
Base Course	DBM	55
Upper Roadbase	DBM	80
RoadBase	D/Lean	190
Upper Sub-base	CBGM	140
Sub-Base	Gravel	265

CONTRACT 6 - MILE POST NO.45 AVERAGE TRANSVERSE CRACK SPACING = >100
PAVEMENT CONSTRUCTION

LAYER	MATERIAL	THICKNESS(mm)
Wearing Course	HRA	48
Base Course	DBM	60
Upper Roadbase	DBM	75
Roadbase	D/Lean	190
Upper Sub-Base	CBGM	265
Sub-Base	Type 2	250

Strain at yield during the creep test gives an indication of a bituminous material's resistance to tensile cracking. The brittle wearing course of contract 3 yielded at 0.13% strain, contract 4 at 0.57%, contract 5 at 0.54% and contract 6 at 1.8%.

The binder softening point was determined on samples taken from all layers of each contract and, from the wearing course, the bitumen and filler contents were also determined, Table 7.3.

TABLE 7.3

ANALYSIS OF BINDER AND FILLER CONTENTS
AND RECOVERED BINDER SOFTENING POINTS (SP_r)

CON.	LAYER	SP_r(°C)	CORE REF.	BIT.CONT. %	FILLER CONT.%
3	w/c	61.2	105/OWB 103/OE	9.6	10.1
3	b/c	53.9	"	-	-
3	URB	58.4	"	-	-
4	w/c	57.9	83/OE 82/OB	8.5	4.6
4	b/c	54.5	"	-	-
4	URB	43.7	"	-	-
5	w/c	56.2	69	8.2	8.4
5	b/c	55.3			
5	URB	55.7		-	
6	w/c	47.2	45	6.6	7.7
6	b/c	49.3	"	5.8	2.6
6	URB		"	-	

The brittleness of the wearing course on contract 3 is due to both extreme hardening of the binder and a high filler content creating a dry mix. Susceptibility to bitumen hardening during use is associated with more open textured DBM mixes[9] rather than dense asphalts and therefore extensive oxidization during mixing seems the most likely cause.

7.6.3 Calculation of Coefficients of Thermal Contraction of Low Penetration Asphalts

At low temperatures stiff asphalts tend to act as an elastic material rather than exhibiting visco-elastic characteristics. Consequently, thermal movements in the bituminous layers must be considered as contributing to the overall thermal movements in the road structure.

The thermal coefficient of asphalt is a function of its aggregate type, bitumen grade and void content. The effect of bitumen grade and

void content has been quantified for standard HRA[8]. It has been assumed that different aggregate types may be accounted for by considering their individual thermal coefficients as a ratio of the standard aggregate used.

7.6.3.1 Test Procedure

The thermal coefficient of contraction (C') was measured on beams of 20mm nominal sized HRA wearing course[8] . The aggregate grading is given in Appendix 5. Seven grades of binder were used ranging from 200 PEN to 17 PEN. These beams were mould compacted under the action of a vibrating hammer and cut to a size of 100 x 100 x 400mm. In addition to the laboratory produced material, beams cut from each of the surfacing layers of contract 3 (M4) were also included within this investigation. The test rig used to measure contraction is shown in fig.7.2 and consists of a 500mm length of Mild Steel channel section with upstands at either end each supporting a L.V.D.T. The bituminous sample was positioned between the transducers with their probes butted up to steel platens araldited to the end of the asphalt. The rig was calibrated to allow for thermal movement within the apparatus, thus giving a direct reading of thermal contraction of the test sample. Enclosure of the rig in a thermally controlled cabinet allowed cooling from + 10°C to -10°C.

7.6.3.2 The Thermal Coefficient of Contraction of Asphalts

Asphalts incorporating a hard binder grade have a coefficient of contraction approximately 1.5 times greater than asphalts containing a soft binder, Table 7.4.

Differing void contents have a significantly greater effect; the value of C' increases as the void content decreases.

The values of coefficient obtained from a beam of bituminous material cut from contract 3 of the M4 is also given in Table 7.4 for each of the bituminous layers. The hard dense mix employed as the wearing course on this contract is shown to have a higher coefficient of contraction than the material produced in the laboratory. However the beam was not cut from an area incorporating material with an exceptionally low binder penetration value. Therefore material exhibiting even higher coefficient values will occur in isolated areas of material in this contract. A maximum value of 7 x $10^{-5}/^{o}C$

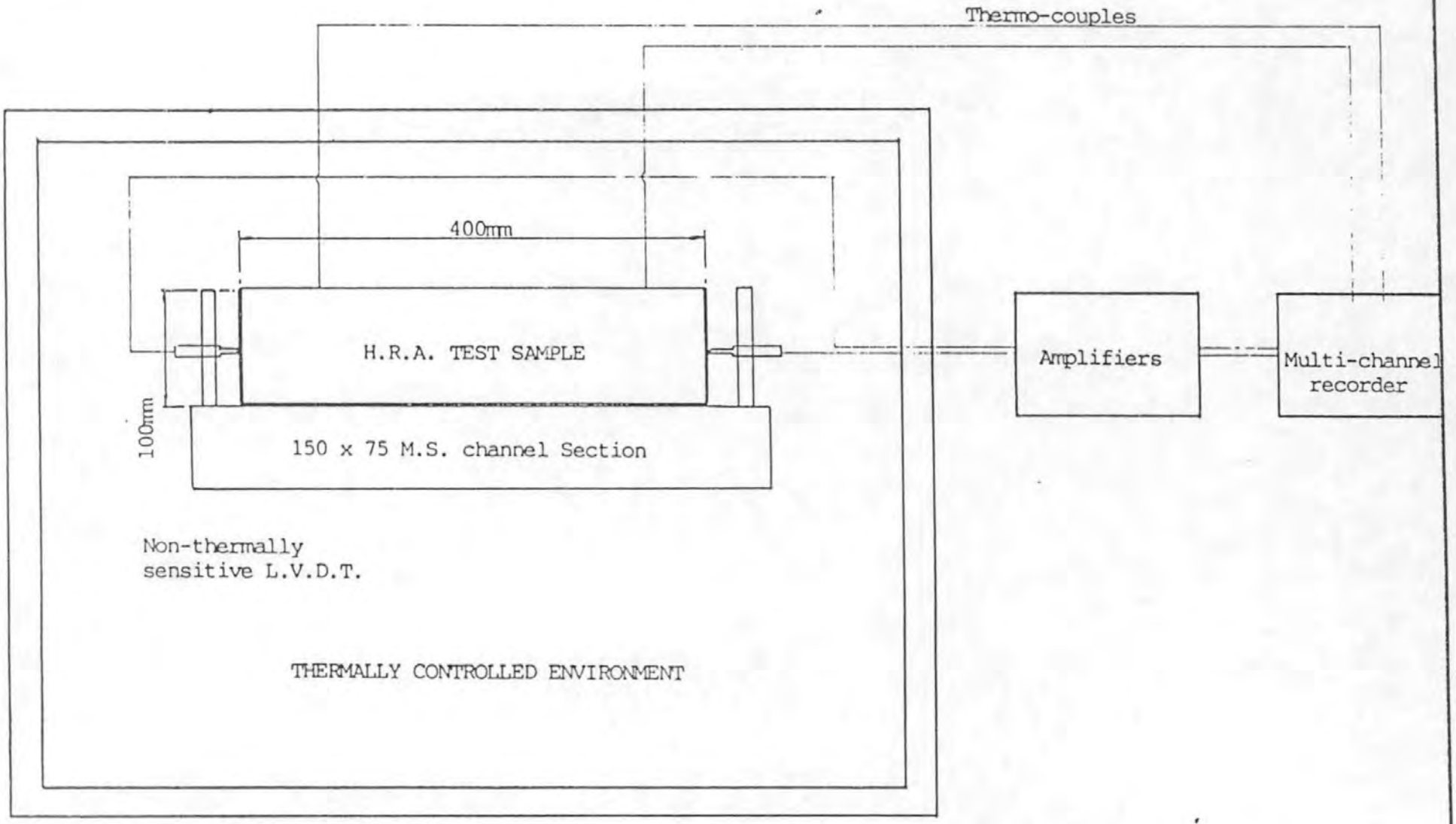

FIG.7.2 TEST LAYOUT FOR THE DERIVATION OF COEFFICIENT OF THERMAL CONTRACTION OF ASPHALTIC BEAMS

and a minimum value of 2.5 x 10^{-5}/°C is assumed for the coefficient of thermal contraction of the wearing course material in the finite element model described in the next section.

TABLE 7.4

COEFFICIENTS OF THERMAL CONTRACTION FOR VARIOUS GRADE BINDERS

Sample No.	Recovered softening point (SP_r) (°C)	Binder grade (Pen)	C'/°C		Void Content (%)
				Aggregate Limestone	
0	42.5	200	2.9	"	4.36
1	47.5	100	3.4	"	4.11
2	56	44	3.13	"	3.95
3	62	34	3.6	"	4.36
4	69	26	3.11	"	4.88
5	78	17	3.93	"	4.22
M4 WC	61.2	-	4.11	Granite	2.1
M4 BC	53.9	-	2.56	Limestone	4.8
M4 URB	58.4	-	2.13	"	5.3

7.7 FINITE ELEMENT MODEL

7.7.1 Thermal Contraction and Warping

A finite element model, F.E.2, simulates thermal contraction and slab warping of the individual pavement layers. Thermal contraction is dependent upon slab length, thermal gradient, coefficient of thermal movement and the restraint offered by shear forces acting along the interface of each layer. The model assumes that no yielding occurs along the interfaces.

Bending moments induced by a night-time or cold period thermal gradient through the pavement are greatest at the slab centres and decrease to zero at the slab centres, fig.7.3. There must, therefore, be some unrestrained warping at the slab ends. The magnitude of this warping is related to the temperature gradient and coefficient of thermal movement of each layer. However, it is independent of slab length.

Upward warping of the slab ends will occur either at night or during periods of cold weather. This is of interest as tensile strains are induced into the surfacing material and overall slab contraction reduces the vertical restraint to warping offered by interlock with adjoining slabs. The model assumes that no end restraint occurs.

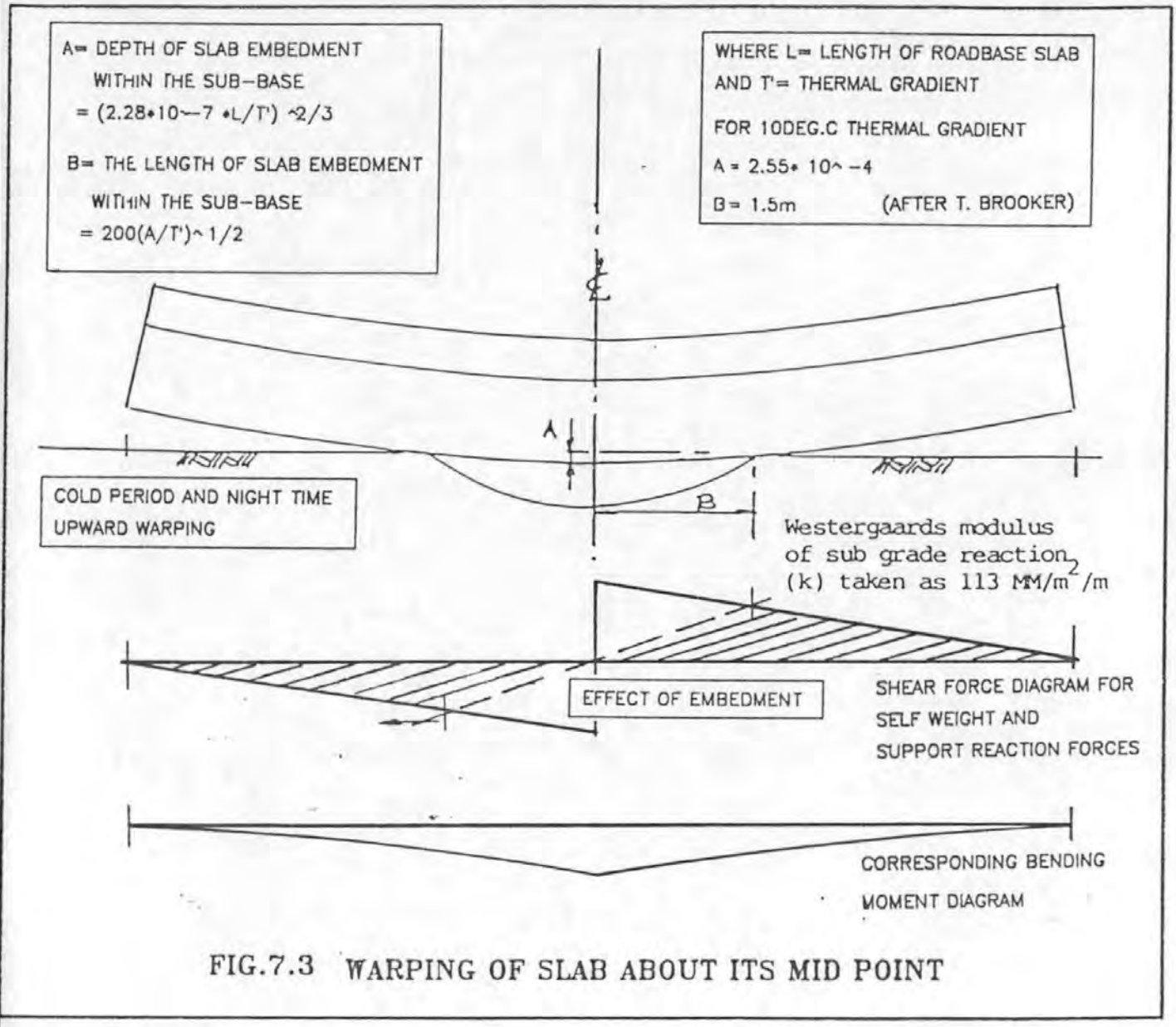

FIG.7.3 WARPING OF SLAB ABOUT ITS MID POINT

The self weight of the slab will tend to restrain the warping action and therefore the density of each layer must be considered. These self weight forces are mobilized because the support reaction forces become concentrated at the slab centre. In practice, with a non-rigid foundation, there will be embedment of this portion of the slab; fig.7.3, and the full self-weight forces will not be mobilized. Previous studies at the Polytechnic undertaken by T. Brooker[76] have shown the length of embedment (B), in fig.7.3, to be 30% of the slab length for typical moduli values of sub-base and roadbase. This factor has been built into the model and the density of each layer is included with the input data.

7.7.2. Description of the Model

The model, fig.7.4, simulates half a pavement slab, 5m in length, with dimensionally similar thicknesses to the M4 and with a vertical crack through the lean concrete roadbase. It is assumed that no granular interlock exists between adjacent concrete slabs, the worst condition, as interlock would tend to inhibit warping displacements. Cracks of predefined length were input above the adjoining slabs at the top of the surfacing. The stiffness values for each of the bituminous layers were derived from respective creep tests and are given in Table 7.5 together with the material characteristics for the stress intensity factor calculations.

TABLE 7.5
RANGE OF STIFFNESS AND THERMAL COEFFICIENT VALUES
DEFINED FOR INDIVIDUAL PAVEMENT LAYERS AS INPUT PARAMETERS
FOR FINITE ELEMENT ANALYSIS OF CRACK MECHANISM

Unit stiffness N/m^2	layer	coefficient of thermal contraction/°C
1,5, 10 x 10^8	bituminous wearing course	(2.3 - 7) x 10^{-5}
1 x 10^8	bituminous base course	2.3 x 10^{-5}
1 x 10^8	bituminous upper roadbase	2.3 x 10^{-5}
30 x 10^9	lean concrete roadbase	1.0 x 10^{-5}

Temperature gradients through the pavement structure were subdivided into short term (daily cycles) of extreme winter temperatures and longer term conditions where low temperatures penetrate deeper into the pavement structure, fig.7.5.

Thermal values for short term were input in the form of a parabolic curve for severe and very severe conditions with gradients of 9, 15 and 20°C, through the surfacing and roadbase layers.

Strains ahead of the crack tip will be greater during sustained periods of low temperatures which are associated with more uniform thermal gradients assumed to be 4, 7 and 10°C.

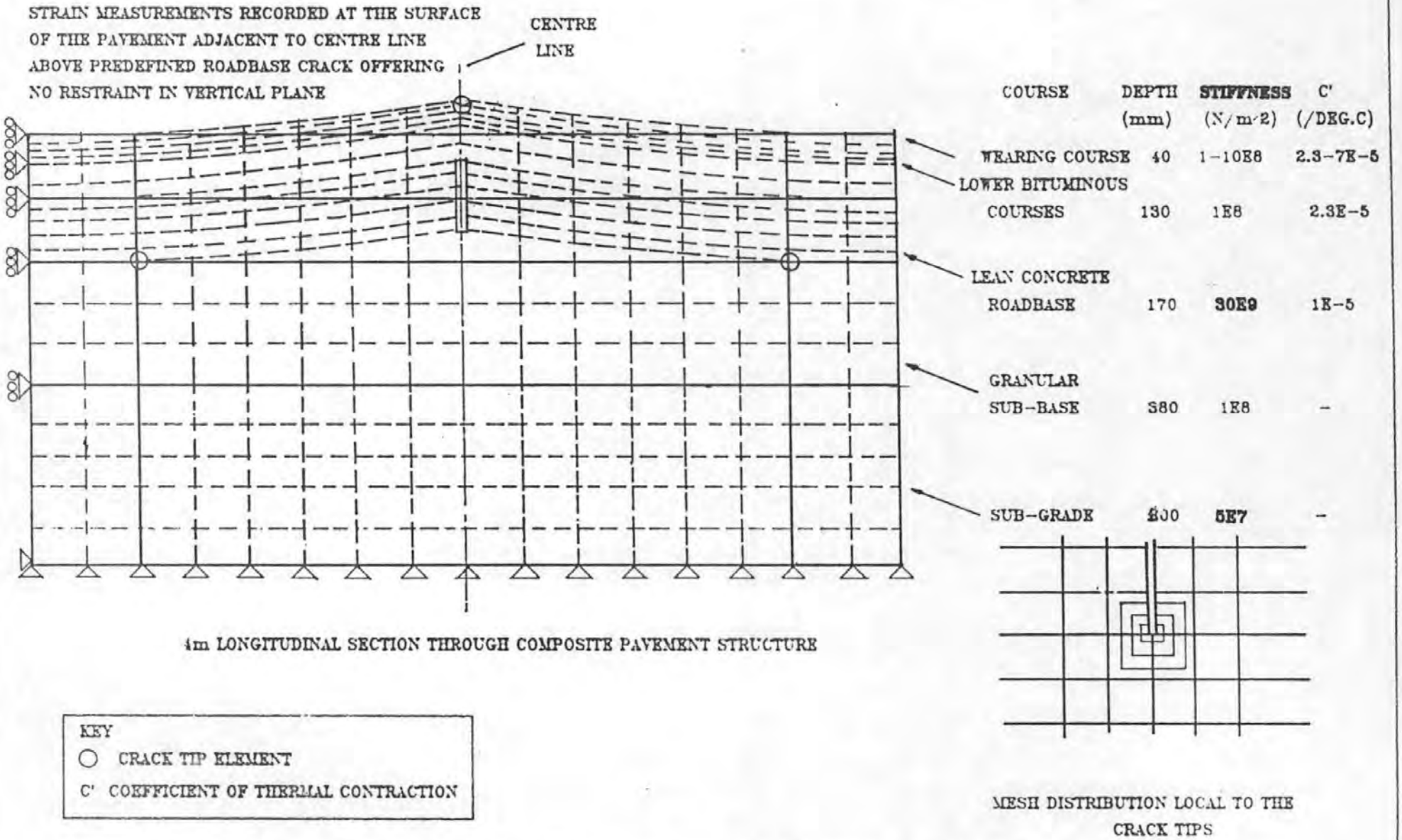

FIG.7.4 FINITE ELEMENT MODEL MESH ORIENTATION AND DEFORMED SHAPE. SIMULATION OF THERMAL CONTRACTION AND SLAB WARPING OF PAVEMENT STRUCTURE

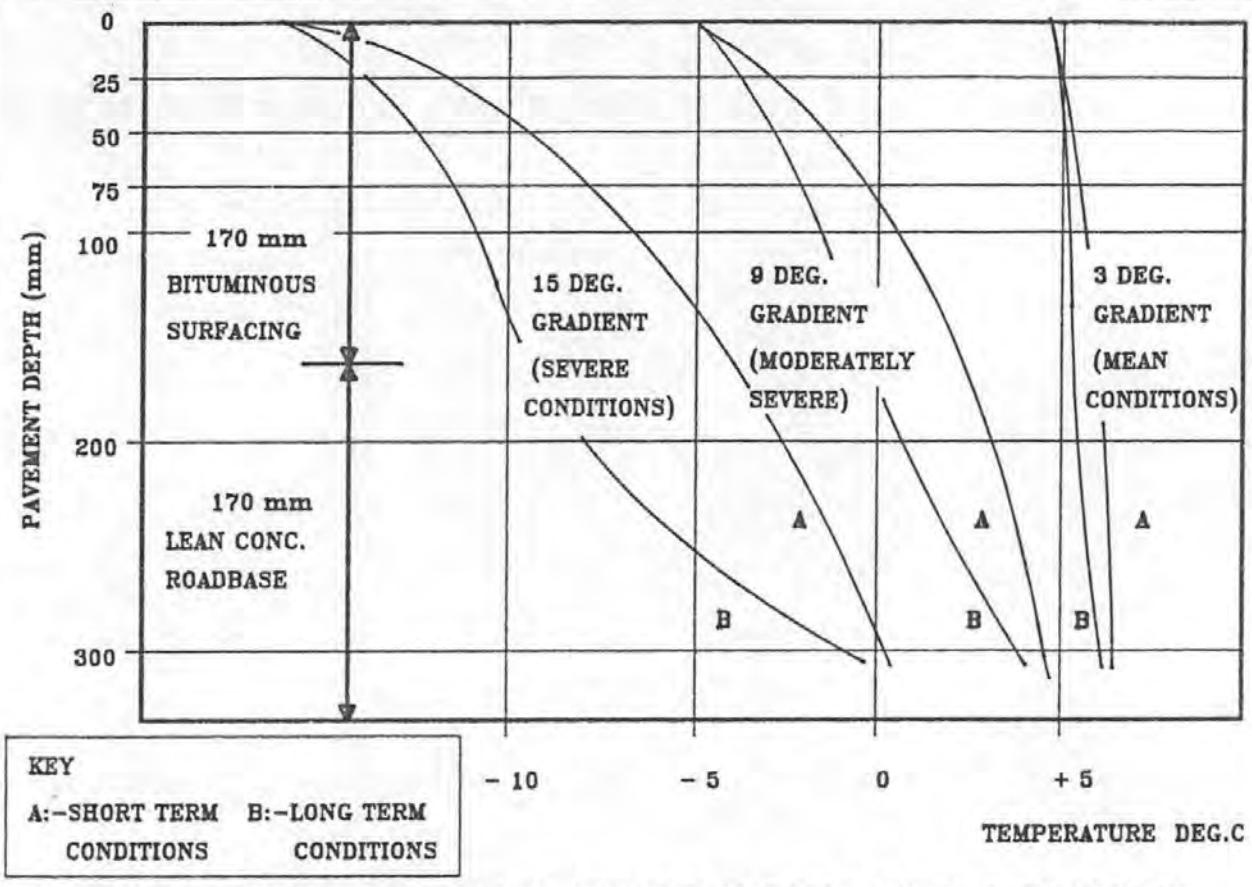

FIG.7.5 THERMAL GRADIENTS THROUGH COMPOSITE PAVEMENTS FOR LOW WINTER TEMPERATURES

7.8 DISCUSSION OF MODEL RESULTS

Predefined cracks have been input into the finite element model to investigate the most likely position for cracks to initiate under daily fluctuations of temperature. The two locations considered were at the pavement surface with downward crack propagation and at surfacing/roadbase interface with subsequent upward propagation. Figures 7.6 and 7.7 indicate the stress intensity factors determined for the surface cracking. They also define the stiffness ratios between the bituminous layers and thermal expansion coefficients.

A comparison of stress intensity factors for cracks originating at both the top and bottom of the surfacing layers is given in fig.7.8. The investigation of crack growth from the base incorporates the temperature data for the four seasons given in section 6. For the surface crack condition, an extreme winter temperature gradient of 9°C across the structural layers of the pavement has been adopted.

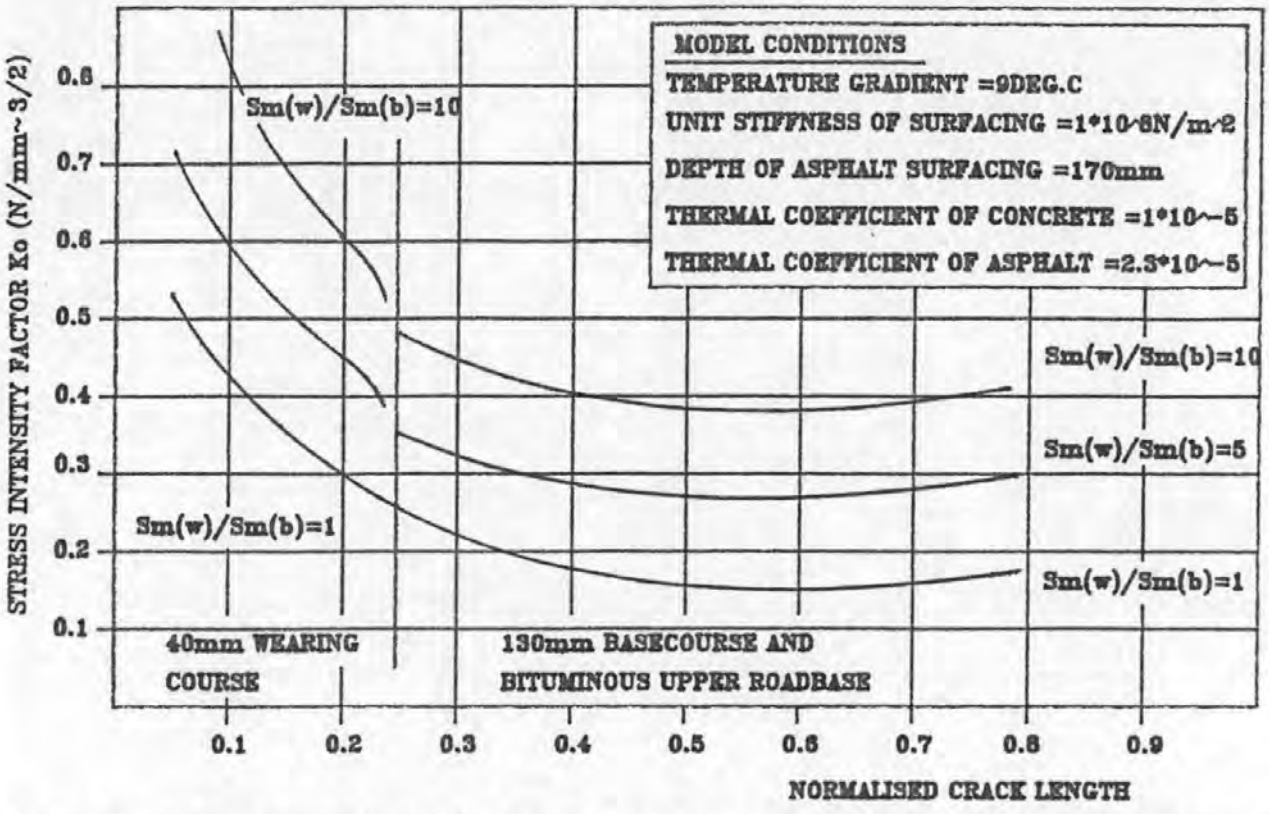

FIG.7.6 STRESS INTENSITY FACTOR (Ko) VERSUS NORMALISED CRACK LENGTH FOR CRACK INITIATION AT THE SURFACE AND CRACK PROPAGATION DOWNWARDS DUE TO SLAB WARPING AND THERMAL CONTRACTION

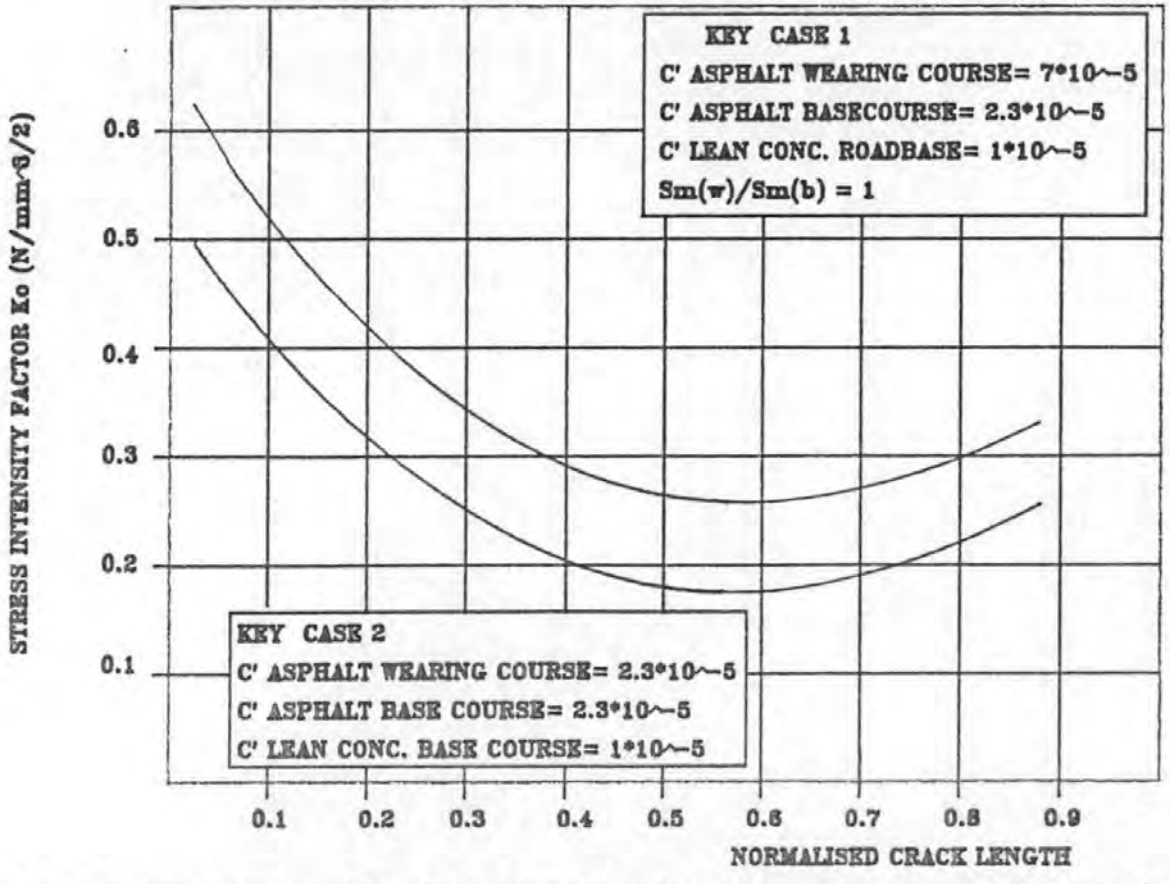

FIG.7.7 STRESS INTENSITY FACTOR (Ko) VERSUS CRACK LENGTH FOR CRACK PROPAGATION DOWNWARDS TOTAL DEPTH OF ASPHALT= 170mm TEMP.GRAD= 9 DEG. UNIT STIFFNESS= 1*10^8 N/m^2

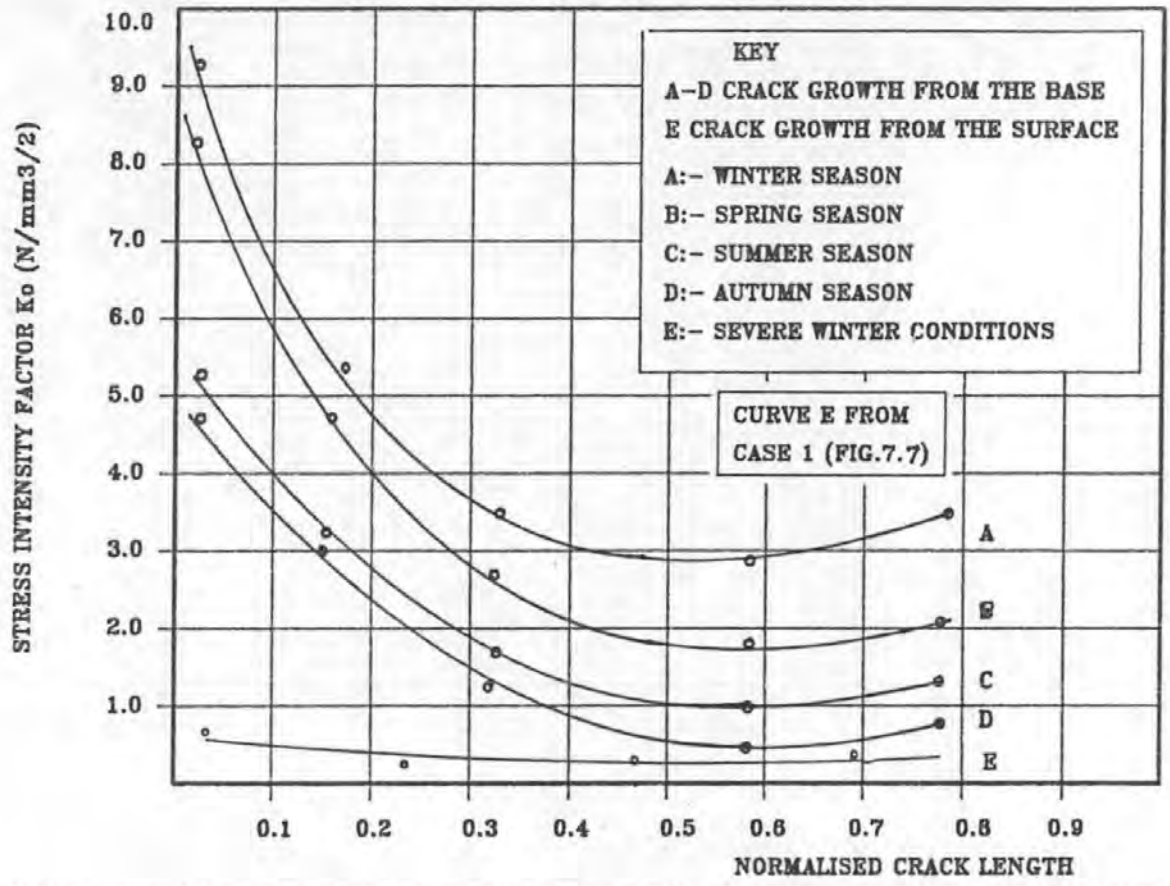

FIG.7.8 COMPARISON OF STRESS INTENSITY CURVES FOR CONDITIONS OF CRACK PROPAGATION FROM THE BASE AND THE SURFACE

The results illustrate that the surface crack condition is not a fatigue phenomenon as its respective stress intensity factor curve, (curve E; fig.7.8) is of lower order of magnitude than that pertaining to base cracking; curves A to D.

Yielding of the surfacing material has been considered to account for field observations of cracks restricted to the upper bituminous layer with no cracking in the base course or bituminous upper roadbase. If the strains induced in the surface under the combined action of warping and contraction are greater than the restraint exhibited by this layer, the material will yield. Therefore, the strains at the surface above a crack in the lean concrete roadbase have been recorded from the finite element model for a range of pavement temperature gradients; fig.7.9. The temperature gradients have been categorised into short term and long term; fig.7.5.

A comparison has been drawn between the strain values derived from the model and the values derived from the creep tests on wearing course material from each of the M4 construction contracts. The yield point, from the creep tests, has been defined from the plot of mix

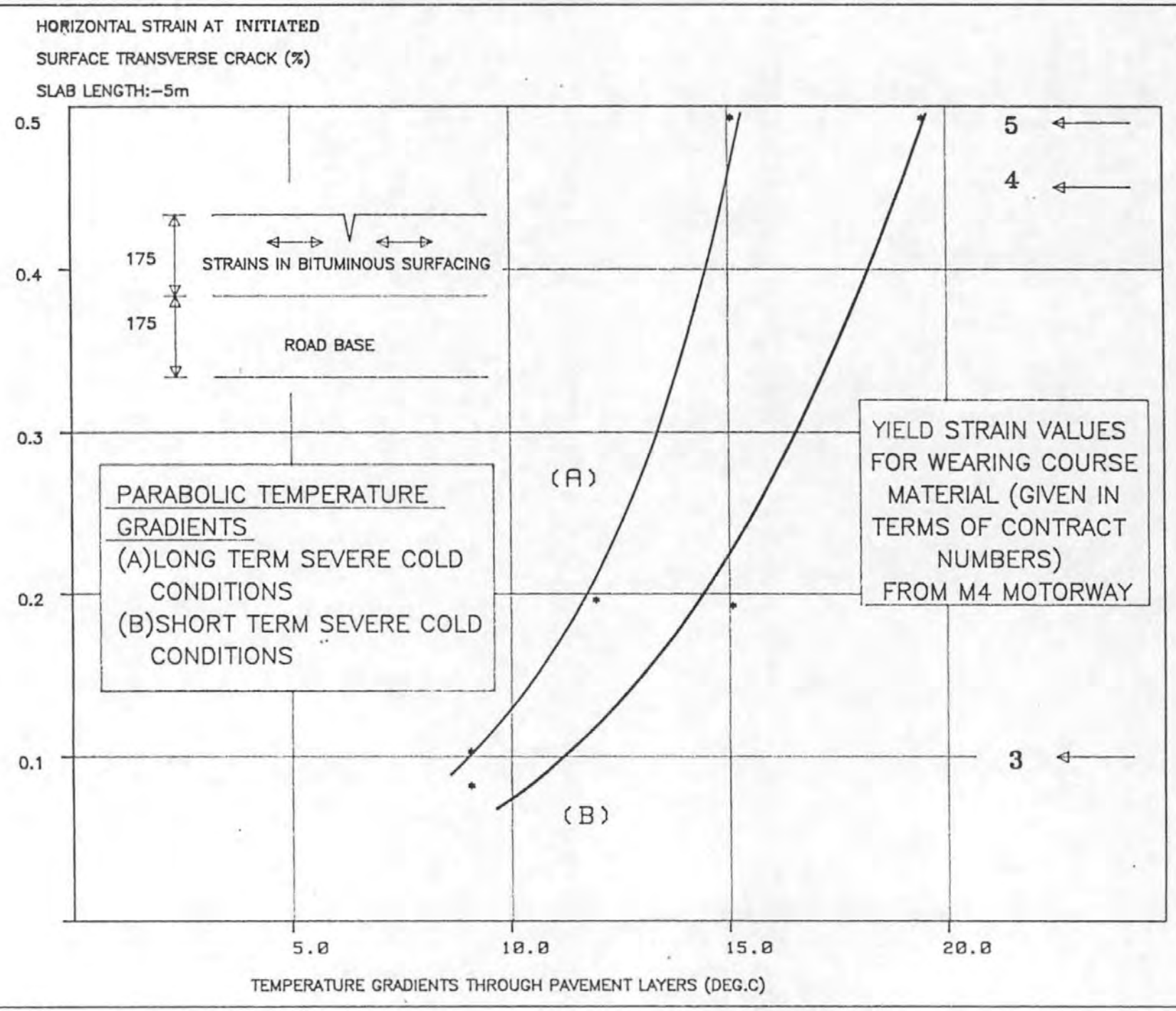

FIG.7.9 HORIZONTAL STRAIN INDUCED INTO THE WEARING COURSE AT AN INITIATED CRACK FOR GIVEN PAVEMENT TEMPERATURE GRADIENTS

stiffness against loading time as the change in gradient between the curve described by the unyielded and yielded material and the yield strain recorded from the experimental results.

The creep test results, fig.7.10, showed the tensile yield strain of the wearing course material on contract 3 to be less than 0.13%, on contract 4 and 5 to be approximately 0.5%, and on contract 6 1.8%. For extended periods of cold weather through the pavement a 9°C temperature gradient will exceed the yield strain of contract 3 and a 14.5°C gradient is greater than the restraint shown by the wearing course material of contracts 4 and 5; fig.7.9. The equivalent short term low temperature differences, also given in fig.7.9 show that the yield strains may be exceeded by a 11.5°C and 19.5°C gradient for the respective contracts.

These results therefore indicate that the tensile yield mechanism will induce surface cracking under temperature gradients which can occur under U.K. climatic conditions.

The concept of using yield strain values measured at 20°C to relate to yield strains at all temperatures and loading is over simplistic due to non uniform thermal and stress susceptibility of the binder. However, the concept has been partially validated through a creep test carried out at 0°C which showed little variation in yield strain with a control test carried out at 20°C; fig.7.11.

Tensile creep tests therefore provide a standardized method by which the tensile resistance to cracking of an asphaltic mix may be derived. This relationship is further verified through additional data presented in Section 7.10.

The incidence of reflection cracking under the mechanism of tensile yield may be related to long term effects requiring a number of winters prior to crack initiation or a single intensely cold winter period or a combination of both.

Observations from the M4 indicate that crack initiation is a combination of both effects as new cracks appear every year. However, the number of new cracks to appear in any specific year is not detailed and therefore the influence of an individual winter

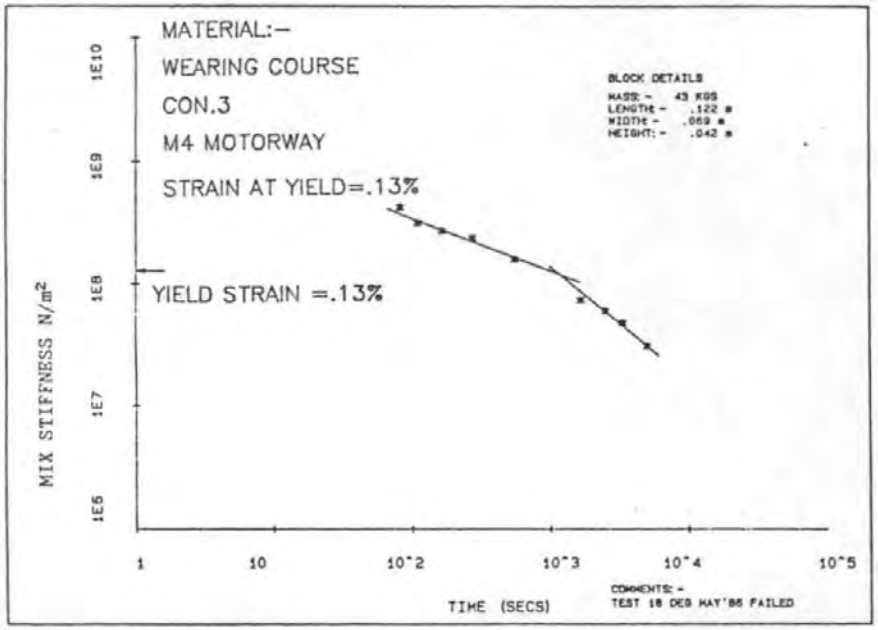

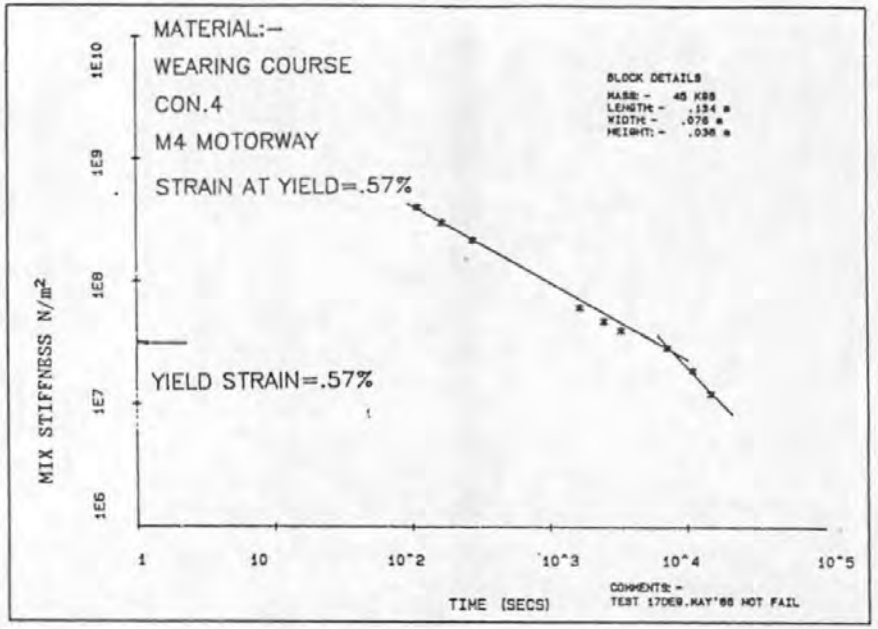

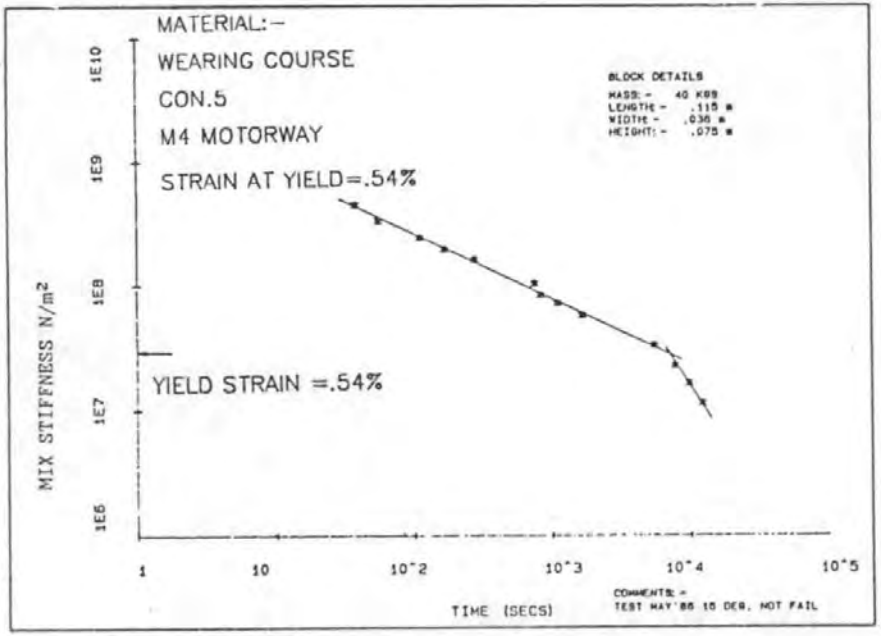

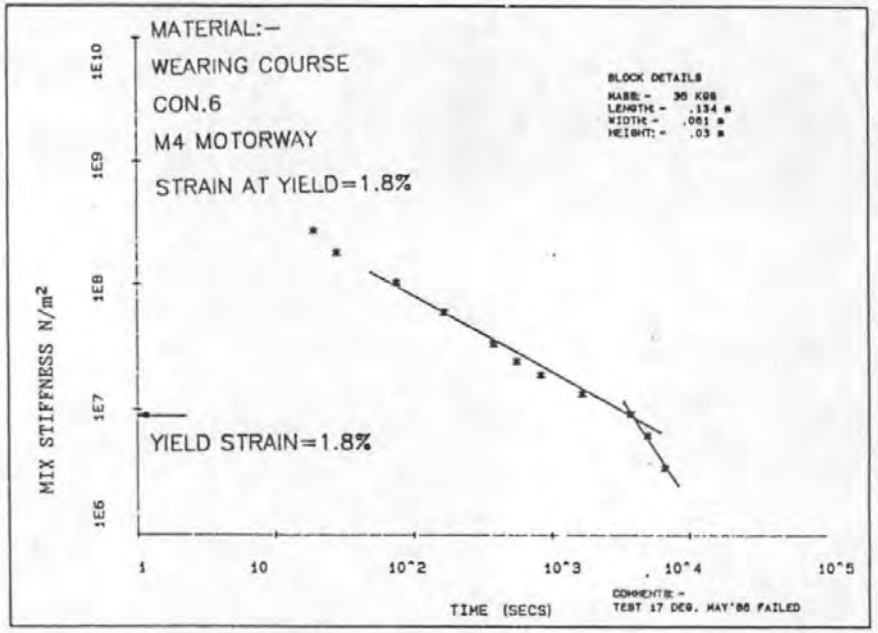

FIG.7.10 TENSILE CREEP TEST RESULTS FROM M4 MOTORWAY (BERKSHIRE) SHEET 1

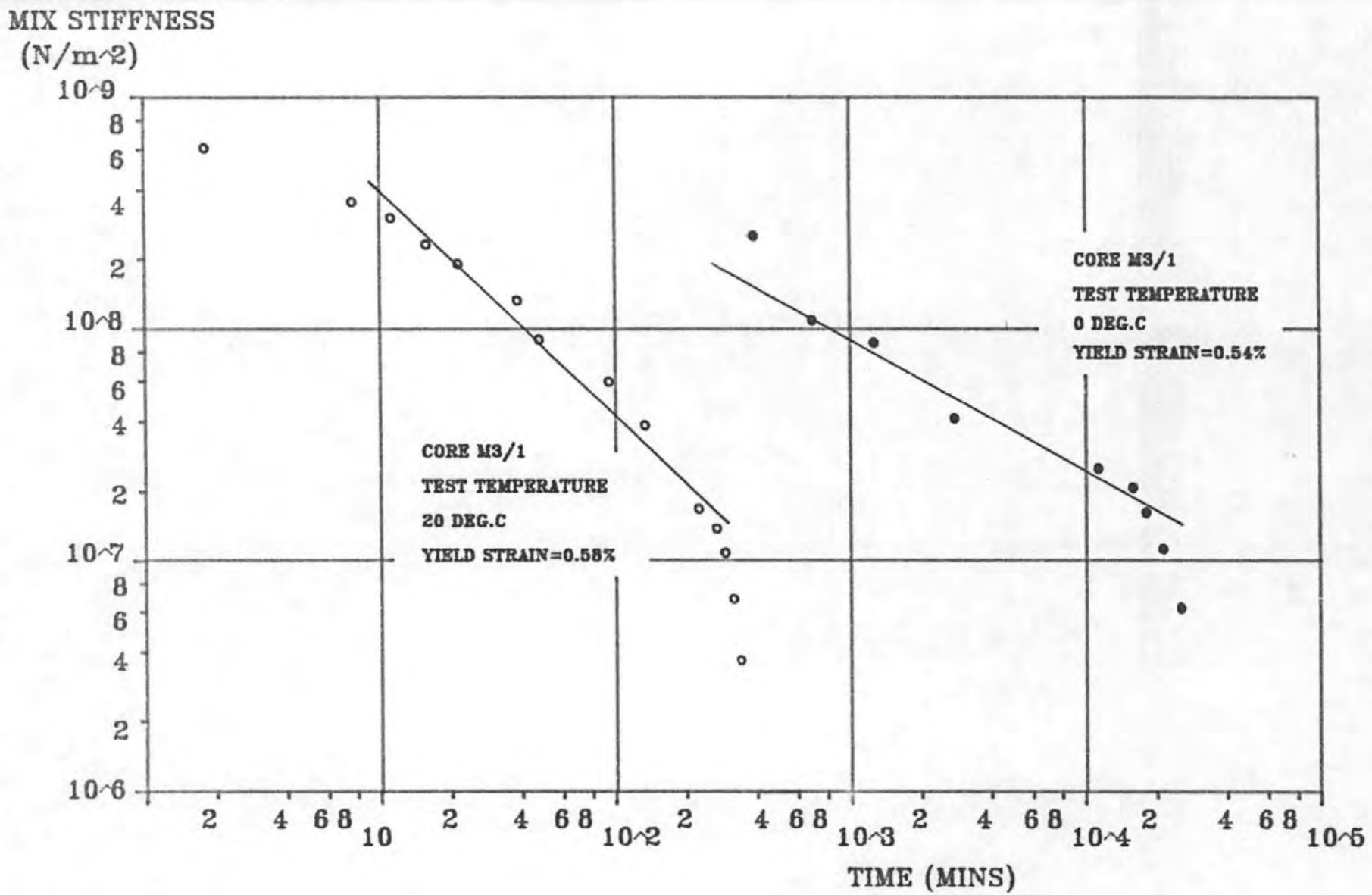

FIG.7.11 VERIFICATION OF YIELD STRAIN CONCEPT AT LOW TEMPERATURES

CREEP TEST RESULTS ON CORES M3/1 PAVEMENT STATE:- WELL DEVELOPED REFLECTION CRACK PATERN

cannot be ascertained.

The probability of cracking occurring in any given year after construction of the pavement for a defined value of winter temperature is also influenced by the change in the wearing course yield strain characteristics.

A further investigation is therefore required to enable the incidence of surface reflection cracking to be accurately predicted. This would entail the collection of crack initiation, pavement temperature and yield strain data from a number of pavements through their service lives.

7.9 COMPARISON OF FIELD OBSERVATIONS WITH MODEL RESULTS

Cracking was confined to the wearing course in several of the cores taken from the M4. The results from the model would account for this as crack propagation would be inhibited at the interface between wearing course and base course through:-

1) Higher yield strain values exhibited by the base course materials
2) Reduction of strain with pavement depth
3) Increased pavement temperature with depth causing a decrease in binder stiffness.

The finite element model produced horizontal crack opening widths at the surface, fig.7.12, of less than 1mm for the extreme case with a pavement temperature gradient of 15°C and a wearing course coefficient of contraction (C') of $7 \times 10^{-5}/^{o}C$, a magnitude of 5 times smaller than recorded field observations from the M4. The plot shows that a coefficient of thermal contraction of $3.5 \times 10^{-4}/^{o}C$ would be required for the bituminous material to produce crack openings of 5mm width which is unrealistically high.

Two further factors may however by considered to account for surface crack opening widths of this magnitude.

Firstly, the possibility of a creep effect within the asphalt which occurs during long periods of cold weather giving the surfacing a higher long term coefficient of thermal contraction.

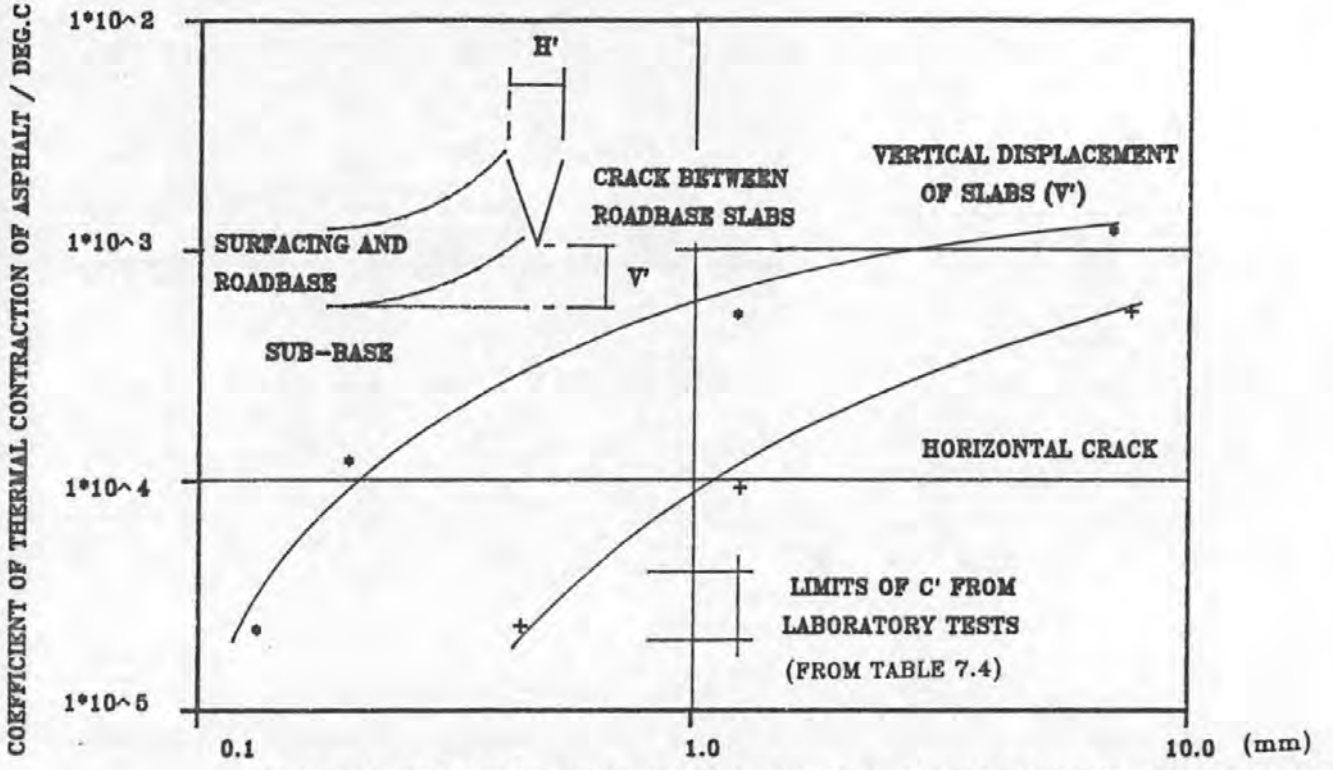

FIG.7.12 HORIZONTAL CRACK WIDTH FOR A CRACK FULLY DEVELOPED THROUGH THE SURFACING AND VERTICAL WARPING DISPLACEMENTS AT THE SURFACE VERSUS THE COEFFICIENT OF THERMAL CONTRACTION OF ASPHALT

Secondly, debris being forced into the crack preventing even limited expansion during the slight increase in the day time temperatures but flow mechanisms within the asphalt allowing it to contract further during the night time fall in temperature. With a moderation in weather and a rise in temperature, the surfacing material adopts more visco-elastic characteristics and its flow mechanisms allow the crack to close.

Simulation of vehicular loading was not undertaken by the finite element model but the 'rocking' of slabs by traffic induces a shearing stress in the surfacing material at the slab ends and therefore its influence must be considered.

The magnitude of the vertical warping displacements at the slab ends for extreme winter temperature conditions as shown in fig.7.12 were 0.08mm. Previous studies[95] have shown that differential vertical displacements between the slab ends greater than 0.5mm are required

for traffic loading to be a significant factor in reflection crack propagation. However, the surfacing material is more brittle at low temperatures and therefore smaller movements will be required to produce similar surfacing deterioration.

7.10 VALIDATION OF YIELD STRAIN CONCEPT

7.10.1 Introduction

The investigation has included further tensile creep tests on cored sample blocks from 4 sites. The sites include the M4 Motorway (Berkshire), A38 (Litchfield By-Pass), Redhouse Road (Northampton) and the M3 Motorway (Hampshire). The cored sections of pavement have been selected to provide diverse material data and comparisons are drawn between the yield properties of materials extracted from areas exhibiting long term cracking, recently developed cracking and those free from this form of pavement deterioration. This is achieved by relating the test results to the frequency and distribution of cracks at the surface adjacent to individual cores.

The constructional thickness of the four pavements were similar consisting of 180-200mm of lean concrete roadbase overlaid by 175mm of bituminous surfacing.

The yield strain results from the wearing courses of these pavements are given in Figs.7.13 to 7.16 and the associated crack distributions are described in the following sections. The presentation of the creep test results in these figures is similar to the format described in section 7.8.

7.10.2 Further Investigation of Crack Development/Strain Relationships

7.10.2.1 M4 (Berkshire)

Three further tests have been conducted on material cored from Contract 4 at locations 88/8, 75/9 and 89/3. Each location exhibited a different crack frequency. The yield strain results are given in Table 7.7 and the recovered binder properties and crack spacing are presented for these cores only in Table 7.6.

The results demonstrate that the greatest crack frequency occurs on

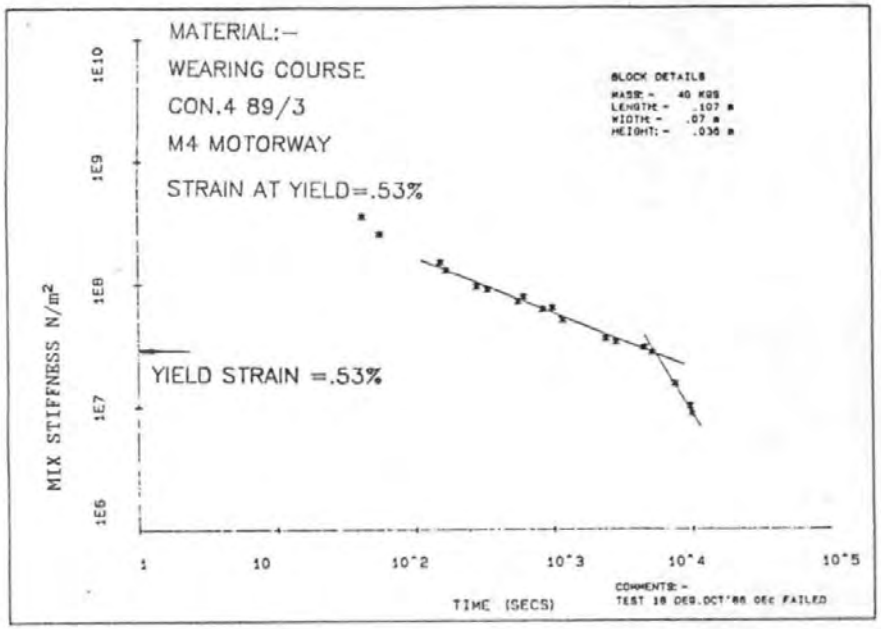

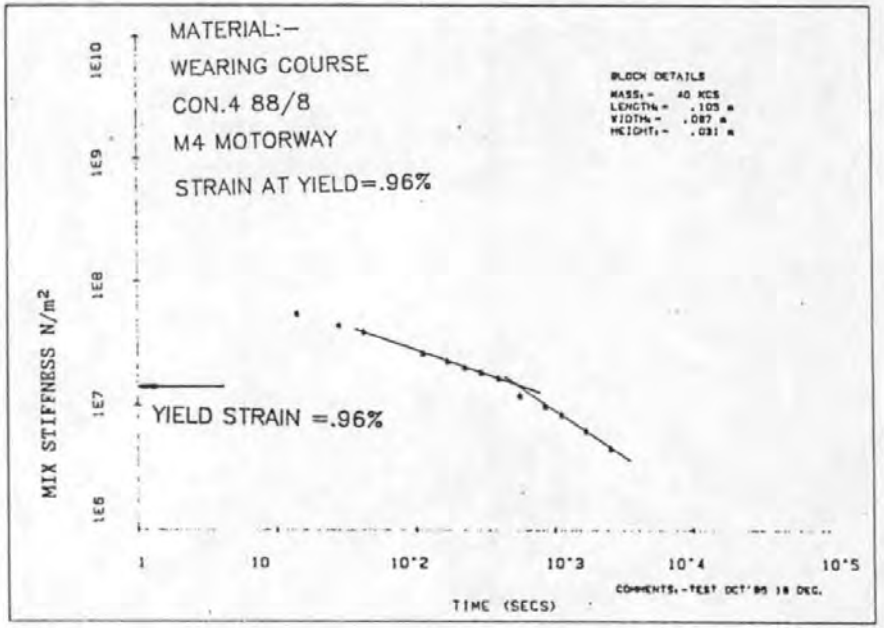

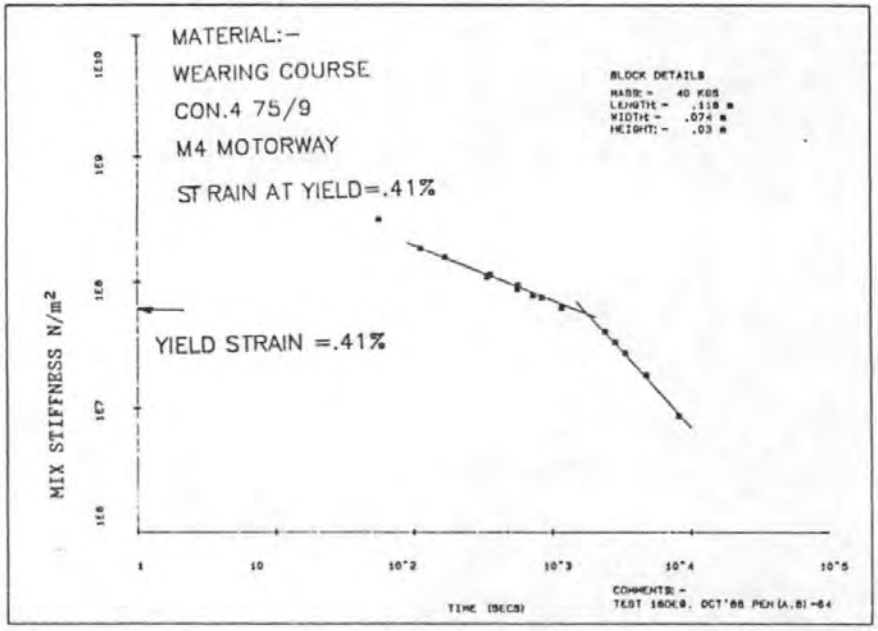

FIG.7.13 TENSILE CREEP TEST RESULTS FROM M4 MOTORWAY (BERKSHIRE) SHEET 2

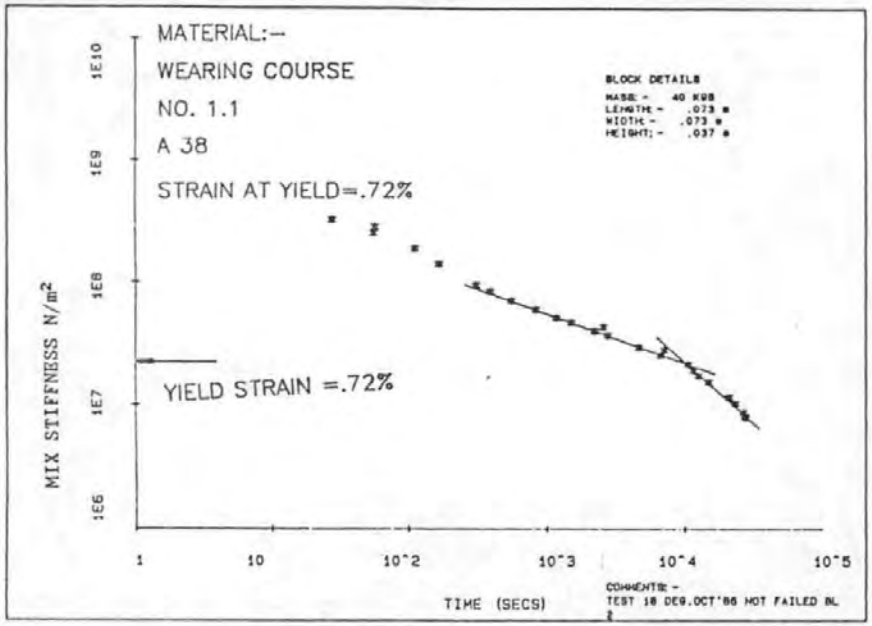

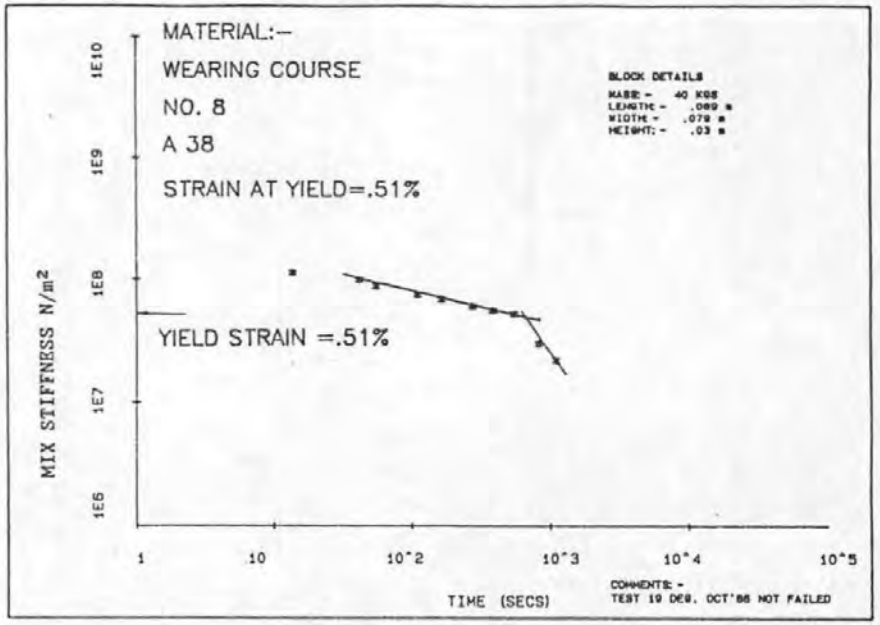

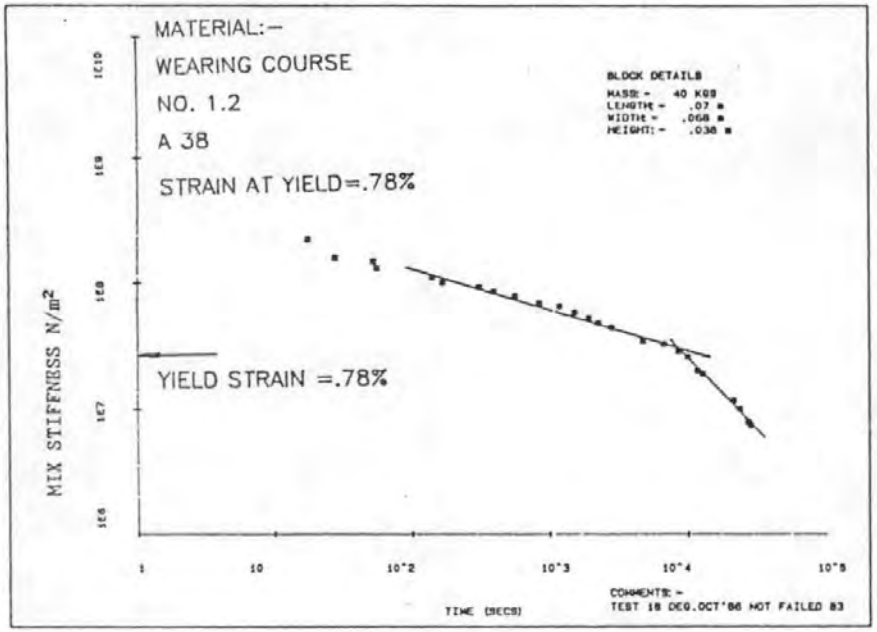

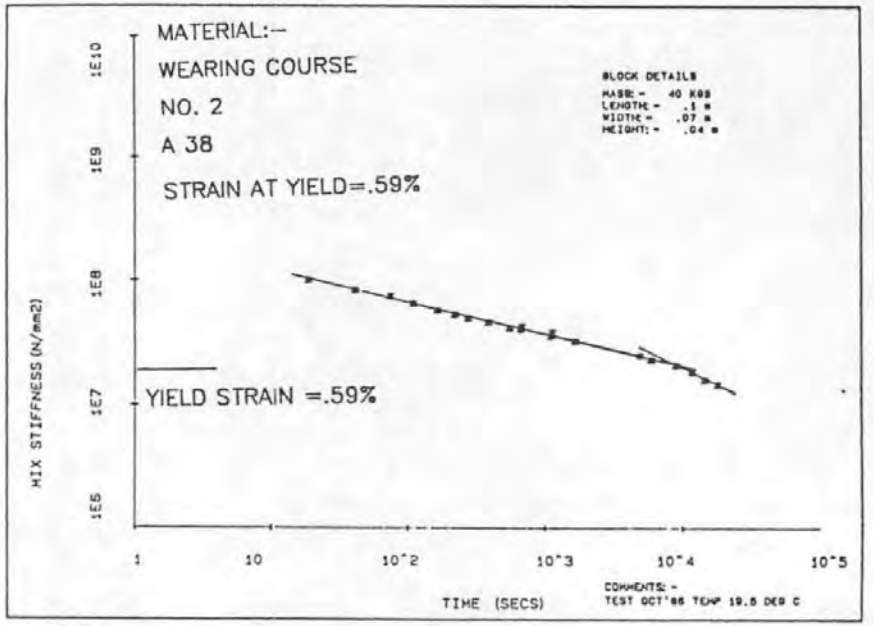

FIG.7.14 TENSILE CREEP TEST RESULTS FROM A38 (LITCHFEILD BY-PASS)

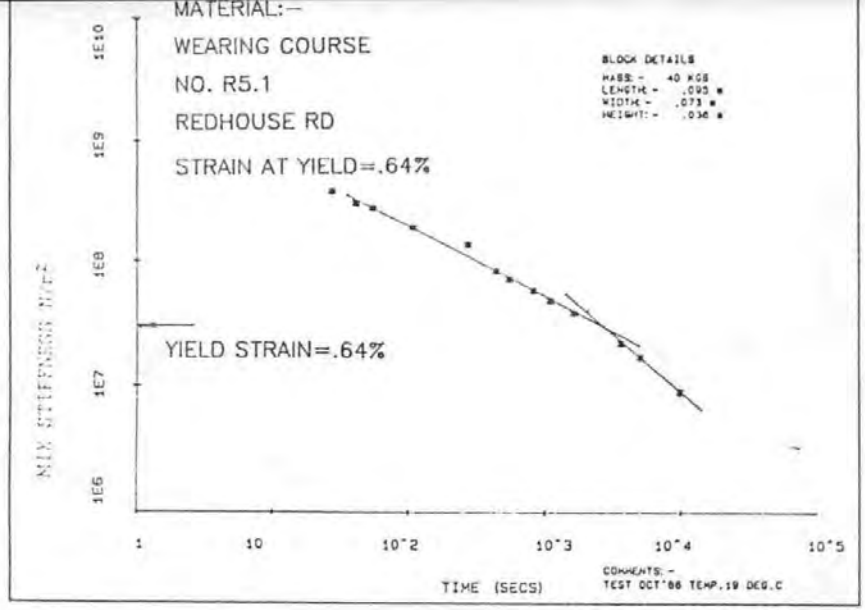

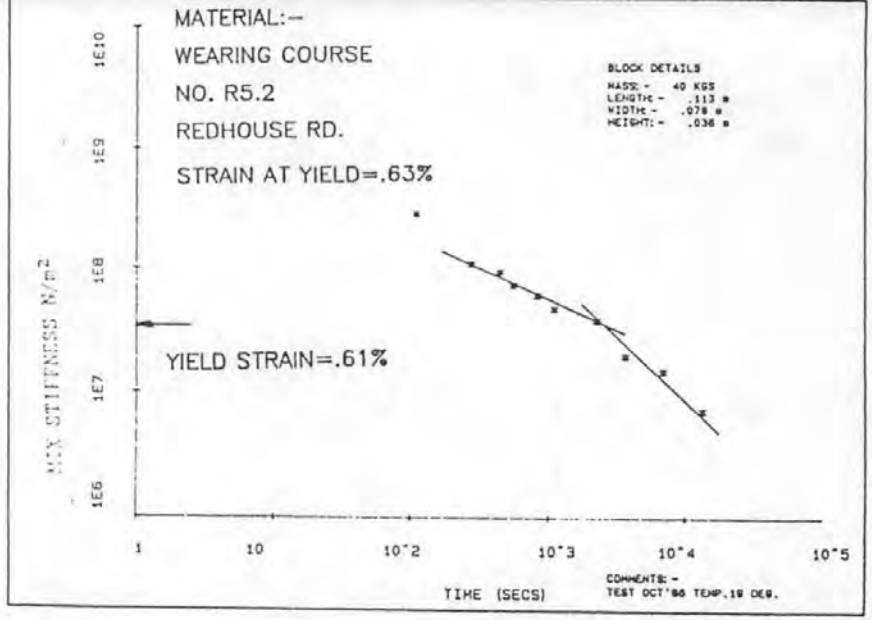

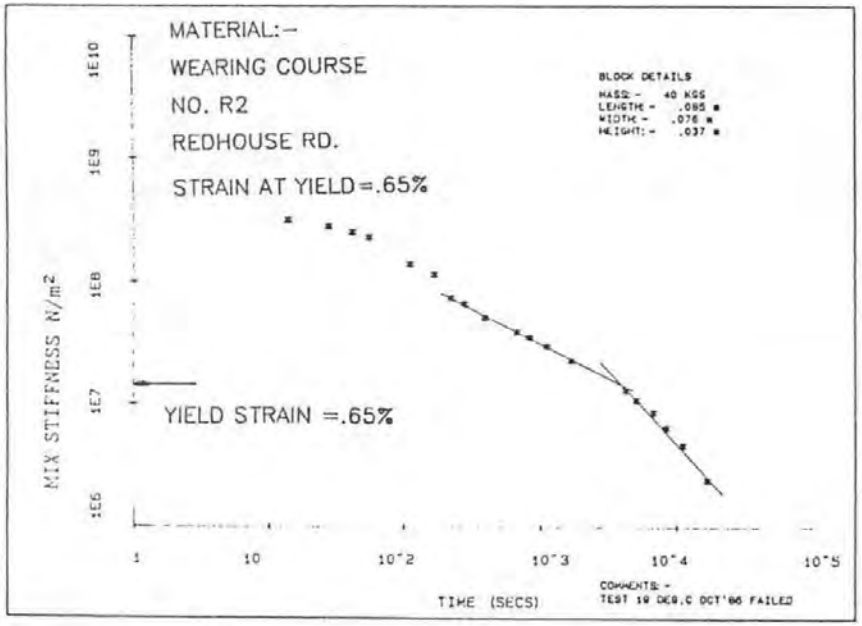

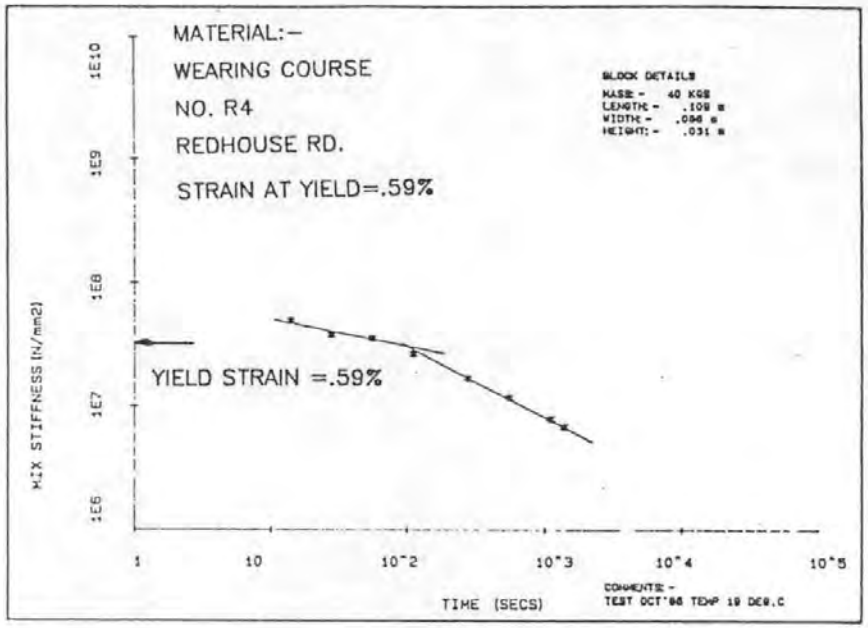

FIG.7.15 TENSILE CREEP TEST RESULTS FROM REDHOUSE ROAD (NORTHAMPTON)

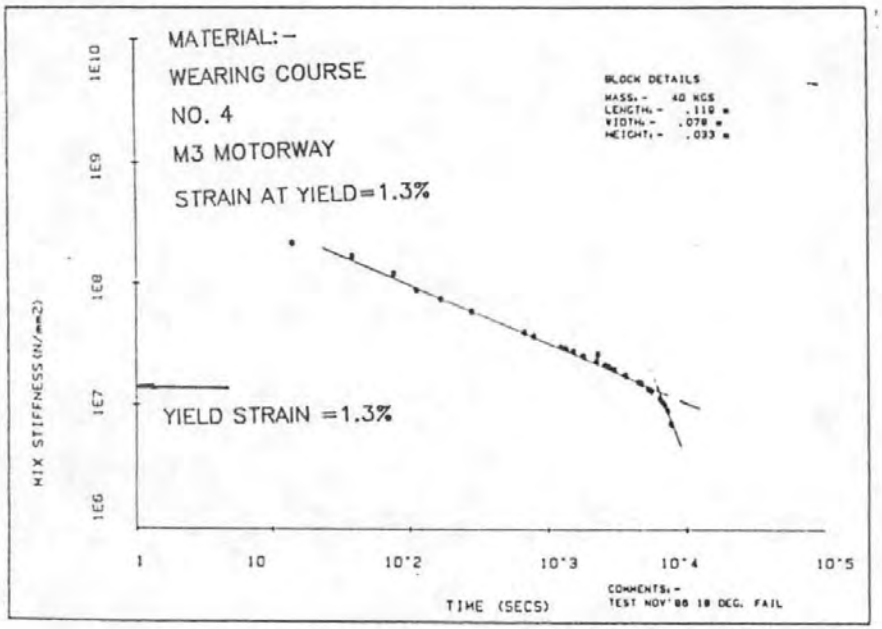

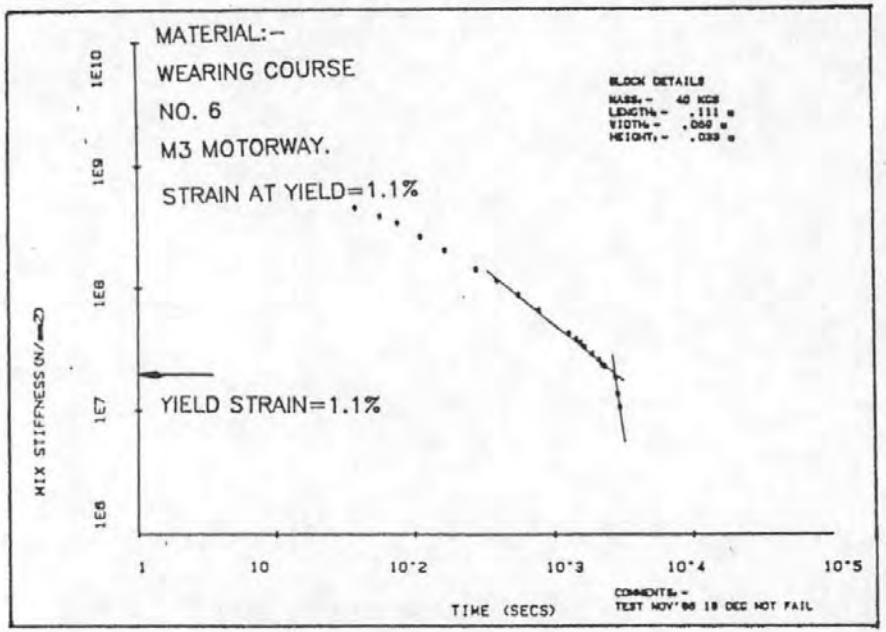

FIG.7.16 TENSILE CREEP TEST RESULTS FROM M3 MOTORWAY (HAMPSHIRE)

sections with the lowest binder penetration and lowest yield strain values. For example, the kilometre adjacent to marker post 88/8 is relatively free of transverse cracking which is reflected by its yield strain value of 0.96%. In the absence of a detailed crack survey at the cored sites, and the resultant yield strains cannot be associated directly with the location of individual cracks.

7.10.2.2 A38 (Litchfield ByPass)

The existence of a characteristic crack spacing is confused by the general deterioration of the pavement. The crack survey indicates an original crack spacing of 10 to 12m which has been halved and quartered by secondary cracking.

The material from three cores were tested, numbers 1, 2 and 8. Cores 1 and 2 were taken from the off-side wheel path of the slow lane, a section where cracking is evident in the nearside wheel path but has not occurred across the full carriageway width. Therefore, the surface cracks are an indication of cracks within the underlying lean concrete but the wearing course material directly adjacent to the cored area has yet to yield.

The yield strain values of 0.72% and 0.78% exhibited by core 1 and 0.69% by core 2 are consistent with the M4 results indicating that full width reflection cracking will occur but that cracking has been delayed by the level of yield strain recorded.

Core number 8 was taken in an area which the crack survey indicates a trace of a crack and therefore at the point of yield. The yield strain value was 0.51%.

7.10.2.3 M3 Motorway (Hampshire)

A section of the M3 in Hampshire constructed in the early 1970's between chainages 68.5 and 68.6 is extensively cracked in the hard shoulder and lanes 2 and 3 but is free from cracking in lane 1. No major maintenance or overlaying has been carried out so therefore the surfacing material is all of a similar age.

Material from the uncracked lane, cores M3/4 and M3/6, exhibited high yield strains of 1.1% and 1.34% respectively and therefore consistent with the results derived from other uncracked pavements. Further

TABLE 7.6
CRACK SPACING AND MIX DETAILS OF THE THREE LOCATIONS CORED ON THE M4 MOTORWAY

Marker post	Week No. of Construction	Cracks /km (no)	Binder pen. (pen)	Binder Soft.pt (deg.c)	Binder Content (%)	Filler Content (%)
75/9	85	50	23	64	7.5	9.8
89/3	69/70	305	31	62	8.1	11.8
88/8	74	22	42	57	7.0	10.6

(after A. Burt)

TABLE 7.7
YIELD STAIN VALUES OF WEARING COURSE MATERIAL FROM THE FOUR TEST SITES

ROAD	CORE	YIELD STRAIN (%)
Redhouse Road (Northampton)	R2	0.65
	R4	0.59
	R5	0.64
	R5	0.61
A38 (Litchfield Bypass)	A38/1	0.78
	A38/1	0.72
	A38/2	0.69
	A38/8	0.51
M4 (Berkshire)	89/3	0.53
	88/8	0.96
	75/9	0.41
	M4/C3	0.13
	M4/C4	0.57
	M4/C5	0.54
	M4/C6	1.8
M3 (Hampshire)	M3/4	1.34
	M3/6	1.1

tests on cores from cracked areas will be carried out under a second phase of this test programme.

7.10.2.4 Redhouse Road (Northampton)

Inspection of the crack survey suggests a primary crack frequency of 8 to 9m although it is not fully developed along the entire length of the surveyed section. Evidence also exists as to occasional secondary cracking at half this frequency.

R2, illustrated in Plate 7, has been cored between a crack which is visible in the wheel path of the slow lane and middle of lane 2. It may be assumed that further hardening of the binder is required prior to full width transverse cracking. This assumption is consistent with its yield strain value of 0.65%.

Cores R4 and R5 have been taken at similar locations and little variation is shown in their yield strain values (0.59% to 0.64%).

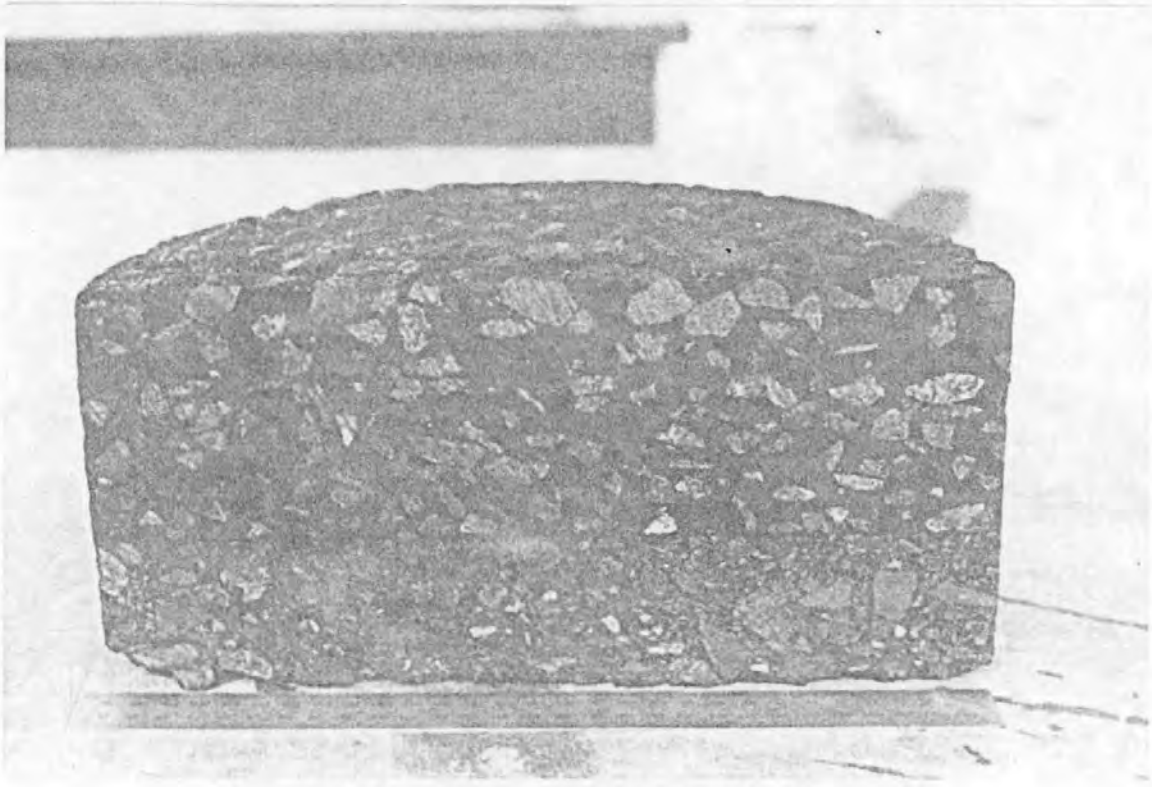

UNCRACKED CORED SECTION

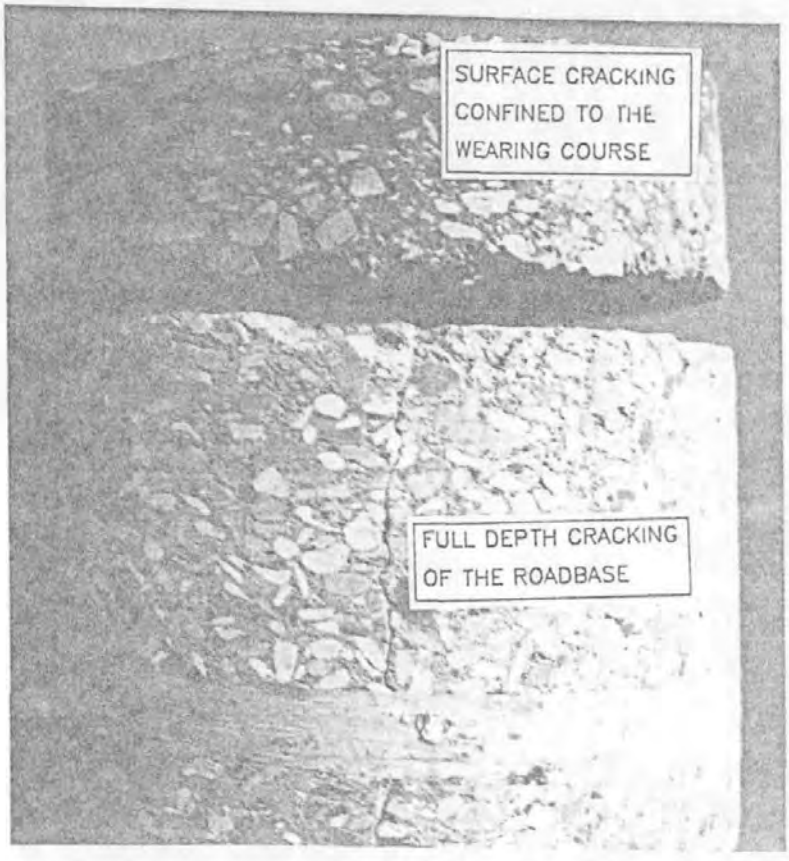

FULL DEPTH CRACKING OF LEAN CONCRETE ROADBASE BUT CRACKING IN THE SURFACING LIMITED TO THE WEARING COURSE

PLATE 7 CORE ON CRACKED SECTION OF THE REDHOUSE ROAD (NORTHAMPTON)

8.0 MECHANISM OF SHEAR FATIGUE

8.1 Introduction

The passage of traffic induces shear stresses into surfacing material through differential movement between the slab ends of the cracked cement bound roadbase.

The investigation into the influence of vehicular loading is confined to combining the results from a literature search, finite element simulation of a cracked pavement section under standard axle loading and laboratory testing to evaluate the overall contribution to the rate of crack propagation attributable to traffic. The literature and finite element results provide an estimate of the range of vertical movements to be used as an input into the laboratory modelling.

Whereas simulation of thermally induced stresses may be satisfactorily represented by horizontal crack opening, limited to a single mode of cracking (mode 1), crack mechanisms due to the traffic condition are more complex involving both mode 1 and mode 2, fig.8.1. Furthermore, initially the condition is stress controlled but as the effective restraint offered by the surfacing decreases proportionally with crack growth, together with the gradual breakdown of granular interlock and compression of the sub-grade, strain rather than stress controlled displacements occur. However, the stress intensity curves were obtained for both crack mechanisms which reinforced the conclusions drawn from the limited laboratory investigation.

The influence on crack propagation through the trafficking of composite pavements is further investigated through the presentation of survey data collected by the TRRL. This data allows crack spacing to be related to cumulative traffic flow for pavements of similar age, and provides a comparison of their structural condition.

8.2 Field Test Data

Test undertaken by TRRL in the early 1960's at Slough[41] recorded vertical displacements at the joints of concrete road sections caused by passing traffic, categorising the movements in terms of the

LOADING FOR REFLECTION CRACKING

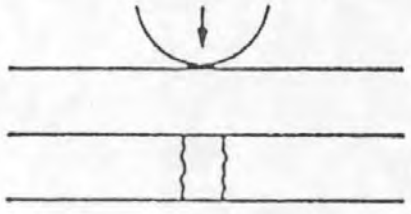

(c)Centred vertical load

MODE I

LOADING FOR REFLECTION CRACKING

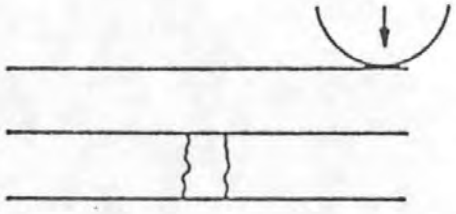

(b)Offset vertical load

MODE 2

CRACK OPENING MODE I

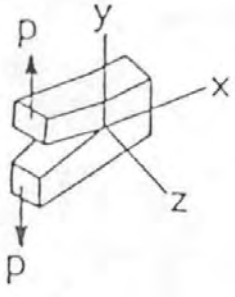

OPENING

CRACK OPENING MODE 2

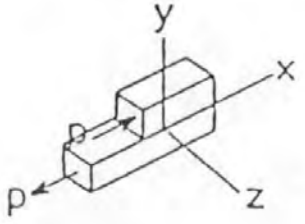

SHEARING

FIG.8.1 MODES OF CRACK OPENING CAUSED BY TRAFFIC

pavement quality.

Relative vertical movements between the two sides of joints in a good concrete road were considered to be of the order .13mm or less but varied according to the freedom of joints. On poor concrete roads movements in excess of 2.5mm were measured. Vertical movements in concrete joints in excess of .38mm led to rapid propagation of the reflection cracks.

The results obtained on the Trunk Road A4 at Slough after three years are shown in fig.8.2

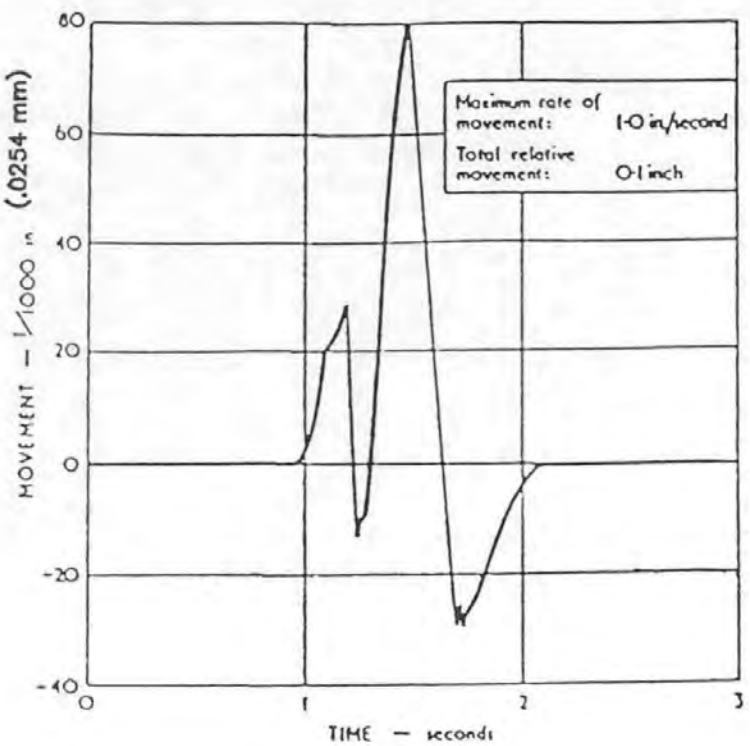

FIG.8.2 TRACE OF THE VERTICAL MOVEMENT AT A JOINT CAUSED BY A PASSING VEHICLE

Although this data was derived from the expansion joints of overlaid structural concrete pavements it shows the magnitude of vertical deflection that will produce rapid crack propagation.

8.3 FINITE ELEMENT MODEL

8.3.1 Model Description

The finite element model (F.E.3) was developed with the PAFEC system [102] to model the differential vertical deflections between the ends of cracked roadbase slabs and to estimate the stresses in the surfacing under the action of standard wheel load.

The sub-base and sub-grade were assumed to be continuous along the length of the pavement while a vertical discontinuity of 0.1mm width was input into roadbase layer. The extent of cracking within the surfacing was designated as a user input through an option varying the position of a crack tip element vertically above the roadbase discontinuity. Additional user inputs included the properties of each layer and position and magnitude of the wheel load.

The dimensions of the pavement structure simulated by the model and an example of its input physical properties are given in fig.8.3. The results from the model provide an estimation of the range of vertical differential displacements between the cracked pavement sections under the influence of a wheel load as it traverses the cracked region. The crack tip element and fine mesh spacing with the surfacing layer also allows the stress intensity factors to be calculated for input increments of crack length.

A wheel of standard .5kN/m^2 loading was exerted, in case 1) fig.8.3, centred over the road base crack and in case 2) offset from the crack at the position of maximum differential deflection between the slabs. A typical example of the deflected shape is illustrated in Fig.8.4 reproduced from the Phase 7 output of the PAFEC Program.

The first run, for each load case, provided the surface deflection with no cracking in the surfacing material. Subsequent runs of the program represented crack propagation through the surfacing layers. The vertical deflection was recorded at the surfacing/roadbase interface adjacent to the crack path.

The accuracy of results in estimating the deflections within the pavement is influenced by simplifications made in the modelling

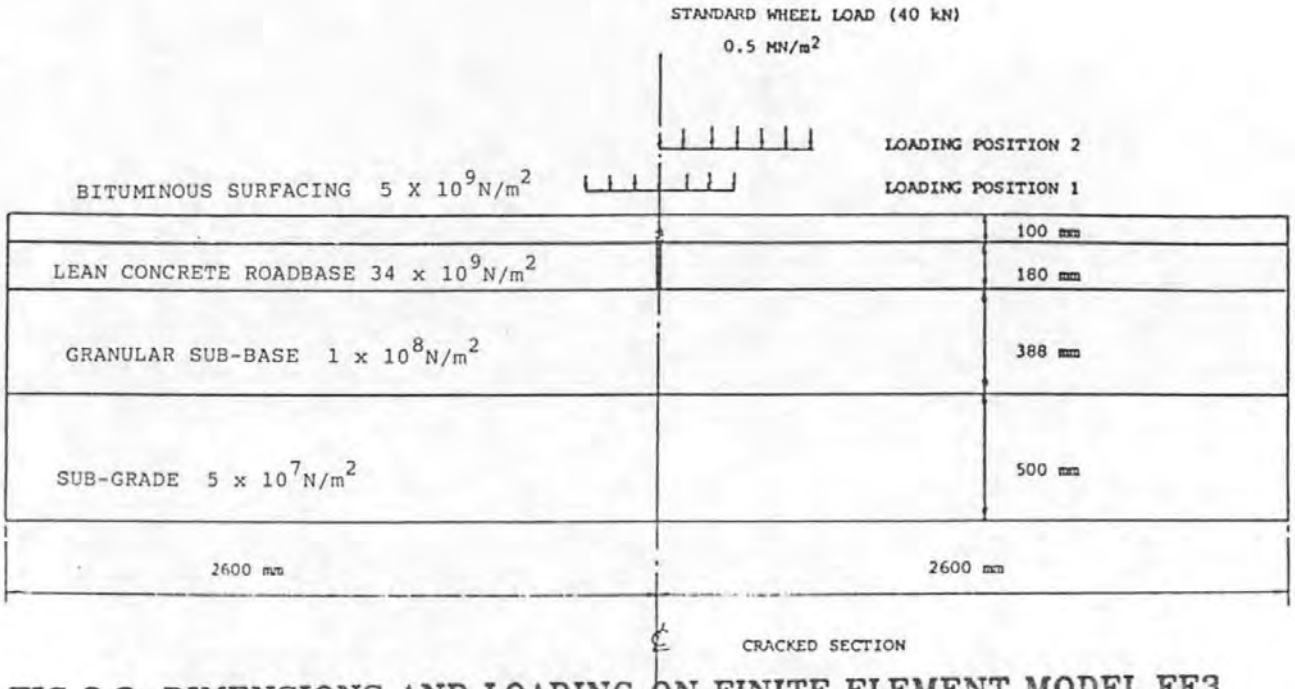

FIG.8.3 DIMENSIONS AND LOADING ON FINITE ELEMENT MODEL FE3 SIMULATING TRAFFIC LOADING ON CRACKED PAVEMENT SECTION

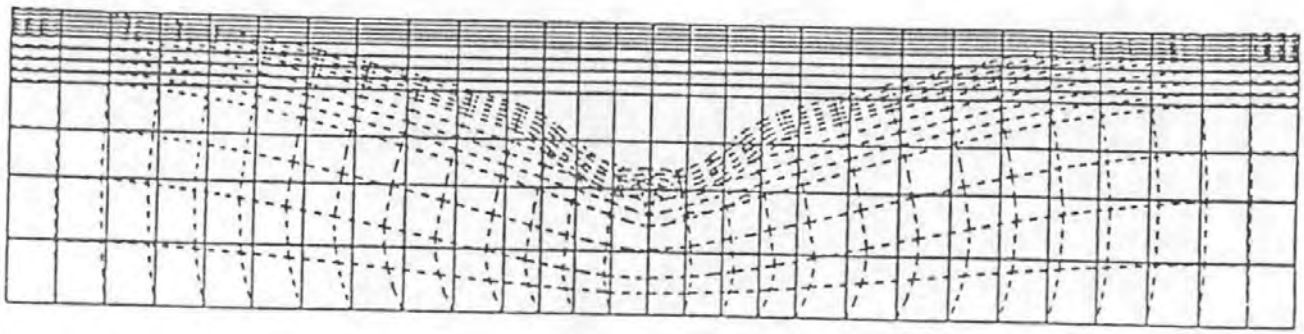

FIG.8.4 EXAMPLE OF DEFLECTED SHAPE OF CRACKED PAVEMENT SECTION (CRACK LENGTH IN SURFACING = 80mm)

technique. The model is limited to elastic analysis, and therefore unable to allow for plastic deformation within the sub layers or frictional restraints between the slab ends. It does, however, provide an indication of the range of relative movement to be adopted in a laboratory study.

8.3.2 Stress Intensity Factor Curves

The stress intensity curve for the various increments of crack development are shown diagrammatically in fig.8.5, shown also is the curve generated by thermal movement. The relative magnitude of the two curves depend on several different variables. The curve relating to tensile fatigue is dependent on the crack opening width and the stiffness of the pavement layers. The curve relating to traffic loading is dependent on axle load in addition to pavement stiffness. The shape of the curves is significant, as they are related to crack growth rate and therefore indicate that thermally induced stresses are responsible for the initial 50-80% of crack growth combining with traffic only in the later stages.

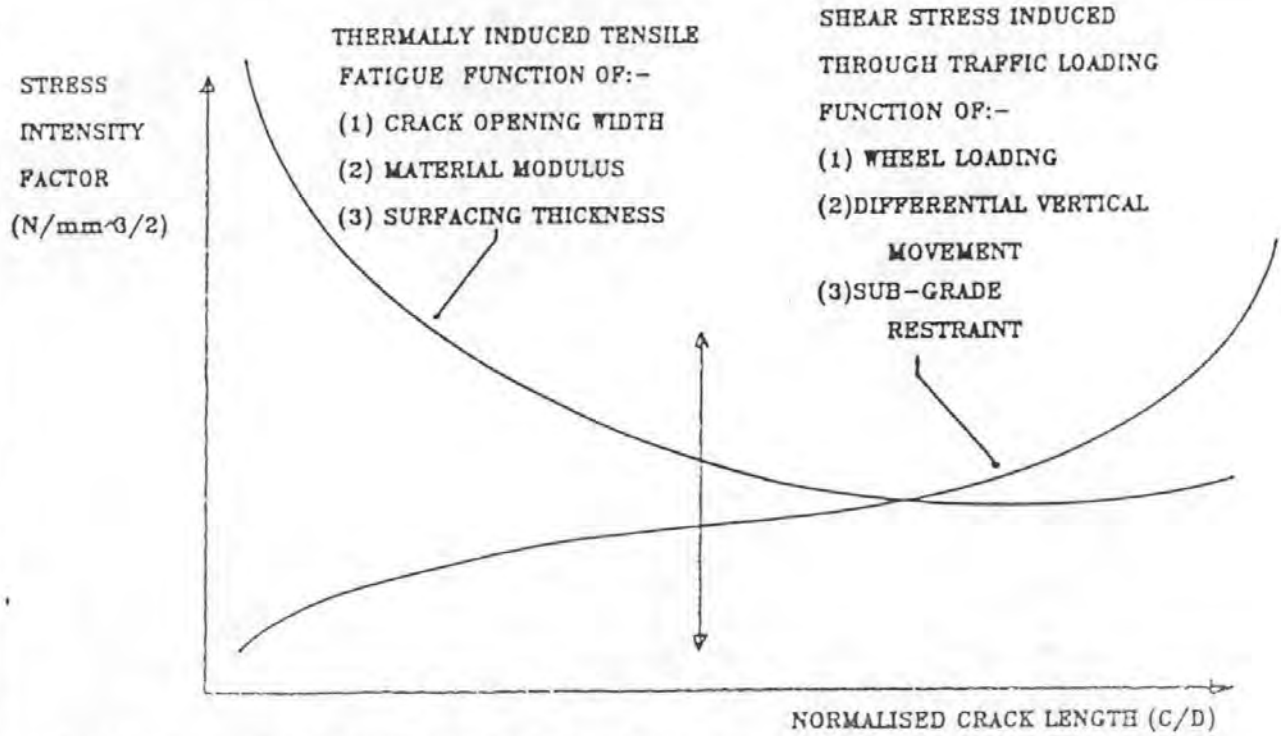

FIG.8.5 STRESS INTENSITY FACTORS FOR TENSILE FATIGUE AND SHEAR FATIGUE VERSUS NORMALISED CRACK LENGTH AS A CRACK PROPAGATES THROUGH A BITUMINOUS SURFACING (DIAGRAMMATIC ONLY)

8.3.3 Deflected Shape

The deflections at the roadbase/surfacing interface adjacent to the crack path are tabulated in figs.8.6 and 8.7 for both load cases. The crack length, generated in the 100mm of surfacing was varied between 0 and 80mm. The maximum deflection for a standard wheel load in position 2 was .83mm with a differential deflection between the loaded and unloaded slab of 0.15mm.

8.4. LABORATORY SIMULATION OF TRAFFIC LOADING CONDITIONS

8.4.1 Rig Description

A laboratory rig, shown in plate 8, was designed with the primary aim of investigating the influence of traffic loading on overall crack development within the surfacing.

The cracked roadbase section was simulated by two 6mm thick spring steel plates cantilevered from fixed end supports and butted together at their free ends, fig.8.8. A 400 x 100 x 100mm asphaltic surfacing beam was adhered to the plates with a high strength epoxy resin.

Sinusoidal loading was applied vertically through a 100kN hydraulic actuator to the sample via a semi-circular rubber platen. The diameter of the platten was based on the mean diameter of a car wheel. The platen acts directly onto the upper surface of the beam offset 100mm to one side of the crack, simulating a wheel approaching the end of the slab;(position 2), fig.8.3. The complete working area is enclosed by a thermal control cabinet which provided a constant temperature range 20-60°C.

8.4.2 Instrumentation

The deflection on the underside of each steel platen was recorded by vertical displacement gauges. These gauges, fig.8.9, were specifically developed to fit between the platens and machine table. They consist of 'L' shaped brackets supporting a cantilevered section on which four 120 ohm strain gauges were adhered. The voltage change within the energised bridge system is recorded as the cantilever deflects and is calibrated to give equivalent vertical displacement. The calibration showed the gauges to be accurate to 0.05mm.

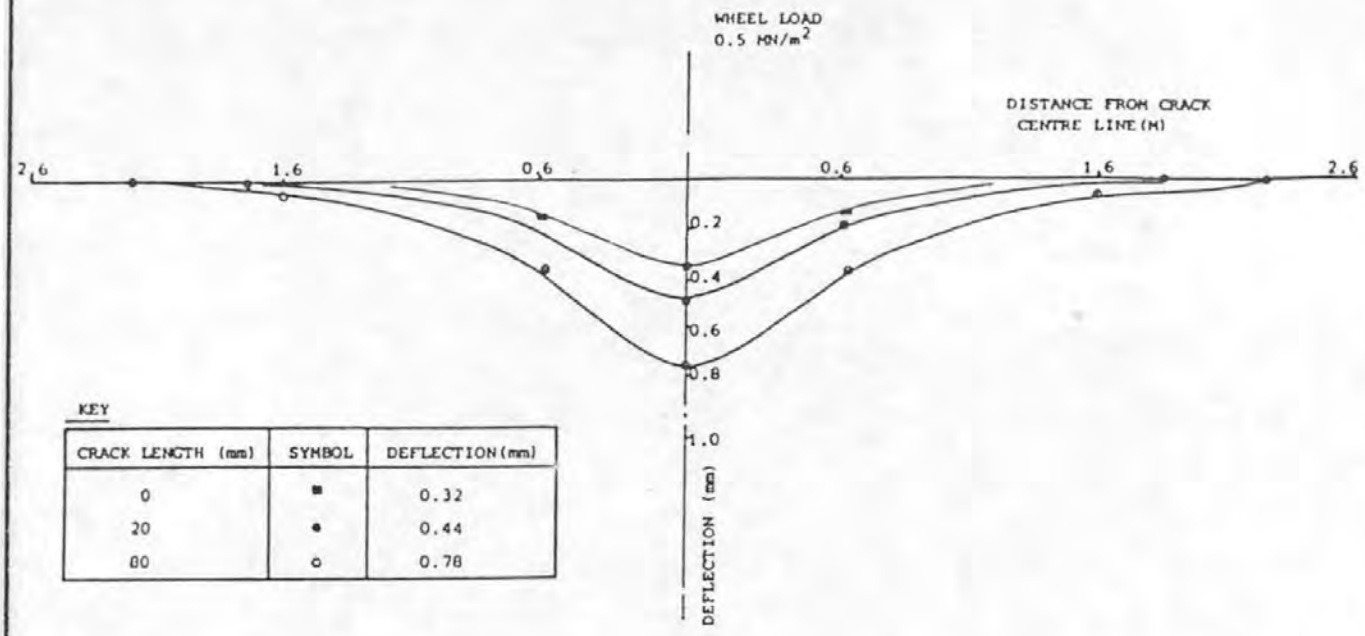

KEY

CRACK LENGTH (mm)	SYMBOL	DEFLECTION (mm)
0	■	0.32
20	●	0.44
80	○	0.78

FIG.8.6 DEFLECTION OF ROADBASE/SURFACING INTERFACE AT CRACK CENTRE LINE DUE TO LOAD CASE 1 FROM FINITE ELEMENT MODEL FE3 OUTPUT

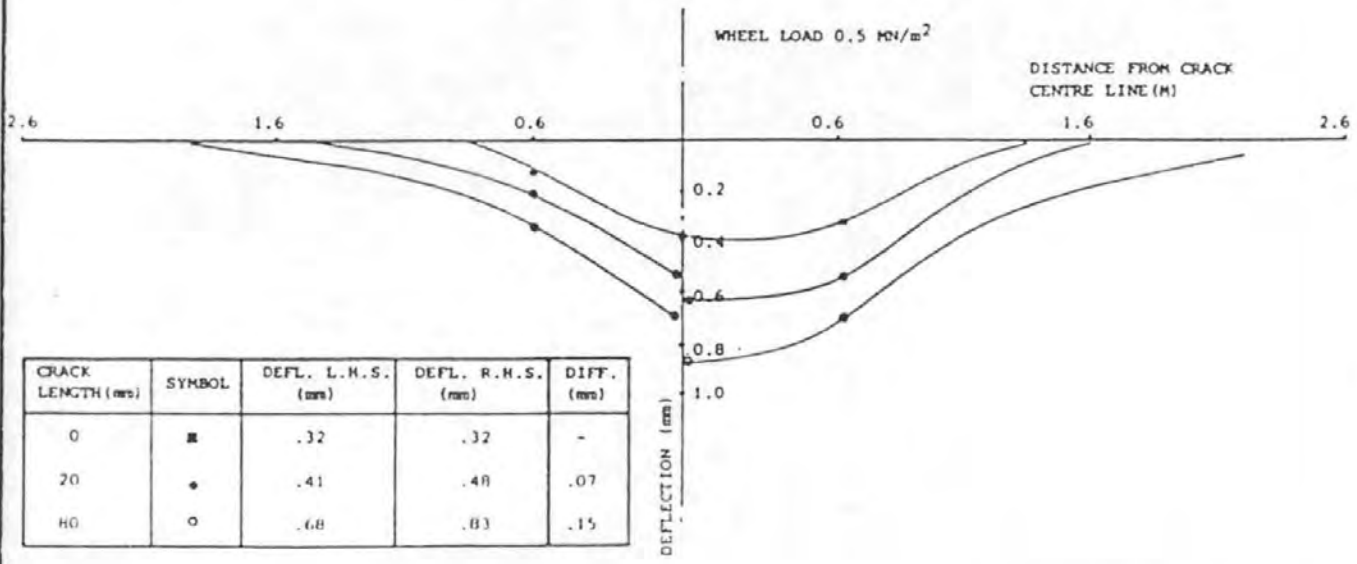

CRACK LENGTH (mm)	SYMBOL	DEFL. L.H.S. (mm)	DEFL. R.H.S. (mm)	DIFF. (mm)
0	■	.32	.32	-
20	●	.41	.48	.07
80	○	.68	.83	.15

FIG.8.7DIFFERENTIAL DEFLECTIONS OF ROADBASE/SURFACING INTERFACE AT CRACK CENTRE LINE DUE TO LOAD CASE 2 FROM FINITE ELEMENT MODEL FE3 OUTPUT

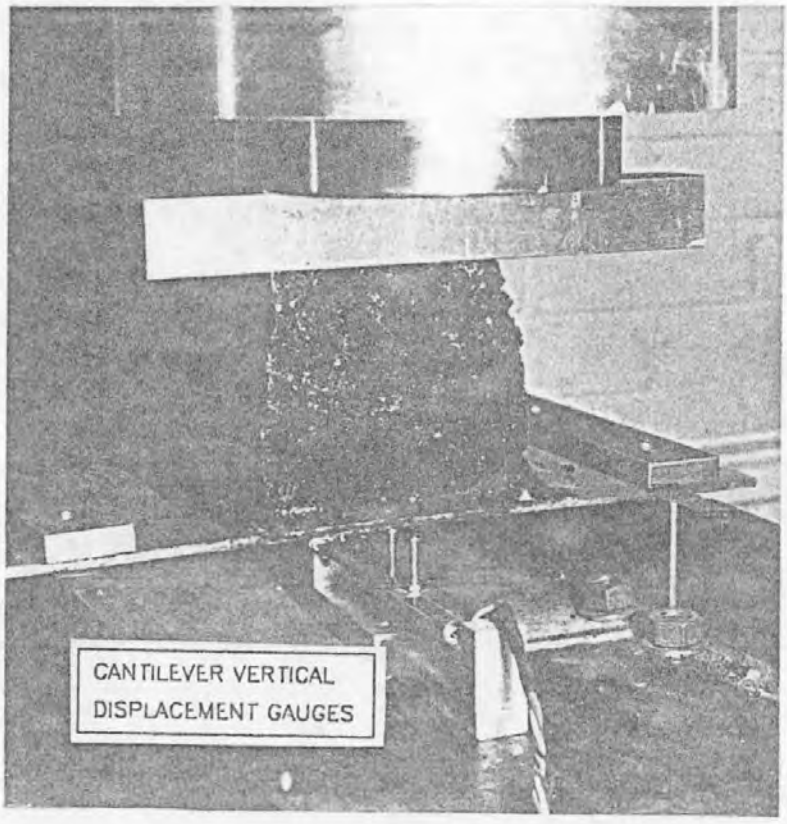

VERTICAL DISPLACEMENT GAUGES TO MONITOR DIFFERENTIAL MOVEMENT BETWEEN SIMULATED CRACKED ROADBASE SLABS

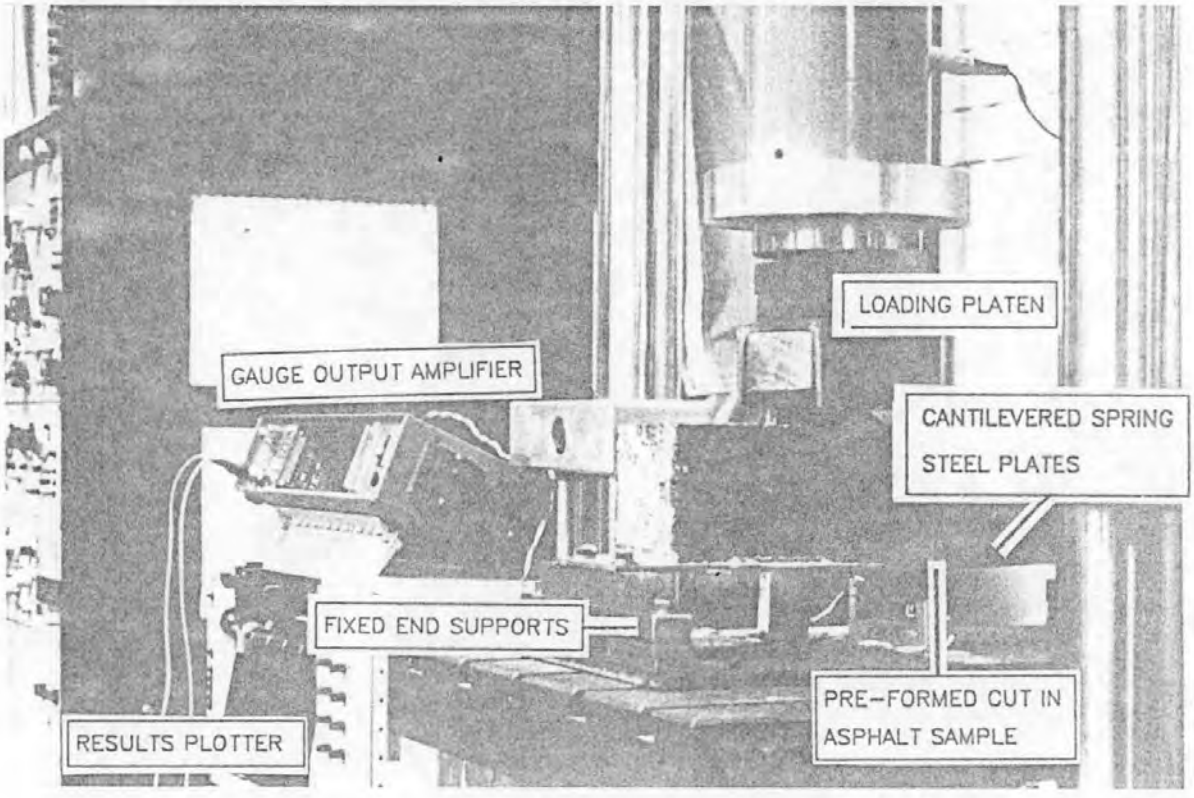

TEST LAYOUT

PLATE 8 TRAFFIC LOADING SIMULATION TEST

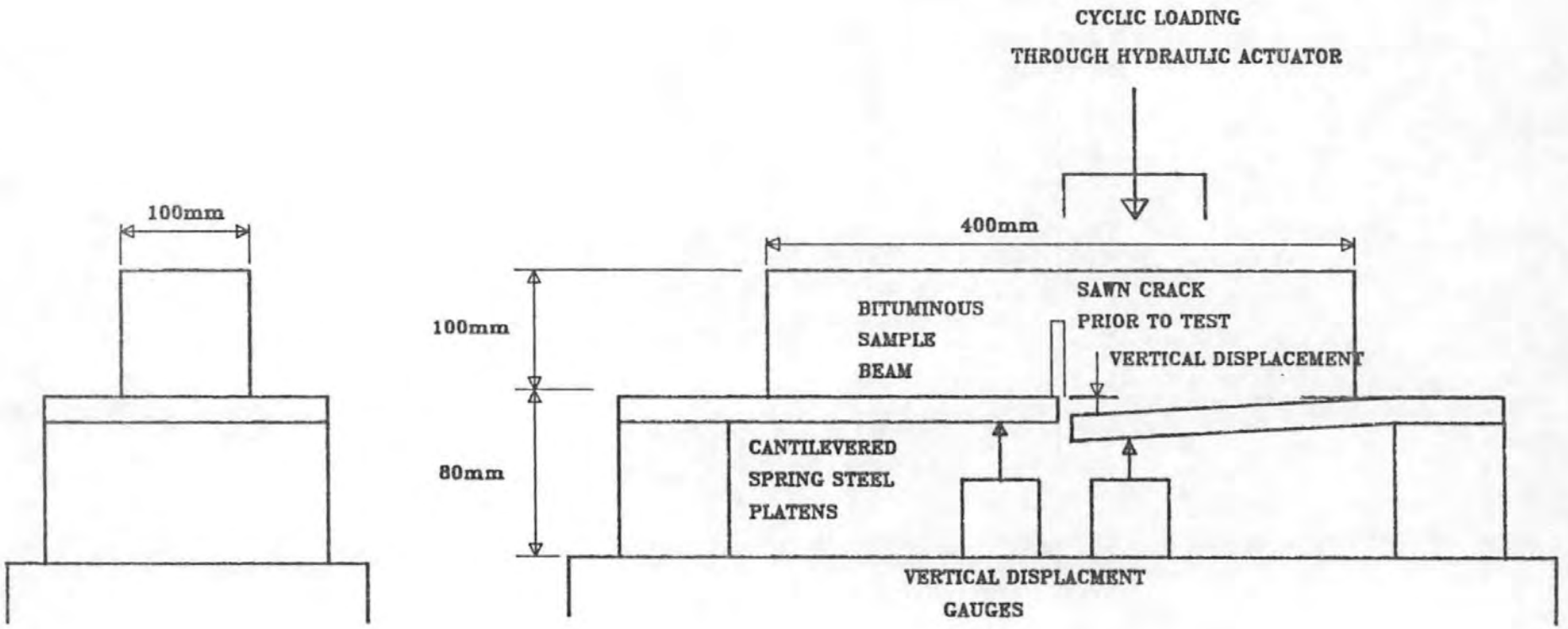

FIG.8.8 TEST RIG CONFIGURATION FOR SIMULATIVE TRAFFIC LOADING

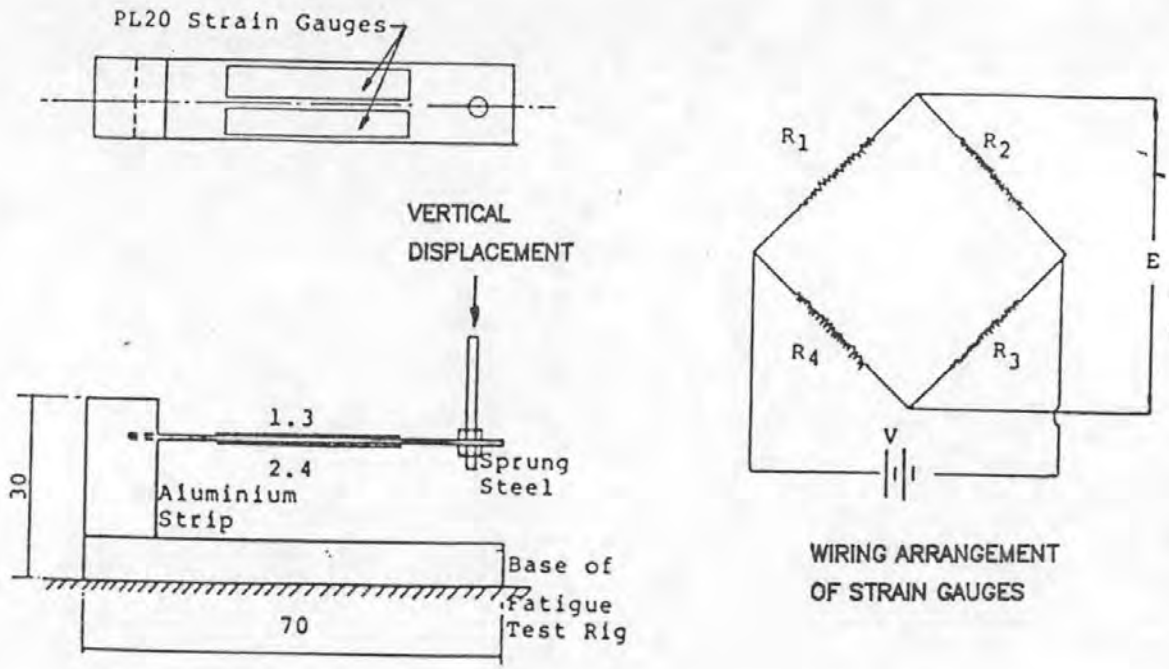

FIG.8.9 VERTICAL DISPLACEMENT MEASUREMENT GAUGES

8.4.3 Test Results

A limited number of tests were carried out on the rig solely to investigate the overall effect of trafficking on crack development. The beams tested were confined to a single mix type to ensure consistency of results. The comparison of stress intensity curves indicates that initial crack growth is induced through the thermal mechanism of tensile fatigue. This condition was therefore simulated through saw cuts of various length at the mid-point of the test beam adjacent to the butted ends of the platens.

The test arrangement was calibrated to provide a frequency consistent with the load/deflection relationship derived from the finite element results. A constant load was applied to provide an experimental increase in differential deflection with a maximum of 1mm at failure of the surfacing.

Stable crack growth was found to occur on beams incorporating a

predefined crack of at least 50mm.

Initial cracking occurred at the top of the saw cut and extended vertically to the surface. The failure conditions of full depth cracking occurred after 5 x 10^5 load applications. Limited surface cracking also formed through a combination of stress concentrations at the platen contact point with the beam and a region of the surface being subjected to tensile stresses during the loading cycle. The beams with shorter crack lengths failed through extensive surface cracking combined with unconfined deformation in the region of the loaded surface.

These observations therefore suggest that the influence of traffic loading is confined to accelerating crack growth in the final stages of propagation through the surfacing layer. Furthermore, although inducing limited surface cracking the predominant direction of crack propagation is vertically upward.

8.5 ANALYSIS OF TRANSVERSE CRACK FREQUENCY DATA

8.5.1 Introduction

Data acquired by the 'Reflective Cracking Working Group' (TRRL) [2] in their study of the performance and reflective cracking of roads with cement bound roadbases was analysed to investigate the influence of both lean concrete compressive strength and cumulative traffic flow on the frequency of transverse cracking.

8.5.2 Crack Spacing

The data derived from various sites (table 8.1) was standardised through the establishment of pre-defined conditions which are detailed on the respective plots (figs.8.10 and 8.11). The analysis included pavements with a common completion date without recent major maintenance and constructed with lean concrete roadbase material.

The plot of lean concrete compressive strength versus crack spacing shows the frequency of observed crack spacing is not directly related to the strength of the roadbase. This conclusion was drawn from eight pavements constructed before 1975 with a combined length of 34.8km. The 28 day compressive strength of the roadbase material ranged from 5N/mm^2 to 40N/mm^2.

TABLE 8.1
SURVEY SITES AND TRAFFIC DATA (AFTER TRRL WORKING PAPER 112mm)

REFLECTIVE CRACKING WORKING GROUP (TRRL) SURVEY SCHEME REF.NO.	TRRL REF.UNIT NOs	LENGTH OF PAVEMENT RELEVANT TO CRITERIA A,B,C (km)	TRAFFIC CARRIED SINCE OPENING (MSA)	TRAFFIC CATEGORY	YEAR OF OPENING	LOCATION
5	1-62	12.4	6	L	1971	A38 Plympton by Pass
15B	147-196	9.8	19	M	1971	M4 Junctions 15-16
21	1-11	2.2	-		1965	-
28	1-12	2.4	19	M	1971	A108 Tilbury Docks
33	61-90,101-108	11/20	21	H	1971	M4 Junctions 9-10
34A	35-98	8.0	18	M	1971	M4 Junctions 10-12
34C	109-141	6.40	18	M	1971	" "
35A	1-6,66-70	2.0	17	M	1971	M4 Junctions 12-14
35B	142-183,208-225	18.0	17	M	1971	" "
35C	275-305	6.00	17	M	1971	" "
36	1-100,117-200	36.0	17	M	1971	M4 Junctions 14-15
38A	1-53	10.6	9	L	1971	M3 Junctions 4-6
38C	1-60	12.0	9	L	1971	" "
39	4-18,25-61	10.0	9	L	1971	M3 Junctions 6-7
41	1-11	2.2	-		1963	-
42C	1-66	13.2	-		1963	-
51	1-45	9.0	9	L	1971	A1 South Witham
59	1-52	10.4	-		1963	-
62	1-28	5.6	-		1963	-
63	1-12	2.4	24	M	1971	A5 Muckley Corner
64	1-60	12.2	10	L	1971	A38 Lichfield by Pass
65	1-24	4.8	8	L	1971	A38 Lichfield East by Pass
67	1-20	4.0	-		1963	-
69	1-62	12.4	35	H	1971	M6 Junctions 4-5
70	1-14,41-60,196-204	24.4	32	H	1971	M6 Junctions 2-6
70B	145-167	4.4	29	H	1971	" "

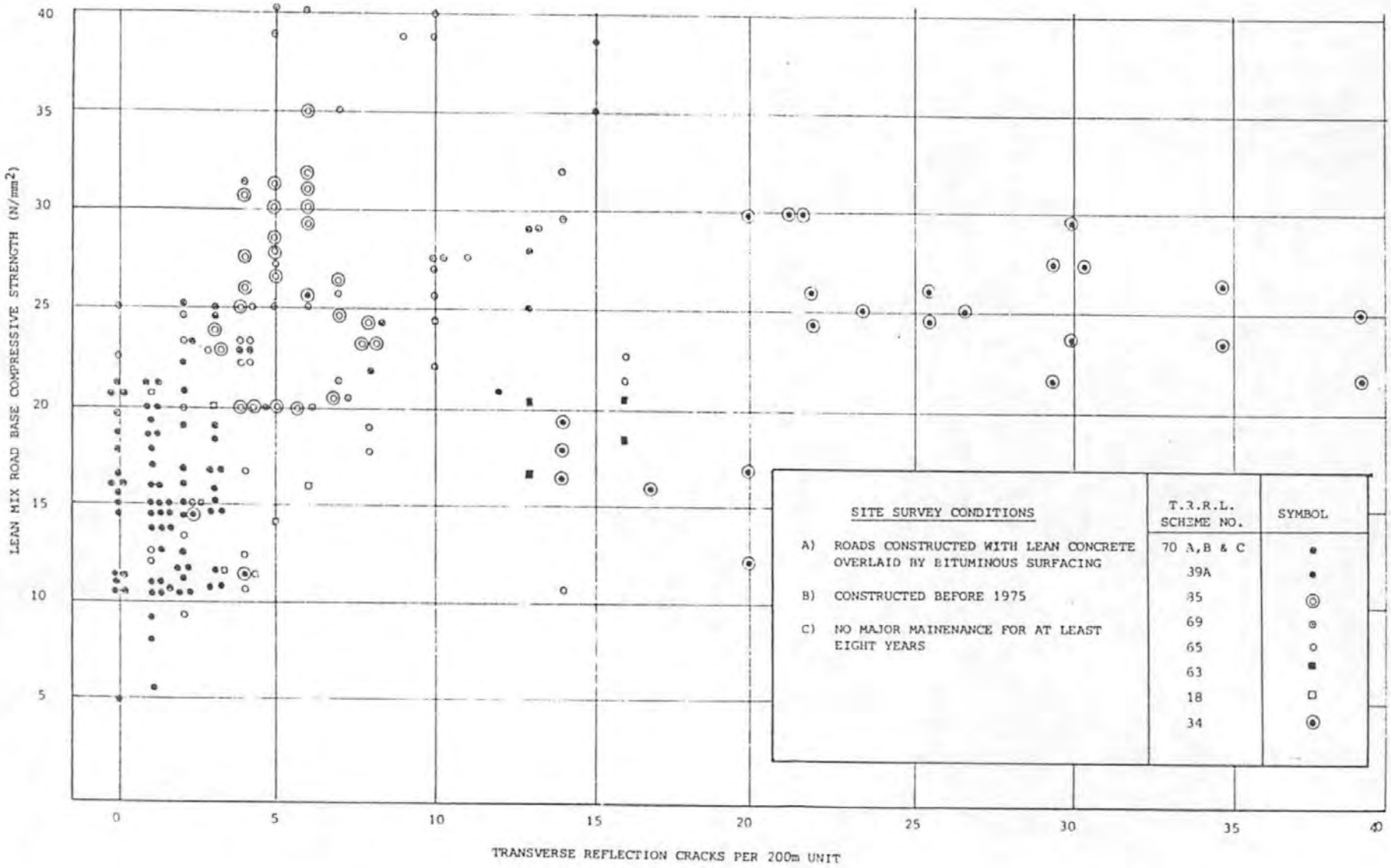

FIG. 8.10 LEAN CONCRETE ROADBASE COMPRESSIVE STRENGTH VERSUS TRANSVERSE TRANSVERSE REFLECTION CRACKS PER 200m UNIT FROM REFLECTION CRACKING WORKING GROUP (T.R.R.L) DATA FOR GIVEN SITE SURVEY CONDITIONS

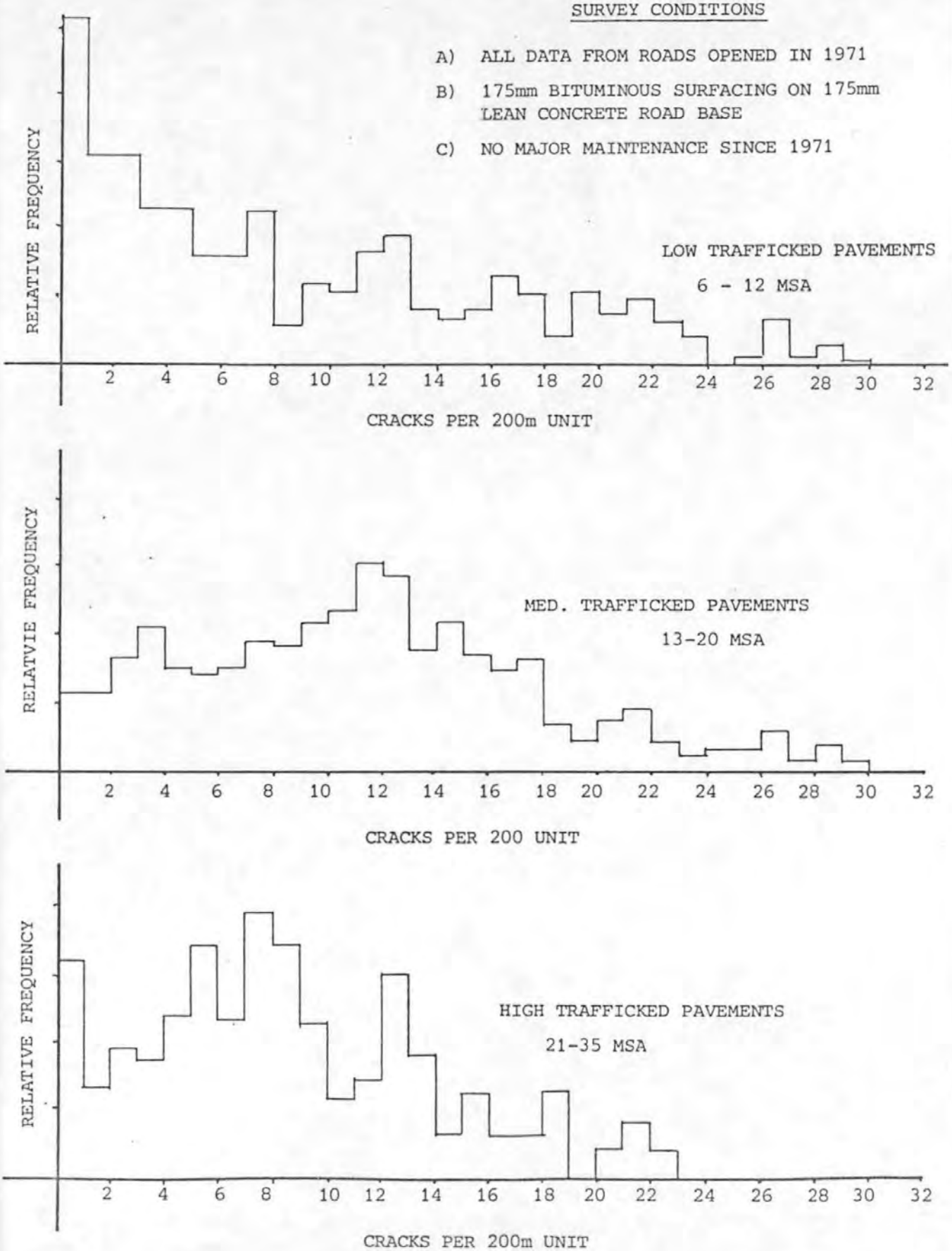

FIG8.11 RELATIVE CRACK FREQUENCY VERSUS THE NUMBER OF CRACKS PER 200M UNIT FOR GIVEN TRAFFIC LOADINGS. DATA FROM REFLECTION CRACKING WORKING GROUP (T.R.R.L.) (2)

Furthermore a definable relationship could not be established between the various levels of cumulative traffic carried by the pavements and transverse crack spacing. For all traffic levels the mean 'slab' length was within a range of 15 m to 20 m after 15 years service without major maintenance. However, for the heaviest traffic category, 21-35 m.s.a., some evidence did exist that the mean spacing was reduced to the lower end of the range.

The variation in crack spacing is therefore related more closely to conditions relevant to individual sites than roadbase strength or traffic flow, which again supports the conclusion from both the finite element modelling and limited experimental results that traffic loading, only contributes to the final phase of crack growth through the surfacing layer on an otherwise defined crack pattern.

9.0 GEOGRIDS AS CRACK INHIBITORS

9.1 Introduction

The influence of surfacing mix properties on the rate of crack growth and the benefit derived from an improvement in mix design has been considered in the previous sections. Two further methods to inhibit reflection cracking have also been considered as part of this investigation;

i) the use of geogrids discussed in this section, and
ii) the use of modified binders discussed in section 10.

The inclusion of geogrids within the bituminous layer increasesthe tensile strength of the pavement surfacing. Theoretically, its optimum position within the pavement is at the level of maximum tensile stress. This is produced, under conditions in which the tensile fatigue mechanism is dominant at the surfacing/road base interface.

The inclusion of a geogrid within the surfacing layer may inhibit reflection cracking in either of two ways. Firstly by acting as a stress relieving layer, in which it reduces the bond between the surfacing and roadbase. The tensile stresses included within the surfacing by movements within the roadbase are therefore reduced. Secondly, as a reinforcing medium dissipating the induced tensile stresses within the matrix of the geogrid. In this case the yield strain of the material must not be exceeded. Additional advantages provided by the use of a geogrid layer include an improved shearing resistance of the pavement by increasing its lateral restraint and providing coherence of the pavement structure if cracking occurs.

The engineering properties of two types of stretched polypropylene fabrics have been evaluated and a comparison drawn between them.

Both materials were manufactured from polypropalyne polymer. Material 1 was specifically designed for asphalt pavement reinforcement with a bi-axial open mesh structure. Material 2 consisted of more closely spaced, thicker strands, and were stretched unidirectionally during manufacture. Dimensional details of both grids are given in fig.9.1.

ALL DIMENSIONS IN mm

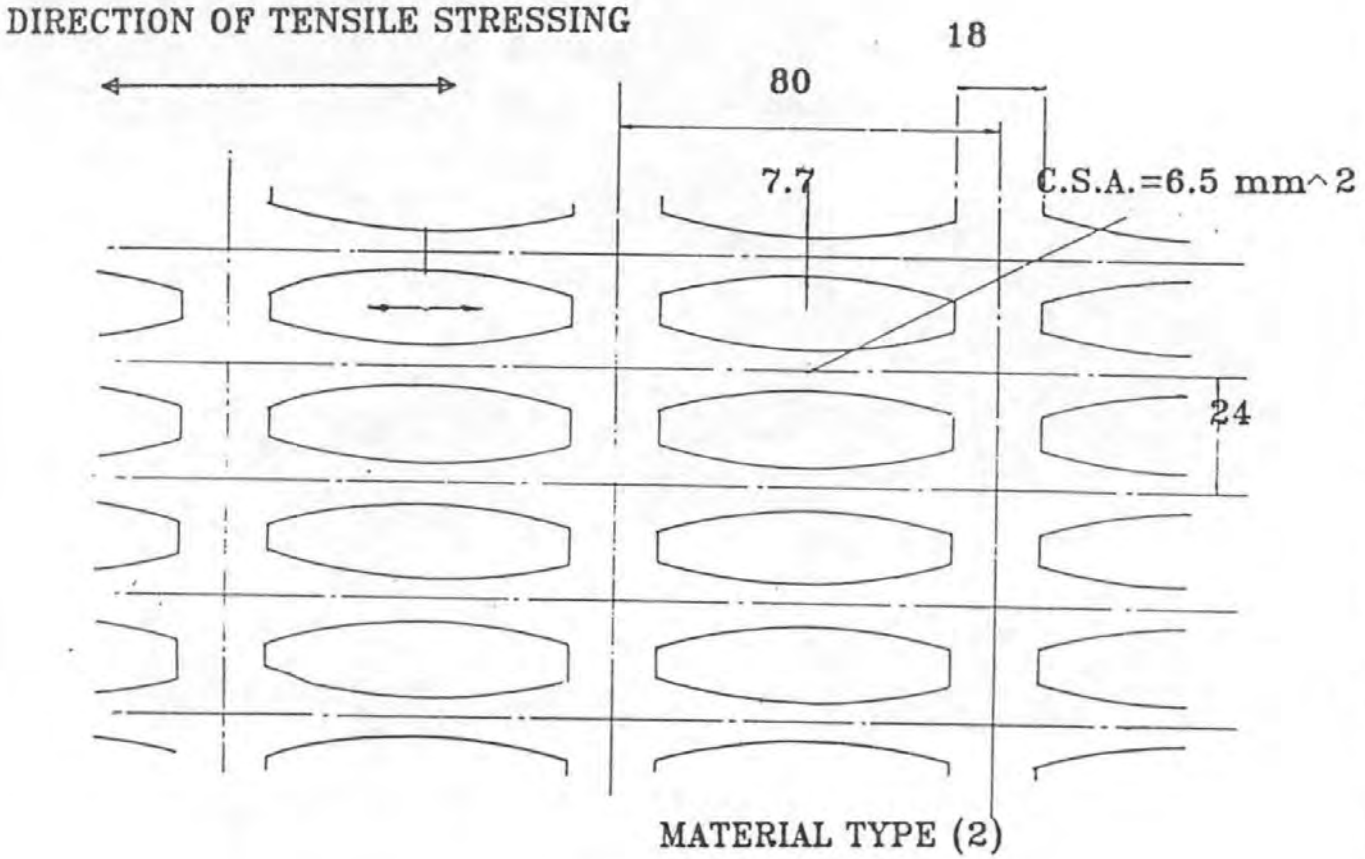

MATERIAL TYPE (2)

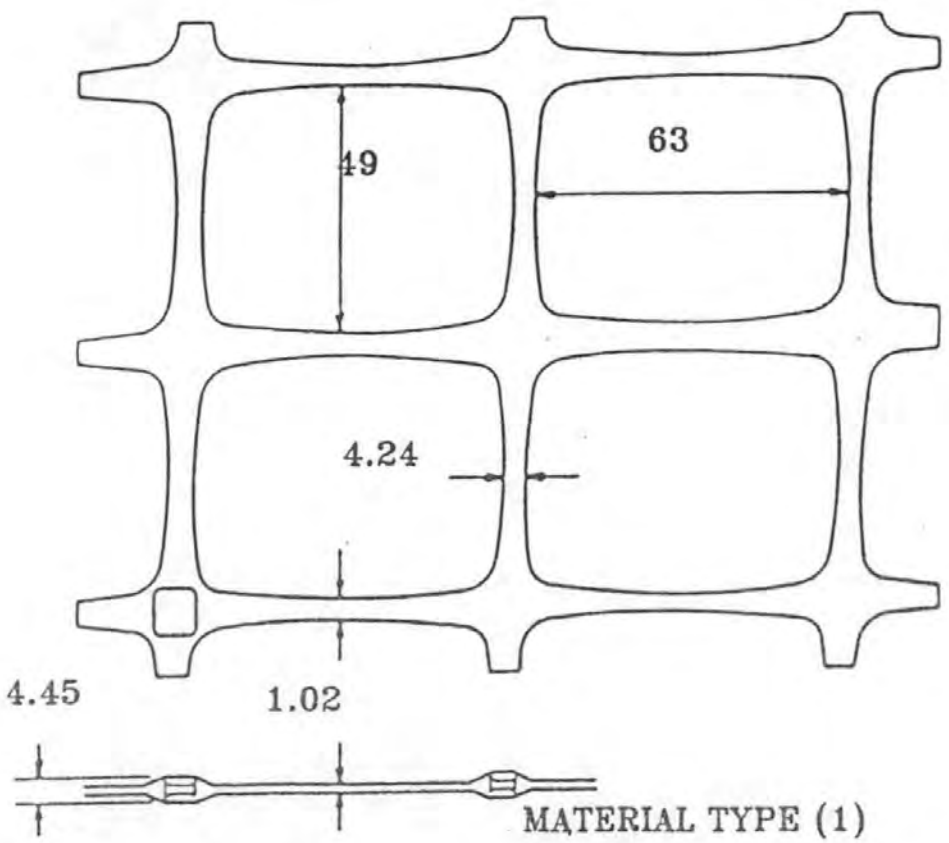

MATERIAL TYPE (1)

FIG.9.1 DIMENSIONAL LAYOUT OF GEOGRIDS

9.2 Engineering Properties of the Geogrids

The characteristics of composite materials may be appraised by isolating the mechanical properties of the components. Therefore, testing was carried out on both types of geogrid to quantify their load-extension and strength properties.

The properties of direct tensile yield and cyclic tensile yield were determined from individual strands cut from the grid mats. A standardised test temperature of 25°C was maintained to an accuracy of ±1°C.

The direct tensile properties of the grid were determined by locating the upper and lower horizontal ribs of material within a clamping device prior to tensioning through a 100 kN actuator. A resultant time/extension relationship was established for a series of extension rates, varied from 1mm/sec to 0.001mm/sec.

From these results the maximum stress prior to yield, the strain at failure and initial Young's modulus were calculated.

The stress was defined as the load on a single strand over the cross sectional area at the mid point of the strand. The results, figs.9.2 and 9.3 show material 1 to have a yield strain at failure of 10-12% independent of loading rate while material 2 exhibited plastic characteristics with strains of over 100% at low loading rates (less that 0.001 mm/sec), comparable to the rate of thermally induced displacement within the pavement structure.

Strands of both materials after failure are shown in plate 9.

Visual inspection showed material 1 to exhibit fibrous characteristics at failure while material 2 showed a typical plastic failure characterized by 'necking' at the ultimate failure point.

A similar clamping method was utilised for the cyclic testing but the strain level varied from 5% to 50% and the number of sinusoidal cycles at failure recorded. It was necessary to increase the mean strain level as the strain amplitude was increased to ensure

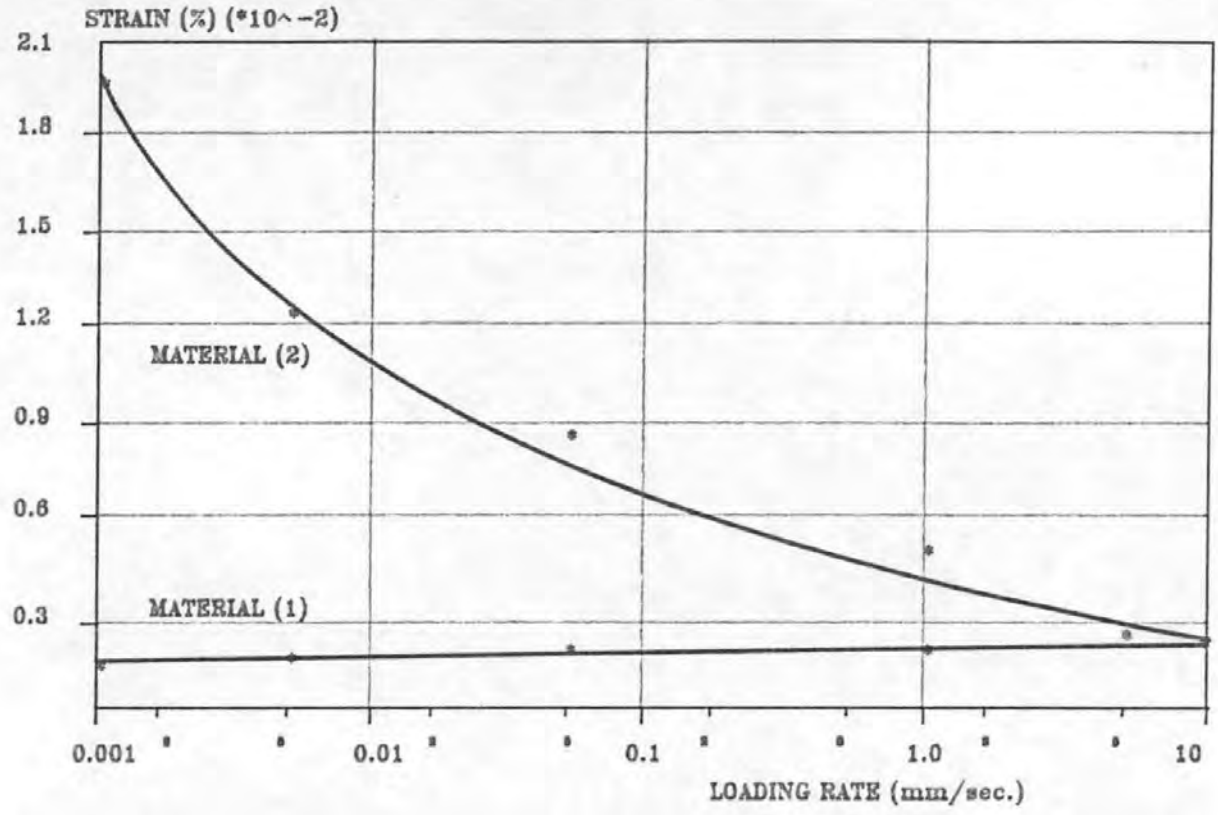

FIG.9.2 GEOGRID STRAIN AT FAILURE VERSUS LOADING RATE IN DIRECT TENSION AT 25 DEG.C. FOR MATERIALS (1) AND (2)

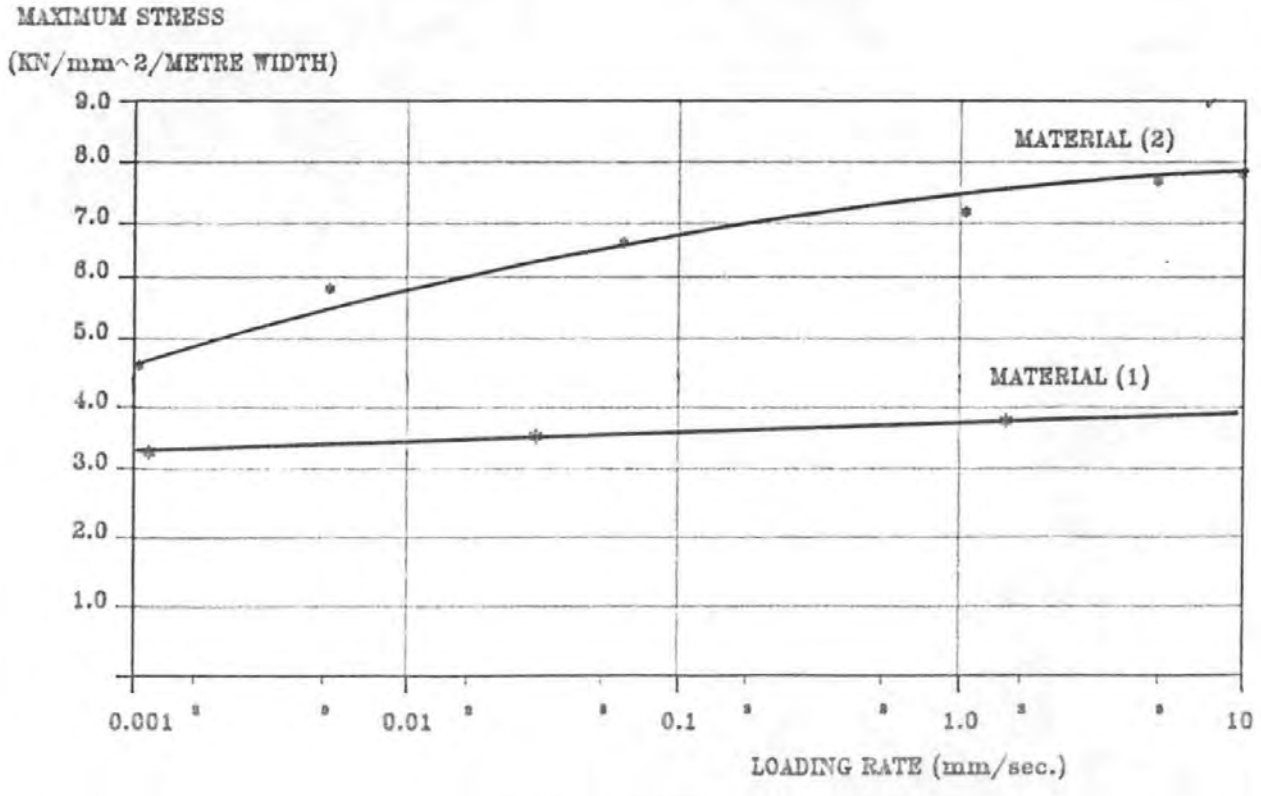

FIG.9.3 GEOGRID MAXIMUM STRESS VERSUS LOADING RATE IN DIRECT TENSION AT 25 DEG.C. FOR MATERIALS (1) AND (2)

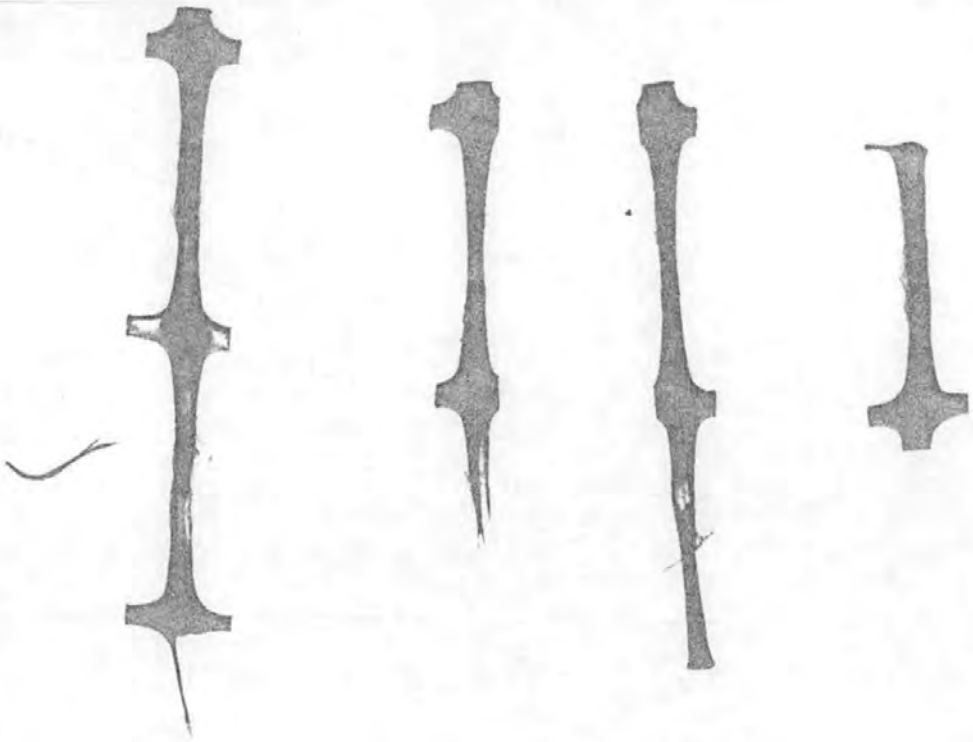

FAILURE CONDITION OF TYPE 1 GRID; FIBROUS END STRANDS

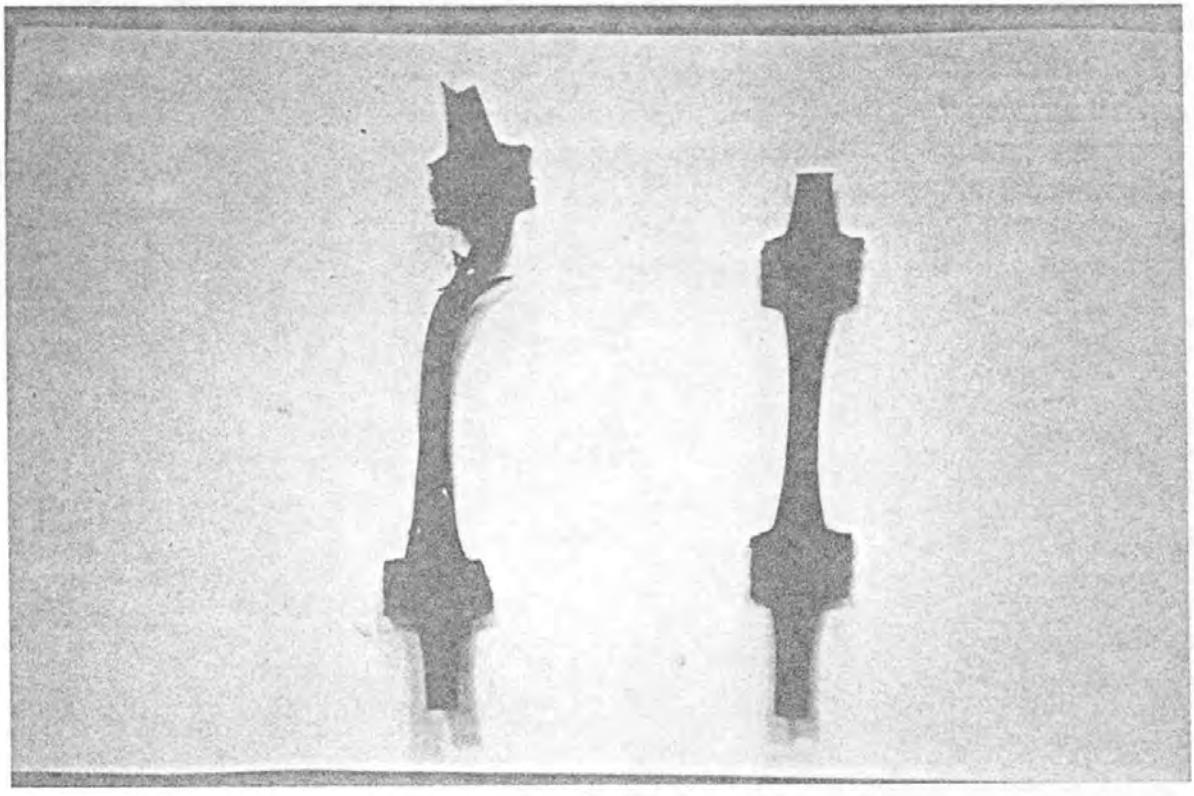

FAILURE CONDITION OF TYPE 2 GRID; EXTENSIVE ELONGATION AND NECKING

PLATE 9 TENSILE TESTING OF GEOGRIDS

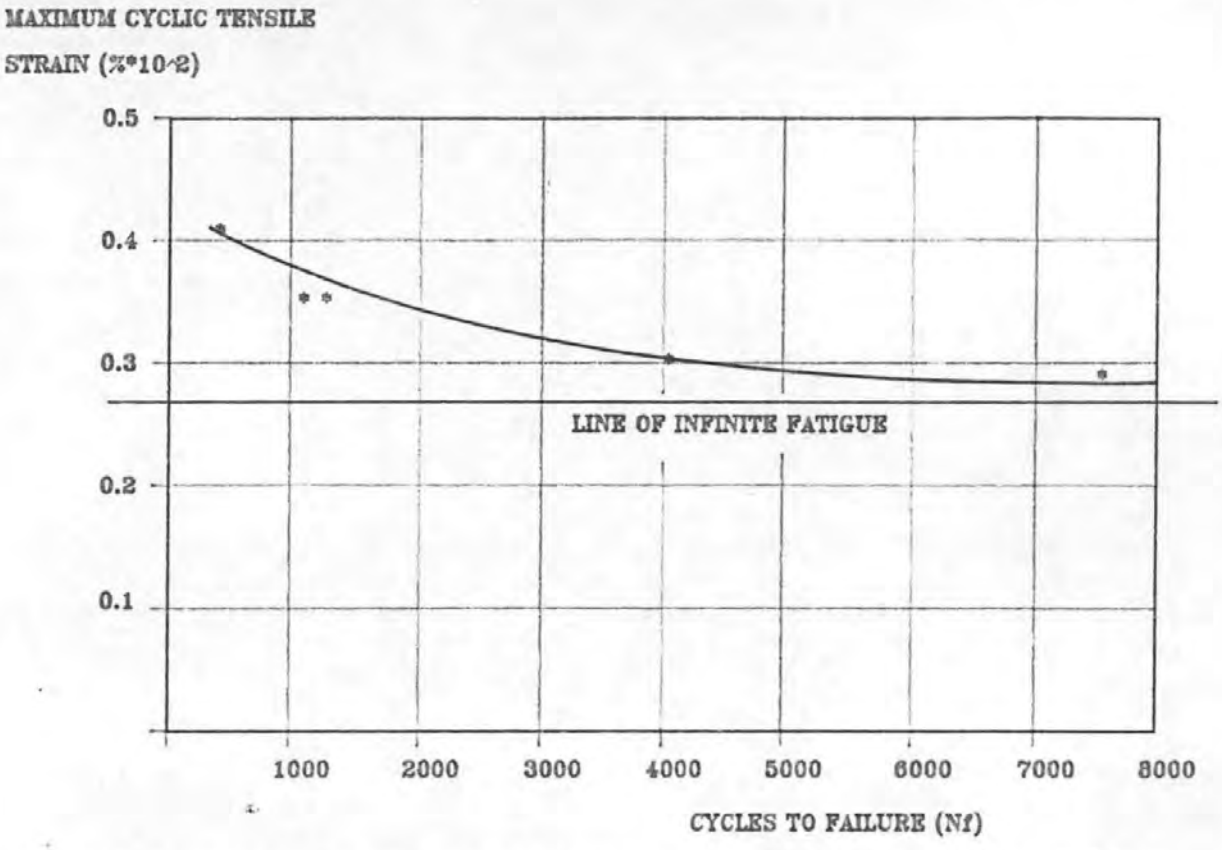

FIG.9.4 CYCLIC TENSILE TESTING OF GEOGRIDS AT 25 DEG.C

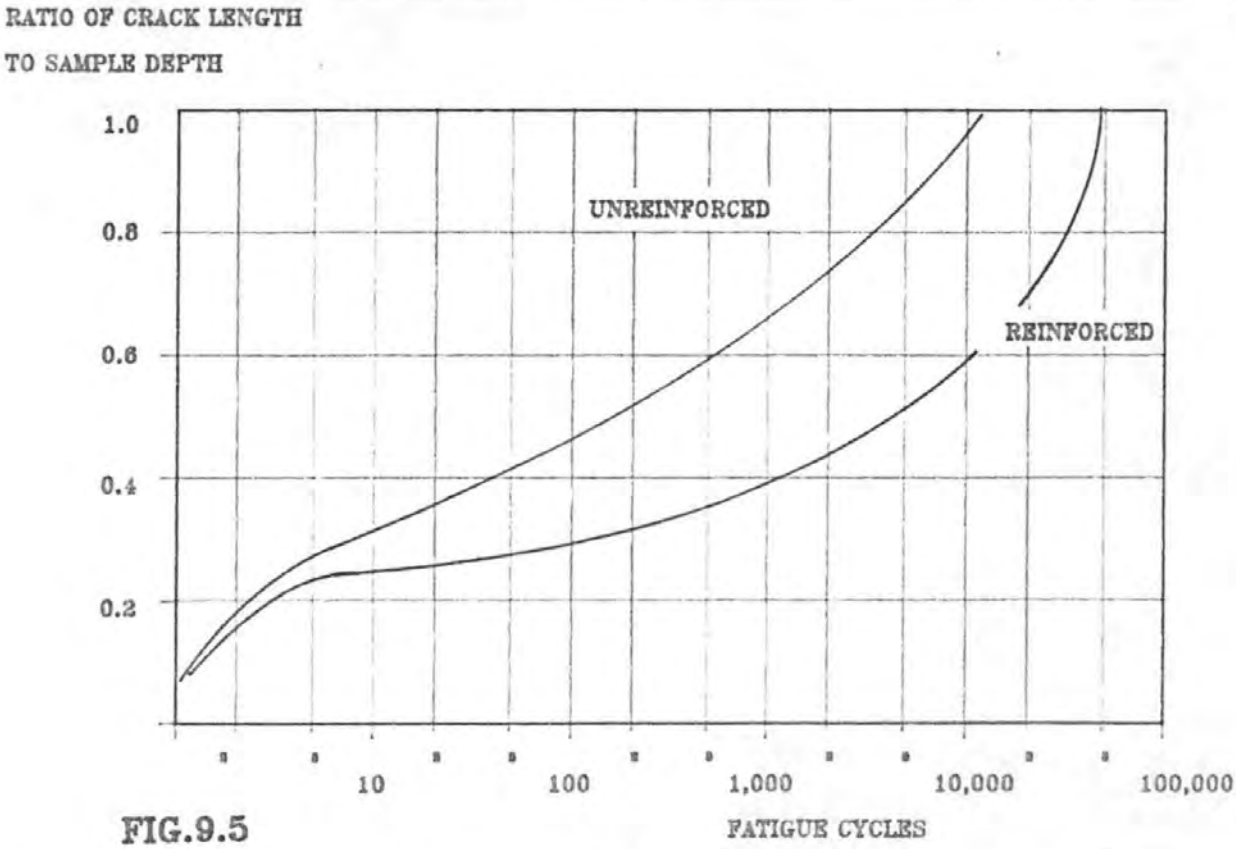

FIG.9.5

CRACK LENGTH VERSUS FATIGUE CYCLES FOR REINFORCED AND UNREINFORCED D.B.M SAMPLES

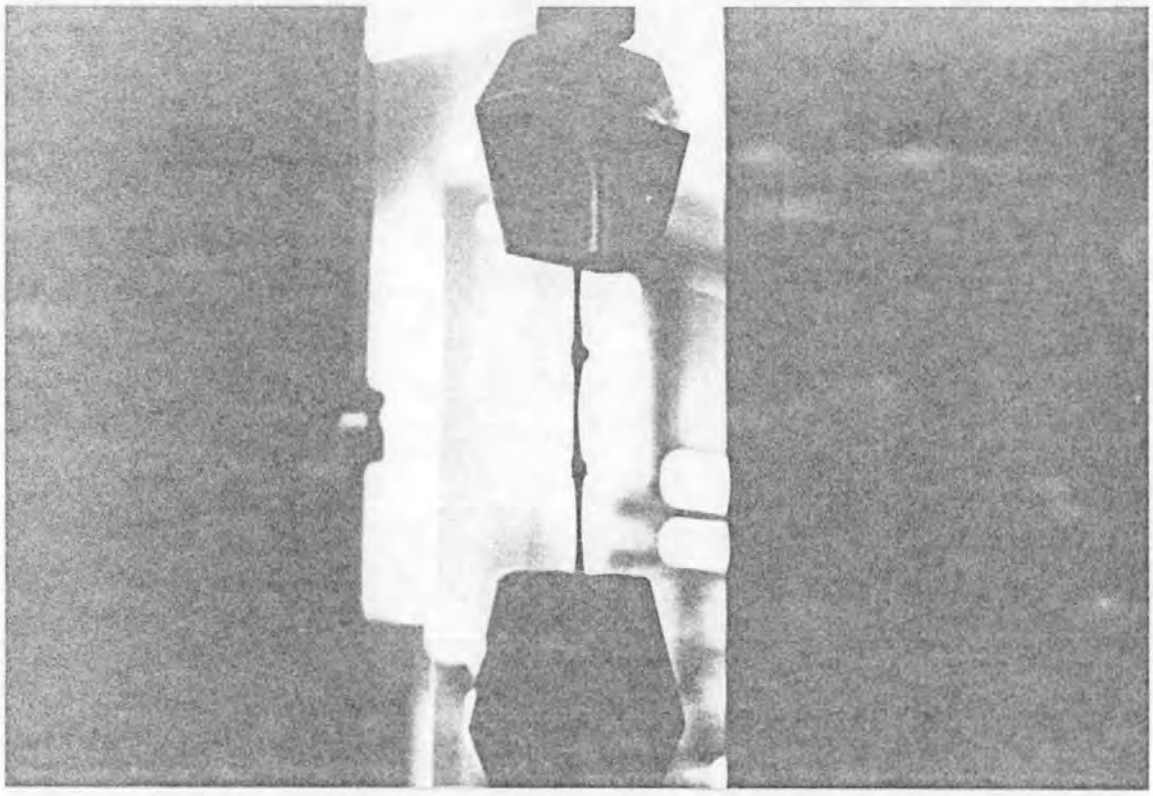

TENSILE TESTING CONFIGURATION

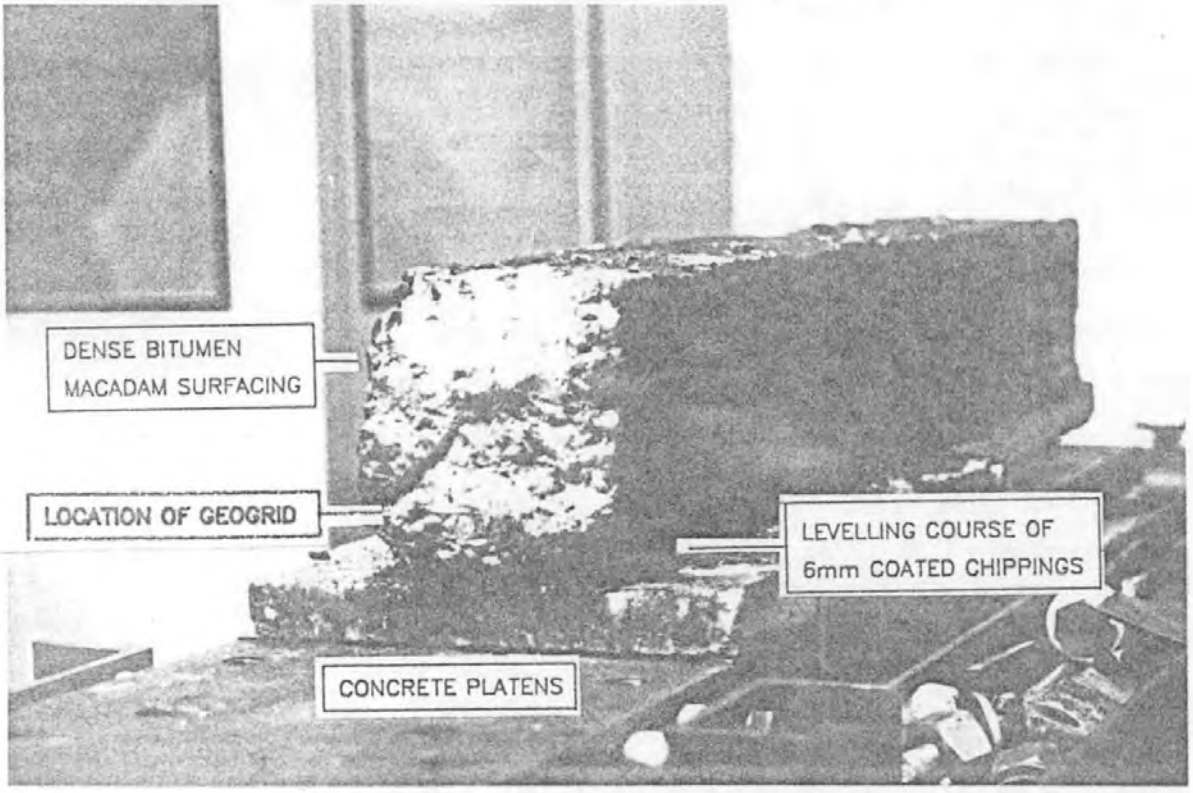

INCLUSION OF GEOGRID AT ONE THIRD DEPTH IN A TEST BEAM OF DENSE BITUMEN MACADAM

PLATE 10 GEOGRID AS A STRESS RELIEVER

material which in turn was bonded to steel platens with no levelling course of chippings.

The length of all test beams was kept constant at 1800mm although in the final series of tests the grid was laid in a range of widths over the anticipated crack path. These tests simulated maintenance projects which incorporated strips of interlayer laid over cracks in the wearing course prior to overlaying. Observations from these projects however, indicated that subsequent crack propagation to the surface was simply offset from the original crack path around the interlayer.

9.4 Test Results

9.4.1 Test Configuration a)

Vertical crack propagation was prevented by a horizontal shear plane developed in the levelling course of chippings extending the length of the test beam. The shear plane rather than interlayer, prevented the cyclic displacements of the platens transmitting as tensile strains into the surfacing layer.

9.4.2 Test Configuration b)

Bonding to steel platens created a stress relieving plane at the chippings/ geogrid interface due to a breakdown in bond between the composite materials. After several thousand strain cycles, the bond failure extended horizontally along the length of the beam with no vertical crack growth.

9.4.3 Test Configuration c)

Sample beams incorporating the type 1 interlayer showed no improvement in fatigue life over a control beam of similar surfacing material without the interlayer. However, a four fold increase in fatigue life was shown by the type 2 interlayer. The crack length versus crack opening cycles is shown in fig.9.5, together with the resultant plot from the control beam.

The benefit associated with type 2 interlayer was due to the increased plan surface area of the strands and superior stress/strain characteristics which created a stress relieving plane within the surfacing layer.

The samples incorporating short widths of type 2 interlayer exhibited reduced fatigue lives compared with the unreinforced control beams up to a grid width upon surfacing depth ratio of approximately 12. These short lengths of grid exhibited rapid shear failure and eventual debonding along the interface with stress concentrations developed at the outer ends of the interlayer. Rapid crack propagation to the uppermost surface resulted at these points. The interlayer acted as an inducer rather than retarder.

However, an improved performance was exhibited by sample beams incorporating long lengths of interlayer. These longer lengths allowed a bond to be developed along the grid/surfacing interface beyond a limited, horizontal debonded zone immediately adjacent to the crack.

10.0 POLYMER MODIFIED BINDERS AS CRACK INHIBITORS

10.1 Introduction

The binders associated with conventional mixes have showed considerable shortcomings, not only in the susceptibility to reflection cracking, but also in various other forms of pavement deterioration.

Polymer modified bitumens are being introduced which improve the characteristic rheological and mechanical properties of the mix. These binders are manufactured by combining conventional bitumen with polymer chains treated with suitable chemical compounds (additives) to improve their properties. These include increasing their resistance to ultra-violet radiation, improving their tensile strength and aggregate adhesion properties and providing a binder less prone to softening under ambient temperatures.

The resulting bitumen elastomer blend is unaffected by the high mixing temperatures but is more elastic in behaviour than conventional bitumen under service conditions. The improvement in stiffness characteristics is illustrated in Fig.10.1 which gives a comparison between the results of creep tests conducted on samples incorporating a modified binder and a conventional binder of similar penetration grade.

According to the manufacturers the benefits provided by these modified binders include;

i) resistance to abrasive, salt and organic contamination,
ii) excellent viscoelastic behaviour at high as well as low temperatures,
iii) increased frictional restraint between tyres and road surface,
iv) improved resistance to cracking, corrugation and rutting,
v) reduced compressive strain between the wearing course and basecourse and
vi) increased impermeability to water.

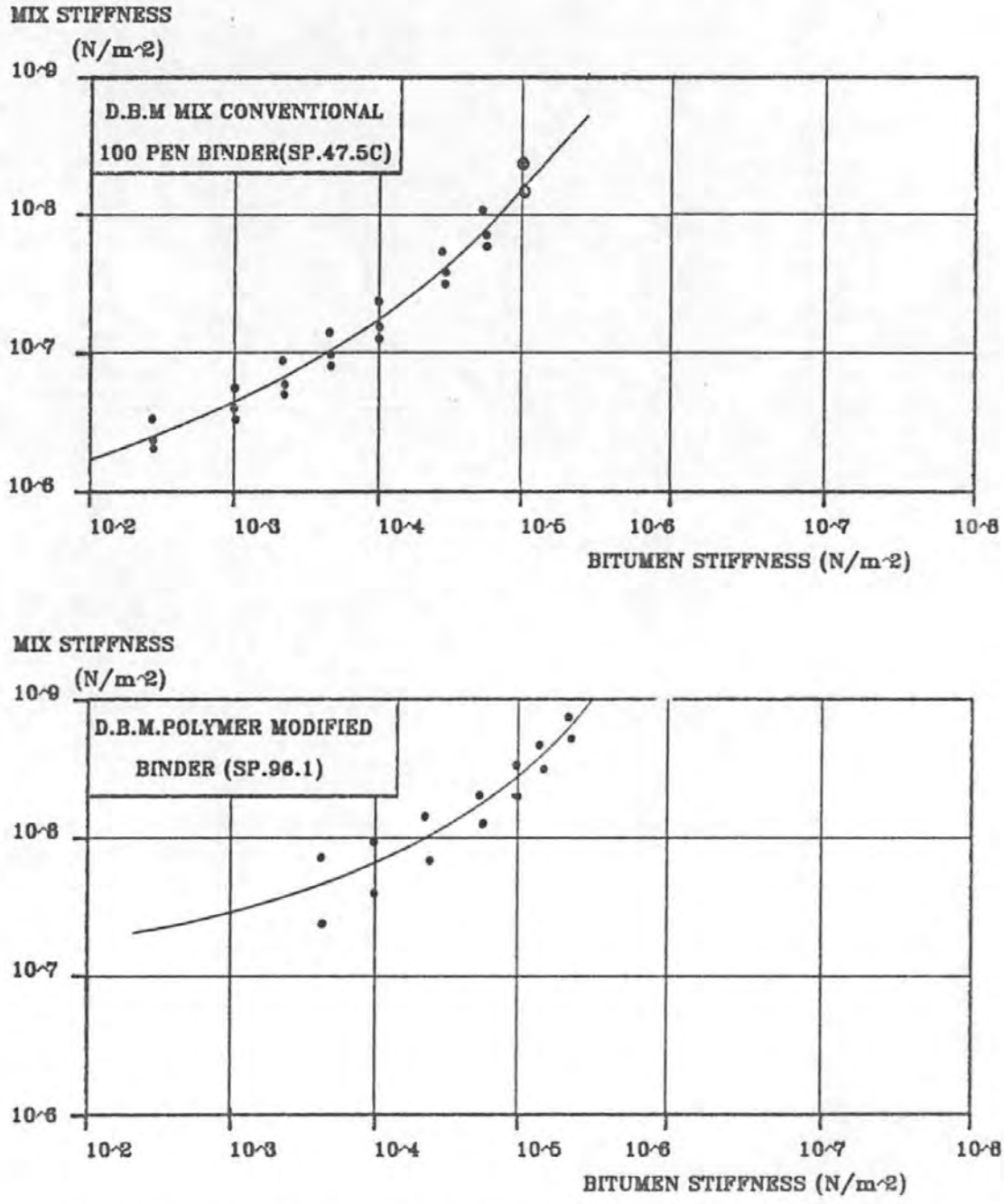

FIG.10.1 RESULTS OF TENSILE CREEP TESTS ON A D.B.M MIX INCORPORATING BOTH A CONVENTIONAL BITUMEN BINDER AND A POLYMER MODIFIED BINDER

10.2 Details of Modified Polymer Binder

To investigate the potential of these materials to inhibit reflection cracking, the test programme was limited to a single material, SBS 'Capiphalte OA' manufactured by Colas Ltd.

The results of standard tests carried out to establish its rheological properties showed a high softening point value of 94°C in relation to the penetration value of 115.

The modified bitumen was incorporated into a DBM mix with a nominal aggregate grading of 20mm, bitumen content of 4.2% and void content of 3%. Control beams containing conventional bitumen were of similar compaction level, bitumen content and grading and incorporated a binder of similar penetration. The depth of both test beams was 100mm.

10.3 Test Results

10.3.1 Tensile Fatigue Tests

Initially, the standard cyclic crack opening amplitude of 1.4mm, adopted for the testing of conventional mixes, was used to test this material. A crack propagated to a length of 20mm within the first few test cycles and thereafter remained constant for a further 20,000 cycles. Under similar test conditions the resultant fatigue life of the control beam was 12,000 cycles.

The modified binder therefore produced a significant increase in the crack opening fatigue life, but the exact increase was not defined. The results of further tests carried out to ascertain the amplitude of crack opening width required to induce failure (reflection cracking through the full depth of beam), showed final propagation to occur at a width of 2.2mm.

The data given in table 6.2, based on mean U.K. environmental conditions, shows that crack opening widths of 2.2mm or greater would be produced in roadbase slab lengths in excess of 30m. Statistical evidence provided in previous publications [38] shows that slabs of this length or greater occur in fewer than 5% of the trunk roads surveyed. Therefore, on pavements with lesser slab lengths the DBM

incorporating the modified binder would resist reflection cracking under the mechanism of tensile fatigue.

10.3.2 Tensile Creep Tests

The plot of Mix Stiffness versus Bitumen Stiffness for both the modified and conventional mixes from the creep test data is given in Fig.10.1.

The ultimate yield strain was 2.1%. This value is significantly higher than the estimated 1.0% strain displayed by wearing course surfacings at the onset of surface initiated reflection cracking through the mechanisms of tensile yield. Surfacing materials with higher yield strains are not susceptible to reflection cracking through this mechanism.

11.0 ENGINEERING SIGNIFICANCE OF RESULTS

11.1 GENERAL

11.1.1 Introduction

Previous sections of this thesis have described, in detail, the development of a predictive model of reflection cracking together with the associated laboratory and field testing and mathematical analyses. The purpose of this section is to put the results of the investigation into the context of highway engineering practice.

11.1.2 Crack Mechanisms

Three crack mechanisms have been identified which may act independently or in combination to produce reflection cracking. The mechanisms are;

a. tensile fatigue of the bituminous layer which results from daily thermally induced movements within the roadbase. Stresses within the surfacing are concentrated above roadbase cracks producing crack growth vertically upwards through the surfacing. The magnitude of these stresses is dependent upon the crack opening width between adjoining roadbase slabs, and is therefore, a function of slab length, daily temperature range and coefficient of thermal expansion of the roadbase material. The rate of crack propagation is influenced by surfacing material properties and thickness. This mode of cracking is normally confined to pavements with long slab lengths and thin surfacings.

b. tensile yield of the bituminous materials which is caused by a combination of thermal contraction and slab warping of the roadbase and surfacing, together with long term shrinkage of the bituminous surfaces. The tensile surface strains exceed the yield strain of the wearing course materials and cracking propagates downwards from the surface. Crack propagation due to thermal contraction and slab warping is a function of both the magnitude and duration of winter low temperatures and the ultimate yield strain of the surfacing layers. Evidence has been published[21] which indicates that bitumens prone to oxidization are also prone to long term shrinkage. Therefore the occurrence of cracks due to this condition is dependent upon climate, the pavement age, mix characteristics and the susceptibility of the binder to oxidization.

However, the effects of both conditions are adequately considered by relating the onset of surface reflection cracking to the tensile strain characteristics of the wearing course material. This form of cracking is normally associated with pavements incorporating significant thicknesses of surfacing and roadbase and is only partially dependent upon roadbase slab length.

c. shear fatigue of the bituminous materials which is caused by transient vertical differential movements between adjoining slabs induced by vehicular loading. The restraints provided by granular interlock between adjoining slabs and sub-grade support limits these differential movements. The effects of the induced shear stresses is normally confined to accelerating crack growth in the final stages of propagation.

Reflection cracking may also be caused by long term differential settlement of adjacent roadbase slabs on areas of variable sub-grade. Field observations made during the course of this investigation have shown that longitudinal cracking is often associated with settlement or shrinkage of the sub-grade on embankments causing construction joints to open to widths in excess of 25mm.

11.1.3 Dominant Crack Mechanisms

The models of the crack mechanisms presented in this thesis indicate that the thermally induced mechanisms are dominant during the early stages of crack growth through the surfacing layers. Tensile yield is the more important mechanism as this will affect the majority of roads and motorways which incorporate a lean concrete roadbase and have a surfacing thickness in excess of 150mm. Shear fatigue becomes dominant in the later stages of crack development initially associated with thermally induced tensile fatigue on pavements with thinner surfacings.

The tensile fatigue mechanism will cause full depth reflection cracking to occur within a 20 year design life of a typical pavement structure incorporating;

(i) a surfacing of 40mm H.R.A. and 60mm DBM,

(ii) a roadbase constructed with limestone or aggregate with similar coefficient of thermal expansion and contraction and

(iii) a slab length of 15m or less.

The life of the pavement may be extended by a greater thickness of surfacing, the use of roadbase aggregates with lower thermal coefficient and a shorter slab length. The slab length required for a 20 year design life is increased to 18m for 120mm of surfacing.

Under conditions of short slab length and surfacing thickness greater than 120mm tensile yield can initiate reflection cracking as a tensile failure at the surface with the subsequent downward propagation of cracks. The severity of the tensile yield mechanism is dependent upon the winter temperature regime and the tensile characteristics of the wearing course material. The susceptibility of a wearing course is related to its tensile strain at the point of yield. Isolated reflection cracks occur in surfacings with yield strains between 0.5% and 1% and develop at regular intervals in surfacings with yield strains below 0.5%. During the life of the pavement the rate of binder oxidisation will reduce the yield strain of the surfacing material. This may be regularly monitored by tensile creep testing of cored material. The testing, described in section 6.9, does not require complex equipment and is of short duration. Therefore, prior to the onset of cracking, a prevention strategy of routine maintenance may be undertaken when wearing course materials exhibit increasing susceptibility to reflection cracking. Existing material may be planed off and replaced by material less prone to reflection cracking. Surface initiated reflection cracking will be prevented in U.K. pavements incorporating layer thicknesses typical of motorway construction, if the yield strain of the surfacing is maintained above 1%.

A more complex relationship may exist between the onset of surface cracking, pavement construction thicknesses and wearing course tensile strain criteria under extreme climatic conditions. This relationship would depend upon the probability that a defined winter temperature occurs once in any given number of years or the frequency of prolonged periods of cold weather. Traffic flow and roadbase and sub-base conditions would also influence this relationship.

The combined influence of tensile fatigue and shear fatigue on crack growth is governed by their relationships with the crack tip stress intensity factor. These show opposing trends. Crack initiation and initial development occurs under the influence of tensile fatigue

while shear fatigue accounts for the final 20 - 40% of crack growth. This acceleration of crack growth in the final stages of crack development will reduce the length of roadbase slab required to produce full depth cracking within a 20 year design life by tensile fatigue alone by up to 30%. The traffic stresses which cause shear fatigue will accelerate crack growth initiated by tensile yield but the effect has not been quantified. Shear fatigue may be the dominant mechanism under conditions where poor sub-grade support is provided under the slab ends and the strength of the lean concrete roadbase material is too weak to afford good granular interlock.

Due to the complex interaction between the three dominant mechanisms of tensile fatigue, tensile yield and shear fatigue no single method exists to prevent their combined influence. However, extensive computer and laboratory evaluation of the individual mechanisms has indicated a number of significant variables which may be considered to limit crack growth.

11.2 FACTORS INFLUENCING CRACK GROWTH

11.2.1 Slab Length

Crack growth rate is influenced significantly by a combination of the length of the lean concrete roadbase slab and its coefficient of thermal expansion. Short slab lengths with low thermal coefficients substantially increase the time to full depth cracking for roadbase initiated cracking. From the example given in section 6.13 an increase in fatigue life by a factor of 20 is produced by a reduction in slab length from 20m to 10m.

The continuous process associated with cement bound roadbase construction inhibits the use of crack inducers to regulate the length of roadbase slabs. However, no satisfactory non-mechanical method of inducing short slab lengths exists. Although short slab lengths may be achieved by incorporating coarse aggregates of high coefficient of thermal contraction, this will result in high thermal movements at the slab ends. Taylor and Williams[89] indicate that crack spacing may be regulated by reducing the strength of the lean concrete to its lower specified limit of 10 N/mm^2. This, however, may be detrimental to the granular interlock between adjacent roadbase slab ends which provides a restraint to the mechanism of shear fatigue. In addition, differential settlement of the slabs may

not be restrained on areas of variable sub-grade. The likelihood of this occurring will increase as the stiffness of the surfacing material is reduced through crack growth.

Tensile yield of the surfacing is less dependent upon slab length as the contribution made by warping action is largely independent of this parameter. An increase in crack frequency within the roadbase will, however, reduce the tensile strains induced in the surfacing, thus reducing the probability of surface yield.

11.2.2 Thickness of Surfacing

The occurance of reflection cracking is influenced significantly by the thickness of the bituminous surfacing layer. A thickness in excess of 150mm will effectively prevent cracking by the mechanism of tensile fatigue. However, cracking caused by tensile yield of the surface is more likely to occur in thick pavements, as stresses caused by warping and thermal contraction will increase with pavement thickness. Thicker surfacings will, however, reduce the traffic induced shear stresses.

11.2.3 Binder Grade

The use of soft binders in the asphalt mix will inhibit crack growth due to both thermally induced mechanisms. For tensile fatigue a change from 50 pen to 200 pen binder can increase the fatigue life of a 100mm thickness of surfacing by a factor of 5. The viscous nature of well compacted rich D.B.Ms containing a soft binder prevents reflection cracks propagating to the surface and therefore a thin layer of this type of material overlying the lean concrete would inhibit the formation of reflection cracks.

11.2.4 Binder Oxidisation

Tensile yield of the bituminous surfacing occurs when the yield strain of the material is less than the tensile strain developed in the pavement surface at low temperatures. Results from the laboratory investigation and field observations indicate that under U.K. climatic conditions bituminous material with a yield strain of approximately 1.0% or less will be susceptible to reflection cracking initiating at the surface. Material within this catagory was generally found to contain oxidized 50 pen. binders reduced to 35 pen. or less. Conversely, pavement sections with less severe cracking

contained material with less oxidized binders. This indicates that the occurance of surface reflection cracks and the rate of their subsequent propagation is partially dependant upon the rate of binder oxidization. It is inevitable that limited binder oxidization will occur during the construction process and later. Therefore the effect has to be considered as a part of mix design. Design options include the use of either softer grades of binder which will oxidize to an acceptable penetration value or of binders less prone to oxidization. Ideally 50 pen. binders contained in traditional dense wearing course mixes should not oxidize to below 40 pen. during the design life of the pavement.

11.2.5 Bitumen Content

The investigation into tensile fatigue cracking indicates that an increase in the bitumen content from 4.2% to 6.2% will improve the fatigue life of a D.B.M. surfacing from 10 to 45 years for a pavement with a 25m roadbase slab. These mixes may be expected to provide poor permanent deformation characteristics. However, it is significant that a slight increase in bitumen content from 4.2% to 4.7% increases the stiffness of the mix, indicating an improvement in stability, while also doubling the tensile fatigue life. An increase in bitumen content will also result in a denser mix which is less prone to bitumen oxidisation.

11.2.6 Void Content

The air void content appears to influence the fatigue life considerably, probably because fatigue crack growth occurs by a mechanism of void coalescence. Well compacted material will retard crack growth and also give the additional benefit of reducing hardening of the binder during the service life of the pavement. A four fold increase in the fatigue life of a 100 pen. D.B.M. has been shown to result by reducing the air voids from 11% to 3% demonstrating the advantage of a greater compactive effort.

Generally hot rolled asphalt mixes are superior to dense macadams because of their lower void and higher binder contents. Tensile fatigue tests have shown that a hot rolled asphalt wearing course mix has four times the fatigue life of a D.B.M. wearing course mix containing a similar grade of binder .

Open graded mixes which have high void contents have shown poor resistance to tensile fatigue reflection cracking. Tests carried out on this material showed a reduction in fatigue life over a dense mix by a factor of approximately 2.5.

Tensile yield is also influenced by void content; with higher yield strain values resulting from poorly compacted material. This has been demonstrated by field observations from the M4 which show surface cracking to generally initiate between traffic lanes where the surfacing has been less well compacted.

11.2.7 Aggregate Grading

Aggregate grading has only a marginal effect on the rate of crack growth under the action of tensile fatigue. Larger aggregate sizes increase the cracking resistance slightly, presumably because the crack path is lengthened.

11.2.8 Reinforcement

The use of steel welded mesh reinforcement within the surfacing material had no effect on the rate of crack propagation in laboratory specimens. The flow characteristics of the bituminous material allow the mechanism of tensile fatigue to operate irrespective of the bond achieved between the surfacing and reinforcement.

11.2.9 Stress Absorbing Layers

The effectiveness of geogrids to inhibit crack growth is dependent upon the construction technique involved and the material and dimensional properties of the grid. Tensile fatigue cracking can be reduced significantly, if not eliminated by the use of a composite layer of geogrid and coated chippings as an additional course between the roadbase and conventional surfacing layers.

The geogrid is subjected to high stress levels as the crack tip makes contact with it. These stress levels may be reduced if debonding occurs between the geogrid and the surfacing material over a limited length. Debonding also reduces the stress being transmitted to the material above the geogrid. However, extensive debonding will be detrimental to the structural integrity of the pavement.

To inhibit crack growth, the geogrid must not yield locally at the

crack tip and must be stiffer than the surrounding bituminous material. Satisfactory performance was provided by geogrids with modulus values approximately 5 times the stiffness of the asphalt. However, if the geogird is too rigid it will be detrimental to the flexible nature of the pavement surfacing.

The width of geogrid has to be considered when it is to be laid over a crack prior to the road being strengthened by an overlay. The geogrid should extend at least 2m each side of the crack to ensure that the cracks are arrested at this level and do not propagate around the edges of the geogrid and then on up to the surface.

Geogrids were shown to be effective in inhibiting cracks propagating upwards. However, though the inclusion of geogrids in the bituminous layers should arrest downward propagation of cracking they will not prevent cracks initiating at the surface unless placed close to the surface, which is impractical.

11.2.10 Mastic Debonded Zones

A reduction in the stress induced in the bituminous surfacing by expansion and contraction of the roadbase may be achieved through the creation of a debonded zone at the interface between the surfacing and roadbase. Debonded zones may be created by spraying a layer of mastic material between roadbase and surfacing. Debonded lengths of 100 and 200mm either side of a crack between two 20m long roadbase slabs increased the fatigue life of the standard D.B.M. material used in the laboratory study from 20 to 25 and 35 years respectively.

Surface tensile yield cracking will be unaffected by this treatment.

11.2.11 Modified Binders

Asphalts incorporating modified binders are not prone to tensile fatigue but will yield at high strains. However, strains of sufficient magnitude to cause yield will only occur under normal UK climatic conditons in pavements with roadbase slab lengths over 30m and surfacings less than 80mm thick.

The use of an asphalt incorporating a modified SBS binder withstood strains of over 2% prior to yield. This value is in excess of the 1.2% exhibited by the wearing course on sections of the M4 free from

reflection cracking and a factor of 4 greater than the estimated yield strain at which reflection cracks will initiate due to tensile yield for a 5m road slab under UK climatic conditions.

11.3 FUTURE RESEARCH

Although limited to a range of D.B.M. and H.R.A. mixes for which crack opening fatigue results are available, the model developed to predict the rate of crack propagation under the mechanism of tensile fatigue is both comprehensive and versatile. A method is provided by which any bituminous mix may be tested within the laboratory and its resistance to this crack mechanism subsequently appraised. The ease and speed of computation is increased through use of the 'Basic' Program RFT100.

Although it has been suggested to manufacturers of products designed to inhibit reflection cracking that an assessment may be made of the effectiveness of individual materials and working practices, no further research into this mechanism alone is planned.

However, a parallel project is currently being undertaken at the Polytechnic to investigate the combined effects of this mechanism and traffic induced shear stresses. Results and conclusions from the project are expected by the late Spring of 1988.

The investigation into the mechanism of tensile yield has been based on pavements with over 10 years service where a good correlation was found to exist between the wearing course yield strain and the corresponding state of pavement crack development. Further research is required to produce and verify a method of testing newly laid bituminous surfacings to provide an end product specification. This may be achieved by the use of statistical techniques and computer modelling to analyse test data from newly constructed pavements. This would provide a 'shift' to allow for the range of yield strain values derived during the course of this project to be applied to recently laid pavement material. The contributory effect of wearing course shrinkage could also be satisfactorily accounted for by this approach.

Recommended tolerances for the yield strain values should include an assessment of pavement ageing using meteorological projections,

traffic data and material characteristics to predict the service life prior to surface crack development.

The program RFT100 may be modified to include the results and to provide a comprehensive predictive model capable of describing both the predominant thermally induced reflection crack mechanisms.

12.0 CONCLUSIONS

12.1 Continuously laid cement bound roadbases crack transversely during curing. The lengths of the slabs formed depend on the temperature regime immediately after construction, the coefficient of thermal contraction of the roadbase material and the ratio between its tensile strength and stiffness. Surveys on local trunk roads indicate crack spacings of between 3m and 30m with a mean of 13.5m. Although pavement deterioration does not necessarily occur as a direct result of cracks in the roadbase these provide focal points for stresses to be induced into the surfacing material.

12.2. Three dominant mechanisms of reflection cracking have been identified and modelled;

a) tensile fatigue which results from horizontal movements at the interface between ajoining roadbase slabs inducing upward crack propagation through the bituminous surfacing,

b) tensile yield which results from tensile failure of the surfacing and induces crack propagation downwards from the surface and

c) shear fatigue which results from traffic producing transient vertical differential movements between adjacent roadbase slabs and accelerates crack growth initiated by the thermally controlled mechanisms.

12.3. The research has produced four principal results;

(a) the development of a comprehensive model to predict the rate of crack growth due to the mechanism of tensile fatigue,

(b) the determination of strain criteria for the onset and development of cracking due to the mechanism of tensile yield,

(c) the development of a simple creep test to derive the yield strain of bituminous material and

(d) the determination of the significant factors influencing shear fatigue.

12.4 The models developed predict that the tensile yield mechanism is the more important as it will affect all roads

with lean concrete roadbases. The tensile yield mechanism will cause cracks to grow more rapidly during the coldest part of the year, when stresses due to thermal contraction are greatest and the wearing course is at its most brittle.

12.5 Tensile yield of the surface can be prevented if the ultimate yield strain of the wearing course is maintained above 1.0% during its service life. This has been verified from the results of an investigation into four sites which exhibit surface reflection cracking. Isolated reflection cracking will occur with surfacing whose yield strain is between 0.5% and 1.0%. Frequent and regularly spaced reflection cracking will occur if the yield strain is less than 0.5%.

12.6 The resistance of bituminous surfacing material to tensile yield may be increased through mixes of adequate design producing non-brittle characteristics. This may be achieved by quality control supervision to ensure the binder is not over oxidized during mixing, the use of softer bitumens and those not prone to oxidization. The comparison of creep test results on mixes of different gradings show dense mixes to have a superior performance. Reflection cracks occur initially between the traffic lanes indicating that good compaction is beneficial.

12.7 Further research is needed to determine how the ductility of the wearing course can be maintained during its design life and to define parameters by which newly laid material may be tested by a tensile creep test to appraise its future ability to resist reflection cracking.

12.8 The tensile fatigue mechanism is significant for roads with bituminous surfacings less than 100mm thick and reqires a roadbase slab length greater than 15m to produce full depth cracking within 20 years. Tensile fatigue cracking will be at its most active during the periods of greatest daily temperature range in the roadbase. This occurs in the Spring and Autumn.

12.9 Tensile fatigue cracking can be prevented or reduced by using mixes with softer binders, higher binder contents, better compaction and coarser aggregate gradings, by increasing the thickness of the bituminous layer or by placing a viscous layer on the lean concrete in the region of the crack. The use of geogrids and polymer modified binders can also be beneficial.

12.10 A computer program to model the tensile fatigue condition has been developed for the HP85. This model is based on the fracture mechanics approach and incorporates the results derived from simulative laboratory testing. The program provides an estimation of reflection cracking fatigue life, in days, for a semi-flexible pavement with a one or two layered bituminous surfacing. The input variables include the coefficient of thermal expansion of the cement bound layer, slab length, surfacing thickness and bituminous mix variables. Temperature conditions within the pavement are defined for mean U.K. conditions but may be varied to allow other climatic regimes to be studied.

12.11 The implications for pavement maintenance resulting from this study suggest a revision of present procedures is necessary. An effective, cost efficient method of inhibiting reflection crack growth may be obtained by placing a geogrid, or other stress relieving layer, over the existing pavement surface. This layer would to prevent upward crack growth and would combine with an overlay incorporating a polymer modified binder to provide greater resistance to tensile yield.

13.0 REFERENCES

1. POWELL, W.D., POTTER, J.F., MAYHEW, H.C., NUNN, M.E. The Structural Design of Bituminous Roads. TRRL Report No.1132 1984

2. CHANDLER, J.W.E., GOULD, P., MAYHEW, H.C., A Study of the Performance and Reflective Cracking of Roads with a Cement Roadbase. TRRL Working Paper No.112, Crowthorne. 1985

3. KENNEDY, C.K., and LISTER, N.W., Prediction of Pavement Performance and Design of Overlays, T.R.R.L., Report No. LR 833, Crowthorne 1978.

4. DEPARTMENT OF TRANSPORT. Specification for road and bridge works. H.M.S.O., London 1976

5. WILLIAMS, R.I.T., Properties of Cement Stabilized Materials, Jour.Inst.Highway Engineers, Vol XIX, No.2, 1972

6. BRITISH STANDARDS INSTITUTE, Testing of Concrete BS 1881, 1983

7. ROAD RESEARCH LABORATORY, A Guide to the Structural Design of Pavements for New Roads. Road Note 29, 3rd Ediction, HMSO, London, 1970

8. BRITISH STANDARDS INSTITUTION. Specification for Rolled Asphalt (Hot Process) BS 594, British Standards Institution London 1985

9. BRITISH STANDARDS INSTITUTION. Specification for Coated Macadam for Roads and other paved areas. BS 4987 British Standards Institution, London 1973.

10. BRITISH STANDARDS INSTITUTION. Penetration Test for Bitumens. BS 4691, British Standards Institution, London 1974.

11. BRITISH STANDARDS INSTUTITION, Softening Point Test for Bitumens. BS 4692, British Standards Institution, London 1971.

12. ULLIDTZ, P., A Fundamental Method for the Prediction of Roughness, Rutting and Cracking in Asphalt Pavements, Proc. Assn. of Asphalt Paveing Techs., Vol.48, 1979, pp557-586

13. VAN DER POEL, C. Time and Temperature Effects of Asphaltic-Bitumen and Bitumen-Mineral Mixtures, SPE Journal, pp 47-53, Sept. 1955.

14. HEUKELOM, W., and KLOMP, A.J.G., Road Design and Dynamic Loading, Proc.Assn. Asphalt Paving Technologists, Vol.33, 1964, pp. 92-125.

15. VAN DRAAT, W.E.F., and SOMMER, P. Engerat zur Bestimmung der Dynamischen Elastizitatsmoduln von Asphalt, Strasse und Auutobahn 6, 1965, pp 206-211.

16. KALAS, B.F., Dynamic Modulus of Asphalt Concrete in Tension and Tension Compression, Proc.Assn of Paving Technicians, Vol.39, 1970, pp 1-20.

17. BROWN, S.F., Material Characteristics for Analytical Pavement Design, Development in Highway Engineering, Vol.1, Applied Science Publishers Ltd., London 1978 pp 41-92

18. TINGLE, E.D. and GREEN, E.H., Changes in the Preparation of Bitumen in the Surface Layer of Rolled Asphalt Wearing Courses Pt.II, J.Highway Res.Rec. (134), 1966, pp51-62.

19. CALIFORNIA DEPARTMENT OF HIGHWAYS AND TRANSPORTATION. The Zaca-Wignore Asphalt Test Road, California, 1970.

20. DICKENSON, E.J., The Performance of Thin Bitumonous Surfacings in Australia. PROC. A.R.R.B. Vol.II, part 3, Australia. pp35-51. 1982.

21. ROLT, J., SMITH, M., and JONES, C., The Design and Performance of Bituminous Overlays in Tropical Environments. T.R.R.L. (overseas div.), Proc. Conf. Bearing Capacity of Roads and Airfields, Plymouth, 1986.

22. SHAHIN, M.Y., and McCULLOUGH, F.B., Prediction of Low-Temperature and Thermal Fatigue Cracking in Flexible Pavements RR No.123-14, Highway Design Devision, Texas Highway Dept., Austin, Texas, 1972.

23. LUND, J.W. and WILSON, J.E., Evaluation of Asphalt Ageing in Hot Mix Plant, Proc. A.A.P.T. Vol53, Arizona, 1984.

24. BRITISH STANDARDS INSTITUTE, Loss on Heating of Bitumen and Flux Oil, BS 2000 pt.45. 1982.

25. RAITHBY, K.D., and RAMSHAM, J.T., Effects of Secondary Compaction on the Fatigue Performance of a Hot Rolled Asphalt, TRRL Report no. LR471, Crowthorne 1972.

26. PELL, P.S., Developments in Highway Pavement Engineering Vol.1, Applied Science Publishers Ltd., London 1978.

27. BROWN, S.F., and BRUNTON, J.M., An Introduction to the Analytical Design of Bituminous Pavements, 3rd Ed, University of Nottingham, 1986.

28. HIGHWAY RESEARCH BOARD, The AASHO Road Test Report 5; Pavement Research, Special Report 61E, National Academy of Science, National REsearch Council, Publs. No.594, Washington, U.S.A. 1962.

29. FREEME, C.R., MEYER, R.G. and SHACKEL, B., A Method for Assessing the Advantages of Road Pavement Structures Using a Heavy Vehicle Simulator, Int. Road Fed. World Meeting, Stockholm, Sweden 1981.

30. ADDIS, R.R. and WHITMARSH, R.A., Relative Damaging Power of Wheel Loads in Mixed Traffic. Dept. of the Environment, TRRL, LR 979, Crowthorne, 1981.

31. O'FLAHERTY, C.A., Highway Engineering, Vol.2, Edward Arnold (pub) Ltd., London 1979.

32. LAKE, J.R., Road Pavement Design, Technical memorandum No.H6/78, Dept. of Transport, London 1978.

33. CURRER, E.W.H. AND O'CONNER, M.C.D. Commercial Traffic: Its Estimated Damaging Effect, 1945-2005. T.R.R.L., LR 910, Crowthorne 1979.

34. CURRER, E.W., Commercial Traffic Studies, D.O.E., T.R.R.L. Report No.LR628, Crowthorne, 1974.

35. JAMES, J.C., Quantities and Prices in New Road Construction, 1969, A Brief Analysis of 60 Successful Tenders T.R.R.L. Report LR 513 Transport and Road Research Labortory, Crowthorne 1972.

36. BROOKS, J.A., Quarry Managers, Journal 56, pp9-21, 1972

37. WRIGHT, P.J.F., A Survey of Roads Constructed with Lean Concrete Bases, RRL NOTE LN/305/PJFW 1963 (Unpub)

38. GARRET, C., Deflection Surveys of Road Pavements with Cemented Roadbases, Kent County Council, 1982.

39. WESTERGAARD, H.M., Bearing Pressures and Cracks, Journal of Applied Mechanics, Vol.61, A49, 1939.

40. BONNELL, D.G.R. and HARPER, F.C., The Thermal Expansion of Concrete, Building Research Station Technical Paper No.7, London 1951.

41. CRONEY, D., The Design and Performance of Road Pavements, HMSO, 1977.

42. T.R.R.L. Bituminous Materials in Road Construction, RRL HMSO 1962.

43. KORFHAGE, G.R., Effect of Pavement Breaker Rolling on the Crack Reflection of Bituminous Overlays, Hwy.Res.No.327 1970.

44. ROBERTS, S.E., Cracks in Asphaltic Resurfacing Affected by Cracks in Rigid Bases, Proc. HRB. Vol.33 (1954).

45. WAY, G., Prevention of Reflection Cracking, Minnetonka East (A Case Study): Arizona Dept of Transport, May 1976.

46. HAAS, R.C.G. et al, Low Temperature Pavement Cracking in Canada - The Problem and Its Treatment, Canadian Goods Roads Assoc., Proc. 1970 pp69-96.

47. KUMAR, A., and GEOTZ, W.M., Asphalt Hardening as Affected by Film Thickness, Voids and Permeability in Asphaltic Mixtures; Proc.Ass. Asphalt Paving Techs., Vol.46, 1977

48. CHANG, H.S., LYTTON, R.L. and CARPENTER, Prediction of Thermal Reflection Cracking in West Texas; Texas Transp. Inst., Res. Report 18-3, 1976.

49. LYTTON, R.L. and SHANMUGHAM, U., Analysis and Design of Pavements to Resist Thermal Cracking Using Fracture Mechanics,

V. INT. CONF. The Structural Design of Asphalt Pavements, Delft University of Technology, Holland 1982.

50. BONE, A.J., CRUMP, L.W., and ROGGEVEEN, V., Control of Reflection Cracking in Bituminous Resurfacing over old Cement-Concrete Pavements. Proc. Highway Research Bulletin No.33 1954.

51. ROGGEVEEN, V., and TONS, E., Progress of Reflection Cracking in Bituminous Concrete Resurfacings, Highway Research Bulletin No.131 1956.

52. JAMES, J.G., A Full-scale Road Experiment with Rubberised Asphalt on Concrete using Metal over a Concrete Joint, RRL Note 3511.1959

53. JIMENEZ, R.A., Testing Method for Asphalt Rubber, University of Arizona, Tucson, Report No. ADOT-R5-15. (164) 1978.

54. MORRIS, G.R. and McDONALD, C.H., Asphalt Rubber Stress Absorbing Mechanics Field Performance and State of the Art. T.R.B. Conf. 1976.

55. McGHEE, K.H., Attempts to Reduce Reflection Cracking of Bituminous Concrete Overlays on Portland Cement Concrete Pavements, Virginia Highway and Transport Research Council, Charlottesville, 1980.

56. DUVAL, J., The Renovation of Concrete Roadways using a thin Carpet of Asphapol, Ass.Asp.Int.Rpt., 1982.

57. BONE, A.J. and CRUMP, L.W., Several Resurfacing Projects, Massachusetts Inst. of Technology Report No.8 Cambridge, Mass, 1954.

58. TYNEER, H.L., GULDEN, W., BROWN, D., Resurfacing of Plain Jointed Concrete Pavements, Transportation Research Record 814, 1981, pp 41-45

59. BUSHEY.R.W., Experimental Overlays to Minimise Reflection Cracking Report No. FHWA-CA - FL - 3167-76-28 California State Dept of Transport, Sacramento, California, 1976.

60. ZUBE, E., Wire Mesh Reinforcement in Bituminous Resurfacing, H.R.B. 131, 1956.

61. SMITH, L.L. and CARPENTER, W., Welded Wire Fabric Reinforcement for Asphaltic Concrete, H.R.B. 322, 1962.

62. BROWN, S.F., BRUNTON, J.M., HUGHES, D.A.B., BRODRICK, B.V., Polymer Grid Reinforcement of Asphalt, Association of Asphalt Paving Technologists, Texas, Vol.55, 1985.

63. HAYWARD, D., Grid Preference, Art. N.C.E., Thomas Telford Pub, London, July, 1986.

64. PICKETT, D.L., and LYTTON, R.L., Labortory Evaluation of selected Fabrics for Reinforcement of Asphalt Concrete Overlays. Report No.261-1, Texas Transportation Ins., Texas A and M University, 1983

65. MAJIDZADEH, K., A Laboratory Investigation of the Use of Petromat for optimizing of Pavement Performance, Ohio State University Sponsored by Phillips Petroleum Company 1976.

66. GULDEN, W., Rehabilitation of Plain Portland Cement Concrete Pavements with Asphalt Concrete Overlays, Asphalt Paving : Technology Procs.,Vol 47, 1978.

67. MULLEN, W.G., and HADER, R.J., Effectiveness of Fabric and Non-Fabric Treatments in Controlling Reflection Cracking, North Carolina State University, North Carolina 1980.

68. WOOLLEY, W.R., Some observations on Resurfacing Portland Cement Concrete Pavements with Bituminous Mixtures. Proc. H.R.B. No.26 Washington 1946.

69. CRAWFORD, C., Cracking and Sealing of PCC Pavements prior to Overlaying with Hot Mix Asphalt. National Asphalt Pavement Association. Information Series No. 91 1985.

70. McLOUGHLIN, A.L. Reflection Cracking of Bituminous Overlays for Airport Pavements, A State of the Art. Report No. FAA-RD-79-57, U.S. Dept of Transport Federal Aviation Administration, Washington, D.C., May 1979.

71. BRITISH STANDARD INSTITUTION. Specification for Hot Applied Joint Sealants for Concrete Pavements, BS 2499 London 1973.

72. SCHAPERY, R.A., A Theory of crack Growth in Viscoelastic Media. Mechanics and Materials Research Centre, Texas A & M University, College Station, Texas, 1973.

73. GERMANN, F.P., and LYTTON, R.L., Methodology for Predicting the Reflection Cracking Life of Asphalt Concrete Overlays, Res. Rpt. No. 207-5, Texas Trans. Inst., Texas Univ. 1979

74. BARENBLATT, G.I., The Mathematical Theory of Equilibrium Cracks in Brittle Fracture, Advances in Applied Mechanics, Vol.VII, Academic Press 1962.

75. RAMSAMOOJ, D.V., Prediction of Reflection Cracking in Pavement Overlays. Highway Research Board H.R.R. 434 Washington D.C. 1973

76. MARCHAND, J.P. and GOACOLOU, H. Cracking in Wearing Courses, V INT. CONF., The Structural Design of Asphalt Pavements, Delft University of Technology, Holland, 1982.

77. McCULLOUGH, B.F. and SEEDS, S.B., Field Validation of an Overlay Design Procedure to Prevent Reflection Cracking, V INT CONF. The Structural Design of Asphalt Pavement, Delft University of Technology, Holland, 1982.

78. MAJIDZADEH, K., and SUCKARIEH, G., The Study of Pavement Overlay Design: Final Report, Ohio State University, Columbus, 1977.

79. COETZEE, M.F., Some Considerations on Reflection Cracking in Asphalt Concrete Overlay Pavements, Ph.D. Thesis, University of California, Berkeley, 1979.

80. BROOKER, T.N., The Determination of Crack Propagation Rates of Reflection Cracking through Asphalt Surfacings, Ph.D. Thesis, Plymouth Polytechnic, Plymouth 1986.

81. PARIS, P. and ERDOGAN, F.J. A Critical Analysis of Crack Propagation Laws. Journal of Basic Engineering, ASME Series D. Vol 85, 1963.

82. WILLIAMS, C., ROSSI, A., and FOULKES, M.D. Some Aspects of Instrumentation, Conf. Teaching of Vibration and Noise, Sheffield Polytechnic 1985.

83. BRITISH STANDARDS INSTITUTION. Specification for Sampling and Examination of Bituminous Mixtures for Roads and other Paved Areas, BS.598, British Standards Institution, London 1974

84. MONISMITH, C.L. and DEACON, J.A., J. Transp.Eng.Div., ASCE, 95, pp317-46, 1969.

85. MINER, M.A., Cumulative Damage in Fatigue, J. Applied Mechanics 67, 1945.

86. SALAM, V., Characterisation of Deformation and Fracture of Asphalt Concrete, C.U.I.T.T.E. Dissertation Series, Univ. of California, Berkeley, 1979.

87. ROBERTS and ERODOGAN. Some Aspects of Fatigue Cracking, Eng. Fracture Mech., Vol.2, No.3, May 1971.

88. FOULKES, M.D. and KENNEDY, C.K., Reflection Cracking of Bituminous Surfacing on Composite Pavements, Int. Conf. The Bearing Capacity of Roads and Airfields, Plymouth 1986. pp105-115

89. GALLOWAY, J.W., Temperature Durations at Various Depths in Bituminous Pavements, R.R.L. Report LR 138, Crowthorne 1968.

90. MAJIDZADEH, K., BURANOM, C. and KARAKOUZIAN, M., Application of Fracture Mechanics for Improved Design of Bituminous Concrete Vol.I, Plan of Research State of the Art and Mathematical Report FHWA-RD-76-91, Federal Highways Administation, Washington D.C. 1976.

91. SHACKLOCK, B.W., Concrete Constituents and Mix Proportions, Cement and Concrete Assn., London 1974.

92. MEYERS, S.L., Thermal Coefficient of Expansion of Portland Cement - Long Time Tests, Industrial and Engineering Chemistry, 32, No.8, pp 1107-112 (Easton, Pa.,) 1940.

93. POWERS, T.C. and BROWNYARD, T.L., Studies on the Physical Properties of Hardened Portland Cement Paste, J.Amerc. Conc.Inst. 48, pp661-79, 1952.

94. TAYLOR, G.D. and WILLIAMS, R.T., Restrained Thermal Contraction in Lean Concrete Roadbases., Highways and Public Works, July 1981.

95. BROOKER,T., FOULKES, M.D. and KENNEDY, C.K., Influence of Mix Design on Reflection Cracking Growth Rate Through Asphalt Surfacing, Proc. 6th Ann.Arbor Conf. Vol.57, 1987.

96. SPARKS, F.N., Stresses in Concrete Road Slabs, Struct.Eng., 17(2) 1939 pp98-116.

97. STOTT, J.P., Tests on Materials for use in Sliding Layers under Concrete Road Slabs" GU Eng.56, London 1961.

98. ROAD RESEARCH LABORATORY, Concrete Roads: Design and Construction. HMSO London 1956.

99. IRWIN, G.R., Analysis of Stresses and Strains near the End of a Crack Traversing a Plate. Transactions, ASME, Journal of Applied Mechanics, Vol.24, 1957.

100. HAYES, D.J., Practical Approach of Beuchner's Formulation. Int.J.Fract.Mech., 8, Pt.II, 1972

101. GUYDISH, J.J. and FLEMING, J.F., Optimisation of the Finite Element Mesh for the Solution of Fracture Problems, Engineering Fracture Mechanics, Vol.10, Pergamon Prerss, U.K., 1978 pp31-42.

102. PAFEC PREPARATION MANUAL. Level 6. PAFEC Ltd Nottingham 1986.

103. BURT, M.A., M4 Motorway, a Composite Pavement: the Mechanism of Failure. Int.Conf. The Bearing Capacity of Roads and Airfields, Plymouth 1986. pp397-408

104. REFINED BITUMEN ASSOCIATION. Technical Bulletin No.3. Penetration Grade Bitumen - Manufacture and Specification, 1979.

105. DEPARTMENT OF TRANSPORT. Specification of Highway Works. H.M.S.O.,1986.

106 DUGDALE, D.S., Yielding of Steel Sheets Containing Slits, Jnl Mech. Phys. Solids, 8, 1960, pp100-104

107 VAN DYKE. Pratical Fatigue Characteristics of Bituminous Mixes, Proc AAPT, Vol 44 1975.

108 CLASSEN, A.J.M., et al. Asphalt-Pavement Design -The SHELL Method Proc 4th.Int. Con. on the Structural Design of Asphalt Pavements, Univ. of Michigan, Ann Arbor, 1977.

109 MAJIDZADEH, K and HERRIN, M., Modes of Failure and Strength of Asphalt Films Subjected to Tensile Stresses, Highways Research record 67, Washington D.C. 1985.

110 SHELL INTERNATIONAL PETROLEUM Co. Ltd, Shell Pavement Design Manual,1978.

APPENDIX 1

CALCULATION OF STRESS INTENSITY FACTOR k_o

PHASE 9 FINITE ELEMENT OUTPUT ELEMENT STRESSING ROUTINE				
Node Number	E Number	Distance Ahead of Crack (r)mm	Stress in Element in the Crack Plane (σx) (E8)	Stress Intensity Factor (k) ($N/mm^{3/2}$)
156	48	1.875	0.382	134.2
165	48	2.875	0.312	132.6
182	48	3.75	0.246	119.41
191	56	4.68	0.205	111.25
208	56	5.62	0.178	104.03
217	56	6.56	0.158	100.45

where $k_o = \sigma x \sqrt{2\pi r}$
F.E. model run for defined increment of crack length.

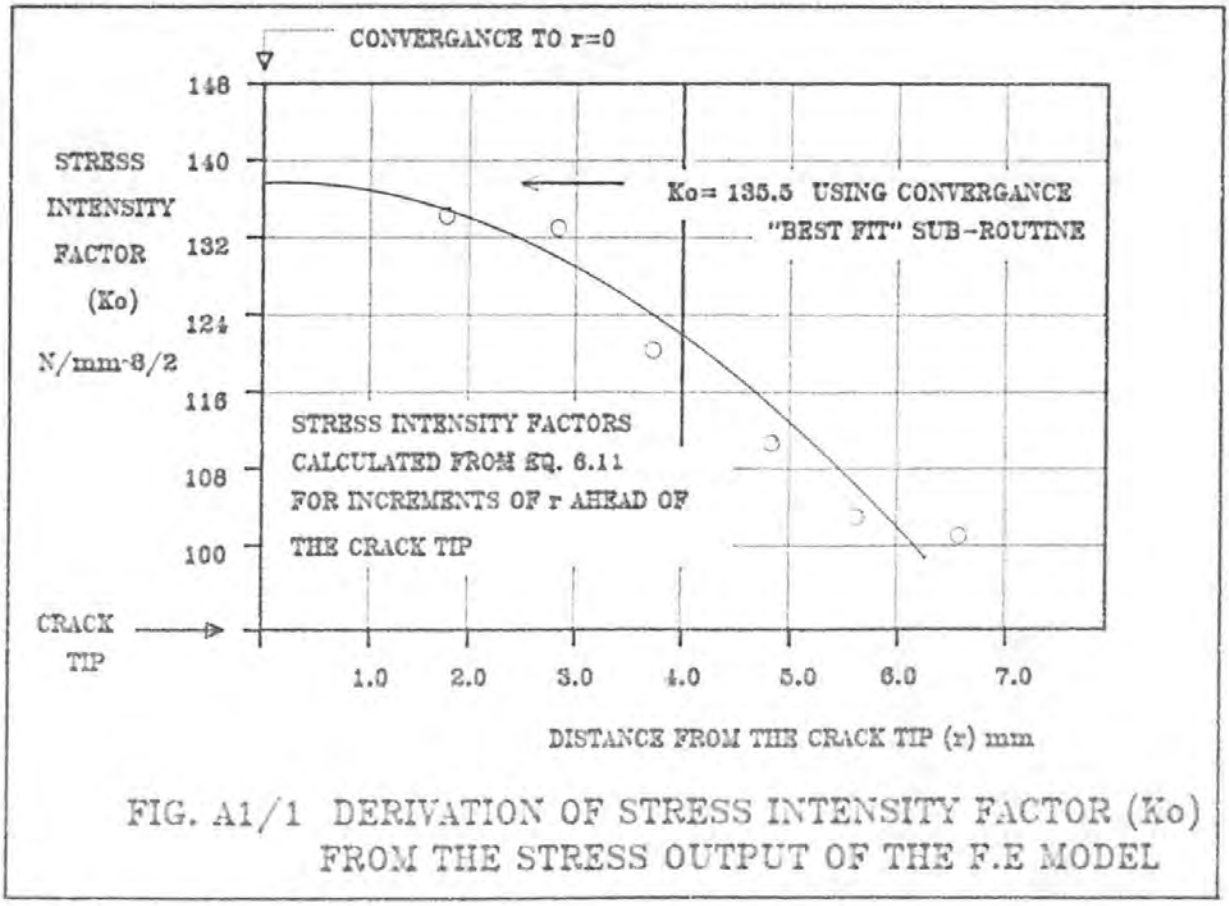

FIG. A1/1 DERIVATION OF STRESS INTENSITY FACTOR (Ko) FROM THE STRESS OUTPUT OF THE F.E MODEL

APPENDIX 2

EXAMPLE CALCULATION OF FATIGUE CONSTANTS A and n

The fatigue constants A and n are calculated from the results of cyclic crack opening tests on beams of bituminous material, described in section 6. A numerical example is presented in this appendix from the test results of a D.B.M. material.

STAGE 1 MIX SPECIFICATIONS

20mm Nominal aggregate size DBM
Mid range grading to Cl.2.2.6. BS. 4987
Bitumen content = 4.2%
Bitumen grade = 50 pen.
Limestone Aggregate from Chipping Sodbury

STAGE 2 TEST SPECIFICATIONS

Frequency of crack opening cycle	= 0.026Hz
Test Temperature	= 40°C
Crack Opening Width	= 1.4mm

STAGE 3 STIFFNESS CHARACTERISTICS UNDER CONDITIONS OF TEST FREQUENCY AND TEMPERATURE

A value of bitumen stiffness is read from Van der Poel's nomograph for test temperature and frequency conditions. A corresponding value of mix stiffness is read from a mix stiffness/ bitumen stiffness plot derived from a static tensile creep test on the bituminous material.

Bitumen Stiffness = 1×10^4 N/m^2

Mix Stiffness = 8.2×10^7 N/m^2

Yield Strain at failure of creep test = 0.7%

STAGE 4 TEST RESULTS TABLE A2.1

COL I Test data recorded at increments of crack opening cycles (N)

COL II The displacement (mm) on the upper surface of the beam recorded from the output of strain gauges mounted on a portal frame, described in section 6.

COL III The crack length (mm) corresponding to the displacement on the upper surface of the beam derived from elastic finite element analysis, fig.6.4.

COL IV Correction to crack length, (COL III), to allow for the

plastic zone ahead of the crack tip, fig.6.8.; in terms of the yield strain of the test material. A 'best fit' curve, fig.A2.1 is derived from a plotting routine in the form $c = A_1 N^{A_2}$ where c is the crack length and N is the number of crack opening cycles

COL V The equation of the curve is differentiated to derive the crack propagation rate dc/dN

COL VI For each increment of crack length the unit stress intensity factor, k_o, is read from fig.6.21.

COL VII The stress intensity factor is modified for values of pavement surfacing thickness, crack opening width and surfacing stiffness.

STAGE 5 DERIVATION OF FATIGUE CONSTANTS

Plot of crack propagation rate versus the modified stress intensity factor, k_r, fig.A2.2. The fatigue constants, A and n, are the intercept of the curve on the y axis and the gradient respectively, fig.6.24.

TABLE A2.1
CALCULATION OF FATIGUE CONSTANTS A AND n

COL I	COL II	COL III	COL IV	COL V	COL VI	COL VII
'CRACK OPENING' FATIGUE CYCLES N (No.)	STRAIN GAUGE READOUT(mm)	CRACK LENGTH FROM FINITE ELEMENT OUTPUT mm.	CORRECTION TO CRACK LENGTH ALLOWING FOR PLASTIC ZONE(mm)	CRACK RATE FROM 'BEST FIT CURVE' (dc/dN)	STRESS INTENSITY FACTOR k_o ($N/mm^{3/2}$)	STRESS INTENSITY FACTOR k_r($N/mm^{3/2}$) where $k_r = \frac{k_o \, u \, S_m}{10^8}$
3	.118	30	8	5	13.5	10.39
10	.136	37	21	1.18	8.7	6.69
20	.163	42	30	.64	7.0	5.39
30	.172	46	37	.37	6.2	4.77
47	.186	49	41	.16	5.8	4.46
125	.20	50.5	43	.068	5.6	4.31
360	.220	54	46	.034	5.4	4.16
822	.234	56	48	.019	5.2	4.00
1290	.247	59	52	.015	5.1	3.93
1602	.261	62	55	.013	5.0	3.85
254	.269	64	57	.011	4.95	3.81
4650	.286	66	61	.0064	4.9	3.77
5274	.321	71	66	.0059	4.85	3.73
5896	.373	78	73	.0055	4.75	3.65
7766	.515	89	85	.0046	4.50	3.46
8390	.539	90	86	.0044	4.40	3.36
9638	.626	93	90	.0040	4.20	3.23
11510	.765	97	95	.0035	3.60	2.77
12500	.92	99	98	-		

COL V 'Best fit' curve $c = 4.4N^{-.35}$
COL VI Crack propagation rate $dc/dN = 1.57\ N^{-.65}$

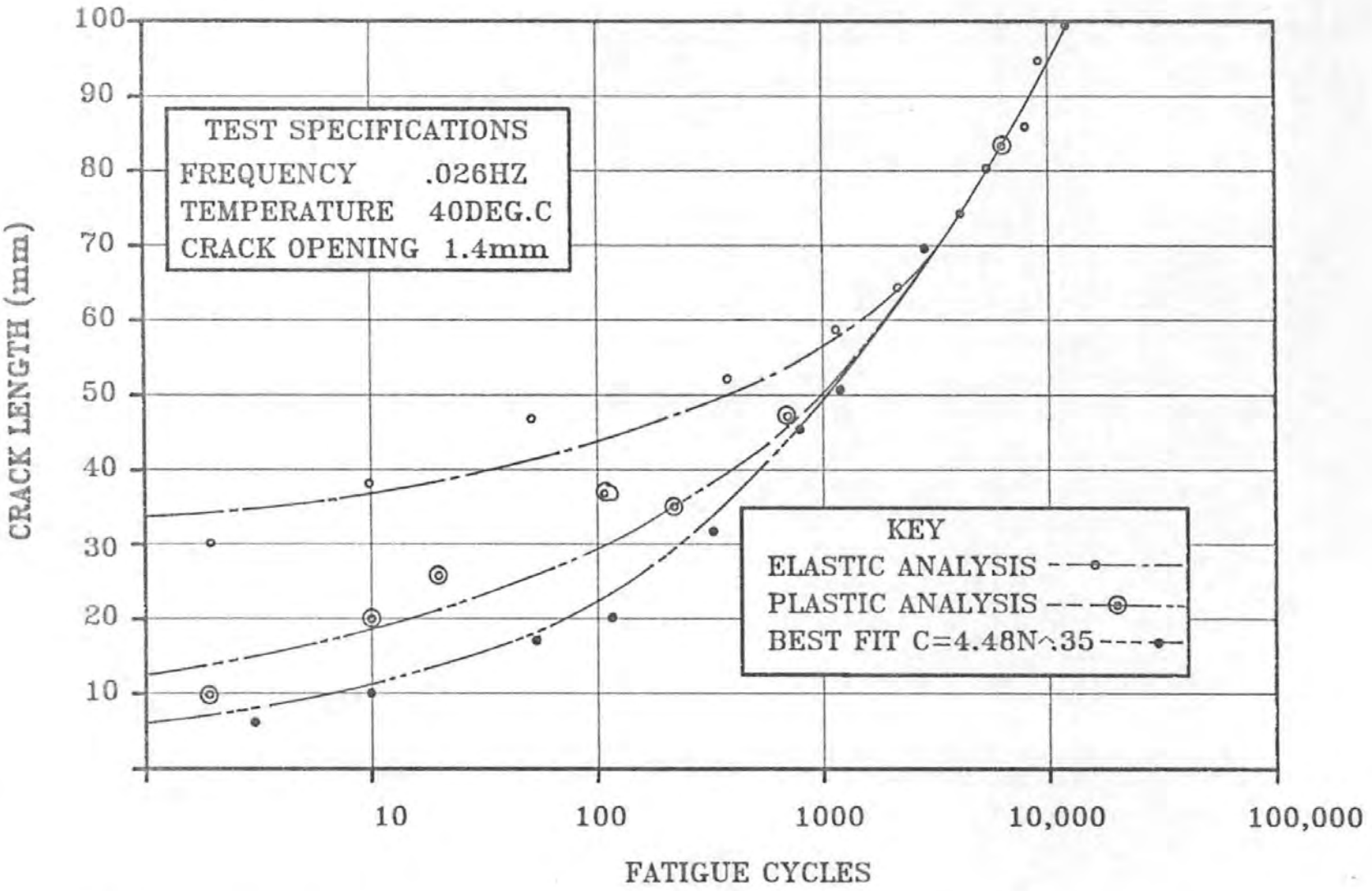

FIG.A2.1 CRACK LENGTH VERSUS FATIGUE CYCLES FROM ELASTIC AND PLASTIC ANALYSIS WITH A 'BEST FIT'POLYNOMINAL CURVE TO DERIVE THE CRACK PROPAGATION RATE

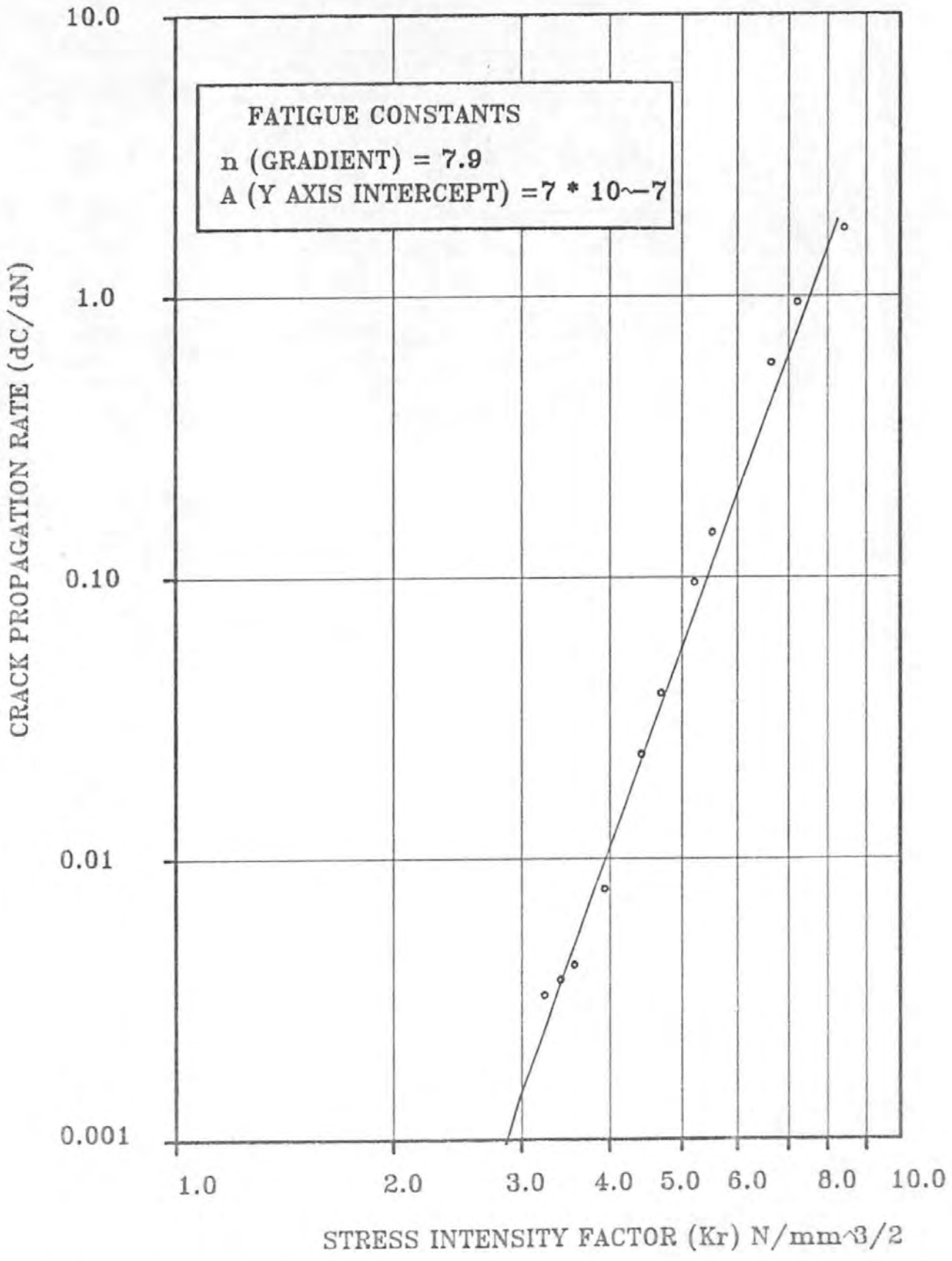

FIG.A2.2 PLOT OF CRACK PROPAGATION RATE VERSUS STRESS INTENSITY FACTOR FOR GIVEN D.B.M. MIX

APPENDIX 3

EXAMPLE ON THE ESTIMATION OF REFLECTION CRACKING FATIGUE LIFE DUE TO THE MECHANISM OF TENSILE FATIGUE

The mixes used to demonstrate the design procedure have been selected from those for which creep test data is available. The surfacing is assumed to consist of a 60mm basecourse and a 40mm wearing course.

Stage 1

1. ASPHALT TYPE:-

   (a) BASECOURSE

   40mm Nominal Aggregate size D.B.M.

   Limestone Aggregate, P_i = 100 Pen

   (b) WEARING COURSE

   14mm Nominal Aggregate size D.B.M.

   Limestone Aggregate, P_i = 100 Pen

2. ESTIMATION OF ROADBASE SLAB LENGTH

Statistical analysis of the crack spacing survey presented in section 6.8 indicates a mean roadbase slab length 15m.

3. ESTIMATED SEASONAL DAILY MEAN AND DAILY RANGE OF TEMPERATURE IN THE SURFACING AND ROADBASE (TYPICAL U.K. CONDITIONS)

The pavement temperatures for the four seasons, used in this example, are represented by the values attributed to the months of January, April, July and October given in Table 6.3. The pavement is assumed to consist of 200mm of cement bound roadbase material overlaid by 100mm of bituminous surfacing material.

4. CREEP TEST DATA

A tensile creep test has been carried out on samples of the proposed mix using the method described in section 6.9. The samples are representative of the pavement material. The results are presented in figure A3.1 as plots of mix stiffness versus bitumen stiffness.

5. VOID CONTENTS

The void contents of both bituminous layers have been calculated:-

(i) Basecourse:- 6%

(ii) Wearing course:- 3%

Stage II

6. CALCULATION OF CRACK OPENING WIDTH (U)

The crack opening width data provided in Table 6.2 for 15m slabs is given below. Assume that warping is not restrained.

MONTH	JAN.	APRIL	JULY	OCT.
CRACK OPENING WIDTH (U) mm	0.32	1.25	1.31	0.69

7. BITUMEN STIFFNESS (S_b)

Values of bitumen stiffness for a daily thermal cycle at seasonal mean temperatures have been derived from Van der Poel's Nomograph; figure A3.2 and are presented below.

MONTH	JAN.	APRIL	JULY	OCT.
BITUMEN STIFFNESS (N/m^2) S_b	7×10^4	2×10^4	5×10^2	3×10^4

Laboratory testing has shown the bituminous mix acts as a viscous medium below a bitumen stiffness value of 1×10^4 N/m^2, therefore no cracking is deemed to occur during the summer season (July).

8. MIX STIFFNESS (S_{md})

Values of S_{md} corresponding to the values of S_b given in section 7 are derived from figure A3.1 and are given below.

MONTH	JAN.	APRIL	JULY	OCT.
MIX STIFFNESS WEARING COURSE (N/m^2) $S_{md}(w)$	2.0×10^8	4.0×10^7	-	7.5×10^7
MIX STIFFNESS BASECOURSE (N/m^2) $S_{md}(b)$	1.0×10^9	2.0×10^7	-	3.0×10^7

9. ESTIMATION OF STRESS INTENSITY FACTORS

The unit stress intensity factors, k_o, are derived from figure 6.21 in terms of the stiffness ratios between the bituminous layers for each season and are presented in Tables A3.1 and A3.2.

The modified stress intensity factors, k_r, calculated from Equation 6.13 are also presented in Tables A3.1 and A3.2

Stiffness Ratios

MONTH	JAN.	APRIL	JULY	OCT
$\frac{S_{md}(w)}{S_{md}(b)}$	2.0	2.0	-	2.5

10. ESTIMATION OF FATIGUE CONSTANTS

The values of fatigue constant "A", given in figures 6.25 to 6.27 are modified for the mix properties of the bituminous layers and presented in figure A3.3. Constant "A" varies with respect to S_b and therefore the season. The seasonal values for the wearing course and the basecourse are given below as A_w and A_b.

MONTH	JAN	APRIL	JULY	OCT
A_w	2×10^{-7}	1.5×10^{-6}	-	8×10^{-7}
A_b	6×10^{-7}	1.5×10^{-5}	-	7×10^{-6}

$n = 6.6$ for P_i = 100pen.

11. NUMERICAL INTEGRATION OF PARIS LAW

Numerical integration of Paris Equation, Tables A3.1 and A3.2, is used to derive the seasonal fatigue life of the basecourse and wearing course individually. These are combined to give the seasonal fatigue life for the bituminous layer.

$$Nf = \int_0^{60} \frac{\Delta c}{A_b k_r^n} + \int_{60}^{100} \frac{\Delta c}{A_w k_r^n} \quad \text{where } \Delta c = 10mm$$

12. DERIVATION OF ANNUAL FATIGUE LIFE

The damage per daily cycle at each seasonal stress level may be defined from Miners' Law.

$$\text{Seasonal damage per cycle} = \frac{1}{\text{Seasonal } Nf}$$

$$\text{Average Damage per cycle} = \left[\frac{1}{3 \Sigma \text{ Seasonal } Nf}\right] \quad \text{from tables A3.1 and A3.2}$$

$$= \frac{1}{3}\left(\frac{1}{10569} + \frac{1}{5510} + \frac{1}{2397}\right)$$

$$= \frac{1}{3}\left(9.43 \times 10^{-5} + 1.81 \times 10^{-4} + 4.17 \times 10^{-4}\right)$$

$$= \frac{1}{3}\left(6.82 \times 10^{-4}\right) = 2.27 \times 10^{-4}$$

$$\text{Annual fatigue life} = \left(\frac{1}{2.27 \times 10^{-4}}\right) \frac{4}{3} = 5862 \text{ Days (16.06 years)}$$

TABLE A3.1
NUMERICAL INTEGRATION OF PARIS' EQUATION FOR JANUARY AND APRIL

CRACK LENGTH			JANUARY				APRIL			
C1 (mm)	C2 (mm)	C(AV) (mm)	k_o ($N/mm^{3/2}$)	k_r ($N/mm^{3/2}$)	Ak_r^n	N (DAYS)	k_o ($N/mm^{3/2}$)	k_r ($N/mm^{3/2}$)	Ak_r^n	N (DAYS)
0	10	5	16.6	10.6	3.55	3	16.6	8.3	-	
10	20	15	13.2	8.5	0.780	13	13.2	6.7	4.25	2
20	30	25	9.6	6.1	0.095	105	9.6	4.8	0.470	21
30	40	35	7.7	4.9	0.022	447	7.7	3.8	0.101	99
40	50	45	6.2	4.0	0.0056	1771	6.2	3.1	0.026	382
50	60	55	6.5	4.2	0.0073	1367	6.5	3.3	0.040	253
N_{bc}						3706				756
60	70	65	7.0	4.5	0.0098	2500	7.0	5.2	0.0058	1724
70	80	75	6.6	4.6	0.0079	2000	7.2	5.4	0.0070	1428
80	90	85	6.8	4.9	0.0032	1430	7.6	5.7	0.0101	1000
90	100	95	8.1	5.2	0.0104	960	8.1	6.1	0.0166	602
N_{wc}						6890				4754
N_t						10596				5510

Where N_{bc} is the Number of Days for Crack Propagation Through the Basecourse
N_{wc} is the Number of Days for Crack Propagation Through the Wearing Course
N_t is the Combined Total

TABLE A3.2
NUMERICAL INTEGRATION OF PARIS' EQUATION FOR OCTOBER

CRACK LENGTH						
C1 (mm)	C2 (mm)	C(AV) (mm)	k_o (N/mm$^{3/2}$)	k_r (N/mm$^{3/2}$)	Ak_r^n	N (DAYS)
0	10	5	16.5	8.5	-	-
10	20	15	13.5	7.0	2.3	5
20	30	25	9.8	5.0	0.29	35
30	40	35	8.0	4.1	0.077	130
40	50	45	6.7	3.4	0.023	435
50	60	55	7.3	3.8	0.042	239
N_{bc}						844
60	70	65	9.0	4.6	0.019	534
70	80	75	9.0	4.6	0.019	534
80	90	85	9.8	5.0	0.033	303
90	100	95	10.4	5.4	0.055	182
N_{wc}						1553
N_t						2397

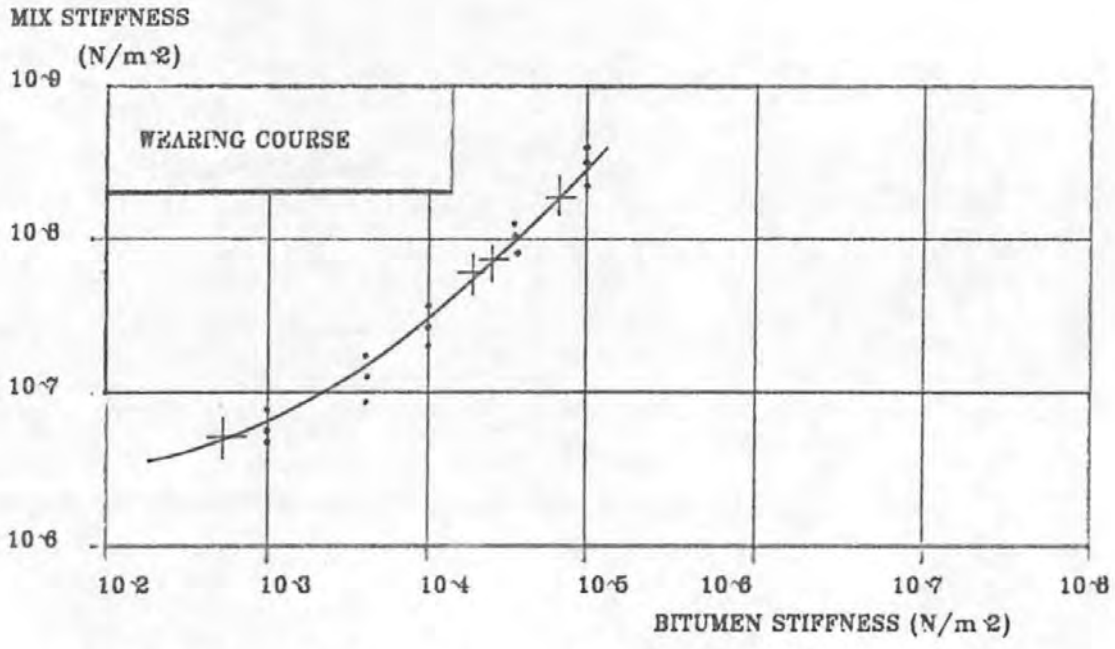

WEARING COURSE :- 14mm NOMINAL SIZED D.B.M
4.2% BITUMEN CONTENT 3% VOID CONTENT Pi = 100pen Pr = 65 pen

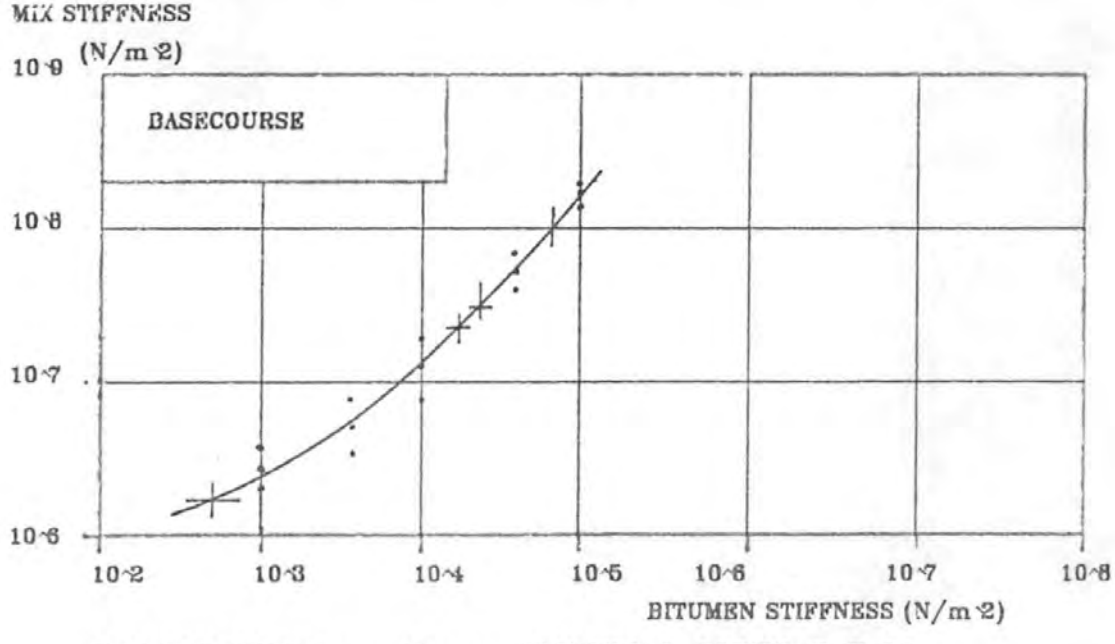

BASECOURSE :- 40mm NOMINAL SIZED D.B.M
4.2% BITUMEN CONTENT 6% VOID CONTENT Pi = 100pen Pr = 65pen

FIG. A3.1 TENSILE CREEP TEST RESULTS ON WEARING AND BASECOURSE MATERIALS

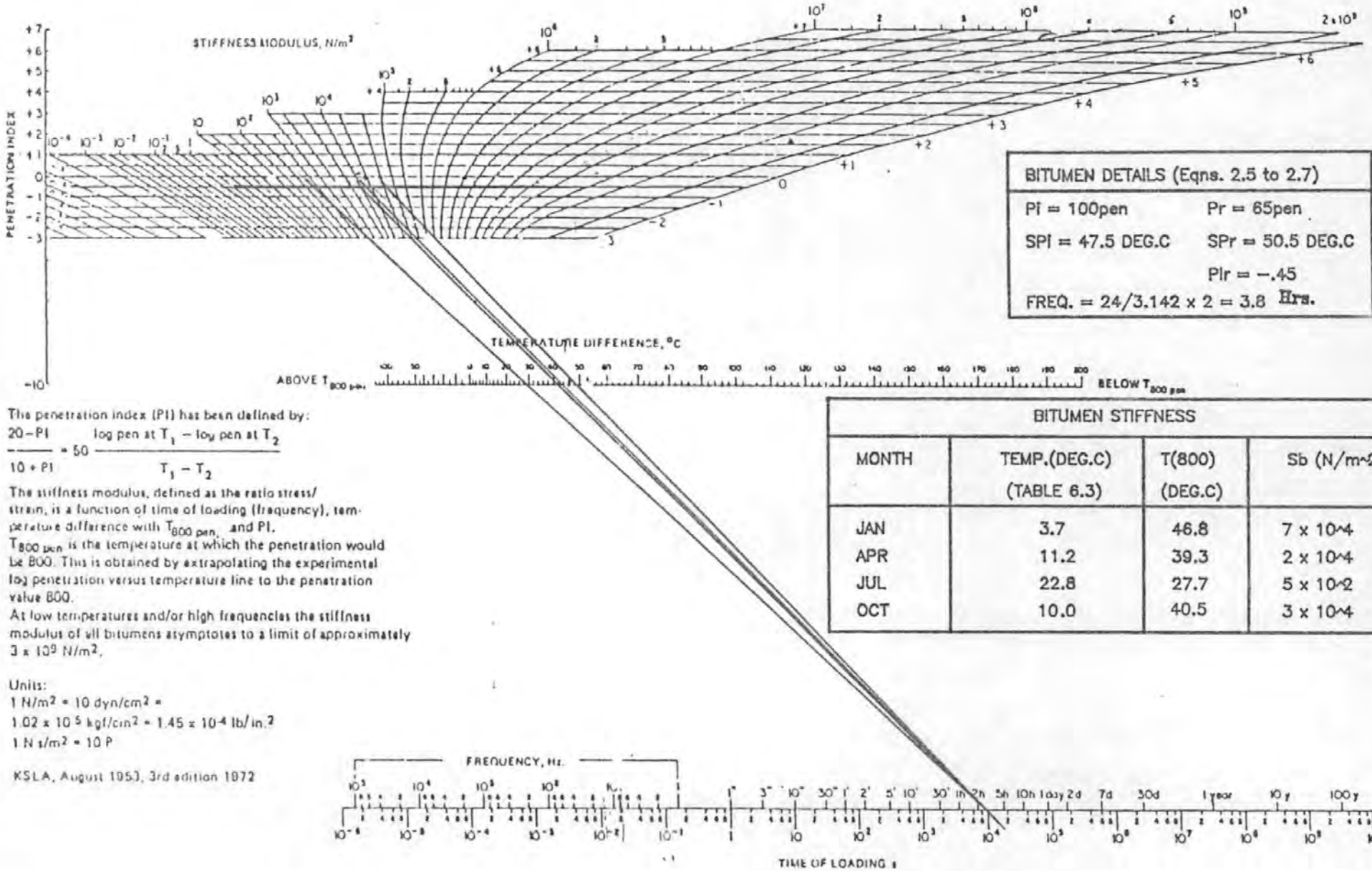

BITUMEN DETAILS (Eqns. 2.5 to 2.7)	
PI = 100pen	Pr = 65pen
SPI = 47.5 DEG.C	SPr = 50.5 DEG.C
	PIr = −.45
FREQ. = 24/3.142 x 2 = 3.8 Hrs.	

BITUMEN STIFFNESS			
MONTH	TEMP.(DEG.C) (TABLE 6.3)	T(800) (DEG.C)	Sb (N/m^2)
JAN	3.7	46.8	7 x 10^4
APR	11.2	39.3	2 x 10^4
JUL	22.8	27.7	5 x 10^2
OCT	10.0	40.5	3 x 10^4

The penetration index (PI) has been defined by:

$$\frac{20-PI}{10+PI} = 50\,\frac{\log \text{pen at } T_1 - \log \text{pen at } T_2}{T_1 - T_2}$$

The stiffness modulus, defined as the ratio stress/strain, is a function of time of loading (frequency), temperature difference with $T_{800\ pen}$ and PI.

$T_{800\ pen}$ is the temperature at which the penetration would be 800. This is obtained by extrapolating the experimental log penetration versus temperature line to the penetration value 800.

At low temperatures and/or high frequencies the stiffness modulus of all bitumens asymptotes to a limit of approximately $3 \times 10^9\ N/m^2$.

Units:

$1\ N/m^2 = 10\ dyn/cm^2 =$

$1.02 \times 10^{-5}\ kgf/cm^2 = 1.45 \times 10^{-4}\ lb/in.^2$

$1\ N\,s/m^2 = 10\ P$

KSLA, August 1953, 3rd edition 1972

FIG.A3.2 BITUMEN STIFFNESS DETAILS FOR TEST MIXES

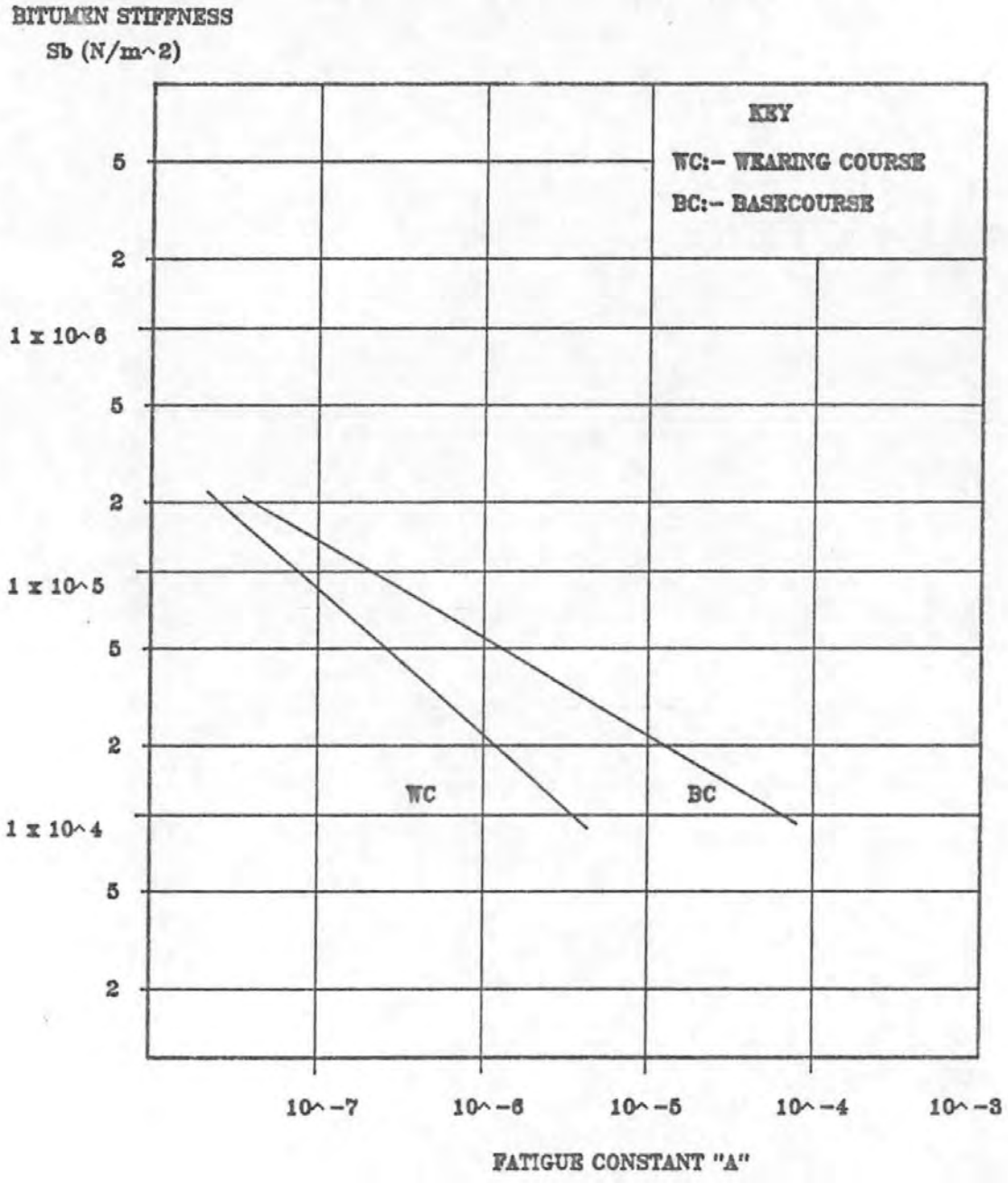

FIG. A3.3 BITUMEN STIFFNESS VERSUS FATIGUE CONSTANT "A" FOR TEST MIXES

(MODIFIED FROM FIGS.6.25 TO 6.27 WITH RESPECT TO THE AGGREGATE GRADING AND THE VOID CONTENT OF THE TEST MIXES)

APPENDIX 4

MODIFICATION OF PREDICTIVE METHOD TO ALLOW FOR BINDER HARDENING WITH AGE

1. Introduction

The example given in Appendix 3 provides a method of estimating the fatigue life under the mechanism of tensile fatigue. The properties of the mix, however, are assumed to remain constant throughout its service life.

The action of the elements, solar radiation, and traffic, induce a hardening of the binder which effects the resistance of the surfacing material to reflection cracking. The influence of this factor is described in section 2. The equations presented by Lytton [49], also detailed in section 2, consider the change in binder hardness in terms of the binder softening point. The work by Lytton has been incorporated with a modified fatigue life design method given in the form of a flow chart, Fig.A4.1. The complexity of this modified method is increased by the fatigue constant A and the stress intensity factor both varying as the binder hardens with age. Therefore a solution may only be formed through an iterative process.

2. Method

To demonstrate the various stages of the method a base course of 60mm of DBM is assumed for which the binder, mix and fatigue properties are known. The input data required is tabulated in table A4.1. For each month of the year the pavement age (Col.I) is calculated from the time of laying, and modified softening point calculated for the relevant formula (Col.III). For each ageing increment (Col.IV) the bitumen stiffness is read from Van Der Poel's nomograph, Fig.A4.2 and the mix stiffness (Col.VI) from creep tests carried out on the original material, Fig. A3.2. Bitumen stiffness is also related to fatigue constant 'A' derived from the results of crack opening fatigue tests (Col.V).

The second stage involves the calculation of the stress intensity factor for each increment of age and crack length. The data is confined to the first month after laying but a similar procedure is

required for all subsequent months of the year.

The iterative calculations, using Paris' Equation, are carried out in the third stage of the procedure to derive the days required for the crack to propagate each crack length increment. The calculations required for the first three increments are given and may be repeated for subsequent crack growth through this layer.

After full depth cracking the respective time, in days, is summed to provide the ultimate life of the layer.

TABLE A4.1

(I) PAVEMENT AGE (N) DAYS	(II) MONTHS	(III) MODIFIED SP. $SP_r(t)$·C (LYTTON)	(IV) S_b (N/m^2) (NOMOGRAPH)	(V) CONST.A.	(VI) S_{md} (N/m^2) (CREEP TESTS)
10	0.32	-	1×10^4	$1.5 \times 10^{-3}(A_1)$	2.5×10^7
20	0.64	-	1×10^4	$1.5 \times 10^{-3}(A_1)$	2.5×10^7
50	1.61	47.9	1.5×10^4	$2 \times 10^{-4}(A_2)$	3.2×10^7
75	2.41	50.71	4×10^4	$1 \times 10^{-5}(A_3)$	6.8×10^7
100	3.22	52.71	6×10^4	$3 \times 10^{-6}(A_4)$	8.0×10^7
200	6.45	56.4	9×10^4	$9 \times 10^{-7}(A_5)$	1.2×10^8
400	12.9	60.47	3×10^5	$9 \times 10^{-9}(A_6)$	2.2×10^8
500	16.1	61.7	5×10^5	$8 \times 10^{-10}(A_7)$	3.1×10^8
800	25.8	64.1	9×10^5	$1 \times 10^{-10}(A_8)$	5.5×10^8
1000	32.2	65.8	2×10^6	$6 \times 10^{-12}(A_8)$	1.0×10^9

Bitumen Ageing Regression Equation (LYTTON)[49]

$$SP_r(t) = -30.6 + 1.23\ SP_i + 10.5 \log_e t \qquad - (1)$$

where SP_i is original softening point in °F (47.5°C) 117.5°F

$SP_r(t)$ is the softening point of the recovered bitumen, in °F, after time t in months

therefore $SP_r(t) = 114 + 10.5 \log_e t$

3 Numerical Integration of Paris Equation[81]

$\Delta N \times A k_r^n = \Delta c$ - (2)

where ΔN increment of fatigue life (Days)

A and n fatigue constants

k_r stress intensity factor

Δc increment of crack growth

4 Iterative Calculations

The increments of pavement age (ΔN) and values of fatigue constant A, Table A4.1, have been combined with the corresponding values of the stress intensity factor (k_r) in an iterative routine on the prime computer. The routine numerically integrates Paris Equation for the range of increments of ΔN and derives the number of cycles required for the predefined increment of crack growth, 10mm, to occur. For example:

1st Increment (c = 0 - 10mm Crack Length) Δc = 10mm

$\Delta N \times A\ k_r^n = \Delta c$

Trial (1) $10 \times 1.5 \times 10^{-3} \times 1.19^{8.5}$ = 0.066mm TOO LOW

Trial (2) $50 \times 2 \times 10^{-4} \times 1.52^{8.5}$ = 0.35mm TOO LOW

Trial (3) $75 \times 1 \times 10^{-5} \times 3.2^{8.5}$ = 14.75mm TOO HIGH

Trial (4) $100 \times 3 \times 10^{-6} \times 3.8^{8.5}$ = 25.4mm TOO HIGH

ΔN_1 derived from iterative routine = 70 Days for 10mm crack growth

2nd Increment ΔN_2 + 70

(Δc = 10mm to 20mm Crack Length)

ΔN_2 from iterative routine = 110 Days

3rd Increment ΔN_3 + 180 Days

(c = 20 to 30mm crack length)

ΔN_3 from iterative routine = 230 Days

Total for 30mm crack = 410 Days

The procedure can be repeated to account for crack growth through the full depth of surfacing however the method is more complex than indicated in this example as fatigue constant n will also vary as the hardness of the bitumen increases with age.

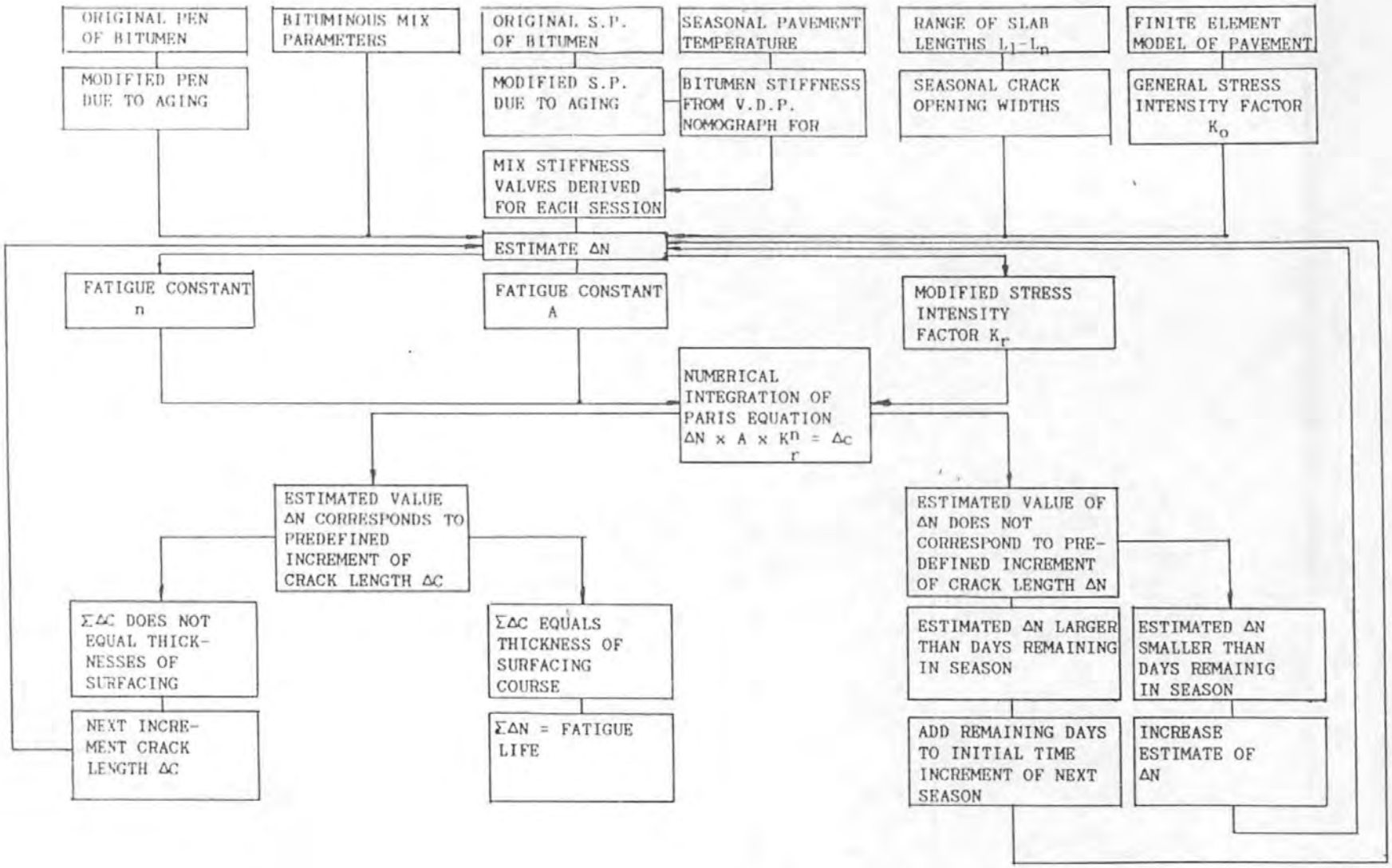

FIG.A4.1 MODIFICATION TO THE TENSILE FATIGUE MODEL ALLOWING FOR BITUMEN HARDENING

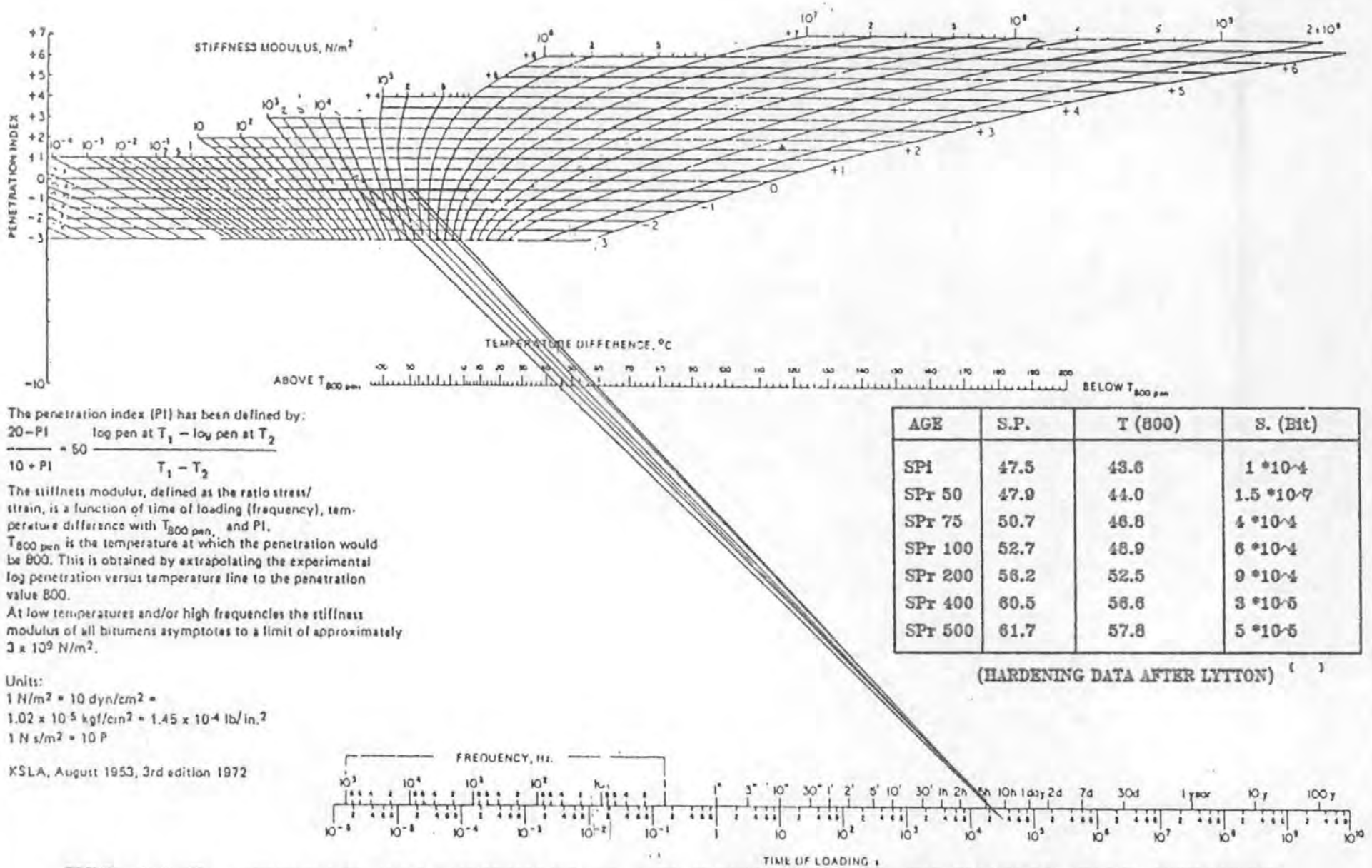

The penetration index (PI) has been defined by:

$$\frac{20-PI}{10+PI} = 50\,\frac{\log \text{pen at } T_1 - \log \text{pen at } T_2}{T_1 - T_2}$$

The stiffness modulus, defined as the ratio stress/strain, is a function of time of loading (frequency), temperature difference with $T_{800\ pen}$, and PI.
$T_{800\ pen}$ is the temperature at which the penetration would be 800. This is obtained by extrapolating the experimental log penetration versus temperature line to the penetration value 800.
At low temperatures and/or high frequencies the stiffness modulus of all bitumens asymptotes to a limit of approximately 3×10^9 N/m².

Units:
1 N/m² = 10 dyn/cm² =
1.02×10^{-5} kgf/cm² = 1.45×10^{-4} lb/in.²
1 N s/m² = 10 P

KSLA, August 1953, 3rd edition 1972

AGE	S.P.	T (800)	S. (Bit)
SPi	47.5	43.6	1 *10^4
SPr 50	47.9	44.0	1.5 *10^7
SPr 75	50.7	46.8	4 *10^4
SPr 100	52.7	48.9	6 *10^4
SPr 200	56.2	52.5	9 *10^4
SPr 400	60.5	56.6	3 *10^5
SPr 500	61.7	57.8	5 *10^5

(HARDENING DATA AFTER LYTTON) ( )

FIG.A4.2 EFFECT ON STIFFNESS OF BITUMEN HARDENING FOR WINTER SEASON (JANUARY) MEAN DAILY TEMPERATURE 3.9 DEG .C

APPENDIX 5

GRADING ENVELOPES FOR TEST MIXES

DENSE BITUMEN MACADAM TO B.S. 4987

OPEN BITUMEN MACADAM TO B.S.4987

HOT ROLLED ASPHALT TO B.S.594

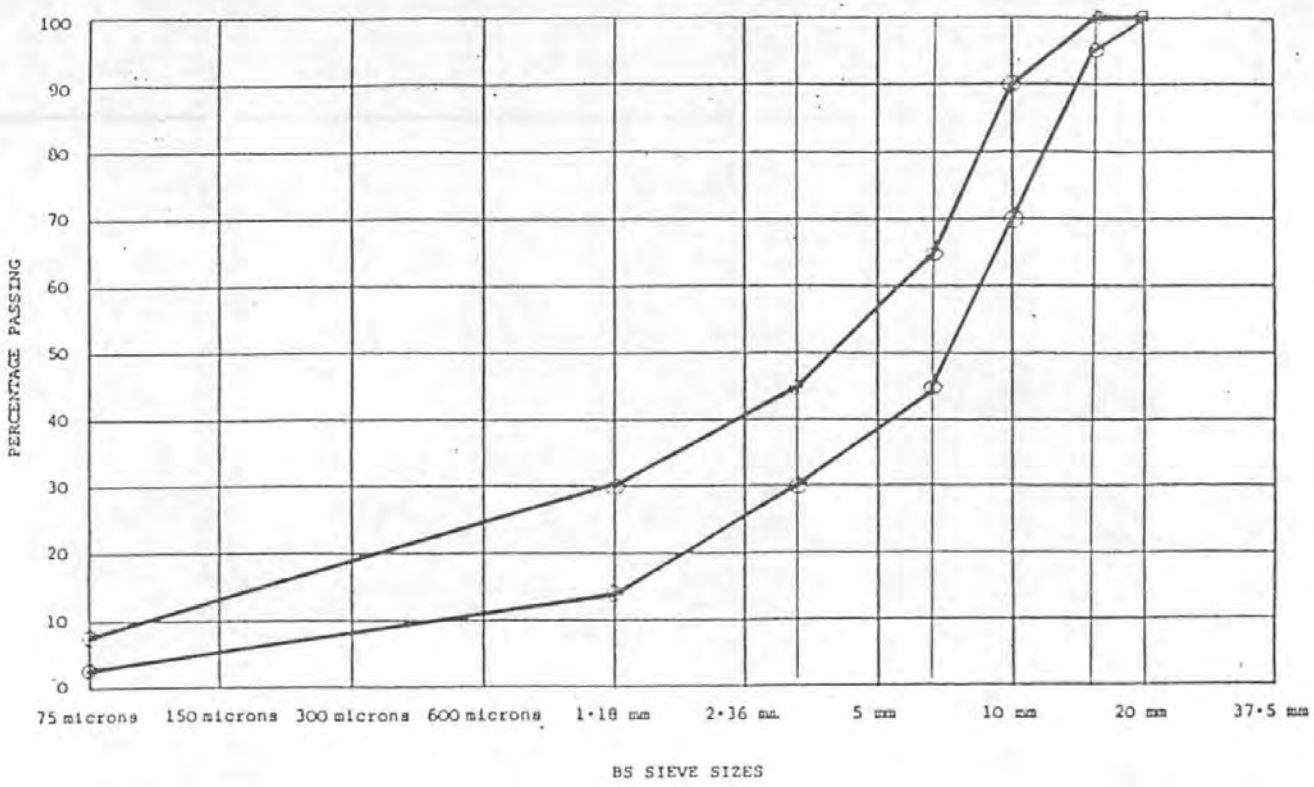

GRADING ENVELOPE FOR 14mm D.B.M WEARING COURSE TO B.S. 4987

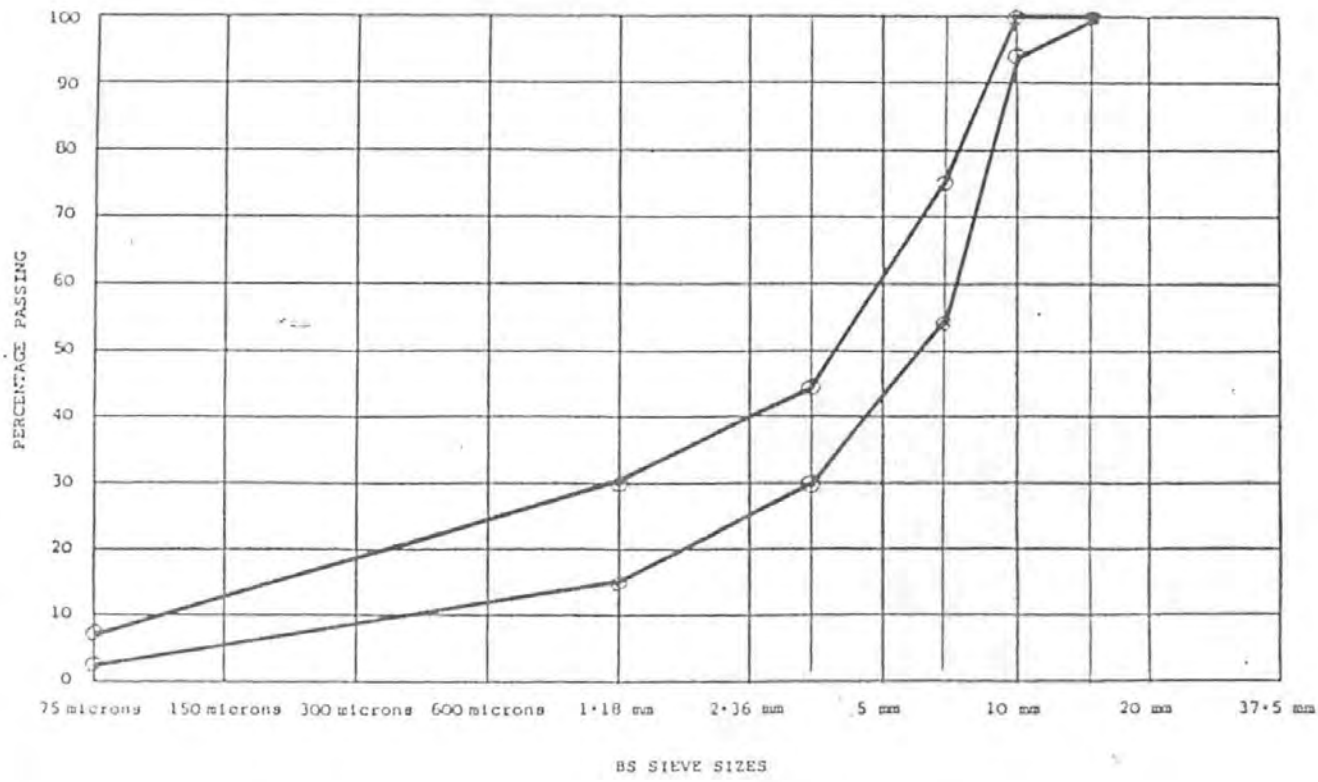

GRADING ENVELOPE FOR 10mm D.B.M. WEARING COURSE TO B.S. 4987

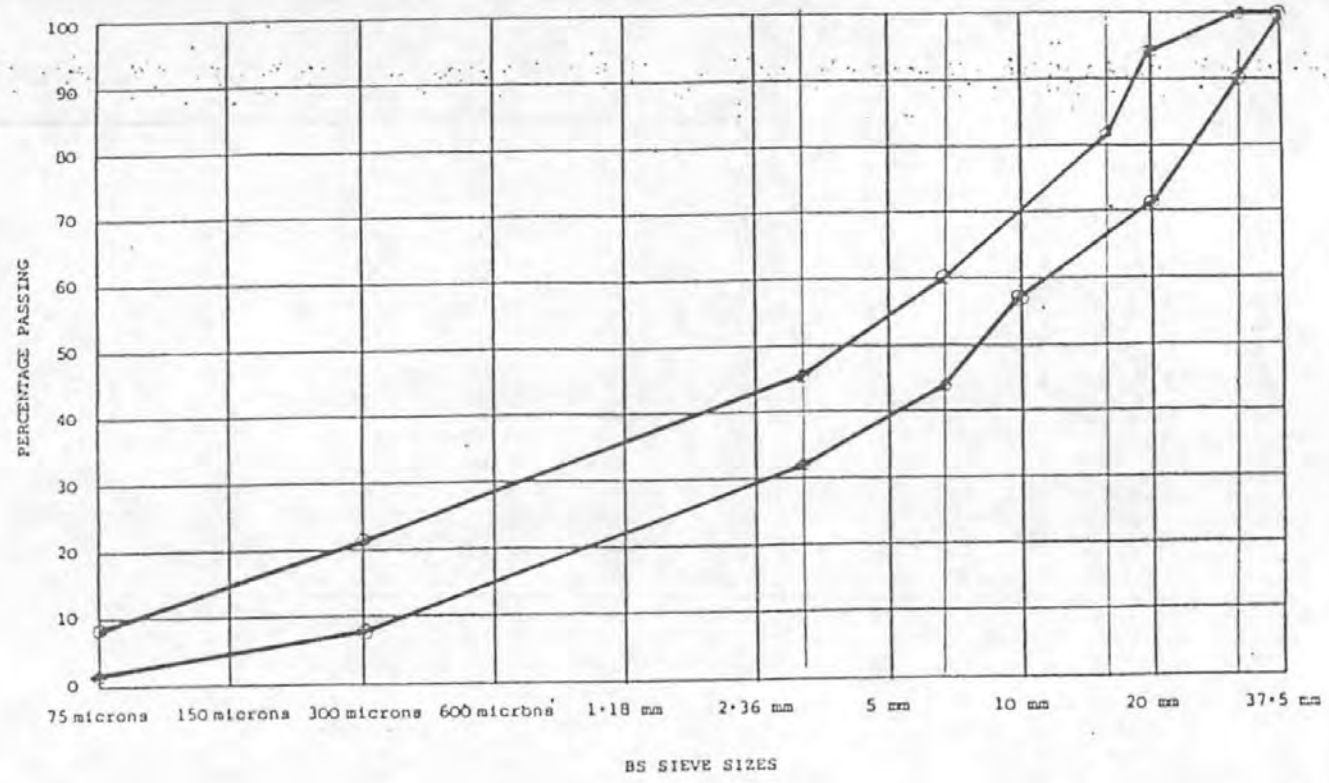

GRADING ENVELOPE FOR 28mm D.B.M BASE COURSE TO B.S. 4987

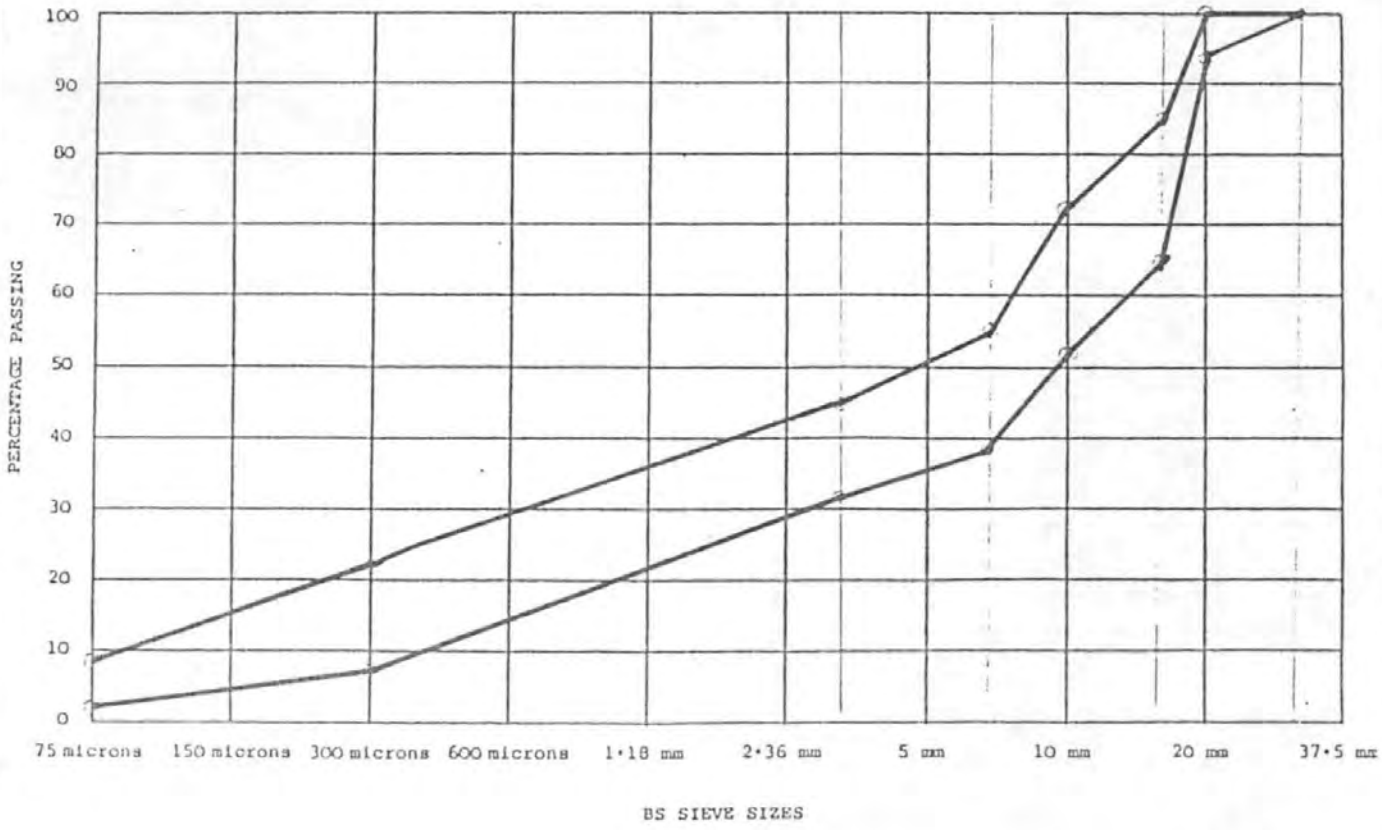

GRADING ENVELOPE FOR 20mm D.B.M. BASE COURSE TO B.S. 4987

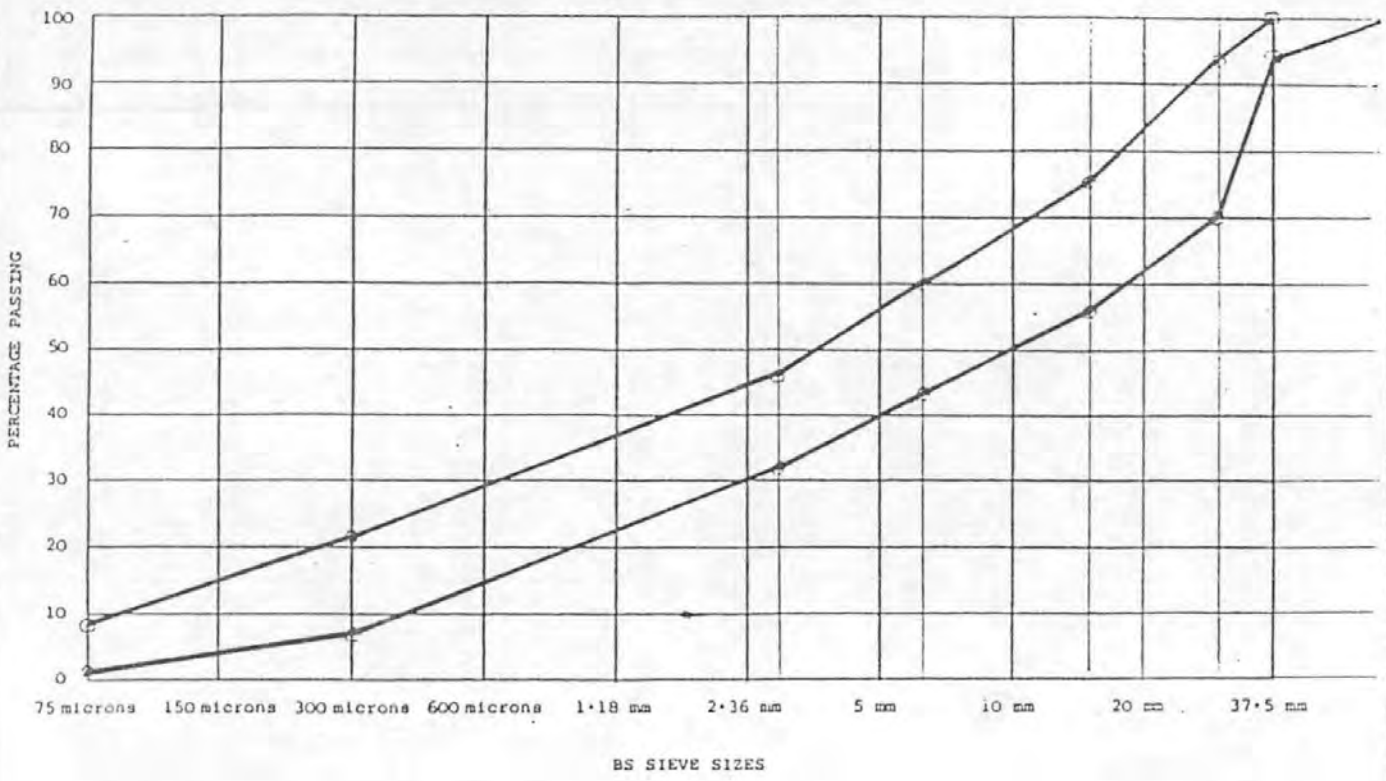

GRADING ENVELOPE FOR 40mm D.B.M BASE COURSE TO B.S. 4987

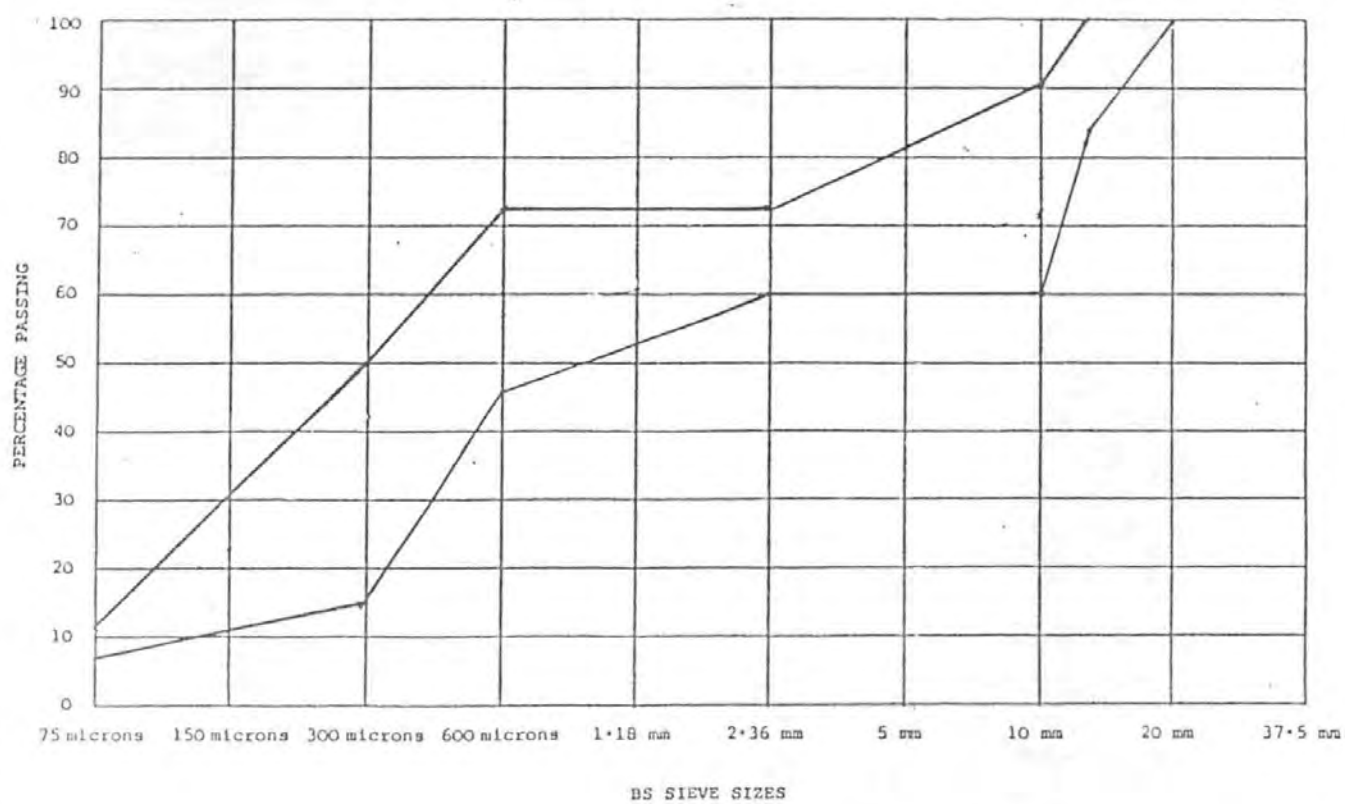

GRADING ENVELOPE FOR H.R.A.TYPE F DES.30/14 TO B.S. 594

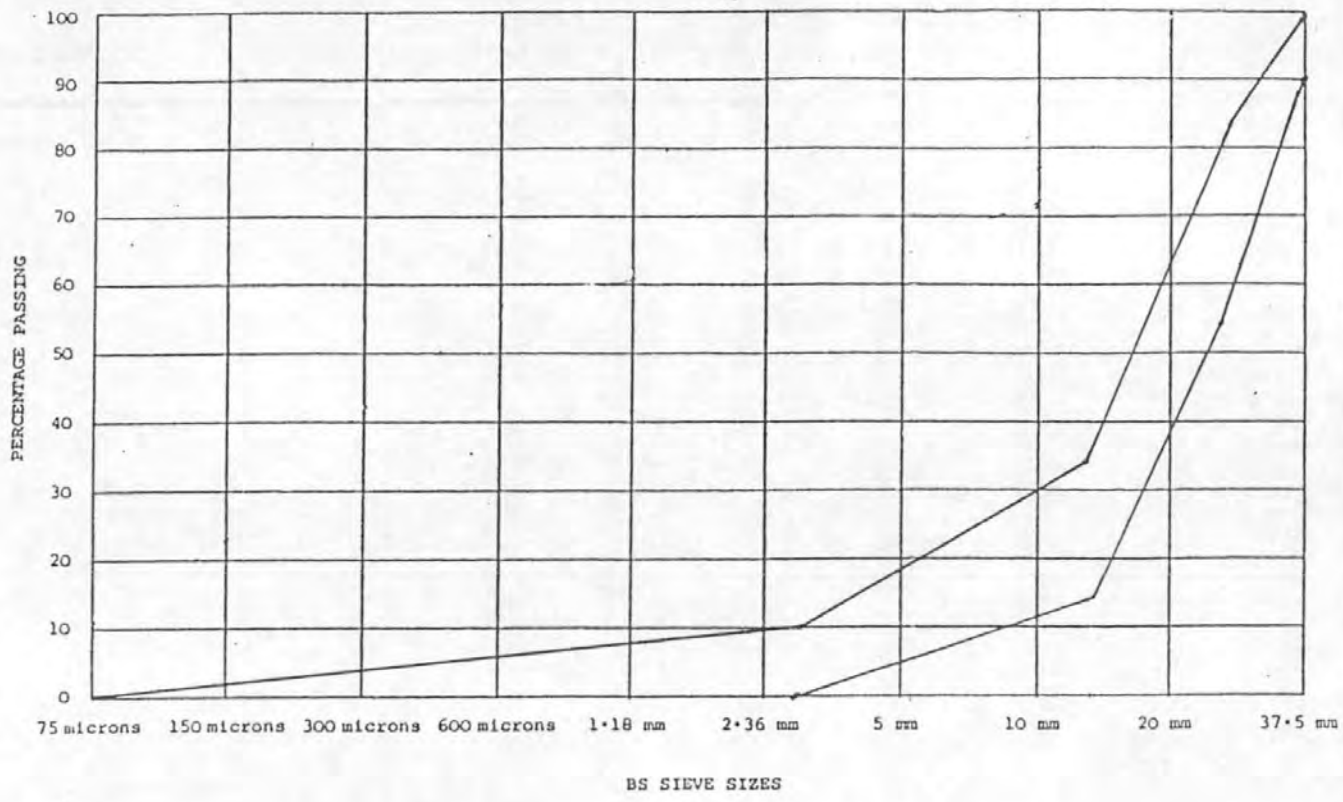

GRADING ENVELOPE FOR 40mm OPEN MACADAM TO B.S. 4987

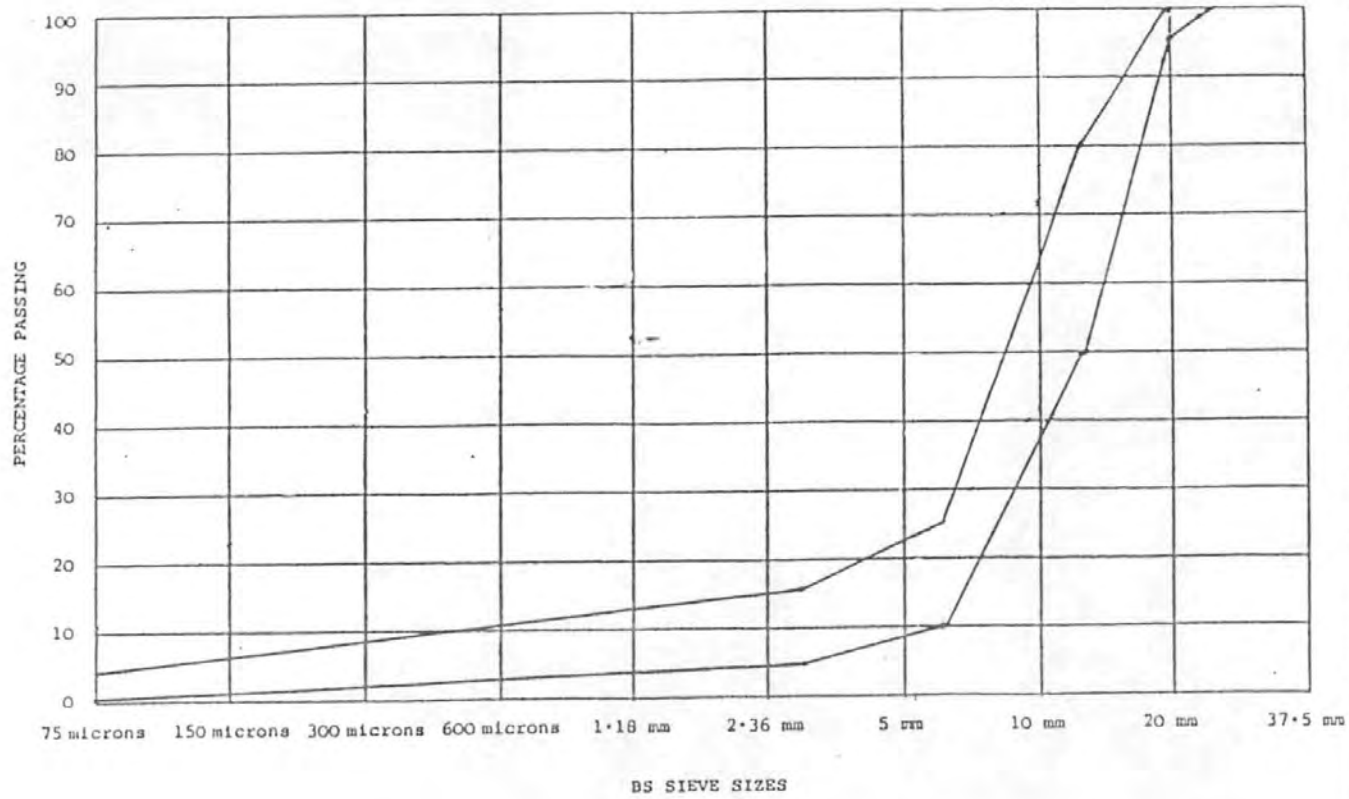

GRADING ENVELOPE FOR 20mm OPEN MACADAM TO B.S. 4987

APPENDIX 6

BASIC PROGRAM LISTINGS

(1) RFT 100 FATIGUE LIFE DUE TO THE MECHANISM OF TENSILE FATIGUE

(2) CRP 100 CALCULATION OF YIELD STRAIN FROM CREEP TEST DATA

(3) PL 11 TENSILE FATIGUE TEST RIG CONTROL PROGRAM

PROGRAM LISTING FOR PL11

TENSILE FATIGUE TEST RIG CONTROL PROGRAM

```
1 REM SPECIAL BLOCK PROGRAM FOR PLYMOUTH POLYTECHNIC SYF 55H VERSION 1B
2 CLEAR @ PRINT @ PRINT @ PRINT @ PRINT
3 REM LAST EDIT. ACJR/5 DEC 84
4 ON TIMEOUT 7 GOTO 1500
5 IMAGE 2,B
6 RESET 7 @ SEND 7 ; TALK 21 UNL LISTEN 0
7 SEND 7 ; CMD 2 @ REMOTE 704 @ OUTPUT 704 ;"HA"
8 Y=SPOLL(700) @ Z=SPOLL(704) @ DISP X;Y;Z @ WAIT 1000
9 OUTPUT 704 ;"HA" @ IF Z>64 THEN ENTER 704 ; Z$@ DISP Z$
10 IF Z=0 THEN 11 ELSE A
11 ! OUTPUT 705 ;"IN"
12 GOSUB 9550
20 REM INITIALISE DATA
21 K=0 @ REAL F0
22 REAL F1
23 DIM M0(500)
24 DIM L1(500)
25 DIM L2(500)
26 DIM B$[100]
27 DIM C(10,2)
28 DIM L(10,2)
29 FOR I=1 TO 10
30 FOR J=1 TO 2
31 C(I,J)=0 @ L(I,J)=0
32 NEXT J
33 NEXT I
34 N9=0 @ P=0 @ N7=0 @ T0=0 @ H1=0
35 C1=1
100 REM LOCATE DATA
102 DISP
105 GOSUB 9500
110 IF K=0 THEN 110
115 K=0
117 REM ORION INFO
118 GOSUB 6700
120 REM WAVEFORM CALCS
121 GOSUB 9550
122 DISP "CALCULATING WAVEFORM DATA"
123 ! PRINT @ PRINT
125 REM NO OF EVENTS/LOW CYCLE
126 E=INT(F1/(F0*N1)) ! -1 ! @ DISP "E=";E
127 IF E>500 THEN F1=.5*F1 @ GOTO 126
128 ! PRINT "EVENT LEVELS";E
129 REM TOTAL CYCLES N8
130 N8=N0*N1*E
131 IF F1>.01 AND F1<9 OR F1=.01 THEN R=64 @ F1=F1*10 ELSE R=0
132 ! PRINT "TOTAL TEST CYCLES";N8
133 REM TOTAL EVENTS TO BE TRANSMITTED TO -015
134 E9=2*N0*E ! @ PRINT "TRANSMITTED EVENTS=";E9 @ PRINT
135 FOR I=1 TO E
140 M0(I)=A0*SIN(2*PI*(I/E))
141 ! PRINT USING "DD,SDD.D" ; I;M0(I)
145 NEXT I
146 M0(0)=0 ! @ M0(E+1)=0
147 A9=A1 ! COPY
150 FOR I=1 TO E
155 IF A1=0 THEN L1(I)=.5*(M0(I)+M0(I-1)) ELSE L1(I)=M0(I)+A1
156 IF A1=0 THEN L2(I)=M0(I) ELSE L2(I)=M0(I)-A1
157 ! PRINT USING "DD,SDD.D,SDD.D" ; I;L1(I);L2(I)
158 NEXT I
159 L2(0)=0 ! @ L2(0)=L2(E)
160 SEND 7 ; TALK 21 UNL LISTEN 0
161 SEND 7 ; CMD 15,11,31
162 !  DISP "PLOT AXES Y/N";@ INPUT Y$
163 ! GOSUB 8000
164 REM START BUTTON
165 GOSUB 6600
170 REM MODE CHANGE
171 GOSUB 6500
172 J=1 @ J1=254 @ I=1 @ 19=1
173 DISP "TRANSMITTING DATA" @ L2(0)=S
174 REM TRANSMIT DATA
175 GOSUB 6000
176 J1=127 ! NO OF UPDATE EVENTS
209 REM START WAVEFORM
210 CLEAR 700
211 OUTPUT 704 ;"RU"
213 WAIT 1000
214 GOSUB 9550 @ DISP "TEST RUNNING" @ GOSUB 2300 @ T1=TIME
215 ON KEY# 1,"STOP" GOSUB 2000
216 ON KEY# 2,"HOLD" GOSUB 2100
218 KEY LABEL
219 Y=SPOLL(700)
220 IF BINAND(Y,65) THEN J1=127 @ GOSUB 6000
225 Z=SPOLL(704)
230 IF Z<>0 THEN GOSUB 6900
235 ! INT "Y=";Y;"Z=";Z;"P=";P;"236 !
240 !  IF P>0 THEN GOSUB 8300
242 IF H1=1 THEN 480
245 T2=INT((TIME-T1)*F9)+T0
480 IF T2<N8 THEN 484 ELSE 2015
484 T4=F0/F1*T2
485 ON KEY# 7,"CURRENT" GOSUB 2400
490 ON KEY# 8,"CYCLES " GOSUB 2400
495 ON KEY# 4,VAL$(T2) GOSUB 2400
496 GOTO 500
497 GOTO 500
500 KEY LABEL
501 IF C1=100 THEN 502 ELSE 900
502 ! PRINT "CURRENT PRIMARY CYCLES";T4*10
503 ! PRINT "T2=";T2
504 C1=0
900 C1=C1+1
1000 GOTO 219
1500 ON TIMEOUT 7 GOTO 1535
1505 Y=SPOLL(700)
1510 ON TIMEOUT 7 GOTO 1540
1515 X=SPOLL(704)
1520 ! ON TIMEOUT 7 GOTO 1545
1525 ! Z=SPOLL(705)
1530 DISP "SOMETHING TIMEOUT" @ RESET 7
1531 STOP
1535 DISP "CONTROL INTERFACE TIMEDOUT" @ RESET 7
1536 STOP
1540 DISP "ORION TIMED OUT" @ RESET 7
```

```
1541 STOP
1545 ! DISP "PLOTTER TIMED OUT" @ PRINT 7 ; STOP
2000 SEND 7 ; TALK 21 UNL LISTEN 0
2005 SEND 7 ; CMD 2
2015 OUTPUT 704 ;"HA"
2020 CLEAR @ GOSUB 9550
2025 DISP @ DISP "TEST STOPPED"
2035 DISP "CURRENT CYCLES";T2
2040 DISP @ DISP "RETURN TO MANUAL Y/N";@ INPUT S$
2045 IF S$="Y" THEN GOSUB 2500
2050 DISP @ DISP "ANOTHER RUN Y/N";@ INPUT S$
2055 IF S$="Y" THEN 1
2060 DISP @ DISP "PROGRAM END" @ STOP
2100 SEND 7 ; TALK 21 UNL LISTEN 0
2105 SEND 7 ; CMD 2
2110 H1=1 @ T0=T2 ! STOP THE CLOCK
2115 OUTPUT 704 ;"PA"
2125 OFF KEY# 2 @ ON KEY# 3,"CONT" GOSUB 2200
2135 KEY LABEL
2140 RETURN
2200 SEND 7 ; TALK 21 UNL LISTEN 0
2205 SEND 7 ; CMD 3
2210 H1=0 @ T1=TIME ! RUN THE CLOCK
2215 OUTPUT 704 ;"GO"
2225 OFF KEY# 3 @ ON KEY# 2,"HOLD" GOSUB 2100
2235 KEY LABEL
2240 RETURN
2300 DISP @ DISP "LOW FREQUENCY ";F0;"HZ"
2305 DISP "AMPLITUDE ";A0;"%"
2310 DISP "NO OF CYLES ";N0
2311 IF R=64 THEN F9=F1/10 ELSE F9=F1
2315 DISP @ DISP "HIGH FREQUENCY ";F9;"HZ"
2320 DISP "AMPLITUDE ";A1;"%"
2325 DISP "NO OF CYCLES PER LEVEL";N1
2330 DISP "TOTAL CYCLES";N8;"LOG EACH";C9
2335 RETURN
2400 RETURN
2500 DISP "PRESS 'ENDLINE' WHEN MANUAL LEVELS ARE SET"
2505 INPUT S$
2510 SEND 7 ; TALK 21 UNL LISTEN 0
2515 SEND 7 ; CMD 28
2530 RETURN
5000 GOTO 5000
5500 REM EXTRA WAVEFORM TO RETURN TO MEAN LEVEL AFTER LAST EVENT
5505 A=INT((A9-S)*20.48)
5506 IF A<0 THEN A=-A @ D1=128 ELSE D1=0
5510 A1=INT(A/16) @ A2=A-16*A1
5515 M=INT((S-A9)*10.24)+2048
5520 M1=INT(M/16) @ M2=M-16*M1
5525 PRINT I9,A1,A2,M1,M2
5530 OUTPUT 700 USING 5 ; W1+R+D1,A1,A2,M1,M2,F1,1,0,1,0,0,128,0,1,0,0
5535 RETURN
6000 ! PRINT "TRANSMITTING DATA,J1=";J1
6005 IF I9=E9 OR I9>E9 THEN GOTO 5500
6010 IF FP(I9/2)=0 THEN 6040 ! 2ND EVENT IF I9 IS EVEN
6020 IF I9=1 THEN L2(0)=0 ELSE L2(0)=L2(I) ! LST EVENT IN PAIR
6021 A=L1(I)-L2(I-1) ! /2 ! AMPLITUDE
6022 M=S+(L1(I)+L2(I-1))/2 ! MEAN LEVEL
6023 IF A<0 THEN A=-A @ D1=128 ELSE D1=0
6024 A=INT(A*20.48) ! CONVERT TO BITS
6025 M=INT(M*20.48)+2048 !
6026 A1=INT(A/16) @ A2=A-16*A1
6027 M1=INT(M/16) @ M2=M-16*M1
6029 ! PRINT J;I;I9;A1;A2;M1;M2 ! ;D1;W1
6030 OUTPUT 700 USING 5 ; W1+R+D1,A1,A2,M1,M2,F1,1,0
6031 J=J+1 @ I9=I9+1
6033 IF J=J1+1 THEN J=1 @ RETURN
6040 REM 2ND EVENT
6041 A=L2(I)-L1(I) ! AMPLITUDE
6042 M=S+(L1(I)+L2(I))/2 ! MEAN LEVEL
6043 IF A<0 THEN A=-A @ D1=128 ELSE D1=0
6044 A=INT(A*20.48) ! CONVERT TO BITS
6045 M=INT(M*20.48)+2048 !
6046 A1=INT(A/16) @ A2=A-16*A1
6047 M1=INT(M/16) @ M2=M-16*M1
6049 ! PRINT J;I;I9;A1;A2;M1;M2 ! ;D1;W1
6050 OUTPUT 700 USING 5 ; W1+R+D1,A1,A2,M1,M2,F1,2*N1-1,0
6051 J=J+1 @ I9=I9+1 @ I=I+1
6052 IF I=E+1 THEN I=1
6053 IF J=J1+1 THEN J=1 @ RETURN
6055 GOTO 6005
6500 GOTO 6505
6501 IMAGE 22A,SDDD.D
6505 SEND 7 ; TALK 21 UNL LISTEN 0
6510 SEND 7 ; CMD 7
6515 WAIT 2000
6520 TRIGGER 700
6525 P1=128 @ P2=0 ! ENTER 700 USING 5 ; D1,P1,P2,L1,L2,S1,S2
6530 S=(2048-P1*16-P2)/20.48
6535 DISP USING 6501 ; "MODE CHANGE TO POS AT ";S;"%"
6555 RETURN
6600 DISP "PRESS GREEN BUTTON ON CONSOLE TO START TEST"
6605 K=1
6610 SEND 7 ; TALK 21 UNL LISTEN 0
6615 SEND 7 ; CMD 22
6620 IF K>0 THEN SEND 7 ; CMD 18
6630 TRIGGER 700 @ ENTER 700 USING 5 ; S1
6635 IF NOT BINAND(S1,1) THEN 6645
6640 SEND 7 ; TALK 21 UNL LISTEN 0
6641 SEND 7 ; CMD 22,19
6642 RETURN
6645 K=-K @ GOTO 6610
6700 GOSUB 9550 @ GOSUB 9555
6705 DISP "LOGGING DATA"
6710 DISP "NUMBER OF STRAIN CHANNELS (1-10)" @ INPUT M9
6711 M1$=VAL$(2*M9)
6715 DISP "NUMBER OF HIGH CYCLES BETWEEN LOGS" @ INPUT C9
6720 REM TIME BETWEEN LOGS T9
6721 T9=INT(C9/F1)
6722 IF T9<60 THEN M8=0 @ S8=INT(T9) ELSE M8=INT(T9/60) @ S8=INT(T9-60*M8)
6725 DISP "COMMUNICATING WITH ORION"
6730 GOSUB 6800
6731 OUTPUT 704 ;"CH 1-";M1$;" SE 611"
```

```
 732 GOSUB 6800
6745 ! OUTPUT 704 ;"IN CH 1-";M1$
6746 ! GOSUB 6800
6747 OUTPUT 704 ;"CH 1-";M1$;" PR MM MU 1"
6748 GOSUB 6800
6750 OUTPUT 704 ;"TA1 OP ME"
6751 GOSUB 6800
6755 OUTPUT 704 ;"TA1 TR TI DE 00-00:";VAL$(M8);":";VAL$(S8);".0"
6756 GOSUB 6800
6760 OUTPUT 704 ;"TA1 CO * RE IN IN 00:";VAL$(M8);":";VAL$(S8);".0"
6761 GOSUB 6800
6765 OUTPUT 704 ;"TA1 CH 1-";M1$;" AT F"
6766 GOSUB 6800
6770 OUTPUT 704 ;"TA1 LO PR MA EV"
6771 GOSUB 6800
6775 OUTPUT 704 ;"TA1 FO CO TO GP"
6776 GOSUB 6800
6780 WAIT 2000
6785 RETURN
6800 Z=SPOLL(704)
6805 IF BINAND(Z,64) THEN ENTER 704 ; B$@ BEEP @ PRINT "ORION RECEIVED MESSAGE "
6810 IF BINAND(Z,62) THEN ENTER 704 ; B$@ BEEP @ PRINT "ORION RECEIVED DATA ";B$
6815 RETURN
6900 ENTER 704 ; B$@ BEEP @ ! DISP B$
6901 REM COLLECT STRAINS FROM ORION
6905 IF B$[1,1]<>"S" THEN RETURN
6910 FOR P=1 TO M9 STEP 2
6915 ENTER 704 ; B$
6918 IF B$[1]="D" THEN GOTO 6915
6919 IF B$[1]="D" THEN GOTO 6905
6920 C(P,1)=VAL(B$[6,13]) @ C(P,2)=VAL(B$[26,33])
6925 IF LEN(B$)>40 THEN C(P+1,1)=VAL(B$[46,53]) @ C(P+1,2)=VAL(B$[66,73]) ELSE RI
6930 NEXT P
6950 RETURN
8000 DIM A$[100]
8010 OUTPUT 705 ;"IN;SP2;IP;"
8020 OUTPUT 705 ;"SC 0 1000 -100 100;"
8021 OUTPUT 705 ;"SL .3"
8022 OUTPUT 705 ;"SI .1 .2;TL 1.5 .1;"
8025 OUTPUT 705 ;"DT !;"
8026 IF Y$="N" THEN RETURN
8030 OUTPUT 705 ;"PU 0 0 PD 1000 0 0 0 0 100 0 -100 PU"
8035 OUTPUT 705 ;"SL .3"
8040 OUTPUT 705 ;"SI .1 .2;TL 1.5 .1;"
8045 FOR I=100 TO 1000 STEP 100
8050 OUTPUT 705 ;"PA";I;" 0;XT;"
8055 READ A$
8060 OUTPUT 705 ;"CP -3 -1;LB";A$
8070 NEXT I
8075 OUTPUT 705 ;"CP -10 -3;LBCYCLES"
8080 FOR I=-100 TO 100 STEP 10
8090 OUTPUT 705 ;"PA 0 ";I;";YT;"
8100 READ A$
8110 OUTPUT 705 ;"CP 1 .2;LB";A$
8120 NEXT I
8125 OUTPUT 705 ;"CP 5 -2;LB%-MICROSTRAIN"
 130 OUTPUT 705 ;"CP -12 2;LB---"
8132 OUTPUT 705 ;"CP 1 0;LBMIN"
8135 OUTPUT 705 ;"CP 10 0;LBMAX"
8140 OUTPUT 705 ;"SP1;CP -8 0;LB---"
8145 OUTPUT 705 ;"CP 80 -1;SI .4 .6;LBINSTRON,LTD."
8150 OUTPUT 705 ;"SI .1 .2;SP2"
8155 OUTPUT 705 ;"PU 0 0"
8160 DATA "100","200","300","400","500","600","700","800","900","1000"
8165 DATA "-100","-90","-80","-70","-60","-50","-40","-30","-20","-10","0.0"
8170 DATA "10","20","30","40","50","60","70","80","90","100"
8175 RETURN
8300 FOR P=1 TO M9
8303 IF N9=0 THEN OUTPUT 705 ;"SP2;LT;PU ";N9+C9;C(P,1);"PD PU 0 0" @ GOTO 830
8305 OUTPUT 705 ;"SP2;LT;PU ";N9;L(P,1);"PD ";N9+C9;" ";C(P,1);" PU"
8306 IF FP(N9/100)>0 THEN 8308
8307 OUTPUT 705 ;"CP 0 -1;LB";VAL$(P)
8308 OUTPUT 705 ;"PU 0 0"
8310 L(P,1)=C(P,1)
8315 NEXT P
8320 FOR P=1 TO M9
8323 IF N9=0 THEN OUTPUT 705 ;"SP1;LT;PU ";N9+C9;C(P,2);"PD PU 0 0" @ GOTO 832
8325 OUTPUT 705 ;"SP1;LT;PU ";N9;L(P,2);"PD ";N9+C9;" ";C(P,2);" PU 0 0"
8326 IF FP(N9/100)>0 THEN 8328
8327 OUTPUT 705 ;"CP 0 -1;LB";VAL$(P)
8328 OUTPUT 705 ;"PU 0 0"
8330 L(P,2)=C(P,2)
8335 NEXT P
8345 P=0 @ N9=N9+C9
8350 RETURN
9300 GOSUB 9550
9305 GOSUB 9555
9310 DISP "LOW FREQUENCY VALUE IN HZ" @ INPUT F0
9315 DISP "AMPLITUDE IN %" @ INPUT A0
9320 DISP "NO OF CYCLES" @ INPUT N0
9325 DISP
9326 GOSUB 9550 @ GOSUB 9555
9327 F1=1
9330 DISP "HIGH FREQUENCY VALUE IN HZ" @ INPUT F1
9335 DISP "HIGH FREQ AMPLITUDE IN %";@ INPUT A1
9336 IF A1=0 THEN N1=1 @ W1=1 @ GOTO 9399 ELSE W1=2
9340 DISP "NUMBER OF CYCLES PER LEVEL" @ INPUT N1
9399 K=1 @ RETURN
9400 K=2 @ RETURN
9500 ! ON KEY£ 1,"FILE" GOSUB 9400
9501 ON KEY£ 2,"KEYBOARD" GOSUB 9300
9502 OFF KEY£ 7
9503 OFF KEY£ 8
9504 OFF KEY£ 4
9505 OFF KEY£ 3
9506 OFF KEY£ 1
9509 KEY LABEL @ RETURN
9550 CLEAR @ DISP @ DISP "BLOCK PROGRAM/PLYMOUTH POLY"
9551 DISP "----------------------------"
9552 RETURN
9555 DISP "KEYBOARD DATA ENTRY"
9556 DISP
9559 RETURN
9999 END
```

PROGRAM LISTING FOR RFT 100

FATIGUE LIFE DUE TO MECHANISM OF TENSILE FATIGUE

```
10    PRINT "THIS PROG FOR PRINT OUT OF RESULTS"
20  ! S1 AND S2 ARE BIT.STIFFNESS VALUES
30  ! A3 IS AN ARRAY FOR BIT STIFFNESS
40    DIM A3(9,12)
50    FOR J=1 TO 9
60      FOR I=1 TO 12
70        READ A3(J,I)
80        DATA 1200,1600,1000,600,180,50,40,60,25,300,900,1000
90        DATA 5400,6600,3000,2160,840,216,120,300,1320,1500,3000,4800
100       DATA 85000,90000,60000,23000,8000,3000,2500,4000,5000,10000,50000,600C
110       DATA 1200,1600,1000,600,180,50,40,60,25,300,900,1000
120       DATA 5400,6600,3000,2160,840,216,120,300,1320,1500,3000,4800
130       DATA 85000,90000,60000,25000,8000,3000,2500,4000,5000,10000,50000,600C
140       DATA 172000,187000,138000,80000,25000,8200,7200,8600,16100,44000,1210C
150       DATA 69000,75000,54000,30000,10000,3200,2800,3400,6300,17300,48000,56C
160       DATA 32000,34000,25000,13400,4400,1400,1220,1480,2800,7800,22000,2500C
170     NEXT I
180   NEXT J
190   DIM S2(12)
200   DIM S1(12)
210   DIM S3(12)
220   DIM S4(12)
230   DIM E1(12)
240   DIM E2(12)
250   DIM E3(12)
260   DIM E4(12)
270   DIM M1(12)
280   DIM K(12,200)
290   DIM Q(12,200)
300   DIM M(133)
310   DIM C(133)
320   DIM T(12)
330   DIM U(12)
340   DIM N1(12)
350   DIM N3(12)
360   DIM N2(12)
370   DIM N5(12)
371 DIM N6(12)
380   DIM G1(12)
390   DIM A1(12)
400   DIM A2(12)
410   DIM T2(12)
420   DIM T3(12)
430   DIM T1(12)
440   PRINT "WEARING COURSE SPEC:- "
450   PRINT "1) H.R.A  2) D.B.M"
460   PRINT "INPUT 1 OR 2"
470   INPUT Tt$
480   IF Tt$="1" THEN Ss$="H.R.A"
490   IF Tt$="2" THEN Ss$="D.B.M"
500   OUTPUT 701;"WEARING COURSE SPEC:- ";Ss$
510   IF Tt$="2" THEN 560
520   PRINT "H.R.A. IS A RECIPE MIX 1(a) TO B.S.594"
530   PRINT "INPUT THE ESTIMATED OXIDIZATION LEVEL 45,35,25 PEN"
540   INPUT Qq$
550   OUTPUT 701;"H.R.A WEARING COURSE OXIDIZED TO";Qq$;"PEN"
560   PRINT " INPUT BASE COURSE DEPTH"
570   DIM A(2,12)
580   INPUT D1
590   PRINT " INPUT WEARING COURSE DEPTH"
600   INPUT D2
610   D3=D1+D2
620   OUTPUT 701;"FULL DEPTH=";D3;"mm"
630   D4=D1+1
640   D5=D3*.8
650   DIM F$[12]
660   FOR I=1 TO 2
670 !
680     IF I=2 THEN 730
690     IF Tt$="1" THEN 750
700     PRINT "INPUT ORIGINAL GRADE OF BITUMEN FOR WEARING COURSE 50,100,200"
710     INPUT G1(I)
720     GOTO 750
730 PRINT "INPUT THE ORIGINAL GRADE OF BITUMEN FOR THE BASE COURSE 50,100,200"
740     INPUT G1(I)
750   NEXT I
760 !
770   PRINT "ARE THE MONTHLY BITUMEN STIFFNESS VALUES TO BE TAKEN ?"
780   PRINT "Y OR N"
790   INPUT Z$
800   IF Z$="Y" THEN 820
810   IF Z$="N" THEN 1320
820   IF Tt$="1" THEN 980
830   IF G1(1)<>200 THEN 880
840   FOR I=1 TO 12
850     S1(I)=A3(1,I)
860   NEXT I
870   GOTO 1150
880   IF G1(1)<>100 THEN 930
890   FOR I=1 TO 12
900     S1(I)=A3(2,I)
910   NEXT I
920   GOTO 1150
930   IF G1(1)<>50 THEN 20
940   FOR I=1 TO 12
950     S1(I)=A3(3,I)
960   NEXT I
970   GOTO 1150
980   IF Qq$="25" THEN 1000
990   GOTO 1040
1000  FOR I=1 TO 12
1010  S1(I)=A3(7,I)
1020  NEXT I
1030  GOTO 1150
1040  IF Qq$="35" THEN 1060
1050  GOTO 1100
1060  FOR I=1 TO 12
1070  S1(I)=A3(8,I)
1080  NEXT I
1090  GOTO 1150
1100  IF Qq$="45" THEN 1120
1110  GOTO 1150
1120  FOR I=1 TO 12
1130  S1(I)=A3(9,I)
```

```
1140  NEXT I
1150  IF G1(2)<>200 THEN 1200
1160  FOR I=1 TO 12
1170    S2(I)=A3(4,I)
1180  NEXT I
1190  GOTO 1480
1200  IF G1(2)<>100 THEN 1250
1210  FOR I=1 TO 12
1220    S2(I)=A3(5,I)
1230  NEXT I
1240  GOTO 1480
1250  IF G1(2)<>50 THEN 20
1260  FOR I=1 TO 12
1270    S2(I)=A3(6,I)
1280  NEXT I
1290  GOTO 1480
1300!
1310!
1320  PRINT "INPUT THE VALUES OF BITUMEN STIFFNESS FROM VAN-DER POELS NOMOGRAPH
1330  PRINT "NOMOGRAPH RECOVERED PROPERTIES IN N/mm^2 FOR EACH MONTH"
1340  A$="WEARING COURSE ,"
1350  B$="BASE     )"
1360  C$="COURSE)    "
1370  D$="(COURSE    "
1380  IMAGE 4X,9A,6X,8A
1390  PRINT USING 1380:A$,B$
1400  IMAGE 4X,9A,6X,8A
1410  PRINT USING 1400;D$,C$
1420  FOR I=1 TO 10
1430    READ P$
1440    PRINT P$;"="
1450    INPUT S1(I),S2(I)
1460    DATA JAN,FEB,MARCH,APRIL,MAY,JUNE,JULY,AUG,SEPT,OCT,NOV,DEC
1470  NEXT I
1480  FOR P=1 TO 2
1490    IF P=2 THEN 1580
1500    IF Tt$="2" THEN 1540
1510    T6=1.79
1520    T7=.354
1530    GOTO 2810
1540    U5=G1(P)
1550   PRINT "INPUT BITUMEN CONTENT 4.2%, 4.7%, 5.2%, 6.2%OF THE WEARING COURSE
1560    INPUT U6
1570    GOTO 1630
1580    U5=G1(P)
1590    OUTPUT 701;"BIT GRADE=";U5
1600 PRINT "INPUT THE BITUMEN CONTENT 4.2%,4.7%, 5.2%, 6.2%, OF THE BASE COURSE
1610    INPUT U6
1620    OUTPUT 701;"BIT. CONTENT=";U6
1630    IF U5=200 AND U6=4.2 THEN 1650
1640    GOTO 1680
1650    T6=2.46
1660    T7=.466
1670    GOTO 2810
1680    IF U5=200 AND U6=4.7 THEN 1700
1690    GOTO 1730
1700    T6=1.85
1710    T7=.466
1720    GOTO 2810
1730    IF U5=200 AND U6=5.2 THEN 1750
1740    GOTO 1780
1750    T6=1.98
1760    T7=.466
1770    GOTO 2810
1780    IF U5=200 AND U6=6.2 THEN 1800
1790    GOTO 1830
1800    T6=3.020
1810    T7=.466
1820    GOTO 2810
1830    IF U5=100 AND U6=4.2 THEN 1950
1840    IF U5=100 AND U6=4.7 THEN 1850
1850    IF U5=100 AND U6=5.2 THEN 1860
1860    IF U5=100 AND U6=6.2 THEN 1870
1870    IF U5=50 AND U6=4.2 THEN 1890
1880    GOTO 1920
1890    T6=2.15
1900    T7=.22
1910    GOTO 2810
1920    IF U5=50 AND U6=4.7 THEN 1930
1930    IF U5=50 AND U6=5.2 THEN 1940
1940    IF U5=50 AND U6=6.2 THEN 1950
1950    FOR J=1 TO 2
1960    IF Tt$="1" AND J=1 THEN 2470
1970      PRINT "INPUT VOID CONTENT AND AGGREGATE GRADING"
1980      IF J=2 THEN 2010
1990      PRINT "WEARING COURSE"
2000      IF J=1 THEN 2020
2010      PRINT "BASE COURSE"
2020      PRINT "RANGE OF METHOD"
2030      PRINT "3% TO 12% AND GRADING 40 28 20 10mm"
2040      INPUT V1,S$
2050      OUTPUT 701;"VOID CONTENT =";V1
2060      OUTPUT 701;"AGG =";S$
2070      IF 3<V1 AND 4.5>V1 THEN 2140
2080      IF V1=3 THEN 2140
2090      IF 4.5<V1 AND 6>V1 THEN 2240
2100      IF V1=4.5 THEN 2240
2110      IF 6<V1 AND 12>V1 THEN 2340
2120      IF V1=6 THEN 2340
2130      IF V1=12 THEN 2340
2140      IF S$="40" THEN 2180
2150      IF S$="28" THEN 2180
2160      IF S$="20" THEN 2200
2170      IF S$="10" THEN 2220
2180      T5=.1146*V1+1.394
2190      GOTO 2440
2200      T5=.71*V1+.01
2210      GOTO 2440
2220      T5=.456*V1+.945
2230      GOTO 2440
2240      IF S$="40" THEN 2280
2250      IF S$="28" THEN 2280
2260      IF S$="20" THEN 2300
2270      IF S$="10" THEN 2320
```

```
2280      T5=.180*V1+1.1
2290      GOTO 2440
2300      T5=.17*V1+2.44
2310      GOTO 2440
2320      T5=.293*V1+1.68
2330      GOTO 2440
2340      IF S$="40" THEN 2380
2350      IF S$="28" THEN 2380
2360      IF S$="20" THEN 2400
2370      IF S$="10" THEN 2420
2380      T5=.128*V1+1.41
2390      GOTO 2440
2400      T5=.11*V1+2.82
2410      GOTO 2440
2420      T5=.086*V1+7.19
2430 !
2440 !
2450      IF J=2 THEN 2530
2460      RESTORE
2470      PRINT "ARE THE FATIGUE CONSTANTS :A: REQUIRED  Y OR N"
2480      INPUT Y$
2490      IF Y$="N" THEN 2550
2500      IF Y$="Y" THEN 2510
2510      PRINT "FATIGUE CONSTANTS FOR THE GIVEN MONTHS  (WEARING COURSE):-"
2520      IF J=1 THEN 2540
2530      PRINT "FATIGUE CONSTANTS FOR THE GIVEN MONTHS  (BASE COURSE):-"
2540      RESTORE 1460
2550      FOR I=1 TO 12
2560      IF Tt$="1" AND J=1 THEN 2580
2570      GOTO 2610
2580      T33=LGT(S1(I))
2590      T11=(-T33+T6)/T7
2600      GOTO 2670
2610        IF J=2 THEN 2640
2620        T33=LGT(S1(I))
2630        IF J=1 THEN 2650
2640        T33=LGT(S2(I))
2650        T11=(-T33+T5)/.25347
2660 !
2670        A(J,I)=10^T11
2680 !
2690        IF Y$="N" THEN 2720
2700        READ F$
2710        PRINT F$,A(J,I)
2711        OUTPUT 701;F$,A(J,I)
2720      NEXT I
2730      IF Y$="N" THEN 2770
2740      PRINT " TO CONTINUE PRESS KEY K1"
2750      ON KEY 1 LABEL "P F C" GOTO 2770
2760      GOTO 2760
2770      IF Y$="N" THEN 2790
2780      IF J=2 THEN 3140
2790    NEXT J
2800    GOTO 3030
2810    IF P=2 THEN 2880
2820    FOR I=1 TO 12
2830      T33=LGT(S1(I))
2840        T11=(-T33+T6)/T7
2850        A1(I)=10^T11
2860      NEXT I
2870      GOTO 2930
2880      FOR I=1 TO 12
2890        T33=LGT(S2(I))
2900        T11=(-T33+T6)/T7
2910        A2(I)=10^T11
2920      NEXT I
2930    NEXT P
2940    J=1
2950    FOR I=1 TO 12
2960      A(J,I)=A1(I)
2970    NEXT I
2980    J=2
2990    FOR I=1 TO 12
3000      A(J,I)=A2(I)
3010    NEXT I
3020 !
3030 !PRINT ":A: VALUES FOR WEARING COURSE AND BASE COURSE"
3040    FOR J=1 TO 2
3050      FOR I=1 TO 12
3060    OUTPUT 701;A(J,I)
3070      NEXT I
3080    NEXT J
3090 !
3100 !
3110 !
3120 !
3130 !
3140    I1=1
3150  GCLEAR
3160    GINIT
3170    GRAPHICS ON
3180    ALPHA OFF
3190    WINDOW 0,100,0,100
3200    VIEWPORT 0,100,0,100
3210    FRAME
3220    LDIR 0
3230    MOVE 5,95
3240    LABEL " INPUT CREEP DATA"
3250    MOVE 5,90
3260    LABEL "IN THE FOLLOWING FORMAT:-"
3270    MOVE 5,85
3280    IF I1=2 THEN 3310
3290    LABEL "WEARING COURSE"
3300    GOTO 3320
3310    LABEL "BASE COURSE"
3320    MOVE 15,80
3330    LABEL " INPUT Sm @ Sb=1E2"
3340    MOVE 15,75
3350    LABEL " INPUT Sm @ Sb=1E6"
3360    MOVE 10,5
3370    DRAW 10,70
3380    MOVE 10,5
3390    DRAW 90,5
3400    MOVE 10,5
```

```
3410  DRAW 90,70
3420  MOVE 40,5
3430  DRAW 40,30
3440  MOVE 60,5
3450  DRAW 60,45
3460  MOVE 12,1
3470  LABEL "BITUMEN STIFFNESS (N/mm^2)"
3480  LDIR PI/2
3490  MOVE 38,12
3500  LABEL "1E2"
3510  MOVE 58,12
3520  LABEL "1E6"
3530  MOVE 8,10
3540  LABEL "MIX STIFFNESS (N/mm^2)"
3550  IF I1=2 THEN 3710
3560  !
3570  !
3580  !
3590  !
3600  MOVE 75,80
3610  INPUT W1
3620  MOVE 75,75
3630  INPUT W3
3640  OUTPUT 701;"Sm @ Sb=10^2 (WEARING COURSE) = ";W1
3650  OUTPUT 701;"Sm @ Sb=10^6(WEARING COURSE) = ";W3
3660  W2=LGT(W1)
3670  W4=LGT(W3)
3680  W5=2*(W2-W4)/4+W2
3690  W6=(W4-W2)/4
3700  IF I1=1 THEN 3810
3710  MOVE 75,80
3720  INPUT B1
3730  MOVE 75,75
3740  INPUT B3
3750  OUTPUT 701;"Sm @ Sb=10^2(BASE COURSE) = ";B1
3760  OUTPUT 701;"Sm @ Sb=10^6(BASE COURSE) = ";B3
3770  B2=LGT(B1)
3780  B4=LGT(B3)
3790  B5=2*(B2-B4)/4+B2
3800  B6=(B4-B2)/4
3810  GCLEAR
3820  I1=I1+1
3830  RESTORE 3550
3840  WAIT 1
3850  IF I1=2 THEN 3150
3860  !
3870  !
3880  !
3890  !
3900  FOR I=1 TO 12
3910    S3(I)=LGT(S1(I))
3920    S4(I)=LGT(S2(I))
3930    E1(I)=W6*S3(I)+W5
3940    E2(I)=B6*S4(I)+B5
3950    E3(I)=10^E1(I)
3960    E4(I)=10^E2(I)
3970    M1(I)=E4(I)/E3(I)
3980  NEXT I
3990  RESTORE 4060
4000  PRINT " THE MODULAR RATIOS (Sm) (base/wearing)  ARE:-"
4010  FOR I=1 TO 12
4020    READ F$
4030    PRINT F$,M1(I)
4040  ! OUTPUT 701;F$,M1(I)
4050  NEXT I
4060  DATA JANUARY,FEBUARY,MARCH,APRIL,MAY,JUNE,JULY,AUGUST,SEPTEMBER,OCTOBER
4061  DATA NOVEMBER,DECEMBER
4070  !
4080  FOR I=1 TO 133
4090    READ M(I)
4100  ! OUTPUT 701;"M(I)=";M(I)
4110  NEXT I
4120  FOR I=1 TO 133
4130    READ C(I)
4140  ! OUTPUT 701;I
4150  ! OUTPUT 701;"C(I)=";C(I)
4160  NEXT I
4170  !
4180  !
4190  !
4200  !
4210  PRINT "INPUT ESTIMATION OF SLAB LENGTH"
4220  INPUT L
4230  PRINT "IS THE 80% FATIGUE LIFE REQUIRED  Y OR N"
4240  INPUT P$
4250  IF M1(1)=1 AND M1(12)=1 AND D3=100 THEN 4270
4260  GOTO 4300
4270  PRINT "INPUT ESTIMATED DEBOND LENGTH AJACENT TO CRACK AT SURFACING/ROAD ?"
4280  INPUT Ee$
4290  OUTPUT 701;"DEBOND LENGTH = ";Ee$;"mm"
4300  PRINT "CALCULATING STRESS INTENSITY FACTORS"
4310  IF D3=80 THEN 5000
4320  IF D3=100 THEN 4350
4330  GOTO 4380
4340  IF Tt$="1" THEN 4410
4350  IF Ee$="0" THEN 4410
4360  IF Ee$="100" THEN 5690
4370  IF Ee$="200" THEN 5850
4380  IF D3=120 THEN 5210
4390  IF D3=150 THEN 5370
4400  IF D3=180 THEN 5530
4410  FOR J=1 TO 12
4420    FOR R=1 TO 100
4430      P1=0
4440      P2=10
4450      IF .075<M1(J) AND .25>M1(J) THEN 4570
4460      IF M1(J)=.075 THEN 4570
4470      IF .25<M1(J) AND .75>M1(J) THEN 4630
4480      IF M1(J)=.75 THEN 4630
4490      IF .75<M1(J) AND 1.25>M1(J) THEN 4690
4500      IF M1(J)=1.25 THEN 4690
4510      IF 1.25<M1(J) AND 1.75>M1(J) THEN 4750
4520      IF M1(J)=1.75 THEN 4750
4530      IF 1.75<M1(J) AND-2.5>M1(J) THEN 4810
```

```
4540      IF M1(J)=2.5 THEN 4810
4550      IF 2.5<M1(J) AND 5.0>M1(J) THEN 4870
4560      PRINT "OUTSIDE RANGE OF METHOD"
4570      FOR I=1 TO 10
4580      IF P1=R THEN 4930
4590      IF P1<R AND P2>=R THEN 4930
4600      P1=P1+10
4610      P2=P2+10
4620      NEXT I
4630      FOR I=11 TO 20
4640      IF P1=R THEN 4930
4650      IF P1<R AND P2>=R THEN 4930
4660      P1=P1+10
4670      P2=P2+10
4680      NEXT I
4690      FOR I=21 TO 30
4700        IF P1=R THEN 4930
4710        IF P1<R AND P2>=R THEN 4930
4720        P1=P1+10
4730        P2=P2+10
4740      NEXT I
4750      FOR I=31 TO 40
4760        IF P1=R THEN 4930
4770        IF P1<R AND P2>=R THEN 4930
4780        P1=P1+10
4790        P2=P2+10
4800      NEXT I
4810      FOR I=41 TO 50
4820        IF P1=R THEN 4930
4830        IF P1<R AND P2>=R THEN 4930
4840        P1=P1+10
4850        P2=P2+10
4860      NEXT I
4870      FOR I=51 TO 60
4880        IF P1=R THEN 4930
4890        IF P1<R AND P2>=R THEN 4930
4900        P1=P1+10
4910        P2=P2+10
4920      NEXT I
4930      K(J,R)=R*M(I)+C(I)
4940  ! PRINT "K=";K(J,R)
4950  P1=0
4960  P2=10
4970    NEXT R
4980  NEXT J
4990  GOTO 6320
5000  P1=0
5010  P2=10
5020  FOR J=1 TO 12
5030    FOR R=1 TO 80
5040      FOR I=61 TO 68
5050        IF P1=R THEN 5100
5060        IF P1<R AND P2>=R THEN 5100
5070        P1=P1+10
5080        P2=P2+10
5090      NEXT I
5100      K(J,R)=R*M(I)+C(I)
5110  !     OUTPUT 701;"K=";K(J,R)
5120  ! FOR I=1 TO 93
5130  !  OUTPUT 701;"C(I)=";C(I)
5140  !  OUTPUT 701;"M(I)=";M(I)
5150  !  NEXT I
5160        P1=0
5170        P2=10
5180    NEXT R
5190  NEXT J
5200  GOTO 6320
5210  P1=0
5220  P2=10
5230  FOR J=1 TO 12
5240    FOR R=1 TO 120
5250      FOR I=69 TO 80
5260        IF P1=R THEN 5310
5270        IF P1<R AND P2>=R THEN 5310
5280        P1=P1+10
5290        P2=P1+10
5300      NEXT I
5310      K(J,R)=R*M(I)+C(I)
5320      P1=0
5330      P2=10
5340    NEXT R
5350  NEXT J
5360  GOTO 6320
5370  P1=0
5380  P2=10
5390  FOR J=1 TO 12
5400    FOR R=1 TO 150
5410      FOR I=81 TO 95
5420        IF P1=R THEN 5470
5430        IF P1<R AND P2>=R THEN 5470
5440        P1=P1+10
5450        P2=P2+10
5460      NEXT I
5470      K(J,R)=R*M(I)+C(I)
5480      P1=0
5490      P2=10
5500    NEXT R
5510  NEXT J
5520  GOTO 6320
5530  P1=0
5540  P2=10
5550  FOR J=1 TO 12
5560    FOR R=1 TO 180
5570      FOR I=96 TO 113
5580        IF P1=R THEN 5630
5590        IF P1<R AND P2>=R THEN 5630
5600        P1=P1+10
5610        P2=P2+10
5620      NEXT I
5630      K(J,R)=R*M(I)+C(I)
5640      P1=0
5650      P2=10
5660    NEXT R
5670  NEXT J
```

```
5680  GOTO 6320
5690  P1=0
5700  P2=10
5710  FOR J=1 TO 12
5720  FOR R=1 TO 100
5730  FOR I=114 TO 123
5740  IF P1=R THEN 5790
5750  IF P1<R AND P2>=R THEN 5790
5760  P1=P1+10
5770  P2=P2+10
5780  NEXT I
5790  K(J,R)=R*M(I)+C(I)
5800  P1=0
5810  P2=10
5820  NEXT R
5830  NEXT J
5840  GOTO 6320
5850  P1=0
5860  P2=10
5870  FOR J=1 TO 12
5880  FOR R=1 TO 100
5890  FOR I=124 TO 133
5900  IF P1=R THEN 5950
5910  IF P1<R AND P2>=R THEN 5950
5920  P1=P1+10
5930  P2=P2+10
5940  NEXT I
5950  K(J,R)=R*M(I)+C(I)
5960  P1=0
5970  P2=10
5980  NEXT R
5990  NEXT J
6000  GOTO 6320
6010  ! DATA FOR M(GRAD) FOR 100mm SURFACING
6020  DATA -.97,-.305,-.135,-.08,-.07,-.035,-.02,-.03,-.05,-.06
6021  DATA -.97,-.305,-.135,-.08,-.07,-.035,-.02,-.03,-.04,-.05
6022  DATA -.97,-.305,-.135,-.08,-.07,-.035,-.015,-.01,-.02,-.04
6030  DATA -.97,-.22,-.17,-.105,-.055,-.02,-.03,-.02,-.023,-.035
6040  DATA -.88,-.245,-.17,-.1,-.04,-.02,-.01,-.02,-.04,-.05,
6050  DATA -.83,-.36,-.18,-.1,-.05,-.05,-.02,-.02,-.03,-.05,
6060  ! DATA FOR M  (GRAD) FOR 80mm SURFACING
6070  DATA -.95,-.275,-.07,-.06,-.06,-.01,-.03,-.04
6080  ! DATA FOR M (GRAD) FOR 120mm SURFACING
6090  DATA -.60,-.25,-.17,-.12,-.04,-.027,-.013,-.03,-.02,-.01,-.015,-.025
6100  DATA -.35,-.365,-.15,-.07,-.06,-.05,-.03,-.02,-.028,-.007,-.005,-.01,-.01
6101  DATA -.01,-.02
6110  DATA -.34,-.36,-.08,-.06,-.05,-.04,-.04,-.025,-.02,-.015,-.02,-.01,-.02
6111  DATA -.005,-.005,-.005,-.01
6120  ! DATA FOR 100mm SURFACING AND DEBONDS OF 100 @ 200mm M(GRAD)
6130  DATA -.48,-.19,-.11,-.08,-.06,-.02,-.01,-.01,-.01,-.02
6140  DATA -.21,-.15,-.06,-.04,-.04,-.02,-.02,-.01,-.01,-.02
6150  ! DATA FOR INTERCEPT (C) FOR 100mm SURFACING
6160  DATA 21,14.35,10.95,9.3,8.9,7.15,8.3,9,10.6,11.5
6161  DATA 21,14.35,10.95,9.3,8.9,7.15,7.7.7,8.4,9.3
6162  DATA 21,14.35,10.95,9.3,8.9,7.15,5.95,5.6,6.4,8.4
6170  DATA 21,13.5,12.5,10.55,8.4,4.8,5.9,5.2,5.6,6.5
6180  DATA 20.3,14.2,12.7,10.6,8.2,5.2,4.1,4.8,6.4,7.3
6190  DATA 20.3,15.6,13.2,10.8,8.8,3.8,3.8,3.6,4.13,6.4
6200  ! DATA FOR INTERCEPT (C) FOR 80mm SURFACING
6210  DATA 19.75,13,8.9,8.6,8.2,6.1,7.3,8.0
6220  ! DATA ROR 120mm SURFACING
6230  DATA 17,13.5,11.9,10.4,7.2,6.55,5.71,6.9,6.1,5.2,5.7,6.8
6240  ! DATA FOR 150mm SURFACING
6250  DATA 15.25,15.4,11.1,8.7,8.3,7.8,6.6,5.9,6.54,4.65,4.65,5,5,5,6.4
6260  !  DATA FOR 180mm SURFACING
6270  DATA 14.2,14.4,8.8,8.2,7.8,7.3,7.3,6.25,5.82,5.4,5.9,4.8,6,4.05,4.05,4.0
6271  DATA 4.05,4.9
6280  ! DATA FOR 100mm SURFACING WITH A DEBOND OF 100mm(INTERCEPT C)
6290  DATA 11.3,9.7,8.8,8.0,7.4,6.3,5.9,5.4,5.4,6.3
6300  ! DATA FOR 100mm SURFACING AND A DEBOND OF 200mm
6310  DATA 9.7,9.1,8.0,7.6,7.0,5.7,5.7,5.1,5.1,6.0
6320  FOR I=1 TO 12
6330    READ T1(I)
6340  NEXT I
6350  FOR I=1 TO 12
6360    READ T2(I)
6370  NEXT I
6380  FOR I=1 TO 12
6390    READ T3(I)
6400  NEXT I
6410  IF 80<=D3 AND 125>=D3 THEN 6440
6420  IF 125<D3 AND 160>=D3 THEN 6490
6430  IF 160<D3 AND 201>D3 THEN 6540
6440  FOR I=1 TO 12
6450    T(I)=T1(I)
6460    U(I)=L*.01*T(I)
6470  NEXT I
6480  GOTO 6580
6490  FOR I=1 TO 12
6500    T(I)=T2(I)
6510    U(I)=L*.01*T(I)
6520  NEXT I
6530  GOTO 6580
6540  FOR I=1 TO 12
6550    T(I)=T3(I)
6560    U(I)=L*.01*T(I)
6570  NEXT I
6580  E$="MONTH"
6590  G$="CRACK OPENING"
6600  H$="DAILY"
6610  I$="WIDTH"
6620  J$="MEAN TEMP."
6630  IMAGE 2X,5A,2X,13A,2X,5A
6640  PRINT USING 6630;E$,G$,H$
6650  IMAGE 13X,5A,4X,10A,
6660  PRINT USING 6650;I$,J$
6670  FOR I=1 TO 12
6680    READ F$
6690    PRINT F$;"          ";U(I);"          ";T(I)
6700  NEXT I
6710  PRINT "CALCULATING FATIGUE LIFE"
6720  !
6730  DATA 2.2,3.3,5.2,8.3,9,9.5,8.2,7.5,6.3,4.6,3.4,2.3
6740  DATA 1.4,2.3,4.2,6.3,7,7.6,6.8,5.8,4.9,3.5,2.6,1.6
```

```
6750  DATA 1,1.5,3,4.6,5.4,5.4,5.3,4.3,3.6,2.6,2,1.2
6760  DATA JAN,FEB,MAR,APR,MAY,JUN,JUL,AUG,SEPT,OCT,NOV,DEC
6770  !
6780  FOR I=1 TO 12
6790    N1(I)=0
6800    N2(I)=0
6810    N5(I)=0
6820  NEXT I
6830  FOR I=1 TO 2
6840  IF Tt$="1" THEN Z1=6.57
6850  IF Tt$="1" THEN I=2
6860    IF I=2 THEN 6910
6870    IF G1(I)=200 THEN Z1=4.8
6880    IF G1(I)=100 THEN Z1=6.6
6890    IF G1(I)=50 THEN Z1=7.2
6900    GOTO 6940
6910    IF G1(I)=200 THEN Z2=4.8
6920    IF G1(I)=100 THEN Z2=6.6
6930    IF G1(I)=50 THEN Z2=7.2
6940  NEXT I
6950  N33=0
6960  N66=0
6970  FOR J=1 TO 12
6980    FOR I=1 TO D1
6990      Q(J,I)=K(J,I)*U(J)*E4(J)/100000000
7000  !
7010  !
7020  !
7030  !
7040  !
7050        N11=1/(A(2,J)*Q(J,I)^Z2)
7060  !     OUTPUT 701;"N1=";N11
7070        N1(J)=N1(J)+N11
7080    NEXT I
7090    PRINT "N(B.C)=";N1(J)
7091    OUTPUT 701;"N(B/C)=";N1(J)
7100  NEXT J
7110  FOR J=1 TO 12
7120    FOR I=D4 TO D3
7130      Q(J,I)=K(J,I)*U(J)*E3(J)/100000000
7140      N22=1/(A(1,J)*Q(J,I)^Z1)
7150    ! OUTPUT 701;"N22=";N22
7160      N2(J)=N2(J)+N22
7170    NEXT I
7180    PRINT "N(W.C)=";N2(J)
7181    OUTPUT 701;"N(W/C)=";N2(J)
7190  NEXT J
7200  FOR J=1 TO 12
7210    N3(J)=N1(J)+N2(J)
7220    N33=1/N3(J)+N33
7230  NEXT J
7240  N4=1/N33*12
7250  PRINT "FATIGUE LIFE =";INT(N4);"DAYS"
7260  OUTPUT 701;"FATIGUE LIFE=";INT(N4);"DAYS"
7270  OUTPUT 701;"SLAB LENGTH=";L;"m"
7280  IF P$="S" THEN 7420
7290  FOR J=1 TO 12
7300  FOR I=1 TO D5
7310  Q(J,I)=K(J,I)*U(J)*E3(J)/100000000
7320  N55=1/(A(1,J)*Q(J,I)^Z1)
7330  N5(J)=N5(J)+N55
7340  NEXT I
7350  NEXT J
7360  FOR J=1 TO 12
7370  N6(J)=N5(J)+N1(J)
7371  N66=1/N6(J)+N66
7380  NEXT J
7390  N7=1/N66*12
7400  PRINT "THE 80% FATIGUE LIFE=";INT(N7);"DAYS"
7410  OUTPUT 701;"THE 80% FATIGUE LIFE =";INT(N7);"DAYS"
7420  END
```

PROGRAM LISTING FOR CRP 100

CALCULATION OF YIELD STRAIN FROM CREEP TEST DATA

```
10 DIM H(4)
20 DIM C$[60]
30 DIM E4(40)
40 DIM W(4)
50 DIM L(4)
60 DIM S1(4)
70 SHORT E1(4,40)
80 SHORT E2(4,40)
90 SHORT E3(4,40)
100 DIM L$[80]
110 SHORT P1(4,40)
120 SHORT P2(40)
121 DISP "NOTE"
122 DISP "IF STRAIN AT YEILD IS REQD.TO BE ADDED AT A LATER TIME THEN TYPE 'RUN
123 DISP "________________________"
130 DISP "IS INFORMATION REQD.TO BE PRINTED ON THE PLOT?"
131 INPUT Y$
132 DISP "IS THE BLOCK INFORMATION TO BE PLOTTED(FIRST BLOCK ONLY)"
133 INPUT Z$
140 DIM D(4,40)
160 DIM A$[40]
170 IF Y$="Y" THEN 240
180 IF Y$="N" THEN 190
190 DISP "ARE THE GRAPHICS POINTS TO BE INPUT MANUALLY"
200 INPUT G$
210 IF G$="Y" THEN 1280
220 IF G$="N" THEN 230
230 IF Y$="N" THEN 690
240 DISP "INPUT THE NUMBER OF MATERIAL TYPES"
250 INPUT N3
260 FOR P=1 TO N3
270 DISP "INPUT THE PLOT SYMBOL"
280 INPUT R$
330 DISP "FOR MATERIAL TYPE";P
340 DISP "INPUT THE MATERIAL "
350 DISP "FOR H.R.A INPUT 1"
360 DISP "FOR D.B.M INPUT 2"
361 DISP "FOR OTHER INPUT 3"
370 INPUT A$
380 IF A$="1" THEN 400
390 IF A$="2" THEN 420
391 IF A$="3" THEN 422
400 A$="HOT ROLLED ASPHALT"
410 GOTO 430
420 A$="DENSE BITUMEN MACADAM"
421 GOTO 430
422 DISP "INPUT MATERIAL"
423 INPUT A$
430 DISP "INPUT THE SOFTENING POINT"
440 INPUT B$
450 DISP "INPUT REF.NO."
460 INPUT C$
470 DISP "AGGREGATE GRADING?"
480 INPUT D$
510 DISP "INPUT VOID CONTENT"
520 INPUT F$
530 DISP "SOURCE OF MATERIAL"
540 DISP "INPUT 1)PLYM.POLY"
550 DISP "       2)T.R.R.L"
560 DISP "       3)M.4 "
561 DISP "       4)OTHER"
570 INPUT H$
580 IF H$="1" THEN 610
590 IF H$="2" THEN 630
600 IF H$="3" THEN 650
601 IF H$="4" THEN 652
610 H$="PLYM.POLY"
620 GOTO 660
630 H$="T.R.R.L"
640 GOTO 660
650 H$="M.4"
651 GOTO 660
652 DISP "INPUT SOURCE"
653 INPUT H$
660 DISP "COMMENTS"
670 INPUT L$
680 GOTO 710
690 DISP "INPUT THE PLOT SYMBOL"
700 INPUT R$
710 DISP " INPUT THE NUMBER OF SAMPLES(N2)"
720 INPUT N2
730 DISP "INPUT THE NUMBER OF POINTS(N1)"
740 REM THE NUMBER OF POINTS IS N1
750 INPUT N1
760 DISP "INPUT THE FORCE IN KGS"
770 INPUT F1
780 F2=F1*9.81+.892
790 FOR I=1 TO N2
800 DISP "INPUT SAMPLE LENGTH IN MM"
810 INPUT L
820 L(I)=L/1000
830 DISP "INPUT SAMPLE HEIGHT IN MM"
840 INPUT H
850 H(I)=H/1000
860 DISP "INPUT SAMPLE WIDTH IN MM"
870 INPUT W
880 W(I)=W/1000
890 A=H(I)*W(I)
900 ! PRINT"CSA=";A
910 S1(I)=F2/A
920 ! PRINT "STRESS=";S1(I)
930 NEXT I
940 FOR J=1 TO N2
950 FOR I=1 TO N1
960 DISP "INPUT DISPLACEMENTS IN MM"
970 DISP "INPUT POINT";I
980 INPUT D(J,I)
990 E1(J,I)=D(J,I)/L
1000 REM STRAIN IS E1 @ MODULUS IS E2
1010 E2(J,I)=S1(J)/E1(J,I)
1020 E3(J,I)=LGT(E2(J,I))
1030 P1(J,I)=20*(E3(J,I)-6)+15
1040 ! PRINT "Y CORD.=";P1(J,I)
1050 NEXT I
1060 NEXT J
1070 FOR J=1 TO N2
1080 FOR I=1 TO N1
1090 PRINT "Emix=";E2(J,I)
1100 NEXT I
1110 NEXT J
1120 DISP "INPUT TIME IN SECONDS FROM THE START OF THE TEST"
1130 FOR I=1 TO N1
1140 DISP "TIME INC.FOR POINT";I
```

```
1150 INPUT E4
1160 E4(I)=LGT(E4)
1170 P2(I)=16*E4(I)+15
1180 ! PRINT "X CORD.=";P2(I)
1190 NEXT I
1200 DISP "PLOT TYPE"
1210 DISP "TYPE 1:- NEW PLOT"
1220 DISP "TYPE 2:- CONTINUATION PLOT"
1230 DISP "TYPE 3:-GRAPHICS ONLY PLOT"
1240 INPUT K$
1250 IF K$="1" THEN 1400
1260 IF K$="2" THEN 1750
1270 IF K$="3" THEN 1280
1280 DISP "INPUT THE NUMBER OF POINTS"
1290 INPUT N1
1291 DISP "INPUT PLOT SYMBOL"
1292 INPUT R$
1300 FOR I=1 TO N1
1310 J=1
1311 N2=1
1320 DISP "INPUT POINT";I;"X Y"
1330 INPUT M1,M2
1340 M3=LGT(M1)
1350 P2(I)=16*M3+15
1360 M4=LGT(M2)
1370 P1(J,I)=20*(M4-6)+15
1380 NEXT I
1390 GOTO 1750
1400 DISP "IF PLOT IS REQD.PRESS KEY K1"
1410 ON KEY# 1,"P F C" GOTO 1430
1420 GOTO 1420
1430 PRINTER IS 705
1440 PRINT "IN;SP1;SC0,100,0,100 CHR$(3)"
1441 IF G$="Y" THEN 1850
1450 PRINT "PA15,95,PD,15,15,95,15,PU"
1460 PRINT "PA15,15;XT;PA31,15;XT;PA47,15;XT;PA63,15;XT;PA79,15;XT;PA95,15;XT;PU;
1470 PRINT "PA15,35;YT;PA15,55;YT;PA15,75;YT;PA15,95;YT;PU;"
1480 PRINT "PA50,2"
1490 PRINT "LB TIME (SECS)";CHR$(3)
1500 PRINT "PA15,9"
1510 PRINT "LB1";CHR$(3)
1520 PRINT "PA28,9"
1530 PRINT "LB10";CHR$(3)
1540 PRINT "PA44,9"
1550 PRINT "LB10^2";CHR$(3)
1560 PRINT "PA62,9"
1570 PRINT "LB10^3";CHR$(3)
1580 PRINT "PA76,9"
1590 PRINT "LB10^4";CHR$(3)
1600 PRINT "PA94,9"
1610 PRINT "LB10^5";CHR$(3)
1620 PRINT "PA4,20;"
1630 PRINT " DI0,1;LB MIX STIFFNESS(N/mm2)";CHR$(3)
1640 PRINT "PA11,16"
1650 PRINT "LB1E6";CHR$(3)
1660 PRINT "PA11,33"
1670 PRINT "LB1E7";CHR$(3)
1680 PRINT "PA11,52"
1690 PRINT "LB1E8";CHR$(3)
1700 PRINT "PA11,72"
1710 PRINT "LB1E9";CHR$(3)
1720 PRINT "PA11,88"
1730 PRINT "LB1E10";CHR$(3)
1740 GOTO 1760
1750 PRINTER IS 705
1760 FOR J=1 TO N2
1770 FOR I=1 TO N1
1780 ! PRINT "PA";P2(I);P1(J,I);
1790 NEXT I
1800 ! PRINT "PU";CHR$(3)
1810 FOR I=1 TO N1
1820 IF J=2 THEN 1850
1830 PRINT "SP2;PA";P2(I),P1(J,I);"PU";
1840 GOTO 1860
1850 PRINT "SP1;PA";P2(I),P1(J,I);"PU";
1860 PRINT "LB";R$;CHR$(3)
1870 NEXT I
1880 NEXT J
1881 IF G$="Y" THEN 2090
1890 IF Y$="N" THEN 2090
1900 IF K$="2" THEN 2090
1910 PRINT "SP2;PA20,95"
1920 PRINT "DI1,0;SI.28,.402;LBMATERIAL:-  ";A$;CHR$(3)
1930 PRINT "SP1;PA20,88"
1940 PRINT "SI.141,.202;LBREF./CORE NO:-  ";C$;CHR$(3)
1950 PRINT "PA20,83"
1960 PRINT "LBSOFTENING POINT:-  ";B$;" DEG.C";CHR$(3)
1970 PRINT "PA20,81"
1980 PRINT "LBAGGREGATE GRADING:-  ";D$;" mm";CHR$(3)
1990 IF Z$="N" THEN 2010
1991 PRINT "PA70,88"
1992 PRINT "LBBLOCK DETAILS";CHR$(3)
1993 PRINT "PA70,85"
1994 PRINT "LBMASS:-  ";F1;"KGS";CHR$(3)
1995 PRINT "PA70,83"
1996 PRINT "LBLENGTH:-  ";L(1);"m";CHR$(3)
1997 PRINT "PA70,81"
1998 PRINT "LBWIDTH:-  ";W(1);"m";CHR$(3)
1999 PRINT "PA70,79"
2000 PRINT "LBHEIGHT:-  ";H(1);"m";CHR$(3)
2010 PRINT "PA20,76"
2020 PRINT "LBVOID CONTENT:-  ";F$;" %";CHR$(3)
2030 PRINT "PA20,74"
2040 PRINT "LBSOURCE:-  ";H$;CHR$(3)
2050 PRINT "PA70,05"
2060 PRINT "LBCOMMENTS:-";L$;CHR$(3)
2070 PRINT "SP2;PA0,0,PD,0,100,100,100,100,0,0,0,PU;"
2071 PRINT "PA100,0,PD,0,0,PU;"
2072 NEXT P
2073 DISP "TO INPUT STRAIN AT YIELD PRESS CONT."
2074 PAUSE
2075 PRINTER IS 705
2076 PRINT "IN;SP1;SC0,100,0,100 CHR$(3)"

2077 PRINT "SI.141,.203"
2078 DISP "INPUT STRAIN AT YIELD"
2079 INPUT E$
2082 PRINT "SP1;PA20,78"
2083 PRINT "LBSTRAIN AT YIELD:-  ";E$;" %";CHR$(3)
2090 END
```

APPENDIX 7

INPUT FILES TO "PAFEC" FINITE ELEMENT PACKAGE FOR THE INVESTIGATION OF THE FOLLOWING CRACK MECHANISMS:-

(1) TENSILE FATIGUE (F.E.1)

(2) TENSILE YIELD (F.E.2)

(3) TRAFFIC INDUCED SHEAR (F.E.3)

```
MODEL OF THE TENSILE FATIGUE MECHANISM (F.E.1)
CONTROL
PLANE.STRAIN
TOLERANCE=10E-8
SKIP.COLLAPSE
CONTROL.END
NODES
NODE.NUMBER X  Y
 1 0 0
 2 0 .0075
 3 .1124999 .0075
 4 .1124999 0
 5 .1125001 0
 6 .1125001 .0075
 7 .225 .0075
 8 .225 0
 9 0 .0375
 10 .1125 .0375
 11 .225 .0375
 12 0 .0825
 13 .1125 .0825
 14 .225 .0825
 15 .225 .08375
PRFBLOCKS
TYPE=1
ELEMENT.TYPE=36210
BLOCK.NUMBER,N1,N2,PROP,TOPOLOGY
 1 3 1 1 1 4 2 3
 2 3 4 2 9 10 2 3
 3 3 2 2 9 10 12 13
 4 3 2 2 11 10 14 13
 6 3 1 1 0 5 7 6 0 15
MESH
REFERENCE  SPACING.LIST
 1 2
 2 1 1 1 1 1 1 2 4 4 4 4
 3 4 4 4 2 1 1 1 1
 4 4
CRACK.TIP
LIST.OF.NODES
 10
PLATES.AND.SHELLS
PLAT  MATE  THIC
 1 11 .075
 2 12 .075
MATERIAL
MATERIAL.NUMBER E NU RO
 11 209E9 0.3 7800
 12 1.124E8 .3 2300
DISPLACEMENTS.PRESCRIBED
NODE.NUMBER DIRECTION DISPLACEMENT.VALL
 8 1 .001
 15 1 .001
 7 1 .001
RESTRAINTS
NODE.NUMBER PLANE DIRECTION
 1 0 0
 4 0 0
 0 0 2
 17 0 0
 19 0 0
 21 0 0
 23 0 0
 25 0 0
 27 0 0
 29 0 0
 844 0 2
 846 0 2
 404 0 2
 850 0 2
 852 0 2
 854 0 2
 856 0 2
STRESS.ELEMENT
STRT FINISH STEP
 1 23 1
 25 39 1
 41 143 1
 145 247 1
 249 1000 1
IN.DRAW
TYPE.NUMBER  INFORMATION
1 123
OUT.DRAW
END.OF.DATA
```

```
MODEL OF THE TENSILE YIELD MECHANISM  (F.E.2)
CONTROL
FULL.CONTROL
SKIP. COLLAPSE
STRESS
PHASE=1,2,3,4,5,6,7,8,9
BASE=1000000
CONTROL. END
NODES
NODE.NUMBER
 1 0 0
 2 0 0.5
 3 2.5 0.5
 4 2.5 0
 5 0 0.00
 6 2.55 0.00
 7 0 1.06
 8 2.5 1.06
 10 0 1.23
 11 2.499 1.23
 12 2.5 1.19
 13 2.505 1.23
 14 2.505 1.19
 15 2.505 1.06
 16 2.505 0.5
 17 2.505 0
 18 2.505 0.070
 19 2.5 .070
 20 1.5 0
 21 1.5 0.5
 22 1.5 0.00
 23 1.5 1.06
 24 1.5 1.19
 25 1.5 1.23
 26 .75 1.23
 27 .75 1.19
 28 .75 1.06
 29 .75 .00
 30 1.9975 1.23
 31 1.9975 1.19
 32 1.9975 1.06
 33 1.9975 0.00
 34 5.5001 1.23
 35 2.5 1.222
 36 2.505 1.222
 37 0 1.222
 38 1.5 1.222
 39 1.9975 1.222
 40 2.495 1.23
 41 2.495 1.22
 42 2.495 1.18
 43 2.495 1.06
 44 2.495 0.00
 45 2.495 .070
 46 2.495 0.5
 47 2.495 0
 48 1.9975 0.5
 49 1.9975 0
 50 1.9975 .070
PRFBLOCKS
TYPE=1
ELEMENT.TYPE=36210
BLOCK.NUMBER, N1, N2, PROPERTIES, TOP
 1 1 0 1 1 20 2 21
 2 1 3 2 2 21 5 22 0 0 0 29
 3 1 4 3 5 22 7 23 29 0 0 28
 4 1 5 4 7 23 9 24 12 0 0 27
 5 1 5 5 9 24 37 38 27
 6 2 5 5 24 31 38 39
 7 7 5 5 12 14 35 36
 8 2 5 4 23 32 24 31
 9 7 5 4 8 15 12 14
 10 2 4 3 22 33 23 32
 11 2 3 2 21 40 22 50
 12 7 3 2 3 16 19 18
 13 2 8 1 20 49 21 40
 14 7 8 1 4 17 3 16
 15 7 7 5 35 36 34 13
 16 1 7 5 37 38 10 25 0 0 0 26
 17 2 7 4 38 39 25 38
 18 7 7 5 41 35 40 11
```

```
 19 7 5 5 42 .2 41 35
 20 7 5 4 43 8 42 12
 21 7 4 3 44 6 43 8
 22 7 3 2 46 3 45 19
 23 7 8 1 47 4 46 3
 24 2 7 5 39 41 38 40
 25 2 5 5 31 42 39 41
 26 2 5 4 32 43 31 42
 27 2 4 3 33 44 32 43
 28 2 3 2 48 46 50 45
 29 2 8 1 49 47 48 46
MESH
REFERENCE SPACING.LIST
 1 15
 2 5
 3 7
 5 4
 6 5
 7 1
 8 10
CRACK.TIP
LIST.OF.NODES
 22 35
PLATES.AND.SHELLS
 1 11 1
 2 12 1
 3 13 1
 4 14 1
 5 15 1
MATERIAL
MATERIAL.NUMBER E NU RO ALPHA
 11 40E6 .4 2700
 12 100E6 .3 2700
 13 30E6 .4 2100 1.0E-5
 14 1E0 .4 2100 2.3E-5
 15 5E0 .4 2100 2.3E-5
GAPS
N1 N2 DIRECTION TYPE
 1695 1547 2 1
 1697 1549 2 1
 1699 1551 2 1
 1701 1553 2 1
 1703 1555 2 1
 2351 2221 2 1
 2353 2223 2 1
 2355 2225 2 1
 2357 2227 2 1
 1737 2025 2 1
 19 6 2 1
 45 44 2 1
 50 33 2 1
TEMPERATURE
TEMPERATURE START FINISH STEP LIST.OF.N
 -9 1930 2002 1
 -9 2090 2100 1
 -7.5 1330 1302 1
 -7.5 1430 1450 1
 -7.5 2080 2094 1
 -7.5 2156 2158 1
 -6.4 1260 1335 1
 -6.4 1412 1436
 -6.4 1460 1466 1
 -6.4 2010 2012 1
 -6.4 2136 2156 1
 -5.0 2114 1256
 -5.0 1390 1410 1
 -5.2 1454 1458
 -5.2 2124 2134 1
 -5.2 2006 2008 1
 -4.1 1170 1212 1
 -4.1 1384 1396
 -4.1 2110 2122 1
 -4.1 2214 2218 1
 -3.5 1514 1522
 -3.5 1524 1528 1
 -5.5 1076 1104 1
 -3.5 1500 1508 1
 -3.45 2100 2196 1
 -2.8 1020 1050 1
 -2.8 1484 1484 1
 -2.8 1532 1534 1
 -2.8 984 1010 1
 -2.2 1470 1492 1
 -2.2 2162 2168 1
 -2.2 2162 2168 1
 -1.6 938 966 1
 -1.6 1576 1584 1
 -1.6 2245 2254 1
GRAVITY
 1
RESTRAINTS
NODE.NUMBER PLANE DIRECTION
 1 1 1
 1 2 12
 17 2 12
 17 1 1
 18 1 1
 16 1 1
STRESS.ELEMENT
START FINISH STEP
 1 254 1
 258 269 1
 271 441 1
 445 468 1
 470 513 1
 515 606 1
 608 610 1
 612 1000 1
IN.DRAW
TYPE INFORMATION
 1 123
OUT.DRAW
PLOT TYPE
 1
 20
 30
END.OF.DATA
```

ASSESSMENT OF ASPHALT MATERIALS TO RELIEVE REFLECTION CRACKING OF HIGHWAY SURFACINGS

by M.D. Foulkes

ABSTRACT

The thesis investigates the mechanisms and restraints which influence transverse crack propagation through the bituminous surfacings of semi-flexible pavements. These pavements incorporate continuously laid cement bound roadbases which, during curing, crack into slabs of varying length, ranging from 4-25m.

Reciprocal crack growth can occur in the surfacing, known as 'reflection cracks', located through stresses concentrated at the discontinuities within the roadbase.

Three mechanisms have been identified and are described as contributing to reflection crack propagation. They have been analysed independently although the majority of conclusions drawn are applicable to their combined action. Their relative importance will vary with respect to pavement geometry, material properties, environmental conditions and traffic intensity.

The first mechanism, 'tensile fatigue', induces crack propagation vertically upward through the surfacing. Tensile strains are developed during daily and annual fluctuations of temperature, which cause expansion and contraction of the cement bound roadbase. This mechanism is most prominent on pavements with thin surfacings and long slab lengths. The rate of crack growth is dependent on the range of temperature within the roadbase, slab length, thermal characteristics of the roadbase material and resistance of the surfacing to this form of fatigue.

A model has been developed based on a combination of results from an extensive testing programme, the use of fracture mechanics theory and computer simulation of the condition. The results quantify the resistance shown by conventional bituminous mixes to reflection cracking in terms of their mix parameters. Also considered are the use of stress relieving membranes, reinforcement material and modified binders to inhibit crack growth.

The second mechanism,'tensile yield' is also thermally induced but associated with cold weather conditions. Temperature gradients through the pavement structure induce warping and contraction within the uppermost layers. Tensile strains developed at the surface can, under U.K. winter temperatures, exceed the ultimate yield strain of the wearing course material.

Preliminary investigations of four pavements constructed in the early 1970's to motorway specifications indicate that reflection cracking will initiate at the surface if the yield strain, as defined through tensile creep tests, is reduced through binder oxidization to a value of 0.5%. This mechanism will operate on pavements with greater structural layer thicknesses and is only partially dependent on slab length.

The influence of a further mechanism,'shear fatigue' induced through trafficking of the pavement, has been shown to be confined to the acceleration of crack growth in the final stages of propagation unless a breakdown of interlock occurs between adjoining roadbase slabs.